UNIVERSITY OF STRASBOURG and CHARLES UNIVERSITY

Université de Strasbourg, Faculté de Géographie et d'Aménagement, LIVE, UMR 7362

Univerzita Karlova, Přírodovědecká fakulta, Katedra fyzické geografie a geoekologie

Extreme precipitation in low mountain ranges in Central Europe: a comparative study between the Vosges and the Ore mountains

Fortes précipitations en moyenne montagne en Europe Centrale : Étude de comparaison des Vosges et Monts Métallifères

Silné srážky ve středně vysokých pohořích střední Evropy: Porovnávací studie Vogéz a Krušných hor

Jana MINÁŘOVÁ

Doctoral dissertation

Thèse présentée pour obtenir le grade de Docteur de l'Université de Strasbourg et Université Charles de Prague
Disertační práce

Supervisors (Directeurs de thèse, vedoucí práce):

Pr. Alain CLAPPIER, Université de Strasbourg
&
RNDr. Miloslav MÜLLER, Ph.D., Univerzita Karlova

Prague, 2017

FACULTY OF SCIENCE
Charles University

Declaration (déclaration, prohlášení)

I hereby declare that I carried out this doctoral thesis independently, and all utilized references have been properly cited. No part of this thesis has been submitted for obtaining any other academic degree.

Je déclare que mon travail de thèse est un travail original et que je cite toutes les références bibliographiques et les sources des renseignements. Aucune partie de ce travail n'a été utilisée pour l'obtention d'un autre diplôme académique.

Prohlašuji, že jsem tuto dizertační práci vypracovala samostatně a že jsem všechny použité informační zdroje a literaturu řádně citovala. Tato práce ani její podstatná část nebyla předložena k získání jiného nebo stejného akademického titulu.

.....

May 27, 2017, Prague

Acknowledgements

(Remerciement, poděkování)

First of all, I owe great thanks to the thesis reviewers D.Sc. Olivier Caumont and Dr. Michal Žák, members of defence jury D.Sc. Radan Huth and Dr. Mario Marcello Miglietta, and the chairperson of the jury D.Sc. Daniela Řezáčová, and the supervisors Dr. Miloslav Müller and Pr. Alain Clappier for investing their precious time and efforts. Thanks for the constructive, critical and in-depth attentive scientific comments by Dr. Miloslav Müller, and for the individual lectures in statistics and programming held by Pr. Alain Clappier, due to which the thesis got very elaborate. I am also very much thankful to both supervisors for their guidance, continuous support and encouragements, and the valuable and fruitful ideas that they provided and shared with me throughout the doctoral studies.

This co-supervised thesis was firstly supported for 15-months by *BGF* (*French Government scholarship*) where I specially thank the Cultural Service of French Embassy in Prague and Campus France for their help in administration procedures during the thesis and for arranging the financial support. The thesis was also supported by the scholarship provided by Charles University, and in the second year by *DBU* (*Deutsche Bundesstiftung Umwelt*) for 6 months, which enabled a study stay at Interdisciplinary Environmental Research Centre at TU Bergakademie Freiberg, where I would like to thank Pr. Jörg Matschullat, Dr. Stephanie Hänsel, and Dr. Andreas Hoy for providing a comfortable environment, a valuable cooperation, and exchange of knowledge about precipitation in the Ore Mountains. Besides, I owe thanks to the 6-months ERASMUS Traineeship for supporting my last stay in Strasbourg, and to project CRREAT (reg. number: CZ.02.1.01/0.0/0.0/15_003/0000481, call number 02_15_003 of the Operational Programme Research, Development, and Education) for financially supporting the last months of the research including writing. I am also thankful to Collège Doctoral Européen (CDE) of the University of Strasbourg for selecting me to be a member of the International Doctoral Programme (cohort Helen Keller) dedicated to excellent Ph.D. students, and for providing extra useful help during my stays in Strasbourg.

Furthermore, I thank the national weather networks, i.e. Météo-France, DWD (Deutscher Wetterdiesnt), and CHMI (Czech Hydrometeorological Institute) for providing the daily precipitation datasets.

I extend great thanks to M.Phil. Syed Muntazir Abbas for his valuable remarks during the revision of the manuscripts and for the language corrections, Dr. Nadège Blond for her help in acquiring data from Météo-France, Dr. Georges Najjar, and M.Sc. Florian Raber for their fruitful discussions mainly in the first phase of the thesis, Ing. Ivo Řezáč for the help in programming in Microsoft Excel to effectively upload the raw data, and Dr. Simon Rougier for the brief introduction to the CRAN R software. Great thanks are also dedicated to the administration staff of both universities, mainly Estelle Baehrel, Dr. Dagmar Chalupová, Laurence Barondeau, and M.Sc. Pavla Pousková.

Last but not least, I would also like to thank my family members for their constant support and encouragements, my colleagues (Fangfang Guo in particular), and friends for their positive approach and support.

Abstract

Extreme precipitation is related to flooding which is one of the most frequent natural hazards in Central Europe. Detailed understanding of extreme precipitation is the precondition for an efficient risk management and more precise projections of precipitation, which include uncertainties, especially at regional scale. The thesis focuses on extreme precipitation in the Ore Mountains (OM) and the Vosges Mountains (VG); two low mountain ranges in Central Europe experiencing orographic effect on precipitation. Based on state of the art about precipitation in OM and VG, a currently missing analysis of the temporal distribution of precipitation in VG was needed prior to the analysis of extremes. The original dataset of daily precipitation totals from 14 weather stations used in the initial study was extended to 168 stations covering a broader area of VG. The study of temporal distribution of precipitation during 1960—2013 led to a classification of stations: (i) mountainous stations with winter maxima and highest mean annual totals due to orographic enhancement of precipitation, (ii) stations on leeward slopes with two maxima (summer and winter), (iii) lee side stations with summer maxima and lowest mean annual totals due to rain shadow and more continental character, and (iv) stations on the windward side with no major influence of the mountains and even (oceanic) regime with autumn maxima.

The analysis of extreme precipitation was based on 1—10 days non-zero totals during 1960—2013 from 168 stations located in VG and 167 stations located in OM. Three common pointwise approaches (i.e. Peaks over Threshold, Block Maxima, and Return Period) were firstly employed in VG to select extreme precipitation totals. The results of the seasonal distribution of the totals were dependent on a criterion and suggest that the orographic influence on extreme precipitation is more perceptible at higher selected threshold. In the end, the selection of 54 extreme precipitation events (EPEs) in OM and VG was conducted based on the areal assessment of precipitation, the so-called Weather Extremity Index (WEI). WEI was firstly employed at the regional scale and its values converted to be comparable between regions using maximum theoretical value. The results showed that the EPEs lasted mostly 1—2 days in both regions, whereas affected a larger part of OM (up to 100 %) as compared to VG. Stationary fronts occurred most frequently during EPEs in VG, while lows in OM. Lows in OM during EPEs often originated from cold air cut-off and most of them had Vb track from Mediterranean towards the northeast, which is typical for widespread precipitation and flooding in Central Europe. Even during two of the ten strongest EPEs in VG, the extreme precipitation was related to Vb lows, this time strongly deflected westwards. The comparison of the characteristics of EPEs between OM and VG show strong relationships between the temporal and synoptic attributes, while the spatial attributes are rather site-specific. The results of the thesis contribute to broaden the current knowledge about extreme precipitation in Central Europe and might be helpful not only for projections of extreme precipitation but also for risk managers and engineers, who deal with risks related to atmospheric precipitation.

Keywords: heavy rainfall, Weather Extremity Index, Grosswetterlagen, weather types, continentality, Erzgebirge, Vosges Mountains, Krušné hory

Résumé

Les fortes précipitations sont fréquemment associées aux crues qui représentent un des risques naturels majeurs en Europe Centrale. Mieux comprendre les épisodes de fortes pluies est nécessaire pour les prévoir de manière plus précise dans le futur et ainsi gérer plus efficacement les risques naturels sur les territoires qu'elles affectent. L'objectif principal de cette thèse est de s'intéresser aux événements de fortes pluies à l'échelle régionale en terrain complexe. Elle se focalise sur deux chaînes de moyenne montagne d'Europe Centrale dont les effets orographiques influencent les précipitations : les Monts Métallifères [ou Ore Mountains en anglais] (OM) et les Vosges (VG). Etant donné le manque d'études récentes portant sur les précipitations dans le VG, ce travail de recherche a débuté par une analyse de la climatologie des précipitations moyennes dans ce massif (avant d'en étudier les précipitations extrêmes). Une première analyse s'est basée sur les données de précipitation journalière (1950—2011) mesurées par 14 stations météorologiques puis a été approfondie par une seconde analyse s'appuyant sur un plus grand nombre de stations (168) pendant 1960—2013. Ce travail a permis de classer les stations de mesures pluviométriques des VG : (i) les stations montagneuses montrant les maximum en hiver et les moyennes annuelles les plus élevées, (ii) les stations situées sur les pentes du côté « sous le vent » du massif des VG montrant des précipitations principalement durant deux saisons, l'été et l'hiver, (iii) les stations situées dans la plaine d'Alsace montrant de faibles précipitions pendant la saison estivale et les totaux annuels les moins élevés, et (iv) les stations situées sur le côté « au vent » du massif des VG, étant peu influencées par les VG et dont les maxima apparaissent en automne.

L'analyse de fortes précipitations s'est basée sur des durées allant de 1 à 10 jours pendant la période 1960—2013 sur l'ensemble de 168 stations dans les VG et 167 stations dans les OM. Trois approches ont été tout d'abord appliquées (i.e. Peaks Over Threshold, Block Maxima et Return Period) dans les VG pour sélectionner les totaux de pluie extrême. Les distributions saisonnières des totaux obtenues à l'aide de ces méthodes se sont montrées très sensibles aux paramètres d'entrées prescrits pour chaque méthode. Ainsi il s'est avéré que l'effet de l'orographie sur les fortes précipitations était d'autant plus marqué que le seuil de précipitation était choisi plus élevé. Une quatrième méthode, moins sensible à ses paramètres d'entrée et considerant l'extension spatiale des épisodes, le Weather Extremity Index (WEI), a donc finalement été choisie pour sélectionner les 54 plus forts évenements des précipitations extrêmes (EPEs) dans les OM et les VG. Les résultats ont montré que les EPEs sont le plus souvent de courte durée (1—2 jours) dans les deux régions. Ils affectent souvent plus grande partie des OM (jusqu'à 100 % de la surface du massif) alors qu'ils ne touchent qu'une partie plus petite des VG. Les EPEs dans les VG apparaissent majoritairement lors de la situation synoptique d'un front froid ondulant. Dans les OM les situations synoptiques entraînant le plus fréquemment des EPEs correspondent à des cyclones générés par une goutte d'air froid isolé et dont le trajet est souvent qualifié de « Vb » (c.a.d. allant de la Méditerranée vers le nord-est). Il faut toutefois noter que deux des dix plus forts EPEs des VG sont apparus lors de situations de cyclones Vb, mais cette fois-ci fortement déviés vers l'Ouest. La comparaison de caractéristiques d'EPEs dans les OM et les VG a montré de fortes similitudes temporelles et synoptiques dans les deux massifs contrairement aux répartitions spatiales qui restent propres à chacune des deux régions. Les résultats de cette thèse contribuent à approfondir les connaissances sur les fortes précipitations dans les moyennes montagnes en Europe centrale. Ils peuvent servir à prévoir l'évolution des fortes précipitations dans le futur et à mieux gérer les risques naturels liés aux précipitations.

Mots-clés : fortes précipitations, Weather Extremity Index, Grosswetterlagen, types de temps synoptiques, continentalité, Erzgebirge, Vosges, Krušné hory

Abstrakt

Silné srážky souvisí s povodněmi, tedy jedním z nejčastějších přírodních ohrožení ve střední Evropě. Podrobné pochopení silných srážek je předpokladem k účinnému řízení rizik a přesnějším projekcím srážek, které zvláště na regionální úrovni zahrnují nejistoty. Tato disertační práce se zabývá silnými srážkami ve dvou středně vysokých pohořích ve střední Evropě — v Krušných horách (OM) a Vogézách (VG), kde se projevuje orografický efekt na srážky. Na základě rešerše dostupné literatury o srážkách v OM a VG bylo před analýzou extrémů zapotřebí provést dosud chybějící analýzu časového rozdělení srážek ve VG. Původní soubor denních úhrnů srážek ze 14 meteorologických stanic byl rozšířen na 168 stanic, čímž bylo zahrnuto širší okolí VG. Analýza časového rozdělení srážek ve VG za období 1960—2013 vedla ke klasifikaci stanic na: (i) horské stanice se zimním maximem srážek a nejvyššími průměrnými ročními úhrny díky orografickému zesílení srážek, (ii) stanice na závětrných svazích se dvěma maximy (letním a zimním), (iii) stanice v závětří (Hornorýnská nížina) s letním maximem a nejnižšími průměrnými ročními úhrny vlivem srážkového stínu a kontinentálnějším rysům, (iv) stanice na návětrné straně s minimálním vlivem pohoří a rovnoměrným (oceánickým) ročním chodem a maximem na podzim.

Analýza silných srážek vycházela z 1—10denních nenulových úhrnů za období 1960—2013 ze 168 stanic ve VG a 167 stanic v OM. Nejprve byly tři bodové běžně používané přístupy (i.e. Peaks Over Threshold, Block Maxima and Return Period) použity ve VG pro výběr silných srážkových úhrnů. Výsledky sezónní distribuce těchto úhrnů byly závislé na kritériu a naznačily, že orografický vliv na silné srážky je patrnější při vyšším zvoleném prahu. Výběr 54 silných srážkových událostí (EPEs) v OM a VG byl nakonec proveden na základě plošného vyhodnocení srážek, tzv. Weather Extremity Index (WEI), který byl prvně aplikován na regionální úrovni a jehož hodnoty byly pomocí maximální možné hodnoty převedeny do podoby porovnatelné mezi územími. Výsledky ukázaly, že EPEs trvaly v obou územích hlavně 1—2 dny, přičemž zasahovaly větší část OM (až 100 %) oproti VG. Zvlněné studené fronty se nejčastěji vyskytovaly při EPEs ve VG, kdežto tlakové níže v OM. Cyklóny v OM během EPEs převážně vznikaly odříznutím zatečeného studeného vzduchu a často měly Vb dráhu ze Středomoří směrem na severovýchod, která je typická pro velkoplošné srážky a povodně ve střední Evropě. I při dvou z deseti nejsilnějších EPEs ve VG došlo ke vzniku silných srážek vlivem Vb cyklóny, tentokrát výrazně západně vychýlené. Porovnání charakteristik EPEs mezi OM a VG ukázalo silný vztah mezi časovými a synoptickými znaky, zatímco prostorové znaky byly spíše vázány na dané zkoumané území. Výsledky disertační práce přispívají k rozšíření stávajících poznatků o silných srážkách ve střední Evropě a mohou být přínosné jak pro projekce silných srážek, tak pro manažery a inženýry, kteří se zabývají riziky atmosférických srážek.

Klíčová slova: silné srážky, Weather Extremity Index, Grosswetterlagen, povětrnostní situace, kontinentalita, Erzgebirge, Vogézy, Krušné hory

Table of contents

1. Introduction and motivation

Precipitation is integral to the hydrological cycle, thus, it is essential to life. The temporal and (mainly) spatial distribution of precipitation that influences the distribution of ecosystems and conditions agricultural yields is more complex than that related to temperature (Oliver, 2008). In orographic areas, where many peculiarities can be found (Barry, 2008), the issue of spatial distribution of precipitation becomes even more complex. As stated by many authors, the processes of precipitation in complex relief have still not been satisfactorily understood (Prudhomme and Reed, 1998; Roe *et al.*, 2003; Smith, 2006).

The precipitation anomalies such as drought or heavy rainfall are associated with many natural disasters and losses worldwide (Cutter *et al.*, 2008), and are considered along with storms as leading natural hazards in Central Europe. For instance, the heavy rainfall in August 2002 and June 2013 led to an extensive flooding in Central Europe with many casualties and economic losses (Boucek, 2007; Goldberg and Bernhofer, 2003; Merz *et al.*, 2014; Schröter *et al.*, 2015; Stein and Malitz, 2013; Thieken *et al.*, 2005; Ulbrich *et al.*, 2003; Van der Schrier, *et al.*, 2013). Flooding (flash or widespread) represents one of the most common indirect impacts of extreme precipitation in Central Europe besides landsliding and enhanced erosion. As compared to the rather local direct impacts of extreme precipitation affecting e.g., the transport safety during the precipitation event, the indirect impacts can affect much larger areas, even beyond the area and duration of heavy rainfall occurrence, which increases the risks related to the extreme precipitation events.

The considerable casualties and the dire financial impacts induced e.g., by the two extreme precipitation events in Central Europe (August 2002 and June 2013), highlighted the ongoing vulnerability of societies to the precipitation extremes despite improved risk management and prediction of heavy rainfall (Cavalcanti, 2012; Décamps, 2010; Kienzler *et al.*, 2015; Lamarre and Groupement de recherches sur les risques liés au climat (France), 2005; Raška and Brázdil, 2015). The ongoing vulnerability of European societies to extreme precipitation events along with the increasing frequency and intensity of weather extremes projected in Europe in the context of global climate change according to the IPCC report (Pachauri *et al.*, 2014) and e.g. Söder et al. (2009), Vautard (n.d.) and Westra et al. (2014) demonstrate the crucial demand to recognize, describe, and understand precipitation extremes (Beniston and Stephenson, 2004) to efficiently improve the risk management and warning systems (Kienzler *et al.*, 2015; Socher and Boehme-Korn, 2008; Thieken *et al.*, 2007).

The presented research is motivated by the need of a broader understanding and a detailed insight into the characteristics of extreme precipitation events and their conditioning factors at diverse temporal and spatial scales. It mainly deals with extreme precipitation in two low mountain regions in Central Europe. The results might not only help in mitigating the hazards associated with extreme precipitation but also reduce the risks (human injuries, losses of life, economic losses, and devastation of construction works, cultural and natural heritage) by improved planning based on detailed information. It might also provide the basis for making better engineering decisions which can withstand the recurring and likely more frequent events predicted in future.

2. State of the art

This chapter reviews the current scientific literature related to the definition of extreme precipitation and precipitation in orographic areas. It contains five sections that summarize: (i) common approaches to define extreme precipitation, (ii) its trends and temporal and spatial aspects, (iii) orographic effect on precipitation, (iv) studies about mean and heavy precipitation in the Ore Mountains, and (v) current knowledge about mean and heavy precipitation in the Vosges Mountains.

2.1. Definition of extreme precipitation (event)

An extreme precipitation is easily recognizable but hardly definable (Stephenson, 2008: 12), because the term "extreme" [noun] might already mean many different things (Strangeways, 2007). Statistically and in Aristotle's logic, an extreme represents a maximum or minimum (one) value. In climatology, it is generally the highest (eventually lowest) value of a climatic feature that is observed during study time period. We call an absolute climatic extreme the highest (lowest) value measured during the whole period of record for which the observations are available (*AMS Glossary*, (n.d.)). However, an atmospheric extreme can also be considered as an anomalously high or low value at a given place during a given period (e.g., season) as compared to the usual (e.g., average) values of the atmospheric feature during that period (Rohli and Vega, 2008), which suggests that the term "extreme" might be relative. Extreme as adjective (e.g., extreme precipitation) might not only mean that the subject reaches particularly high or highest value/degree, but also signify that the reaching value/degree is very unusual, exceptional, severe, and far from being moderate, and includes high risk (*Oxford Dictionaries*|*English*, (n.d.)). Thus the definition of extreme precipitation/precipitation extreme might also meet many different meanings.

Extreme precipitation events, part of weather and/or climate extreme events, are complex subjects, which might involve various attributes such as intensity rate (magnitude), spatial and temporal feature and scale (e.g., area affected by the event, timing and duration), and rate of occurrence (Stephenson, 2008). Beniston *et al.* (2007) considered a weather and climate extreme event as an event which is intense, rare, and severe. The intensity, rarity, and severity are commonly used approaches to define extreme precipitation events in atmospheric research, though they include various methods, as it is shown in the following subsections.

2.1.1. Intensity

The intensity approach is simple and popular, and usually consists of defining a **threshold value of precipitation total** (often daily) that is exceeded at an individual site during a given period e.g., month, season, year (Cox and Isham, 2000). For instance, Štekl et al. (2001) analysed extreme daily precipitation totals in the Czech Republic that exceeded 150 mm during 1879—2000. Expert Team on Climate Change Detection and Indices (ETCCDI) suggest to study e.g., the annual count of days when the daily precipitation totals exceed 10 mm, 20 mm or user-defined value (Zhang, 2013; Zhang *et al.*, 2011). World Meteorological Organisation (WMO, online) also defines heavy rain as rainfall total exceeding a specific value such as 7.6 mm in an hour, or high-intensity rain (WMO and UNESCO, 2013). A similar definition is also given by American Meteorological Society (AMS, online), yet it includes the geographical dependence of the specific precipitation accumulation rate that has to be exceeded.

The approach is useful for a single study period and at a given rain gauge, and was used in many studies (e.g., Muluneh *et al.*, 2016; Ngo-Duc *et al.*, 2016; Tošić *et al.*, 2016; Wang *et al.*, 2016a). However, the analysis of precipitation extremes generally aims at certain areas and focuses on more periods of time (e.g., seasons). For such analysis, the described approach might result in biased findings because a limit of precipitation intensity is arbitrary and favours areas (e.g., mountainous) with high precipitation totals on average. Thus, it does not capture the climate differences when the precipitation totals at rain gauges are considered from the climatologically heterogeneous area (Müller and Kaspar, 2014). For instance, a daily rainfall total of 50 mm might be a common value in tropics although it can be destructive in subtropics or mid-latitudes. Similarly, the 50 mm in winter might not be as heavy as if it occurs in summer. The recent large-scale flood of Elbe and Danube rivers in Central Europe at the beginning of June 2013 that was induced by large-scale long lasting heavy rainfall (Grams *et al.*, 2014; Merz *et al.*, 2014; Schröter *et al.*, 2015; Stein and Malitz, 2013) also demonstrates the sensitivity of fixed precipitation total on an analysis. The highest daily precipitation intensity was around 95 mm in the Czech Republic which is much lower than the defined threshold 150 mm in the above-cited study from Štekl et al. (2001). Thus, based on the criterion of exceeding the 150 mm amount, the event would have been omitted and not considered among extreme precipitation events in the Czech Republic despite the heavy rain that occurred especially in Czech highlands and lowland (Van der Schrier, *et al.*, 2013; Müller and Kaspar, 2014).

A simple solution might consist of defining several or adjusting thresholds according to the study period or location which would better reflect the dispersion of climatic conditions, e.g., Stephenson (2008) described "record-breaking" events based on varying thresholds and trending threshold that takes into consideration the non-stationarity (variability) of climate over longer term. Nevertheless, the definition of many thresholds may need broad knowledge of a specialist on the study area(s) and might be time demanding. It also considers the extreme events as equally strong, i.e. no quantification of their extremity is possible. Another way that is particularly used in hydrological studies is to calculate the **Probable (possible) Maximum Precipitation (PMP)** which indicates the physically possible (theoretical) maximum precipitation total (i.e. upper limit) over an area (e.g., basin) for a certain duration (WMO and UNESCO, 2013). The PMP can be used for designing strongest (possible) flood resisting constructions. However, it might not be of special interest in atmospheric research.

Another option is to standardize the precipitation totals by mean precipitation total or mean maximum total since the resulting dimensionless value might lead to more robust comparison among extreme precipitation events from various climatic locations. Nevertheless, the **standardized values** of precipitation totals might also end in biased results due to favouring those locations which show the highest variability of precipitation (Müller and Kaspar, 2014).

Block Maxima (BM) approach also partly deals with the described problem (Coelho *et al.*, 2008; Coles, 2001; Embrechts *et al.*, 2011; Katz, 2010; Katz *et al.*, 2002; Woeste, (n.d.)) since it takes into consideration the climatic features of given rain gauges. The maximum precipitation totals in given periods of time at rain gauges are considered, most often the yearly (or seasonal) daily precipitation maxima (Balling *et al.*, 2016; Blanchet *et al.*, 2016; Ghenim and Megnounif, 2016). Thus, instead of selecting precipitation maxima in an area from all gauges at one, the BM enables a selection of maxima per rain gauge thereby taking account of climatic peculiarities of gauges. However, the extreme precipitation events are not equally distributed in time (e.g., one per year) as it is assumed in the BM, and the BM does not consider whether the period over which the maximum is taken was dry or wet, which might result in a selection of some very low precipitation totals (although highest during the dry period) at a given rain gauge, as it is pointed in Section 7 (Minářová *et al.*, 2017c).

2.1.2. Rarity

Extreme precipitation events can also be defined estimating their rarity (exceptionally high values/frequencies) at a particular place or from the entire affected area (as in intensity approach), and time of year (Beniston *et al.*, 2007; Stephenson, 2008), yet the definition of rarity is not unified and various approaches are used. The first one, **Peaks Over Threshold (POT)** is similar to the previously described (i.e. exceeding threshold rainfall total), however, this time the threshold is considered as percentile (e.g., 90^{th}) of the observed probability density function, thereby reflecting that the extreme precipitation is variable from location to location in an absolute sense (WMO, (n.d.)). The recommended indices by ETCCDI also include the 95^{th} and 99^{th} percentile as the threshold for heavy precipitation among other wet days (precipitation total ≥ 1.0 mm) during the period 1961—1990 (Zhang, 2013). The POT approach is very commonly used in the analysis of precipitation extremes (Allan *et al.*, 2015; Blenkinsop *et al.*, 2016; Wang *et al.*, 2016b; Wi *et al.*, 2015; Yin *et al.*, 2016), the quantiles are easily computable (Zhang *et al.*, 2011) and provides ranking of precipitation totals, i.e. information about their extremity, and robust results. Nevertheless, the POT does not allow for the actual differences between subsequent precipitation totals (Müller and Kaspar, 2014), and the results are threshold-sensitive (Minářová *et al.*, 2017c). However, an automatically defined threshold proposed by Fukutome et al. (2015) for extreme hourly precipitation totals in Switzerland may improve it. It is also based on an empirical distribution, although Katz (2010) suggested that an analysis of precipitation extremes might be improved when based on theoretical distribution.

According to WMO and UNESCO (2013), the **theoretical distribution** of extreme events is the probability distribution of the largest (smallest) observations in a sample. Among the theoretical distributions that are suitable for analysing precipitation extremes (tails of the distribution), the Gumbel distribution and the Generalized Extreme Value distribution (GEV) are most commonly used. In fact, precipitation, in general, does not fit the Gaussian normal distribution because the lowest values (no rain) are disadvantaged as compared to the highest (Granger, 2005). The fitted distribution to precipitation totals generally assumes randomness, homogeneity, and independency, thus a test of homogeneity of time series is needed (e.g., Wang *et al.*, 2010; Wang and Feng, 2013) prior to fitting any distribution. In fact, the homogeneity has to be tested prior to any analysis of precipitation because of the systematic errors related to the rain gauges. For instance, up to 10 % of liquid precipitation might be underestimated using unshielded rain gauges (in use mostly until 1970s to 1980s) as compared to the shielded rain gauges (the relationship between their observations was considered logarithmic in Johnson and Hanson (1995), and the errors related to snow measurements are still not fully solved (Tucker, 2005). Concerning the assumption of independency, although its degree may vary according to precipitation processes, season, and location of the occurrence, which is difficult to consider, still the precipitation tends to fit statistical distributions such as gamma or lognormal (Granger, 2005). However, this study deals mostly with extreme precipitation events.

The Gumbel distribution of extreme values is two parametric distribution, which is obtained by selecting the maximum amplitude from the time series of e.g., daily precipitation totals, which are assumed to be exponentially distributed (Keeping, 1962; Koutsoyiannis, 2004). The GEV distribution is three parametric and includes the parameters scale, shape, and location (Coles, 2001). It is widely used since the three parameters lead to more robust results (e.g., Ban *et al.*, 2015; Hosking and Wallis, 2005; Panagoulia *et al.*, 2014), and it also enables a direct computation of probability, i.e. **return period estimates (RP)**. The RP (described e.g., by Coelho *et al.*, 2008; Coles, 2001; Katz, 2010; Katz *et al.*, 2002) provides an estimation of the probability of occurrence of precipitation events. For instance, 100-year rainfall total has a probability 1/100 of being exceeded in any 1-year period which

means that 100 years might be the average time until next occurrence of the total if the time to the next occurrence fits geometric distribution (*AMS Glossary*, (n.d.)). The RP approach introduces again thresholds (e.g., 5-year, 10-year totals), which makes the outcomes threshold-sensitive (Minářová *et al.*, 2017c). Coles (2001) proposed to analyse the exceeding over rarity threshold by non-homogenous Poisson process. Moreover, the threshold implies a discrete division between extreme and non-extreme precipitation events, although the transition from strongest to less strong precipitation events is rather continuous and fuzzy (Müller and Kaspar, 2014). The fuzzy approach distinguishes extreme and non-extreme events based on their degree of membership with the extreme (maximum), yet the selected degree limit might be again arbitrary.

The RP is of particular interest for hydrologists and risk managers due to the easy understanding and interpretation of results, thus, it is used in many hydrological and meteorological studies (e.g., Bertoldo *et al.*, 2015; Botero and Francés, 2010; Conradt *et al.*, 2013; Dyrrdal *et al.*, 2014; Gumbel, 1941; Hirabayashi *et al.*, 2013; Maugeri *et al.*, 2015). The approach assumes the randomness of extreme events, i.e. the atmospherically generated extreme events occur independently, the probability of their occurrence does not change from year to year although increases with the increasing considered time period. Thus, only external factors might show dependencies (Nott, 2006). However, several studies have suggested that in certain periods of time in paleoclimate, the extreme precipitation events tended to cluster. For instance, Liu and Fearn (2000, 2002) found maximum hurricane intensity in the period 3200—1000 years BP (before present). Dean (1997) also found periodicity in natural processes in Holocene, and Strangeways (2007) even discussed the cyclic behaviour of precipitation (alternation of dry/wet periods) in recent climate, although he suggested that it is not certain whether the cycles are rather related to decadal variation or to trends in extreme/mean precipitation.

The frequency analysis was even suggested to be insufficient if the magnitude of extreme events is not studied in parallel (Katz, 2010). However, the magnitude might be studied also based on exceeding given probability (Stephenson, 2008). Thus, the frequency analysis such as RP, which proceeds from the theoretical distribution of extreme values, remains helpful mostly because it can be applied for a wide range of weather variables and is not influenced by the accumulation period of precipitation (Ramos *et al.*, 2005).

2.1.3. Severity

International Panel on Climate Change (IPCC) indicated that the weather extremes are complex and might correspond to severe weather related to particular climatic phenomena, often requiring a critical combination of variables (Pachauri *et al.*, 2014). Since the occurrence of extreme precipitation events is relatively low, the losses related to it remain considerable, which makes the events severe for societies that cannot easily adapt. The severity of events can be expressed in terms of e.g., number of casualties, economic and long-term losses, the area flooded subsequent to the event, and RP of flooding (Botero and Francés, 2010; Conradt *et al.*, 2013; Gumbel, 1941; Hirabayashi *et al.*, 2013). Thus it combines the atmospheric hazard with human stakes, i.e. it considers the non-natural risk such as exposure and vulnerability as well (Stephenson, 2008).

Including event consequences, the severity approach is very useful in fields such as insurance (e.g., Mills, 2005), ecology (e.g., Smith, 2011) and risk management (e.g., Kienzler *et al.*, 2015; Socher and Boehme-Korn, 2008; Thieken *et al.*, 2007), where it enables an evaluation of the efficiency of management (protecting measures for citizens and stakes, public awareness, and warning systems). The description of direct and indirect impacts of precipitation events is also widely used in studies of

one particular extreme event (e.g., Boucek, 2007; Grams *et al.*, 2014; Thieken *et al.*, 2005) to justify the analysis without further definition of extreme precipitation. However, a broader dataset of extreme precipitation events is needed to gain insight into the characteristics and atmospheric processes related to the events. Primarily, the atmospheric processes can be better interpreted if the dataset of events is based directly on rainfall data instead of impacts, which makes the severity approach less essential in atmospheric research.

Based on Section 2.1, an **extreme precipitation** might be a precipitation whose intensity exceeds common values in a climatic region (i.e. high observed precipitation total) and occurrence is rare (i.e. high RP) - both the intensity and rarity are significant in comparison with long-term and seasonal totals, and the precipitation is largely responsible for any socio-economic impact. The specific timing of individual extreme precipitation events as compared to surrounding (e.g., seasonal) values was also found important by Stephenson (2008). However, there are many factors influencing the precipitation extremes (e.g., synoptic condition, circulation anomalies, antecedent soil moisture, rate of snow melt, character of precipitation event, topographical structure of the area) which even varies from event to event, season to season, and area to area (Kunkel *et al.*, 1999), thereby the range of studied elements is also wide. Besides case studies about individual extreme precipitation events, the studies deal with climatology and seasonality of extreme precipitation, instability and role of convection in producing extreme precipitation based on sounding measurements (Houze, 2014), thermodynamic variables during or prior events showing that their anomalies might efficiently indicate the causal synoptic features of extreme precipitation (e.g., Kaspar *et al.*, 2013), and large-scale atmospheric circulation patterns including the role of atmospheric oscillations (e.g., El Niño Southern Oscillation ENSO and North Atlantic Oscillation NAO), Rosby waves and anomalies in Sea Surface Temperature (SST) and pressure at sea level and other isobaric levels (e.g., Cavalcanti, 2012). Numerical approach is also widely used to quantify and predict extreme precipitation, and to describe the patterns related to extreme precipitation such as cyclones which can also be combined with satellite data and convection (Augros *et al.*, 2016; Bauer *et al.*, 2015; Hally *et al.*, 2015; Mastrangelo *et al.*, 2011; Miglietta *et al.*, 2013a, 2015; Řezáčová, 2007). The trends and temporal and spatial aspects of heavy rainfall are also very commonly analysed in the papers, and are described in the following Section 2.2.

2.2. Trend analysis, and temporal and spatial aspect of extreme precipitation

2.2.1. Trend analysis of extreme precipitation

Linear regression is commonly used in trend studies of precipitation (e.g., Akinremi *et al.*, 1999; Brázdil *et al.*, 2009; Groisman *et al.*, 2005; Wang and Zhou, 2005; Zhou *et al.*, 2009), though Kendall τ test was suggested to better represent the trends in precipitation extremes due to the non-normal distribution of the extremes (Kunkel *et al.*, 1999). The non-parametric Mann-Kendall test for the monotonic trend can even be used to estimate the statistical significance of the results (Hirsch *et al.*, 1982; Hirsch and Slack, 1984; Kendall, 1975; Mann, 1945). However, the analysis of the variability and trends in precipitation, i.e. including extreme precipitation (e.g., Wang *et al.*, 2013; Zhang *et al.*, 2017) is based on the general assumption that the historical record actually reflects its long-term behaviour, which is assumed for other atmospheric hazards as well. However, the historical record is limited by given time period and usually does not take into consideration the conditions prior the beginning of the measurements, though Kunkel et al. (2003) indicated that the past natural variability

of precipitation (e.g., in 18th and 19th century) has to be considered because it might potentially contribute to the recent increase in extremes.

The historical record might also not show the complete pattern of the variability of the hazard (precipitation). Many authors who analysed trends in extreme precipitation in Europe (e.g., Cantet *et al.*, 2010; Dobrovolný *et al.*, 2015; Osborn *et al.*, 2000) or other places (e.g., Alexander *et al.*, 2006; Groisman *et al.*, 2005; Klein Tank *et al.*, 2006; Kunkel *et al.*, 1999, 2003, 2012) suggested that the findings of trends in extreme precipitation events might be statistically unstable due to their low occurrence, i.e. inherent scarcity of data. For instance, Denhez (2009) who found an increase in heavy rainfall (daily totals above 190 mm) up to 40 % during 1900—2005 in Central and Northern Europe, pointed out that the results might be biased because of the insufficient number of representatives of heavy rainfall events in the examined dataset. Nevertheless, the analysis of extreme precipitation variability is crucial for better forecasting (Ferro and Stephenson, 2011) and preparedness of societies against impacts of the hazard, and the analyses of changes in intensity, frequency, duration and spatial extent, and location of extreme precipitation events are particularly important (Oliver, 2005). The changes cannot be easily analysed under the assumed stationary climate yet because the variance and the relationship between the frequency and intensity remain unchanged.

Although the trend studies are generally based on long data series (e.g., Alexander *et al.*, 2006), which is substantial for the analysis of extreme precipitation events (i.e. more representatives), they frequently do not deal with causal conditions and complex processes related to extreme precipitation.

2.2.2. Temporal and spatial aspect of extreme precipitation

The extreme precipitation always lasts during a certain time (i.e. it is not instantaneous and includes several consecutive values) and affects any area, which makes the duration and spatial extent the important characteristics of extreme precipitation events. The spatiotemporal scales of extreme events should be studied in current atmospheric research (e.g., Zolina *et al.*, 2010). The longer lasting and the larger the area affecting by the event, the stronger the event should be. However, the rain gauges may have difficulties in distinguishing local episodes from large-scale events, and the convective rainfall might produce high intensity and short lasting rain that might affect only small areas (Houze, 2014). Thus, the origin of the extreme precipitation events (e.g., from convective/stratiform clouds) has also to be considered (Řezáčová, 2007). A wide range of potential origin of extreme events was suggested by Stephenson (2008) such as evolutionary or stationary (i.e. local maximum values) origin, origin induced by rapid growth due to instabilities, and displacement of similar events in space and time (i.e. to another area and season). Interestingly, Ferro et al. (2005) indicated that an extreme event can arise even due to the simultaneous coincidence of several non-extreme conditions. Regardless of the event origin, all events have a similar course and can be characterized by a beginning, an increase until reaching a peak, and then a decrease until common conditions. Nevertheless, the definition of the start and the end of an event is not clear (Stephenson, 2008), and leads to a fuzzy concept.

The temporal aspect of extreme precipitation events is usually more frequently considered in papers as compared to the spatial aspect. Diaz and Murnane (2008) suggested that it is useful to distinguish whether the event was short- or long-term thus weather or climate event, respectively. The temporal aspect might be more easily quantified than the spatial aspect. For instance, 5-day totals are easily computable and often compared with 1-day values as analysed e.g., in Frich *et al.*,

(2002). The x-day totals (or their quantiles) are also suggested among the 27 core indices for climate change research by ETCCDI (Zhang, 2013). However, the extremity of precipitation event might be influenced by fluctuation in precipitation during the event, which led Beguería et al. (2009) to consider duration together with magnitude and intensity. The dependence of successively increasing duration during events on return period estimates of precipitation intensity enables to compare the extremity of the events not only among the events but also among the rain gauges in the so-called severity graphs (Ramos *et al.*, 2005). Analogously, the duration of events can be combined with intensity and frequency in the so-called IDF (Intensity-Duration-Frequency) curves (e.g., Chow *et al.*, 1988). However, the curves are mostly used by hydrologists.

The spatial aspect of extreme precipitation events can be easily expressed using mean areal precipitation value(s) (Dawdy and Langbein, 1960) or dependence on altitude (e.g., Desurosne and Oberlin, 1994). Nevertheless, the selection of the spatial units over which the means are calculated may bias the results, and the extremity of events depends on the size of the study area as well (Konrad II, 2001). In fact, Ren et al. (2012) stated that the extreme events affect regions which are series of daily affected areas. He adjusted the area affected by extreme events using several thresholds of daily precipitation totals, though it might provide threshold-sensitive results. Another option is to combine the spatial extent of events expressed by Areal Reduction Factors (ARF) with IDF curves, which was considered suitable for graphical representation of extreme atmospheric events (Ramos *et al.*, 2005). The ARF were assumed independent on return period estimates, thus were applicable to all study area (Svensson and Jones, 2010). Besides the IDF curves, other kinds of curves were also designed such as DAD (Depth-Area-Duration) curves for heavy rainfall and its extended version SAD (Severity-Area-Duration) curves used mostly for analysing droughts. The DAD curves are based on observed values (Nicks and Igo, 1980), whereas the SAD on standardized values (Andreadis *et al.*, 2005; Sheffield *et al.*, 2009). Although the curves are very useful for decision makers and risk managers because they provide easily interpretable visualized results, Müller and Kaspar (2014) suggested that they might not provide synthesized results about the extremes.

A geostatistical approach such as interpolation techniques (e.g., Inverse Weighted Distance IDW, Kriging) is another alternative to deal with spatial distribution of precipitation during the extreme events (Davison *et al.*, 2012; Davison and Gholamrezaee, 2012; Dobesch *et al.*, 2007). Wotling et al. (2000) regionalized the extreme precipitation distribution using multiple Gumbel regression instead of simple kriging (which favours the extremes situated in central part of the area and omit the small-scale effects) to study the topographical environment of rain gauges. The authors applied the Principal Component Analysis (PCA) on variables (e.g., exposure, altitude, slope, height and width of the crest, and distance to the crest) based on Digital Elevation Model (DEM) similar to Johnson and Hanson (1995) or CEMAGREF Aix-en-Provence (1981). It showed the influence of topographical parameters and orographic precipitation on the spatial distribution of extreme and mean precipitation.

Both temporal and spatial aspects, i.e. **spatiotemporal aspect**, of extreme precipitation events should be considered in the analysis together with intensity and potentially also with socioeconomic impacts (Diaz and Murnane, 2008). The spatiotemporal dependence was studied e.g., using the multivariate extreme value modelling (Davison *et al.*, 2012; Stephenson, 2009), max-stable processes (Haan, 1984) combined with pair-wise likelihood fitting (Zhang *et al.*, 2014), and other numerical modelling techniques (e.g., Hally *et al.*, 2015). However, a progressive adjustment of duration and area affected by the events is needed due to rather fuzzy delimitation of events in space and time (Müller and Kaspar, 2014). Although such approach might be complex, based on the analysis of extreme precipitation events in the Czech Republic, Müller and Kaspar (2014) proposed an event-

adjusted method to evaluate weather and climate extremes including adjustable variables, the duration and area affected by the events. The method was applied in the presented study as well (Section 2.2) because it provides quantitative information about the extremity of events by introducing the Weather Extremity Index (WEI), which is crucial to see the differences in causes of more or less extreme events instead of considering all events as (equally) extreme. Besides the complex spatiotemporal aspects of extreme precipitation, the areas with complex relief (i.e. orographic areas) are subject to more complicated processes and spatiotemporal distribution. The next Section describes briefly the recent state of the art about the orographic effect on precipitation and its modelling.

2.3. Orographic effect on precipitation

The orographic areas are known for complex precipitation patterns due to the altitudinal differences, microclimatic peculiarities, and many other factors such as prevailing airflow direction slope, roughness, and possible obstructions (Barry, 2008; Prudhomme and Reed, 1998). Some pioneering studies examined the dependence of mean annual rainfall total on altitude in orographic areas and showed positive anomalies on the windward side and negative anomalies on the leeward side from the trend line (e.g., Dawdy and Langbein, 1960). Many studies appeared since that time which either broadened the current hypotheses or suggested new ideas. For instance, Stern and Blisniuk (2002) indicated that more robust results about orographic precipitation are provided while analysing the water stream isotopes and sapwood isotopes instead of elevation, distance from the coast, and air temperature. Nevertheless, in arid areas above the tree line and when aiming at daily scale of precipitation, such analyses might be difficult.

2.3.1. Orographic effect

The orographic effect on precipitation induces enhancement of precipitation and rain shadow on the windward side and leeward side, respectively (Barry, 2008; Gabl, 2014; Thillet and Schueller, 2010), even at meso-γ scales (Foresti and Pozdnoukhov, 2012). The leeward side usually experiences descending air suppressing the cloud and precipitation formation due to solar heating effects. As many authors stated, instead of generating precipitation the mountain ranges frequently lead to modification and amplification of precipitation. The modification commonly emerges from a pre-existing weather disturbance (Smith, 2006). In mid-latitudes in winter, the precipitation is mainly controlled by deep cyclones related to Rosby waves that can be strongly modified by terrain. The orographic effect is stronger in winter due to the more pronounced western circulation, lower heights, colder temperature aloft, and higher relative humidity, which significantly emphasize the differences in precipitation totals between the windward and leeward side (Johnson and Hanson, 1995). In summer, the orographic effect is reduced by different nature of precipitation (stratiform and convective), increased instability, and relative humidity (Barry, 2008; Johnson and Hanson, 1995).

The obvious orographic effect can be observed on high and large mountain ranges that are situated perpendicular to the steady prevailing airflow (e.g., the Himalayas, the Rocky Mountains, and the Scandinavian Mountains in Europe). However, a little impact on precipitation field can also be induced by only 1—5 km wide mountains. The spatial extent of mountain range influences the spatial distribution of precipitation with maximum totals shifting from the ridge towards the windward side (ranges wider than 30 km) with increasing extension of the range (Smith, 2006). Roe

et al. (2003) also stated that smaller and narrower mountain ranges tend to experience precipitation which maximizes near the divide whereas the precipitation tends to be significantly displaced from the divide in larger ranges. The width together with slope of mountain range also affects the spatial distribution of precipitation so that similarly elevated narrow and steep mountains receive lower precipitation totals than wider mountains with gentle slopes due to attenuated perturbation induced by the topographical obstacle and reduced time for the condensate to precipitate and fall out before crossing the ridge and evaporating in the lee (Kirshbaum and Smith, 2008; Krishbaum and Durran, 2004).

Over sloping terrain, the air is forced to either flow around the obstacle or to rise (Smith, 1979). The horizontal water vapour flux is one of the critical factors influencing the process since strong moist airflow associated with meteorological disturbances such as cyclones and fronts is able to rise over high terrain instead of flowing around it (Smith, 2006). The forced air uplift consists of adiabatic cooling and expansion of the air parcels (Allaby, 2007). The relative humidity eventually reaches 100 %, the water vapour condenses, the cloud droplets are created and can converse to larger hydrometeors (rain or snow particles) and fall out if the forced uplift is exceeded by gravity (Wallace and Hobbs, 2006). The moist air might rise over hills two to three times higher than the dry air might due to the latent heat changes related to the state conversion (Smith, 2006).

The air parcels that are forced to ascent over an orographic barrier try to return to their initial position which induces gravity waves behind the barrier in the main direction of airflow (Holton *et al.*, 2003) and might generate specific non-precipitating clouds such as Ac lenticularis (Hamblyn *et al.*, 2009) that indicates the reversibility of airflow dynamics to air descent and evaporation. According to Smith (2006), all the condensed water that has not precipitated before descent is subject to evaporation. Thus the condensate influenced by topography (slope) and wind speed is considered the key element in the physics of orographic precipitation, and the penetration depth as the key factor determining the fraction of water vapour flux that can be condensed. The time delay related to conversion time between water stages and fallout time of rain/snow is also a factor controlling the precipitation patterns in orographic areas. The fallout, drying ratio (relation between the evaporated and condensed components), and CAPE (Convection Available Potential Energy) influence the precipitation efficiency and depend among other factors also on surface temperature, as suggested in many studies (Colle and Zeng, 2004; Fuhrer and Schär, 2005; Garvert et al., 2007; Kirshbaum and Smith, 2008; Smith et al., 2005). Stronger compensating descent and evaporation is awaited for convective clouds than stratiform clouds since the convective clouds generate more upward motion, whereas the stratiform clouds tend to rise smoothly over the orographic barrier (Kirshbaum and Smith, 2008). Even in general, the convection becomes more probable with increasing roughness of the relief. However, according to Prudhomme and Reed (1998) and Drogue et al. (2002), the convective cells and precipitation are less dependent on the correlation between orography and topographic parameters than on the roughness. On the other hand, based on the NDVI (Normalized Difference Vegetation Index), deeper convection-related clouds were observed over mountainous regions (King *et al.*, 2004).

Several studies also dealt with the impact of orographic effect on precipitation in relation to the development of the relief and resulted in a positive feedback of precipitation to topography - higher precipitation increases the erosion and the probability of flash flood occurrence on the windward side and resulting steeper slopes are then more susceptible to erosion due to orographically related precipitation (e.g., Niedźwiedź *et al.*, 2015; Reiners *et al.*, 2003; Roe *et al.*, 2003). Besides, there was a study showing that the NAO might amplify orographic precipitation and river discharge in the UK

(Burt and Howden, 2013), and other discussing the influence of warmer surface temperature due to climate change on orographic precipitation (Siler and Roe, 2014), and on environment (Fort, 2015).

The above-described processes highlight the complexity of precipitation patterns in orographic areas, which makes the rainfall-runoff models in mountainous areas also difficult (e.g., Le Moine *et al.*, 2013). The research of precipitation in such areas is even more complicated due to the very uneven and poor distribution of rain gauges in mountains (gauges are situated mostly in valleys), errors in observations related to instrumental and location changes, changes in the observation procedures and practices, and due to frequent erroneous radar data (e.g., screening) as stated in many studies (Barstad and Smith, 2005; Germann *et al.*, 2006; Prudhomme and Reed, 1998; Šálek, 2007; Strangeways, 2007), which makes the modelling of precipitation in complex relief challenging.

2.3.2. Modelling of precipitation in orographic areas

Pioneering models of precipitation over an orographic area were based on geostatistical methods of interpolation of observed precipitation totals from gauges. IDW (Inverse Distance Weighting), Kriging, Spline Fitting or other interpolation methods were commonly used and in some cases (e.g., co-kriging, kriging with external drift) included the correlation between the precipitation total and altitude or aspect (e.g., Hutchinson, 1998). However, the models did not take into consideration any physical processes related to precipitation in complex relief. Thus the specialists started also to model the known physical processes in parallel with the interpolation models. Influenced by the computational capabilities, the first models including physics were one-dimensional, such as the air parcel model over terrain proposed by Alpert (1986) or Sinclair (1994). Later on, the quasi-analytical models included processes such as advection and forced uplift but assumed that only upslope regions influence precipitation thus neglecting the evaporation of cloud water and hydrometeors caused by descending air after the barrier and overestimating the precipitation totals (Smith, 2006). To estimate the condensation rate, Neiman *et al.* (2002) proposed an upslope model that took account of terrain slope and wind velocity but assumed that all condensed water falls immediately to the ground, thus again overestimating the precipitation totals.

In 2004, Smith and Barstad proposed a linear model of orographic precipitation, which includes time delays related to the conversion of condensed water and fallout, downslope evaporation, airflow dynamics (e.g., advection), cloud physics, and mountain width, and is applicable to an arbitrary wind direction in complex relief. It was an extension of the upslope model and the upslope-time delay model (Smith, 2003). The model assumed stable atmosphere and steady state air near the saturation level, and its sensitivity was tested in Barstad and Smith (2005). The model prioritizes linear mechanisms and the errors are related to time delay factor, rain gauge errors, and not accurately known wind direction (Barstad and Smith, 2005). Moreover, the model does not consider the nonlinearities such as moist airflow blocking (Jiang, 2003) and cloud physics bifurcation (Jiang and Smith, 2003).

For accurate modelling and prediction of local precipitation in orographic areas, either a model based on detailed environment-to-circulation approach or a fully dynamic local-scale model that considers the terrain effects is needed. Although the mesoscale numerical models are expensive and execution costly, they enable for a complex description of processes, and are nowadays commonly used (Colle and Yuter, 2007; Colle and Zeng, 2004; Gagnon *et al.*, 2013; Kirshbaum and Smith, 2008; Miglietta *et al.*, 2013b; Miglietta and Rotunno, 2012, 2014), even for the heavy precipitation events despite some difficulties (e.g., Chen *et al.*, 2013; Trapero *et al.*, 2013).

2.4. Mean and extreme precipitation in the Ore Mountains

The relationship between weather types [Grosswetterlagen] and spatial distribution of **mean precipitation** characteristics in the Ore Mountains [Erzgebirge, Krušné hory] was detailed in (DWD DDR and HMÚ ČSSR, 1975). The study also described the orographic effect on precipitation in the region; the windward (German) side and mountainous areas are much wetter on average due to the orographic intensification of precipitation as compared to the lee (Czech) side, which often experiences the rain shadow. The rain shadow was even discussed by Brádka (1963) with respect to the lesser occurrence of cyclones inducing heavy rainfall in the region as compared to other regions in Czechoslovakia. In addition, Pechala and Böhme (1975) found that the enhancement of precipitation is the highest on northern (Saxon) slopes (e.g., area of Auersberg) rather than at the highest elevated places. Although the recent studies rather dealt with trends in precipitation over the area, INTERKLIM (2014) has also described the mean precipitation characteristics over the area during 1961—2010, and project REGKLAM (Bernhofer *et al.*, 2009) over Dresden region during reference period 1961—1990 as compared to 1991—2005. Thus, there was no need to study the mean precipitation in detail again in this thesis.

Past and present variations in precipitation in the Ore Mountains were analysed separately for Saxony (Franke *et al.*, 2004; Küchler and Sommer, 2005) including Dresden region (Heidenreich and Bernhofer, 2011) and the Czech Republic (Tolasz *et al.*, 2007) except the project INTERKLIM (2014) which discussed also the projections in precipitation over the Saxon-Bohemian area until 2100. The changes in **extreme precipitation** were studied in Saxony by Hänsel et al. (2015) during 1901—2100. The trend analyses agreed on that the intensity and return period of precipitation increase, while the duration decreases, and the same pattern is expected in future. Brázdil (2002) studied the atmospheric extremes and related floods in the Czech Republic with respect to the global climate change. He found no trends in extreme precipitation (daily totals above 150 mm) from half of the 19th century to 2000 which occurred mostly due to cyclic patterns in precipitation. However, since the 1990s, the frequency of extreme precipitation has increased and August 2002 was found exceptional.

The extreme precipitation event in August 2002, its causes, the subsequent large flood over the Elbe and other river basins, and huge socioeconomic losses (e.g., 3 bil. euro in both Czech Republic and Austria, and 9.2 bil. euro in Germany) were largely discussed by many authors (Boucek, 2007; Brazdil *et al.*, 2006; Brázdil, 2002; Conradt *et al.*, 2013; Kienzler *et al.*, 2015; Rudolf and Rapp, 2002; Socher and Boehme-Korn, 2008; Ulbrich *et al.*, 2003). In fact, the event was particularly important for the Ore Mountains because the maximum daily precipitation total 312 mm was measured in the Eastern Ore Mountains at Zinnwald weather station on August 12, 2002, which according to Munzar et al. (2011) is the third highest daily total since the onset of a dense rain gauge network (late 19th century) in Central Europe except high Alpine regions. Individual 2-years and longer floods of Ohře river, which drains the lee of the Ore Mountains, and Czech part of the Elbe river draining directly small part of Eastern Ore Mountains can be found in Brázdil *et al.* (2005) and Kynčil and Lůžek (1979). It is useful for the identification of the consequences of individual heavy rainfall events, and for some severe floods a brief description of the synoptic situation is given. Kynčil (1983) analysed floods in foreland and the Ore Mountains during 1784—1981, Kakos (1977) the meteorological patterns causing floods in the Ore Mountains, and Hladný and Barbořík (1967) the short-term hydrological predictions in Ohře river basin. Some hydrometeorological studies about exceptional precipitation or flood events that affected local places in the Ore Mountains are given in (e.g., Chamas and Kakos, 1988; Kakos, 1975). Štekl et al. (2001) provided a detailed analysis of synoptic situation during

extreme precipitation (150 mm daily rainfall total threshold) for the period 1879—2000 in the Czech Republic, where several of the events that affected the Ore Mountains are discussed.

Extreme precipitation in the Ore Mountains defined using intensity threshold approach (Section 2.1.1) was studied by Pachala and Böhme (1975), who found that daily totals exceeding 50 mm occurred in 90 % of cases on northern (windward) slopes of Ore Mountains and the totals above 100 mm mainly on northern slopes. The intensity approach together with POT approach (Section 2.1.2; 99th and 95th percentile) was used for the brief analysis of changes in precipitation extremes in (INTERKLIM, 2014). However, no study provided a detailed analysis of various characteristics of extreme precipitation events in the region, which would be based on a larger dataset of events and defined the same way (as in Section 9).

2.5. Mean and extreme precipitation in the Vosges Mountains

Altitudinal differences up to 1,200 m from the highest peak to Upper Rhine Plain, almost south-north orientation of the main crest of the Vosges Mountains (in French regions Alsace, Lorraine and partly Franche-Comté), and the prevailing westerlies from the Atlantic Ocean are mostly responsible for differences in spatial distribution of **mean precipitation** between the windward (western) and leeward (eastern) side in the region (Alsatia, 1932; Ernst, 1988; Gley, 1867; Météo-France, 2008; Sell, 1998). Older literature sources described mean precipitation mostly in Alsace [not Lorraine] region or in broader areal context, i.e. northeastern France (Dion, 1972; Lafontaine, 1986; Lecolazet, 1950; Raulin, 1881; Schock, 1994). Similar to later studies (REKLIP, 1995; Sell, 1998), they suggested that the highest mean annual totals can be found in the Highest (Southern) Vosges near the Ballon d'Alsace peak, whereas the lowest in the southern Upper Rhine Plain. Lafontaine (1986) also discussed the oceanity and continentality of mean precipitation in the area of the Vosges Mountains massif based on the data from the Sewen-Lac Alfeld weather station during 1971—1980, and indicated that there might be a reversal behaviour of precipitation from oceanic patterns with precipitation maxima in winter in the West to more continental features with summer precipitation maxima in the East. Rempp (1937, p. 20) even stated that "the precipitation regime in the Upper Rhine Plain is as continental as in Czechoslovakia". However, the climate in the Czech Republic (Tolasz *et al.*, 2007) is rather considered as in transition from oceanic to continental (rather than pure continental). Moreover the spatially delimited frontier between the oceanic and continental precipitation regime remains unclear and needs quantitative approach in the Vosges Mountains massif (Lafontaine, 1986), though a dependence between precipitation regime on eastern (leeward) slopes and the distance from the crest might be more substantial than the dependence of precipitation on altitude (Rempp, 1937).

Mostly older studies also dealt with mean precipitation and climate at particular places in the area of the Vosges Mountains or Alsace, e.g. in the Fecht river basin (Paul, 1982), Bruche river basin (Hirsch, 1967), Hautes-Vosges [High Vosges] (Météo-France, 2008; Pfister, 1994), and Hohneck peak (Rothé and Herrenschneider, 1963). The study from the Fecht valley (Paul, 1982) also qualitatively discussed the precipitation continentality, however, he divided the precipitation regimes into: oceanic, transitory with oceanic/continental dominance, and continental. Pfister (1994) examined the issue of regionalization of the precipitation totals at rain gauges with the windward exposition. The trends in precipitation in the region were analysed for 1925—1964 in Lecarpentier and Shamsi (1972), locally in Colmar by Schenck (1976), and more recently by KLIWA (Söder et al., 2009), although they studied the climate changes in Southern Germany (including close Baden-Würtenberg

state). A recent description of climate which describes wetter and drier periods for the last 2000 years can be found in (Beck, 2011).

The mean precipitation in Alsace are well described by Sell (1998) and visualized in the atlas of the climate of the Upper Rhine by REKLIP (1995), though they do not consider the windward side of the Vosges Mountains situated in Lorraine region. The conclusion from the available literature was the necessity for a recent study of mean precipitation (temporal distribution) in the area of the Vosges Mountains (Section 6).

The pioneering study of Rempp (1937) also briefly discussed **extreme precipitation** events such as the event from May 1931 and July 1932, which occurred likewise due to a squall line and affected strongly the Upper Rhine Plain instead of the Vosges Mountains. It led the author to a suggestion about a relationship between the squall lines and heavy rainfall in the lee of the Vosges Mountains. The local study of the Bruche river basin (Hirsch, 1967) discussed annual and monthly precipitation maxima, thus used the BM approach (Section 2.1.1). Later on, for the same basin, he compared intensity-frequency curves with a proposed statistical method that enables a division of heavy rainfall to partial showers, although the rain intensities were assumed constant in the clusters (Hirsch, 1972). Spatial distribution of precipitation related to given synoptic situations (i.e. wind direction) were shown in the climate atlas (REKLIP, 1995). The very advanced study was performed by Maire (1979), who analysed 1—48 hourly precipitation totals using adjusted model MONTANA and Gumbel distribution to estimate 2 and 10-year totals. He found that in lowland (i.e. Upper Rhine Plain), the heavy rainfall lasts mainly less than 6 hours (1—2 hours most frequently). However, the study was limited to the summer half-year (May—October) and Ill river basin. Flooding in the Ill basin was studied by Humbert et al. (1987). Many studies dealt with flooding as a consequence of extreme precipitation, e.g. of the Rhine river or the tributary Meuse river which springs in the Vosges Mountains (e.g., Baulig, 1950; Krahe *et al.*, 2004). The January flood in 1995 of Rhine and Meuse river was discussed in detail including comments on the synoptic situation prior the flood in December, and January (Fink *et al.*, 1996; van Meijgaard and Jilderda, 1996). The large flood that occurred in April and May 1983, and heavily affected the Lorraine and Alsace regions was even discussed from the viewpoint of the genesis of extreme precipitation. The event on 5—10 April was related to a stagnation of zonal flux over the northeastern France, while the event on 22—26 May to reversal airflow from east of air masses originated from Mediterranean area [i.e. likely the Vb van Bebber's (1891) cyclone] (Paul and Roussel, 1985). In 1980, two short heavy rainfall events with short-term maxima up to 85 mm (Bayon rain gauge) were described and related to storms and cold fronts (Région Météorologique Nord-Est, 1980a, 1980b).

More recently, the expected changes in extreme precipitation and their uncertainties in the Rhine river basin (Bosshard *et al.*, 2013; Pelt *et al.*, 2014) and southern Germany (Söder *et al.*, 2009) are discussed only in these papers. To the best of our knowledge, the precipitation in the Vosges Mountains were recently considered only in the scope of the COPS (Convective and Orographically-induced Precipitation Study) campaign which studied especially the leeward convection and related precipitation patterns and orographic influence over restricted area, and showed that the convection is more frequently initiated over the leeward slopes of the Vosges Mountains instead of over the Rhine river valley (Labbouz *et al.*, 2013; Planche *et al.*, 2013). The literature review about the mean and extreme precipitation in the Vosges Mountains showed the necessity of a detailed analysis of the issue.

3. Work objectives

The main objectives of this thesis are to study the temporal, causal (synoptic) and spatial characteristics of extreme precipitation in the Ore Mountains (also named Krušné hory or Erzgebirge at the Czech-German border) and the Vosges Mountains (northeastern France), and to compare the results between the two regions. The two mountainous areas are low mountain ranges. The ranges are of similar morphology and the prevailing airflow is almost perpendicular to the main crest of the ranges, which induces the orographic effect on precipitation (Section 2.3.1). Since the Ore Mountains are situated in the middle part of the Central Europe and the Vosges Mountains at the border of Central and Western Europe (Section 4), their mean annual course of precipitation differs likely due to the degree of continentality.

The analysis of extreme precipitation was carried out using the daily rain gauge data recorded during the period 1960—2013. However, due to the missing recent climatological analysis of the temporal distribution of precipitation in the Vosges Mountains in the available literature sources, the temporal distribution of precipitation, as well as several central European continental features in the Vosges Mountains, were analysed beforehand (Section 6). A package to R statistical software RHtests_dlyPrcp proposed by ETCCDI (Wang *et al.*, 2010; Wang and Feng, 2013) was used to test the homogeneity of the time series of daily precipitation totals prior the analysis of extremes, as testing the homogeneity of daily totals is a prerequisite for further analysis of extremes. In order to study the extreme precipitation in the two study regions, a dataset of extreme precipitation totals had to be selected. Therefore, after testing the standard pointwise approaches such as POT, BM, and RP described in Section 2.1.1 and 2.1.2 on the data from the Vosges Mountains (Section 7), the spatial assessment recently developed by Müller and Kaspar's (2014) was applied in the two study regions, and the extremity of events was quantified using WEI (Section 4.3), which is easily event- comparable (Section 4.3, 8, 9). Temporal, causal, and spatial characteristics of 54 (strongest) extreme precipitation events (EPEs) selected this (same) way in the Ore and Vosges Mountains were analysed separately (Section 8 and 9, respectively). They were then compared from one study region to another by investigating the statistical dependence between the pairs of EPE characteristics (e.g., duration, affected area, extremity, synoptic variables, relief) using Cramér's V (1946) and chi-squared residuals (Greenwood and Nikulin, 1996), which enable to identify the positive/negative associations between the variables.

The work objectives of the thesis were achieved taking the following steps:

- Investigation of temporal distribution of precipitation in the Vosges Mountains
- Testing of homogeneity of the time series
- Testing of usual pointwise methods to identify the extreme precipitation totals considering data from the Vosges Mountains
- Using event-adjusted evaluation method (Müller and Kaspar, 2014) to select the extreme precipitation events (EPEs) in both the Ore and the Vosges mountains
- Examination of temporal, synoptic, and spatial characteristics of the EPEs in the two regions
- Comparison of the dependent and independent characteristics of EPEs between the two regions

4. Study area, data, and methods

4.1. Study area: The Ore Mountains and the Vosges Mountains

The Ore and Vosges mountains (Fig. 1) are low mountain ranges in Central Europe (familiar region) that were selected based on higher density of population and more concentrated industries in the surrounding areas (Podkrušnohorské pánve basins, major part of Saxony and Upper Rhine Plain) as compared to that in high mountain ranges such as the Alps. The higher concentration of stakes and societies increases the interest for the knowledge and risk management of heavy rainfall and subsequent flooding, which count among the most severe natural disasters in the two regions. Similar morphology of the Ore and Vosges mountains with gentle windward slopes and abrupt leeward slopes, and prevailing westerlies almost perpendicular to the main crests favour the orographic effect on precipitation (Section 2.3). As a result, the leeward side of both mountain ranges experiences rain shadow and is considered among the driest regions in France (Alsatia, 1932; Ernst, 1988; Sell, 1998) and the Czech Republic (Pechala and Böhme, 1975; Tolasz *et al.*, 2007). Despite the similarities between the Ore and Vosges mountains where microclimatic peculiarities and lowland in the lee can be added, their geographical position differs, i.e. the Ore Mountains are situated eastwards from the Vosges Mountains, which makes their precipitation patterns different, however still with some continental features of precipitation (Section 2.5).

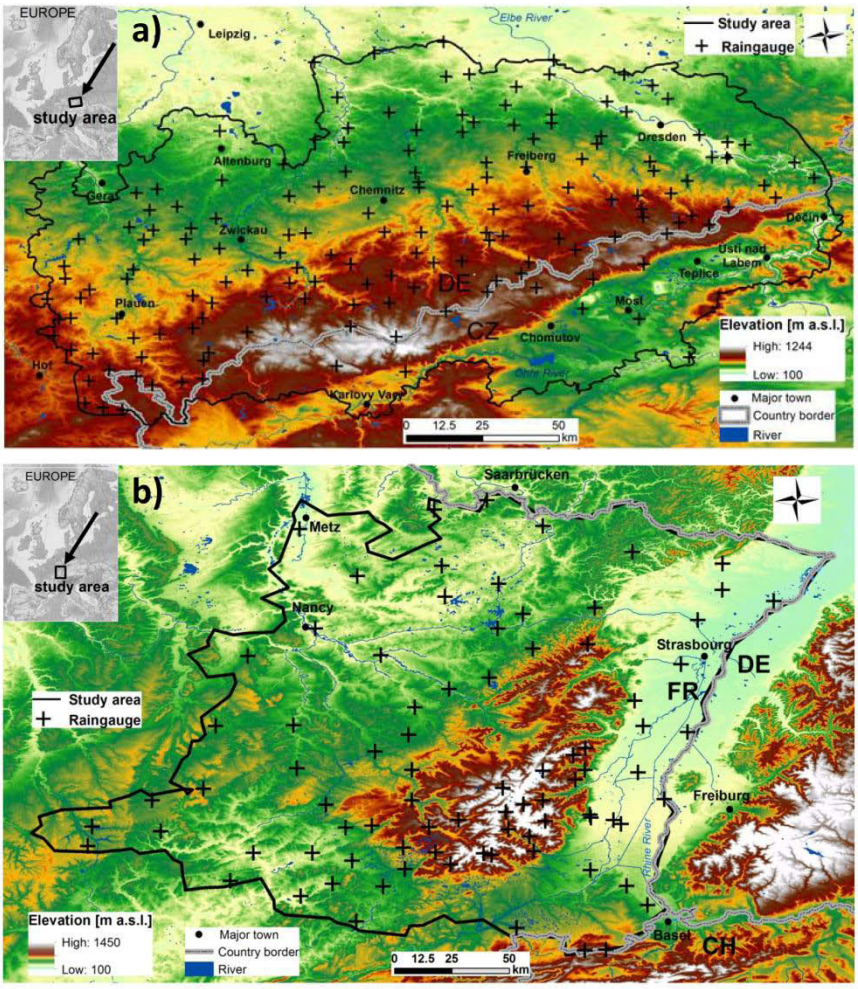

Figure 1 *Study area and the distribution of rain gauges in (a) Ore Mountains and (b) Vosges Mountains*

The study area of the Ore Mountains (OM) comprises 40,600 km^2 and covers major part of Saxony and eastern edge of Thuringia in Germany, and a major part of the Karlovarský kraj (Carlsbad) and Ústecký kraj (Ústí nad Labem) regions in the Czech Republic (Fig. 1a). OM culminates at Klínovec (Keilberg in German; 1.244 m a.s.l.) which is located in the Czech Republic, and Fichtelberg (1.215 m a.s.l.) is the second highest peak situated on the German side. The climate in OM is temperate and transitional from the oceanic in western Europe to continental in eastern Europe (DWD DDR and HMÚ ČSSR, 1975). Although the main precipitation season is summer, a secondary winter maximum can be found in the mountains. The orographic effect on precipitation is mostly responsible for the differences in mean precipitation totals between the (wetter) windward side including the mountainous areas which experience the enhancement of precipitation, and (drier) leeward side, subject to rain shadow (Pechala and Böhme, 1975).

The study area of the Vosges Mountains (VG) comprises 31,400 km^2 and is situated in Alsace, a major part of Lorraine and partly also in Franche-Comté French regions (Fig. 1b). VG culminates at Grand Ballon (1,424 m a.s.l.), and its climate is temperate. Due to the orographic effect on precipitation, the mean annual precipitation totals are the highest near the mountain crest and the lowest in the Upper Rhine Plain. The difference between the mean annual totals at wettest and driest stations can reach 1,700 mm, despite the horizontal distance of only about 40 km (Alsatia, 1932; Ernst, 1988; Sell, 1998). Further details about the temporal distribution of precipitation in VG are given in Section 6.

The boundary of the study areas mostly corresponds to that of the administrative units. However, in order to minimize the extrapolation of precipitation data, the boundaries at some places were reduced based on the spatial distribution of the rain gauges (i.e. the large border areas with no rain gauge in the administrative units were clipped from the selection).

4.2. Data: Daily rain gauge totals, synoptic data, and homogeneity

Daily precipitation rain gauge totals were used in this thesis. Initially, the data were obtained from *Météo-France* French national weather network for 14 meteorological stations situated in North-Eastern France for the period 1950—2011, and were used for the first assessment of temporal characteristics of precipitation in VG (Section 6). Then the *Météo-France* provided a wider dataset of daily precipitation totals from 168 rain gauges covering a broader area of VG. The metadata (e.g., changes in the geographical position of gauges and measuring instrument and techniques) were also acquired. The obtained wider dataset of daily totals for the period 1960—2013 was used to detail the analysis of the temporal distribution of precipitation in VG which was firstly based on the restricted dataset of 14 stations. The homogeneity of the time series was tested, and the resulting data were used to define the extreme precipitation using the pointwise methods POT, BM, and RP (Section 2.1, 7), and spatial assessment - the WEI (Section 8). The daily precipitation totals together with the metadata during 1960—2013 were also acquired from the *Deutscher Wetter Dienst* (DWD) German national weather service for 157 rain gauges, and from *Czech Hydrometeorological Institue* (CHMI) during 1960—2005 for only 10 weather stations due to high costs. The data from DWD and CHMI covered the area of OM. The data were tested for their homogeneity, and used to select the extreme precipitation events in OM using WEI for further study (Section 9). The influence of the low amount of weather stations from the Czech side and their availability until 2005 was not considered significant due to comparatively more uniform weather patterns in the lee (Czech) side than those on the windward (German) side (Barry, 2008; Whiteman, 2000). Minor inconsistencies that can appear in data among the three national weather networks were considered negligible.

Some **discontinuities** can be found in daily precipitation series in both OM and VG, which were mostly related to the installation or shutting down of rain gauges. Data from the gauges with observations not longer than half of the study period 1960—2013 (i.e. 27 years which were not bounded to any part of the period) were not considered for further analysis. In OM, no such case occurred, whereas in VG, 84 rain gauges had to be omitted following this criterion. However, the omission increased the daily totals availability from 35—62 % in the 1960s, and from 50 to almost 100 % since the 1980s, and the missed values in further analysed yearly time series in OM and VG were less than 10 %, which is sufficient for accurate assessment of duration and variability of mean and extreme precipitation (Zolina *et al.*, 2013).

The homogeneity of the time series was tested using the RHtests_dlyPrcp R-package proposed by ETCCDI (Wang *et al.*, 2010; Wang and Feng, 2013), which is designed for testing the daily precipitation series, and includes the metadata in the computation. A data measurement error of 0.2 mm was fixed in OM based on the WMO's suggestion (2008), and 0.4, 0.3 and 0.2 mm were tested in VG, which resulted in the same findings: in OM, no inhomogeneous time series were found, in VG time series from only two rain gauges (Aillevillers and Foucogney) were not homogeneous. The inhomogeneous time series were homogenized using RHtests_dlyPrcp, although the homogenization provided insignificant differences in the order of 10^{-2} mm between the raw and homogenized data. The uneven spatial distribution of rain gauges was assumed insignificant, since it is not crucial for the point data analysis (Section 6), and also does not play any important role in gridding common logarithms of return period estimates from gauges to estimate the spatial extent of extreme precipitation events using WEI (Section 4.3).

The analysis of **synoptic conditions** during extreme precipitation events was based on two weather type catalogues (Section 8 and 9); a common manual "Grosswetterlagen" Catalogue GWLc (Werner and Gerstengarbe, 2010) and an alternative automated SynopVisGWL-Catalogue SVGc (James, 2006 and pers. comm. with Paul James, 2015). For the quantitative estimation of synoptic conditions during extreme precipitation events, the NCEP/NCAR (National Centers for Environmental Prediction/ National Center for Atmospheric Research) daily data reanalysis at 2.5° gridded horizontal resolution (Kalnay *et al.*, 1996) during 1960—2010 (Uppala *et al.*, 2005) were used (Section 8 and 10). **Digital Elevation Models** (DEM) at 100 m horizontal resolution comprising OM and VG were obtained from GeoMappApp and used for the map outputs in *Esri*'s *ArcGIS 10.5*. Outputs of the synoptic analysis were visualized in *Golden* software *Surfer 10*.

4.3. Methods

The climatology (temporal distribution) of precipitation in VG was analysed based on annual and monthly totals, the variability of monthly and daily totals in VG was studied based on cumulative distribution function, and the continentality was quantified using Hrudička's index (1933) of precipitation (ombric) degree of continentality *k* as follows:

$$T_{1/2R_a} = \frac{12(w-35)}{\sqrt{R_a}}, \quad (1)$$

where *w* is the percentage of the sum of mean monthly rainfall totals in the mean annual rainfall total R_a during warmer half-year (April—September), and R_a is the sum of the mean monthly rainfall totals in the mean annual rainfall total during colder half-year (October—March). Greater the $T_{1/2R_a}$ is, greater the continentality becomes, and more uneven precipitation regime is expected.

The index of precipitation seasonality *F* (Markham, 1970) was calculated to express the seasonal concentration of mean monthly precipitation totals and uneven annual distribution of precipitation as in (Brázdil *et al.*, 2009; Tolasz *et al.*, 2007):

$$F = \frac{R}{\sum_{i=1}^{12} r_i} 100, \quad (2)$$

where *R* is the magnitude of the resultant vector (based on addition of monthly rainfall totals r_i expressed as vectors for month *i*=1, 2,..., 12) divided by the annual rainfall total $\sum_{i=1}^{12} r_i$, i.e. scalar addition of monthly rainfall totals. The seasonal concentration corresponds to the direction of the resultant vector, and greater the *F* is, more unevenly distributed are the monthly totals.

In the **analysis of precipitation extremes**, 1—10 days non-zero precipitation totals were studied, since no longer events were expected to occur in OM and VG, and the 10-day totals were found mostly contributing to floods in the Upper Rhine river basin (Pelt *et al.*, 2014). **POT, BM, and RP** (based on GEV) described in Section 2.1 were firstly station-wise used as selection criterions for the **extreme precipitation totals** (EPTs) on the data of VG. Four thresholds (95th, 97.5th, 99th, and 99.9th percentile), three time blocks (seasonal, 1- and 2-year maxima), and three return period thresholds (2-, 5- and 10-year return period estimates) were tested and the resulting datasets were examined and compared based on **seasonal** or monthly **distribution** of EPTs. Note that the seasons in the thesis corresponded to meteorological seasons with spring spanning from March 01 to May 31, and summer half-year (SHY) comprised April—September, and winter half-year (WHY) October—March. The season of EPTs was assigned based on the first calendar day of EPTs because a sensitivity analysis showed that the difference in seasonal assignment of EPTs based on other (i.e., second, third,…, tenth) calendar day of EPTs is negligible.

Based on the selection criterion-sensitive and pointwise results of POT, BM, and RP, a spatial event-adjusted method (Müller and Kaspar, 2014) for precipitation extremes was applied for the first time at regional scale to select the **extreme precipitation events (EPEs)** in OM and VG. The **Weather Extremity Index (WEI)** provides a quantitative estimation of the extremity of EPEs based on event-adjusted information about rarity, spatial extent, and duration of EPEs, which makes the comparison among EPEs and regions easy and robust. The method introduces a variable E_{ta} for any event, which affects an area *a* and lasts *t* days; its maximum value corresponds to WEI. The method starts by rarity assessment of rain gauge precipitation totals (1—10 days in the thesis) using GEV, which is suitable for precipitation extremes also in the Czech Republic (Kyselý and Picek, 2007). The maximal value of return period estimates was set to 1,000 years following the Müller and Kaspar's suggestion (2014). The return period estimates from the gauges of x-day totals are expressed as common logarithms to be less influenced by topography, and the logarithmic values are interpolated into the 2x2 km regular grid using the Ordinary Kriging. After the interpolation, the gridded logarithmic values are converted back to return period estimates and are considered in their decreasing order, i.e. irrespective of the geographical location in the study area and starting from the grid point with a highest return period estimate. The E_{ta} is calculated step-by-step as the grid points are included one by one as follows (Müller and Kaspar, 2014):

$$E_{ta}[\log(\mathrm{yr})\mathrm{km}] = R\log(G_{ta}) = \frac{\sum_{i=1}^{n} \log(\mathrm{N_{ti}})\sqrt{a}}{n\sqrt{\pi}}. \quad (3)$$

The E_{ta} is equal to the multiplication of the radius of a circle *R* [km] (considered over an area *a* [km^2] which consists of *i* number of included grid points), and the common logarithm of the spatial geometric mean G_{ta} of return period estimates N_{ti} [year] for a given duration *t* [day] at grid point *i*.

The step-by-step inclusion of grid points aims at finding a balance between the increasing area which make the E_{ta} greater mainly in the first steps of inclusion, and the decreasing return period estimates which make the E_{ta} lower mainly in further grid point inclusion. Thereby, the E_{ta} exhibits a maximum during the inclusion, which is considered as WEI and corresponds to the optimized area affected by EPEs. Since the EPEs vary in duration, the duration of an EPE has also to be optimized. The optimized duration of overlapping events (e.g., 1-day with 3-day EPE) corresponds to the highest (final) WEI calculated for 1-, 2-,..., x-day long events (up to 10 days in the thesis) for which all the daily E_{ta} are non-zero values, i.e. the daily precipitation totals during the whole event are significant. The WEI enables easy EPE to EPE comparison and can be converted to be region to region comparable as it was shown in the thesis (Section 10). For comparison among regions, the WEI values from one region remain unchanged, while the WEI values from other region(s) are converted as if the region(s) had the same area as that of the first region. The converted WEI values are equal to the multiplication of the unchanged WEI values in other region(s) by the ratio of the maximum theoretical WEI (i.e. 1000 years is the return period estimate in all grid points) value in the first region to that in other region(s).

Based on highest WEI values, **54 strongest EPEs** in OM and VG were further analysed in the thesis and described in detail in hydro-meteorological context. **Characteristics of EPEs** such as duration, affected area, extremity, seasonality, and synoptic condition were studied in individual study regions. The qualitative description of synoptic condition was based on weather types from the weather catalogues GWLc and SVGc mentioned above. If the EPE did not last one day, the weather type that occurred most often during EPE was assigned to it, and if the frequencies of weather types were similar during the EPE, the weather type was assigned based on the day of the highest 1-day E_{ta} value. Inter-annual variability of EPEs was studied based on least-squares linear regression, and the statistical significance of the monotonic trends was estimated using the non-parametric Mann-Kendall Test (Hirsch *et al.*, 1982; Hirsch and Slack, 1984; Kendall, 1975; Mann, 1945).

The **comparison** among characteristics of EPEs **in OM and VG** proceeded from the qualitative categorization of the **temporal, synoptic, and spatial characteristics of EPEs** (Section 10). The spatial characteristics of EPEs included the relationship between the area affected by EPEs and the geographical position and orography, which was based on the centre of gravity of return period estimates. The synoptic characteristics were categorized using the quantitative synoptic variables instead of qualitative weather types due to the high number of weather types occurring during the EPEs in the two study regions, which would influence and substantially lower the robustness of results. The independence of pairs of categorized characteristics of EPEs (12 altogether) was tested using the Pearson's chi-squared test of independence (Greenwood and Nikulin, 1996) at 1 % significance level. When the test resulted in rejecting the null hypothesis of independence, the chi-squared residuals were used to describe the positive/negative association between the categories of EPE characteristics and the Cramér's V (Cramér, 1946) calculated, which shows the strength of dependence. Cramér's V is the percentage of the maximum (possible) variation of the two variables, and varies from 0 to 1 with 1 meaning that the two variables are identical. The dependent characteristics of EPEs were discussed in detail and compared from one study region to another. The WEI values were for the first time compared between two regions using the above mentioned maximum theoretical WEI value. Since the characteristics of EPEs and EPEs itself were defined the same way, the comparison provided robust results identifying site-specific characteristics of EPEs and those which might be more general and valid in other low mountain ranges in Central Europe.

5. Overview of research articles used in the thesis

The thesis is based on five research articles which are focused on mean precipitation in the Vosges Mountains, extreme precipitation in the Vosges and Ore mountains, and comparison of extreme precipitation characteristics between the Ore and the Vosges mountains. The articles were mostly published or submitted to impact factor rated international journals and were all peer-reviewed. The five articles are listed below:

Minářová J. 2013. Climatology of precipitation in the Vosges mountain range area. *AUC GEOGRAPHICA* **48**(2): 51–60.

Minářová J, Müller M, Clappier A. 2017. Seasonality of mean and heavy precipitation in the area of the Vosges Mountains: dependence on the selection criterion. *International Journal of Climatology* **37**(5): 2654–2666. DOI: 10.1002/joc.4871.

Minářová J, Müller M, Clappier A, Kašpar M. 2017. Characteristics of extreme precipitation in the Vosges Mountains region (north-eastern France). *International Journal of Climatology* n/a-n/a [in press]. DOI: 10.1002/joc.5102.

Minářová J, Müller M, Clappier A, Hänsel S, Hoy A, Matschullat J, Kašpar M. 2017. Duration, rarity, affected area, and weather types associated with extreme precipitation in the Ore Mountains (Erzgebirge) region, Central Europe. *International Journal of Climatology* n/a-n/a [in press]. DOI: 10.1002/joc.5100.

Minářová J, Müller M, Clappier A, Kašpar M. [submitted TAAC-D-17-00287]. Comparison of synoptic conditions and characteristics of extreme precipitation between the Ore Mountains and the Vosges Mountains. *Theoretical and Applied Climatology*.

I am the sole author of the first paper, and the first author of the four other articles. In the second, third and fifth article, I applied and prepared all daily datasets, performed all analyses except for the estimation of GEV and WEI which were done by M. Kašpar. I was also mainly responsible for the preparation of the manuscripts. A. Clappier and M. Müller supervised my work, proposed some analytical approaches and helped with the interpretation of results. The fourth article resulted from 6-month collaboration with German colleagues at TU Freiberg in Germany: A. Hoy assisted me in the interpretation of weather types catalogues, S. Hänsel recommended me some literature sources about precipitation in OM and proposed the trend analysis and boxplot approach for visualizing the relationship of affected area, duration, and WEI of EPEs, and J. Matschullat improved the level of the manuscript language and supervised the 6-month collaboration in Germany. M. Kašpar, A. Clappier, and M. Müller helped in a similar way as mentioned above and I prepared the data, mainly performed the analyses, and have written the manuscript following the changes in the structure of the paper proposed by the German colleagues.

6. Article I: ‘Climatology of precipitation in the Vosges mountain range area’

The first article (Minářová, 2013) entitled ‘Climatology of precipitation in the Vosges mountain range area’ describes the climatology (temporal distribution) of precipitation in VG on 14 selected weather stations during the period 1950—2011 at annual, seasonal, monthly and daily resolution. Based on mean monthly totals (i.e. annual course of precipitation), three precipitation regimes are identified: (i) winter precipitation maxima characteristic for mountainous stations, (ii) two precipitation maxima (winter and summer) typical of stations on leeward (eastern) slopes, and (iii) summer precipitation maxima, feature of stations situated in the Upper Rhine Plain frequently subject to rain shadow. The paper also discusses the precipitation (i.e. ombric) continentality in the region using quantitative approaches such as Hrudička’s index (1933) for the degree of continentality and Markham’s index (1970) of precipitation seasonality (Section 4.3). The inter-annual changes are described based on cumulative distribution functions of daily totals.

CLIMATOLOGY OF PRECIPITATION IN THE VOSGES MOUNTAIN RANGE AREA

JANA MINÁŘOVÁ

Charles University in Prague, Faculty of Science, Department of Physical Geography and Geoecology

ABSTRACT

The aim of this work is to study the climatology of atmospheric precipitation in the study area situated in north-eastern France. It is shown that the Vosges mountain range, due to its position almost perpendicular to the prevailing western airflow, affects the spatial and temporal distribution (and thus the seasonality) of precipitation at a regional scale. This is carried out by computing the daily rainfall at 14 meteorological stations over the period 1950–2011. Different levels of rainfall resolution were examined – at first the annual rainfall which varies greatly between the windward side and the highest part of the Vosges mountain range and the Upper Rhine Plain (the difference is as large as 1700 mm per average year), then the monthly rainfall and distribution of precipitation within the year and finally the daily rainfall variability. Three categories of stations were determined according to their annual precipitation distribution: (i) mountain stations with a winter precipitation maximum, (ii) leeward slope stations with two precipitation maxima, i.e. in winter and summer and (iii) leeward stations located in the Upper Rhine Plain eastward of the Vosges with a summer precipitation maximum. Quantitative methods of ombric continentality demonstrate that the Vosges represent a limit between oceanic and a more continental climate. However, the empirical formulas are not satisfying and further research is required.

Keywords: climatology, precipitation variability, ombric continentality, leeward effect, the Vosges

1. Introduction

The distribution of atmospheric precipitation is not uniform in space and time (e.g., Prudhomme, Reed 1998). Taking into consideration the potential impact of precipitation on human beings (e.g., lack of precipitation causes drought, while its excess generates floods) and the incompleteness of knowledge about this domain (Šálek 2007), further research is required. Thus the aim of this study is to contribute to the research concerning atmospheric precipitation using the standard climatological methods (with annual, monthly and daily rainfall resolution) and studying the degree of ombric (rainfall) continentality, while taking into account the potential influence of orography on the precipitation distribution.

The studied area comprises the Vosges, a relatively low-elevation mountain range, situated in north-eastern Metropolitan France near the border with Germany and Switzerland, and their surroundings – the Upper Rhine Plain in particular. The reason for such a choice of area is, that the Vosges represent one of the first orographic barriers to the Westerlies from the Atlantic Ocean (air masses come mostly from West or South-West, in 40.5% of days out of the period 1985–1987, as explained e.g., in REKLIP 1995) which is due to their extension in the north-north-east and south-southwest direction. Another hypothesis is that a limit between oceanic and more continental climate (with a different distribution of precipitation within a year) occurs in this area. The last motivation is that the chosen area (Figure XVII in Colour appendix) presents a considerable altitudinal variability (up to 1300 m) – the Grand Ballon, the highest vosgian peak reaches 1424 metres above sea level (thereafter ASL), while the Upper Rhine Plain keeps a relatively constant altitude of approximately 200 meters and less (Sell et al. 1998).

Among the factors influencing climate variability (and therefore precipitation variability) in the studied area are altitude, slope exposure and geographical position (in the sense of distance and direction from the Vosges), along with specifics of the local relief (convexity vs. concavity) etc. It should be noted that vosgian slopes are typically steeper on the eastern (Alsatian) side, close to the Upper Rhine Plain, than those of the western (Lorraine) part (Troux, Quillé 1951); this influences the precipitation patterns too.

As aforementioned, the orientation of the Vosges mountain range forms a perpendicular orographic barrier to the prevailing western airflow; therefore it would be expected (Barry, Chorley 2003) that on the windward side and on the mountain ridges may occur an orographic intensification of precipitation mainly due to the reinforcement of air uplift while the phenomenon of rain shadow is characteristic for the leeward side (in our case it concerns mainly the Upper Rhine Plain). However at the local scale the description of the precipitation pattern gets more complicated, as many factors and conditions need to be accounted for.

Regarding climate continentality, we recognize two types of continentality in general – thermal and ombric (relating to temperature and precipitation respectively).

To be quoted as:
Minářová, J. (2013): Climatology of precipitation in the Vosges mountain range area
AUC Geographica, 48, No. 2, pp. 51–60

This study analyses only the second one. According to the degree of continentality, we distinguish oceanic, semi-continental and continental climates (e.g., Sobíšek et al. 1993). In European mid-latitudes the oceanic climate is typically humid, with relatively high and uniform temporal distribution of precipitation (with the exception of a small peak in winter at the west coasts). In contrast, the continental climate is generally much drier (precipitation peaks during summer) and the distribution of precipitation is uneven. The semi-continental climate has some combination of the characteristics of oceanic and continental climates (Zíková 2009).

The climate of the studied area is usually classified as temperate and semi-continental and generally under the prevailing influence of western airflow rich in water vapour (e.g., Sell et al. 1998). One of the most important climate characteristics of the region is its well-marked spatial and temporal variability (Météo-France 2008). Both are related to relief (topography), degree of continentality and the related seasonal of the precipitation.

Besides, the mean annual air temperature varies between 10 °C (plain), 7 °C (800 metres ASL) and 5 °C for 1200 m in the Vosges (Sell et al. 1998; Mühr 2007). In terms of average annual rainfall, the variability is much more pronounced. The windward side and the main mountain ridge of the Vosges is the most humid (the average annual rainfall surpassing 2000 mm) whereas less precipitation falls on the leeward side. The minimal rainfall is in the Upper Rhine Plain, typical of the rain shadow (e.g., town Colmar with less than 550 mm per year considered as one of the driest place in Metropolitan France) (Sell et al. 1998). Climate patterns are more pronounced in winter, with winter cyclones more frequent and intense in winter than in summer (Bürger 2010).

Overall, this paper emerges from the need to enhance the knowledge concerning the climatology of atmospheric precipitation in relation to orography in the Vosges area. This will be accomplished by analysing 14 meteorological stations over the studied area, there providing a potential framework for estimating atmospheric precipitation. Some of the results shown here could be specific to the study area but others could be transferable to other orographic regions.

2. Data and methods

The map output for the Vosges mountain range area was processed through the ArcGIS cartographical software (version 9.3.1) operating with geographic information systems (GIS) provided by ESRI (Environmental Systems Research Institute; available from http://www.esri.com/) – using their basemaps (e.g., towns). The topology background was adopted from the Marine Geoscience Data System (project of Columbia University in New York) using their software GeoMapApp (version 3.1.6). This application (http://www.geomapapp.org/) provides a visualisation of the Global Multi-Resolution Topography (GMRT) terrain model, with node spacing of 100-meters. For continental surfaces, NED (National Elevation Dataset) was used.

Access to the meteorological daily data was granted by the Météo-France network. The daily rainfall obtained covered the period from 1950 to 2011 (i.e. 62 years) from 14 meteorological stations (see Figure XVII

Tab. 1 Geographical position, average annual rainfall $\overline{Ra}$ and year with missing data of 14 studied meteorological stations.

Meteorological station (number | name)		Northern latitude [°]	Eastern longitude [°]	Altitude [m ASL]	Average annual rainfall $\overline{Ra}$ [mm]	Year with a missing observation
1	Sewen – Lac Alfeld	47.82	6.87	620	2,334	1952–60, 1964, 2002, 2004, 2006–08
2	Wildenstein	47.98	6.96	560	2,070	1950–56, 1957, 1958, 1960, 1961, 1992
3	Sewen – Foerstel	47.81	6.91	505	1,907	1950–58, 1968, 1974, 1975, 1977, 1978
4	Longemer	48.07	6.95	745	1,865	1961, 1962
5	Mittlach – Erbe	48.01	7.03	552	1,834	1963–72, 1974, 1975, 1976
6	Le Hohewald	48.41	7.35	785	1,226	1952, 1953, 1955, 1963, 1964, 1975, 1976, 1977, 1982, 1983, 1984
7	Aubure	48.20	7.22	796	1,084	1950–1970, 1986, 1989, 2010
8	Strasbourg	48.58	7.77	139	730	–
9	Barr	48.41	7.46	193	722	1953, 1970
10	Kayserberg	48.14	7.27	248	703	1950, 1965, 1967, 1968, 1977, 1978
11	Neuf – Brisach	48.03	7.58	195	640	2002, 2003
12	Ebersheim	48.31	7.49	164	621	–
13	Rouffach – Chs	47.95	7.29	208	612	1961, 1962, 1971, 1981, 1982, 1987, 1989, 1990, 2004
14	Oberentzen	47.94	7.38	205	606	1956, 1964

in Colour appendix). The dataset was not continuous (Table 1) – some series were interrupted within the observation period (with the exception of the stations *Ebersheim* and *Strasbourg*), mostly in winter or summer. The list of meteorological stations is presented in Table 1, which displays the geographical position of the studied stations, the average annual rainfall ($\overline{Ra}$) as well as any years with at least one day of missing observations. While some data were available during the listed years (the listed years do not mean that for all the year we have "no data", however, data from these years were omitted when calculating the average annual rainfall). The stations are listed in order of their average annual rainfall ($\overline{Ra}$) for the studied period, from greatest (*Sewen-Lac Alfeld*, no. 1) to least (*Oberentzen*, no. 14). The meteorological stations displayed in Figure XVII are divided according to their average annual rainfall in intervals of 500 mm. The first interval includes stations with annual rainfall between 500 mm and 1000 mm; no station had less than 500 mm.

Any time period containing missing values was discarded in the calculations. That is, for the daily resolution, only days with missing precipitation data were omitted, while for the monthly resolution, the whole (incomplete) months were discarded if data were missing, even on a single day. Listing all the days with missing values in Table 1 is beyond the scope of this paper.

It was chosen not to homogenise the data because inaccuracies may occur – especially in the case of outlying values (extreme precipitation), contrary to original data. Homogenization of the dataset may result in filtering out of the marginal values (Štěpánek 2007). Another reason is that future research will examine these extremes.

The standard climatological approach was used on the collected data. This consists in analysing rainfall from large to small temporal levels (e.g., years to days) and of the rainfall variability (Sobíšek et al. 1993). For some cases, 5 meteorological stations were selected as representative of a part of the studied area (their position is indicated in Figure XVII) – *Longemer* (no. 4), the sole representative of the windward side of the Vosges, *Sewen-Lac Alfeld* (no. 1) and *Wildenstein* (no. 2), both situated closest to the main mountain crest, *Aubure* (no. 7) located on the leeward side but still in the Vosges, and finally *Oberentzen* (no. 14), which represents purely a leeward lowland station (within the rain shadow area) in the Upper Rhine Plain.

2.1 Annual rainfall and distribution of precipitation within an average year

Firstly the average annual rainfall ($\overline{Ra}$) was analysed using Microsoft Excel 2010 within the period 1950–2011 for each station in order to determine the general magnitude of rainfall in the examined area. Then the average monthly rainfall ($\overline{Rm}$) was studied for each station and each month, allowing to ascertain the variability of precipitation within an average year. The calculation was based on the following equations:

$$\overline{Ra} = \frac{\sum_{i=1}^{j} Ra_i}{n}, \quad (1)$$

$$\overline{Rm}_{J-D} = \frac{\sum_{i=1}^{j} Rm_i}{n}, \quad (2)$$

where i is the i-th year; j last year with observations and n represents the total number of years with observations (*J-D* signifies months from January to December), while Ra_i (Rm_i) is the sum of the daily rainfall (Rd) within a year (month) i and the number of days within the year (month) i.

It is important to note that for the entire study the afore described procedure was followed.

Subsequently, the season (or day) of highest concentration of precipitation within the analysed period (1950–2011) was determined for the five characteristic meteorological stations. The method shows the intra-annual variability of precipitations. The yearly centre of gravity of rainfall was computed using the percentage of $\overline{Rm}$ in $\overline{Ra}$ expressed as a vector with a direction representing a month and magnitude equal to this percentage. The closer in value these percentages are for each month, the more uniformly the precipitation is distributed in an average year. The results were plotted into a polar chart (Figure XIX in Colour appendix) which was divided into 12 parts corresponding to each month in a year (30° for every month). The 12 coordinates for the 5 examined stations were found this way, aligned in the graph. The centre of gravity (resultant vector) for each station was calculated as the sum of 12 vectors representing 12 months for such stations. The date (placed on the "auxiliary" circle in Figure XIX) was matched with each centre of rainfall gravity, i.e., the resultant vector, to indicate the centre of gravity of the humid period.

Finally to make the graph more meaningful, a dashed "average" circle (with magnitude equal to the average of resulting vectors for five stations) was added into the graph. The radius of this circle Rm_{result} centred at the origin of the polar coordinate system was calculated as:

$$|Rm_{\text{J–D}}| = \sqrt{\left[\left(\frac{\sum_1^n Rx_{J-D}}{n}\right)^2 + \left(\frac{\sum_1^n Ry_{J-D}}{n}\right)^2\right]}, \quad (3)$$

$$Rm_{result} = \frac{\sum_J^D |Rm_{J-D}|}{12}, \quad (4)$$

where $|Rm_{\text{J–D}}|$ means the value (calculated as a distance of a vector using the Pythagorean theorem) of a resultant average monthly rainfall for all stations from January (J) successively up to December (D). This results in 12 values. The variable n is the number of examined stations (in our case equal to 5); Rm_{result} represents the sole resultant average monthly rainfall (for all months – from January to December).

2.2 Ombric continentality

The ombric continentality was also examined. Three empirical formulas describing the degree of ombric continentality were selected: (i) the time of the half annual rainfall, (ii) the degree of continentality by Hrudička (1933) and (iii) Markham's index of uneven distribution of precipitation (*F*).

The time of the half annual rainfall (i) represents the time in months counted from April to reach the half of the annual average rainfall ($\overline{Ra}$). The shorter the calculated time, the greater the ombric continentality (Hrudička 1933).

The degree of continentality *k* (ii) proposed by Hrudička (1933) is calculated as follows:

$$k = \frac{12(l-35)}{\sqrt{s_z}} \ [\%], \tag{5}$$

where *l* is the percentage of the sum of the average monthly rainfall from April to September in the average annual rainfall and s_z is the sum of the average monthly rainfall for the cold period (from October to March) expressed in milimeters.

When the increase of the *k* value is greater, the ombric continentality is becoming more pronounced and the distribution of precipitation in an average year less uniform.

The last approach (iii) involved the use of the precipitation seasonality index *F* (Markham 1970). This index has been applied in several studies to demonstrate the degree of annual inequality in the distribution of precipitation or the degree of ombric continentality (e.g., in the Climate Atlas of Czechia, Tolasz et al. 2007). In this paper, it was calculated for five selected meteorological stations as follows (Shver 1975):

$$F = \frac{R}{\sum_{i=1}^{12} r_i} \times 100 \ [\%], \tag{6}$$

where *F* is the percentage of the magnitude of the resultant vector *R* (calculated as the sum of vectors representing monthly rainfall r_i, where $i = 1, 2, \ldots, 12$) divided by the total annual rainfall (equal to the scalar sum of all monthly rainfall).

Notice that the monthly rainfalls were transformed into vectors (with two components) as in the previous case (the determination of a day with the highest concentration of precipitation) described above. In general, lower value of *F* means more balanced distribution of precipitation within a year and thus typically lower degree of ombric continentality (Brázdil et al. 2009).

2.3 Variability of monthly and daily rainfall

The best way to express the inter-monthly and inter-daily variability seemed to be to plot a curve resembling a cumulative distribution function. The monthly (daily) rainfall data were arranged in descending order. The largest observation was assigned the order number 1, the second largest the order number 2, and so on until all observations had an order number. A quotient of an order number and the absolute number of observations was calculated (e.g., 62 for a station measuring within the whole studied period of 62 years) – in this case identical to the largest order number. This quotient was expressed as a percentage and then subtracted from "100" (to form a complement to 100).

Using this approach, we got the values on the y-axis in Figures XXI and XXII, and the x-axis values in Figures XXIII and XXIV (Colour appendix).

In Figure XXII (in Figure XXIV), the values on the x-axis (y-axis) were equal to the monthly (daily) rainfall related to the average monthly rainfall (daily rainfall from days with observations and exceeding 0.0 mm divided by the number of days with this rainfall), expressed as a percentage. For a higher significance of results, the values on the axis expressing the monthly rainfall (*Rm*) or daily rainfall (*Rd*) were divided by the average (monthly or daily) rainfall ($\overline{Rm}$, $\overline{Rd}$). Notice that the inter-monthly variability was expressed only for five selected meteorological stations comparing the months of January and July (as is standardly used in climatological research – e.g., Votavová 2010).

3. Discussion of results

3.1 Average annual rainfall

The values of average annual rainfall ($\overline{Ra}$) calculated by (1) are recorded in the Table 1. Comparing Table 1 with Figure XVII, the mountainous stations (and mostly south-western stations) show a far greater average annual rainfall (> 1000 mm/year) than the leeward side. The average annual rainfall at *Sewen-Lac Alfeld* station (no. 1, with 2334 mm/year) is almost four times greater than at *Oberentzen* (no. 14 with 606 mm/year). This difference is significant, considering the short distance in the west-east direction (only about 70 km). The results demonstrate the important role of the Vosges mountain range as a precipitation barrier, thus leading to the phenomenon of rain shadow in the Upper Rhine Plain (making it relatively dry).

It should be noted that – despite the general trend – the stations situated easternmost in the studied area do not show low values of $\overline{Ra}$. In the case of *Strasbourg* (no. 8), this is because the Vosges are not as high in its surroundings and thus the rain shadow is less pronounced in this region (REKLIP 1995, Bürger 2010).

Neuf-Brisach (no. 11) could be perceived as a station standing at the windward side of Schwarzwald, near-by is Totenkopf (557 m ASL), part of the Tertiary volcano Kaiserstuhl (Scholz 2008).

The dependency between the altitude of a station and its $\overline{Ra}$ was not proved. One explanation is that the altitude does not represent a decisive factor influencing

the rainfall in the studied area. For example, Bankanza (2011) states that for the most humid summers in the Czech Republic (1997, 2002) the slopes and altitudes in the surrounding area were much more important than the altitude of the measuring station.

It is interesting that at *Longemer* station (no. 4), which is the westernmost station and is the only one on the windward side (Table 1, Figure XVII), the average annual rainfall is not the highest as might be expected (1865 mm contrary to, e.g., *Wildenstein* (no. 2) with 2070 mm/year). The reason could lie in the fact that the windward effect is more pronounced close to the main mountain ridge than on the windward side, because the windward western slopes are not so steep, which causes a gradual (not abrupt) air uplift. This might postpone the onset of precipitation. This relationship was described e.g., by the UTD ("upslope-time-delay") model proposed by Smith (2003). Another hypothesis is that *Longemer* station (no. 4) is not situated south-easternmost where the highest rainfall is reached because of the prevailing western and mainly south-western airflow in the studied area as mentioned above (e.g., REKLIP 1995).

3.2 Average monthly rainfall

The resulting values of the average monthly rainfall ($\overline{Rm}$) calculated using formula (2) are represented in Figure XVIII. The uneven monthly distribution of precipitation within an average year is clearly evident – the most humid month is December for the seven first meteorological stations (e.g., at *Sewen-Lac Alfeld* (no. 1) it is about 300 mm), whereas for the remaining seven stations it is the summer months (most frequently June and August, e.g., 67 mm per August at *Oberentzen* station, no. 14). This demonstrates the undeniable spatial and temporal differences in distribution of precipitation and the role of the Vosges mountain range as the most significant factor.

Three categories of stations were distinguished on the basis of the precipitation course of $\overline{Rm}$ in an average year (apparent in Figure XVIII):

(i) stations with one peak of precipitation in winter (the five first meteorological stations – e.g., *Wildenstein*, no. 2),
(ii) stations with two peaks – one main and one incidental (four stations), which could be divided into 2 groups according to the predominant maximum in winter (*Le Hohewald*, no. 6 and *Aubure*, no. 7) or in summer (*Barr*, no. 9 and *Kayserberg*, no. 10),
(iii) stations with one peak in summer (six stations – e.g., *Neuf-Brisach*, no. 11).

It is almost surprising that the annual course of precipitation changes almost gradually from the west (i) to the east (iii) of the studied area with the accompanying progressive decrease of $\overline{Ra}$ (curves between different categories do not cover almost each other – Figure XVIII). This could be generated by the increasing ombric continentality in the west-east direction manifested by the progressive weakening of winter maximum and the gradual increase of summer maximum of precipitation, with the summer maximum dominating for category (iii) stations. This can be explained by a greater participation of convective precipitation in summer for this category (e.g., Sládek 2005). In category (ii) with two maxima of precipitation, the summer convection and the winter intensification of the oceanic western circulation both create local precipitation maxima (McCabe 2001) – the convection is minority for the first group of stations, whereas it prevails in the second group of this category. The higher winter's wind velocity and winter's intensified atmospheric circulation is deciding in the case of category (i) (Heyer 1993).

The role of the Vosges in the course of precipitation could lie in an intensified transition from category (i) to (iii), thus amplifying the transition from oceanic to more continental climate.

3.3 Average day of the highest concentration of precipitation

In Figure XIX the average day with the highest concentration of precipitation within the examined period (1950–2011) is identified using formulas (3) and (4). It leads to an analogous conclusion as in the previous case – meteorological stations closer to the west, that is, category (i) stations, reach the highest concentration of precipitation in winter – in December (e.g., on the 19th of December for *Wildenstein*) whereas precipitation at *Oberentzen* station, category (iii), reaches a maximum on average in July (on the 5th of July). Thus the centre of rainfall gravity is dependent on the geographical position of the stations (Figure XVII).

From Figure XIX, the increase of ombric continentality is also evident. The vectors head towards December for category (i) but get shorter gradually with decreasing $\overline{Ra}$ (Table 1) up to the smallest magnitude of vector for category (ii) – here represented by *Aubure* station (no. 7). Then for category (iii), the vector increases in its magnitude even as $\overline{Ra}$ continually decrease, but the direction is now oriented to summer months, as seen for the *Oberentzen* station (no. 14), which has its vector pointed to July. It is interesting to notice that the influence of orography must represent a very important factor for the studied area, which is manifested by the immediate weakening of winter maximum just after reaching the main crest. Thus the role of Vosges as a generator of ombric continentality can be confirmed (Bürger 2010).

Moreover, from the graph on Figure XIX the ratio between the average rainfall circle (illustrated by a dashed line) and the asymmetrical curve of monthly rainfall dependencies for individual stations can be observed.

With decreasing asymmetricity of the annual distribution of rainfall, the annual course of precipitation is more balanced and the peak of the highest concentration of precipitation is less pronounced. In an ideal case (such as

for rainfall in equatorial areas) no peak can be recognized (Kottek et al. 2006; Trefná 1970), the form of the rainfall dependency approaches a circle and the resultant vector is zero. In our case, the shape of the dependency for the *Aubure* station (no. 7) is the most similar to an average circle. Thus the rainfall at *Aubure* station (no. 7) shows the most balanced concentration – with the winter peak (on 6th of December) just a little greater than the summer secondary peak (in May). This is manifested also by the smallest resulting vector out of the list.

However, this method is not without disadvantages: the information value of the results is limited, because when adding vectors of the same magnitude but opposite directions, their sum would be equal to zero. Hence, the vector would indicate that the highest rainfall for a station occurs in another month that is not counterbalanced. This has partially occurred in the case of *Aubure* (no. 7) where the magnitude of the resultant vector pointing to winter is reduced by the secondary summer maximum.

Nevertheless, the unquestionable advantage of this method lies in accenting the real centre of gravity of precipitation which is much more representative as a result than the bare comparison of $\overline{Rm}$.

3.4 Evolution of annual rainfall

The evolution of annual rainfall (*Ra*) in time during the period 1950–2011 was also explored (as well as for the months January and July) as you can see in Figure XX. But the results of linear trend and moving 5-year average were not statistically significant – the index of determination was on the order of single hundredths, hence the trend curves were not represented in the graph.

Points of inflexion were also studied. The humid (or dry) year is often followed by the opposite extreme (e.g., dry year 1970 followed by a wet one in 1971 or the humid 1985 was succeeded by the dry 1986).

Afterwards, the peaks were compared with literature to see whether or not they were followed by a hydrological (or another) response (e.g., minimum by a drought, maximum by a flood). In a majority of cases, the local maxima of *Ra* were also followed by floods (Schäfer et al. 2012). For example, the year 2001, which was the most humid year for the majority of examined stations (the highest annual rainfall of 3170 mm was collected at *Sewen-Lac Alfeld* station, no. 1), and was also marked by an extreme rainfall in the end of December (264 mm were measured from 28th and 29th of December at *Sewen-Lac Alfeld* meteorological station, no. 1) that was followed by an overflowing of the Moselle, Meuse, Erlenbach and Thur rivers; even a landslide happened with one fatality (IHMÉC 2008).

Minima of *Ra* were frequently followed by a hydrological and agronomical drought. In 2003 the meteorological drought which was transformed even into a socio-economical drought was recorded in almost whole of Western Europe (Söder et al. 2009). In Metropolitan France, it caused (with the heat wave) 15,000 casualties from the 4th to the 20th of August (Hémon, Jougla 2003). Concerning the earlier dry episodes, Amigues et al. (2006) demonstrated that the meteorological drought of 1976, 1991 and 1996 was followed by the pedological or hydrological one.

No available information was found about the adverse impact of the meteorological drought in 1971, even though the data in Figure XX suggest that this episode should have been quite significant. At *Sewen-Lac Alfeld* as well as at the *Strasbourg* station (no. 1 and no. 8) the annual rainfall for 1971 was only about half of the average (1200 mm contrary to $\overline{Ra}$ = 2330 mm at no. 1 and 432 mm in contrast to $\overline{Ra}$ = 730 mm on average at station no. 8). This could be related to the insufficiency of data or due to a systematic error resulting from the conversion of values of solid precipitation to values of liquid precipitation that was much more error-prone in the past (e.g., Štěpánek 2007). The winter period 1970/1971 was not only extremely cold but also rich in precipitation – e.g., from the 1st to the 10th of March in 1971, 25 cm of new snow cover was recorded in North-Western France (Fondevilla 2004). Another reason could lie in the anemo-orogaphic system after Jeník (1961) – the examined station could be at a non-favourable place to accumulate snow (snow could be taken away by wind) as observed for example at Giant Mountains (*Krkonoše* in Czech) situated in the Czech Republic.

3.5 Inter-monthly variability

The inter-monthly variability examined through cumulative distribution curves for the months of January and July is documented in Figure XXI. The variability between the determined categories is greater in winter than in the summer period – the curves are farther apart and oscillate more in winter (from 4 to 670 mm in January compared to 13–347 mm in July). This could be connected with the more frequent occurrence of extra-tropical cyclones in the winter period (Gulev et al. 2001). The cyclones are generally moving from west to east across the Vosges mountains and as a consequence the rain shadow is more present in winter (REKLIP 1995), so that the left outliers are missing in the January curves in Figure XXI. Hence the spatial variability of precipitation is significant in January. However since the January curves are more linear, the precipitation should be more evenly temporally distributed.

The absolute inter-monthly variability is the greatest for the mountainous (i) category of stations (e.g., *Wildenstein*, no. 2). It is interesting that for these stations a relatively few dry months of July are observed whereas dry January is much more frequent for lowland stations – category (iii). The determined categories above (see section 3.2) are evident in January in contrast to July where the differences are less obvious.

To improve data readability, five stations were selected as representatives to compare the inter-monthly variability of rainfall value months for January and July in Figure XXII. The July variability for the most frequent values is smaller than the variability in January. The divergence from the linearity becomes much more visible for the July curves. This could be related to the fact that in July, the precipitation is less predictable (e.g., Buizza et al. 2009), contrary to January where the precipitation is greater and more regular. The convection nuclei arise relatively chaotically and their temporal and spatial distribution is hard to predict (McGuffie, Henderson-Sellers 2005). The missing left outliers for January, and thus the less frequent occurrence of outliers compared to July is also better visible in the relative expression of values.

3.6 Ombric continentality

The ombric continentality was studied using three quantitative empirical formulas – the two latest calculated as indicated in (5) and (6). The resulting values are listed in Table 2.

The two first characteristics show the expected values. The degree of continentality increases with the decreasing $\overline{Ra}$ – this is shown by the simultaneous decrease of the time of half annual rainfall (precipitation is more concentrated in the summer months) and the increasing Hrudička's index *k*. However, contrary to what might be expected, the most continental station is not *Oberentzen* (no. 14) but *Neuf-Brisach* station (no. 11). This could be related to the fact that the highest concentration of precipitation is in the summer months but due to the effect of Schwarzwald, it is not reaching the lowest value of $\overline{Ra}$. This is in agreement with REKLIP (1995), where it is stated that the Schwarzwald precipitation maxima are in summer months and not in winter like in the Vosges.

The three distinct categories of stations can be also clearly identified from the same two characteristics – category (ii) stations have values of the time of half annual rainfall between 5.5 to 6.5 and values of *k* between 5.0 and 12.0. Note that the definition of continental climate proposed by Hrudička (1933), states that the half annual rainfall time must be less than 3 months; by this strict definition, none of these stations is continental. The stations of category (i) and the first group of category (ii) are "oceanic" and the remaining stations are "continental in transition" after the author definition.

However, by the definition of *k*, Hrudička (1933) as well as Nosek (1972) indicated that the smallest value (k = 0.8%) should have been reached at Tórnshavn, the capital city of the Faroe Islands, whereas in the studied area the meteorological station *Sewen-Foerstel* (no. 3) shows a value of 0.6%. This raises some doubts about the empirical formulas concerning the degree of ombric continentality – for example for the meteorological station Valentia in Ireland less than 35% of precipitation is attained in summer (Mühr 2011), hence the numerator in equation (5) is smaller than zero and thus the *k* value is then negative, which is not consistent with the interpretation of *k* proposed by Hrudička.

Concerning Markham's index *F*, the values were calculated for every year of the studied period for the five selected stations (in Table 2 only the average values are listed). The results do not correspond well with the explanation of this index normally found in literature (Tolasz et al. 2007; Brázdil et al. 2009) – for the most oceanic stations, category (i), a smaller value of *F* would be expected according to all the previous results, but

Tab. 2 Degree of continentality for 14 examined meteorological stations for the period 1950–2011.

Meteorological station (number | name)		Time of the half annual rainfall [month]	Degree of continentality *k* [%] by Hrudička	Markham's index *F* [%] for five selected stations
1	Sewen – Lac Alfeld	7.4	0.9	19
2	Wildenstein	7.2	1.7	15
3	Sewen – Foerstel	7.5	0.6	–
4	Longemer	6.8	3.1	10
5	Mittlach – Erbe	7.2	1.6	–
6	Le Hohewald	6.5	5.2	–
7	Aubure	6.5	5.4	5
8	Strasbourg	4.9	17.0	–
9	Barr	5.7	11.0	–
10	Kayserberg	5.6	11.7	–
11	Neuf – Brisach	4.7	21.7	–
12	Ebersheim	4.9	18.2	–
13	Rouffach – Chs	5.1	16.2	–
14	Oberentzen	5.0	18.0	14

these stations show on the contrary the greatest value in the examined area! This could be caused by the same type of error – addition of opposite vectors – as in the case of the centre of gravity of precipitation, mentioned above. But more probably this is caused by a misinterpretation of this index *F*. The index represents whether or not the precipitation is distributed evenly in a year. This means that its values have to be the smallest for the category (ii) with two maxima (neither the summer nor the winter maximum significantly surpasses the other), in Table 2 represented by the *Aubure* station (no. 7). This is obvious from the form of the near-elliptical shape of the curve and the minimal magnitude of resultant vector in Figure XIX.

Thus the index *F* should be interpreted that it could reach high values not only for continental stations but also for purely oceanic stations that are dominated by a winter maximum of precipitation. Small values of *F* are obtained, with a changing time of the maximum or two regular opposing maxima. It should be noted that no relationship between *F* and either the altitude of the station or *Ra* was recognized, and no trend was identified either.

3.7 Daily precipitation totals

The variability of the daily rainfall (*Rd*) was examined. The results of the cumulative distribution functions are presented in Figure XXIII. In term of the absolute values, it can be assumed that a higher variability occurs for category (i) stations situated in the Vosges, compared to category (iii) stations in the Upper Rhine Plain. This statement is consistent with the results of the cumulative distribution function for January and July (Figure XXI).

It is interesting that even in the daily resolution, the effect of the Vosges mountain range is clearly present – most of the precipitation falls in the area of the main crest, somewhat less at the leeward slopes and significantly less precipitation in the Upper Rhine Plain. The curves for the three categories of stations do not cross each other, with the exception of the category (ii) and the category (iii), where outliers of *Kayserberg* station (no. 10) lay in some cases below the outliers for *Strasbourg* station (no. 8).

To make the results clearer, the curves were related to the average daily rainfall ($\overline{Ra}$) only for five selected stations (Figure XXIV). The new curves of the stations situated in the Vosges mountain range differ from the curve of the *Oberentzen* station (no. 14) situated in the Upper Rhine Plain. For *Oberentzen*, the interval of values is much smaller on the x-axis and y-axis compared to the others. Thus the variability of precipitation in the area of the rain shadow is different compared to the mountainous stations – the intensified convection in summer in the lowland stations could not surpass the maxima of category (i) stations. This is supported by the fact that the difference between the average daily rainfalls is about 7 mm: 10.9 mm at *Sewen-Lac Alfeld* (no. 1) in contrast to 3.8 mm for *Oberentzen* (no. 14).

For the category (i), i.e. oceanic stations, precipitation took place on more than 50% of the days, compared to the lowland *Oberentzen* (no. 14) with at most 40% days with precipitation. This supports the statement that for the category (iii) stations the precipitation is more concentrated.

The highest daily totals are typically situated in the Vosges mountain range and the intensified convection in summer in lowland stations could not surpass this maximum.

Nevertheless, the shape of the curves could be influenced by the outliers (extreme precipitation). Thus these outliers could be interesting for future research in this field.

With regards to the absolute daily maxima, surprisingly, in a majority of cases these do not occur at the month of maximum of precipitation. For example, for *Wildenstein* (no. 2), 157 mm of rain fell on the 30th of May in 2000, rather than in December. The very same day a total daily maximum for all the 14 examined stations and the whole study period was reached at the *Mittlach-Erbe* station (no. 5) at 190.5 mm. To examine the synoptic situation is beyond the scope of this paper. However, this is quite frequent in other areas. That is, intensification of convection in one year in summer can produce relatively higher rainfall than in a standard period of maximum rainfall (Heyer 1993). But notice that for the most humid and the driest station the absolute daily maximum occurred in the month of maximum rainfall (169.1 mm for *Sewen-Lac Alfeld* on 29th of December and 68.9 mm on 15th of August for *Oberentzen*).

4. Conclusion

This paper describes a climatological research in a region influenced by orography (the Vosges mountain range and their lee) – from annual to daily rainfall resolution. Three categories of stations are identified based on the differences in the annual temporal distribution of precipitation.

For the first time in the studied area, the ombric continentality is quantitatively described. The Vosges cause a relatively fast transition into a more continental climate in their lee with a maximum of precipitation in summer (Upper Rhine Plain) and not in winter (like in the Vosges). However, some difficulties with empirical formulas are found (e.g. Hrudička's index *k*). For future research in this area it would be interesting to determine a real limit between oceanic climate and climate in transition.

The analysis using the shape of the cumulative distribution function has never been applied before for this region. Nevertheless, the influence of outliers (extreme

values) can be high. Thus it is strongly recommended for future research to examine these values.

Acknowledgements

I would like to thank Dr. Miloslav Müller for his guidance during this research, Ivo Řezáč for help with programming in MS Excel, and finally also to Dr. Martin Přeček and prof. Richard Crago for English language scientific corrections.

REFERENCES

AMIGUES, J. P., DEBAEKE, P., ITIER, B., LEMAIRE, G., SEGUIN, B., TARDIEU, F., THOMAS, A. (2006): Sécheresse et agriculture: Réduire la vulnérabilité de l'agriculture à un risque accru de manque d'eau. Collectif scientific analysis. France, INRA, 72.

BANKANZA, J. C. M. (2011): Time variation of the effect of geographical factors on spatial distribution of summer precipitation over the Czech Republic. IDŐJÁRÁS 115 (1–2), 51–70.

BARRY, R. G., CHORLEY, R. J. (2003): Atmosphere, weather and climate. New York, Routledge, 6, 421 p.

BRÁZDIL, R. et al. (2009): Climate fluctuations in the Czech Republic during the period 1961–2005. Int. J. Climatol. 29 (2), 223–242.

BUIZZA, R., HOLLINGSWORTH, A., LALAURETTE, F., GHELLI, A. (1999): Probabilistic predictions of precipitation using the ECMWF ensemble prediction system. Wea. Forecasting 14 (2), 168–189.

BÜRGER, D. (2010): Conference paper: "Influence of geo-factors (geology, climate) on the land-use patterns in the Upper-Rhine Graben". 26. 8. 2010 within the 4th Summer University about the environment sciences organized by EUCOR, Gunsbach, France.

EASTERLING, D. R. et al. (2000): Observed Variability and Trends in Extreme Climate Events : A Brief Review. Bull. Am. Meteorol. Soc. 81 (3), 417–425.

FONDEVILLA, W. (2004): Les intempéries de 1965 à 1985 [online]. Last modification 12th December 2011. [cit. 2013-04-06]. Available at: http://la.climatologie.free.fr/intemperies/tableau8.htm.

GULEV, S. K., ZOLINA, O., GRIGORIEV, S. (2001): Extratropical cyclone variability in the Northern Hemisphere winter from the NCEP/NCAR reanalysis data. Clim. Dynam. 17 (10), 795–809.

HEYER, E. (1993): Weather and Climate. Leipzig, B.G. Teubner Publisher, 9, 344 p.

HRUDIČKA, B. (1933): Contribution to the research of ombric continentality in Europe. Brno, Offprint from the writings of the Department of Czechoslovakian Geographical Society, rang C3.

HRUDIČKA, B. (1933): Time of the half precipitation and the annual repartition of periodic amplitude in Czechoslovakia. Brno, Documents published at Faculty of Natural Sciences, Masaryk University, 185.

IHMÉC. (2008): Mémoire des catastrophes [online]. France, IHMÉC. [cit. 2013-04-06]. Accessible at: http://memoiredescatastrophes.org/catastrophe/.

JENÍK, J. (1961): Alpian vefetation in Giant Mountains, Králický Sněžník Mts and High Ash Mountains: Theory of anemo-orographic systems. Prague, Czech Republic, NČSAV.

KOTTEK, M. et al. (2006): World Map of the Köppen-Geiger climate classification updated. Meteorol. Z. 15, 259–263.

MARKHAM, C. G. (1970): Seasonality of precipitation in the United States. Annals of the Association of American Geographers 60, 593–597.

McCABE, G. J., CLARK M. P., SERREZE M. C. (2001): Trends in Northern Hemisphere Surface Cyclone Frequency and Intensity. J. Climate 14 (12), 2763–2768.

McGUFFIE, K., HENDERSON-SELLERS, A. 2005. *A climate Modelling Primer*: University of Michigan, John Wiley & Sons. 3, 296 p.

Météo-France (2008): Climatology of the Vosges. Épinal, Météo-France au service des Vosges: le centre dépertemental d'Épinal (Departmental Centre of Météo-France in Épinal), 10 p.

MÜHR, B. (2007): Climate diagram [online]. Offenbach, DWD [cit. 2011-09-29]. Available at: http://www.klimadiagramme.de/Europa/strasbourg.html.

MÜHR, B. 2011. Klimadiagramme [online]. The latest modifications on 20th September 2012 [cit. 2012-09-29]. Available at: http://www.klimadiagramme.de/.

NOSEK, M. 1972. Methods in Climatology. Prague: Academia, 1, 434 p.

PFISTER, L. (1994): Rapport of several stations to spatialisation of precipitation in the High-Vosges [manuscript]. Strasbourg. Master's thesis at Faculty of Geography at University of Louis Pasteur in Strasbourg.

PRUDHOMME, C., REED, D. W. (1998): Relationship between extreme daily precipitation and topography in a mountainous region: a case of study in Scotland. Int. J. Climatol. 18 (13), 1439–1453.

REKLIP (Regio-Klima-Projekt). (1995): Klimaatlas Oberrhein Mitte-Süd = Atlas climatique du Fossé Rhénan Méridional. Offenbach, IFG, 1, 212 p. + annexes.

SCHÄFER, G., LANGE, J., WINTZ, M., SPARFEL-GARRELS, S., SPARFEL, J., MANGOLD, M., MINÁŘOVÁ, J., RABER, F., SPARFEL, Y. (2012): Actes de la 5ème Université d'Eté EUCOR, Gunsbach, France, EUCOR, 5th Summer University of Environmental Sciences EUCOR, 92 p.

SCHOLZ, M. (2008): Classification of Flood Retention Basins: The Kaiserstuhl Case Study. Environ. Eng. Geosci. 14 (2), 61–80.

SELL, Y. et al. (1998): Alsace and the Vosges: Geology, natural environments, flora and fauna. Delachaux et Niestlé, 352 p.

SHVER CA. (1975): Index of precipitation seasonality. Trudy GGO 303, 93–103.

SLÁDEK, I. (2005): Proposal for a new degree of continentality of climate. In: Physical-geographical proceedings 3, Masaryk University in Brno, 144–148.

SMITH, R. B. (2003): A linear upslope-time-delay model for orographic precipitation. J. Hydrol. 129, 2–9.

SOBÍŠEK, B. et al. (1993): Meteorological terminological & explanatory dictionary: with concept names in Slovak, English, German, French and Russian languages. Prague, Academia: Ministry of Environment of the Czech Republic, 594 p.

SÖDER, M., CONRAD, M., GÖNNER, T., KUSCH, W. (2009): Climate changes in the South Germany: Magnitude – Consequences – Strategies. Mainz, KLIWA, 20 p.

SUMMER, G., HOMAR, V., RAMIS, C. (2001): Precipitation seasonality in eastern and southern Coastal Spain. Int. J. Climatol. 21, 219–247.

ŠÁLEK, M. (2007): Orographic intensification of precipitation and its implications for quantitative precipitation estimation by meteorological radars. In: Proceedings from the 10 years of disastrous floods in Moravia in 1997. Brno, Czech Hydrometeorological Institute, p. 20.

ŠTĚPÁNEK, P. (2007): Control of the quality of data: Homogenization of time series. Brno, Czech Hydrometeorological Institute. 68 p.
TOLASZ, R. et al. (2007): Climate Atlas of Czechia. Olomouc, Czech Hydrometeorological Institute, 1, 256 p.
TREFNÁ, E. (1970): Climatography of the World. Prague, Hydrometeorological Institute, 60 p.
TROUX, A., QUILLÉ, A. (1951): The Vosges: Geography and History. Saint Dié, Weick, Hodapp et Cie, 8, 72 p.
VOTAVOVÁ, B. (2010): Analysis of the meteorological dates [manuscript]. Brno, 46 p. Bachelor's thesis at Faculty of Electrical Engineering and Communication, Department of Biomedical Engineering at Brno University of Technology. Supervisor: doc. Ing. Jiří Rozman, CSc.
ZÍKOVÁ, N. (2009): Spatial variability of precipitation annual cycles [manuscript]. Prague, 2009, 116 p. + 1 CD-ROM. Master's thesis at Faculty of Mathematics and Physics, Department of Meteorology and Environment Protection, Charles University in Prague. Supervisor: doc. RNDr. Jaroslava Kalvová, CSc.

Jana Minářová
Charles University in Prague
Faculty of Science
Department of Physical Geography and Geoecology
Albertov 6
128 43 Prague 2
E-mail: minarovj@natur.cuni.cz

RESUMÉ

Klimatologie srážek v oblasti Vogéz

Předmětem článku je klimatologie oblasti Vogéz na základě denních úhrnů atmosférických srážek 14 studovaných meteorologických stanic z oblasti pohoří a jeho závětří (Hornorýnská nížina) za období 1950–2010. Pro odlišnosti v ročním chodu srážek byly stanice rozděleny do tří kategorií: (i) horské s jedním výrazným srážkovým maximem v zimě, (ii) stanice na závětrných svazích se dvěma srážkovými maximy – letním a zimním a (iii) stanice ryze závětrné nacházející se v nížině východně od Vogéz s jedním letním srážkovým maximem. Metody kvantitativního hodnocení stupně ombrické kontinentality vedou ke zjištění, že Vogézy tvoří hranici mezi oceánickým a kontinentálním, resp. přechodným podnebím. Další výzkum zejména extrémních denních úhrnů srážek je však žádoucí.

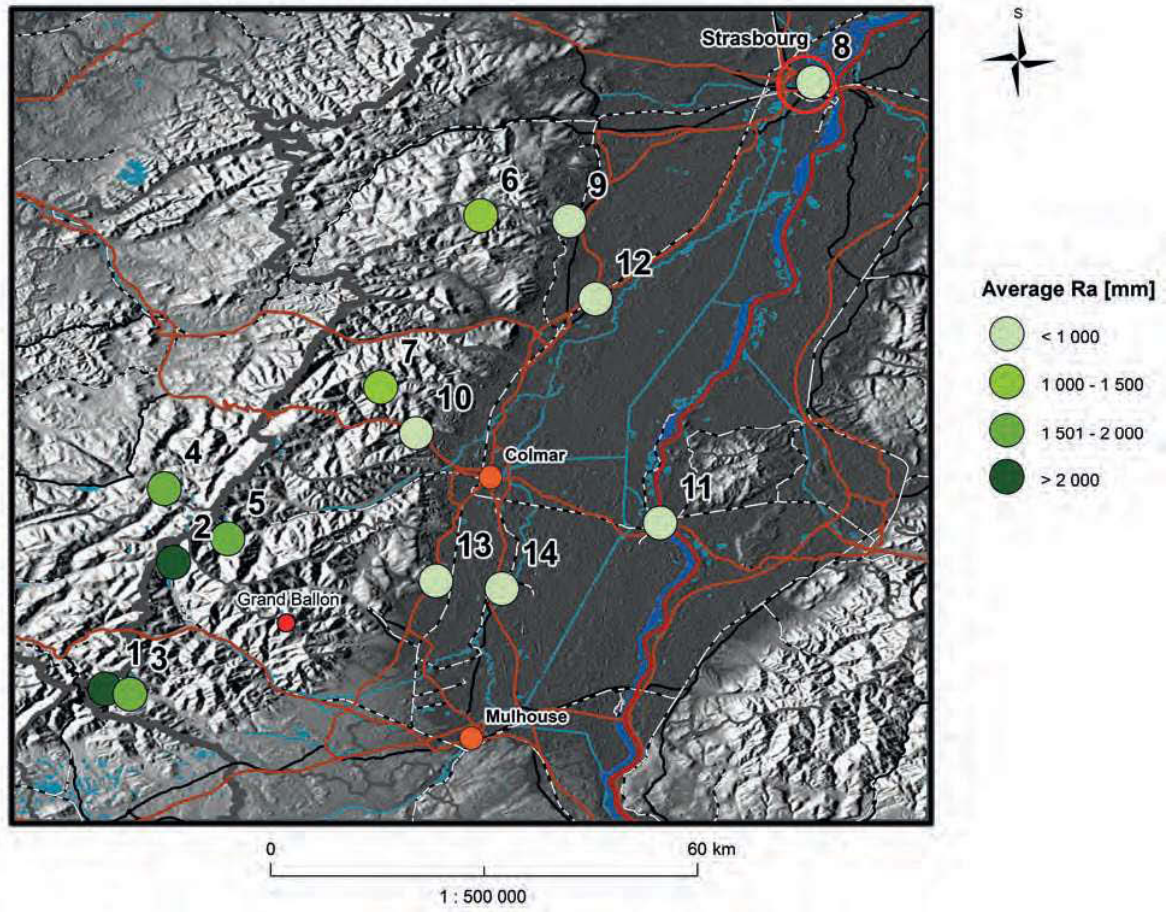

Fig. XVII Geographical position and the average annual rainfall ($\overline{Ra}$) of the 14 examined stations. Numbers represent stations listed in Table 1. The real values of $\overline{Ra}$ are recorded in this table too.

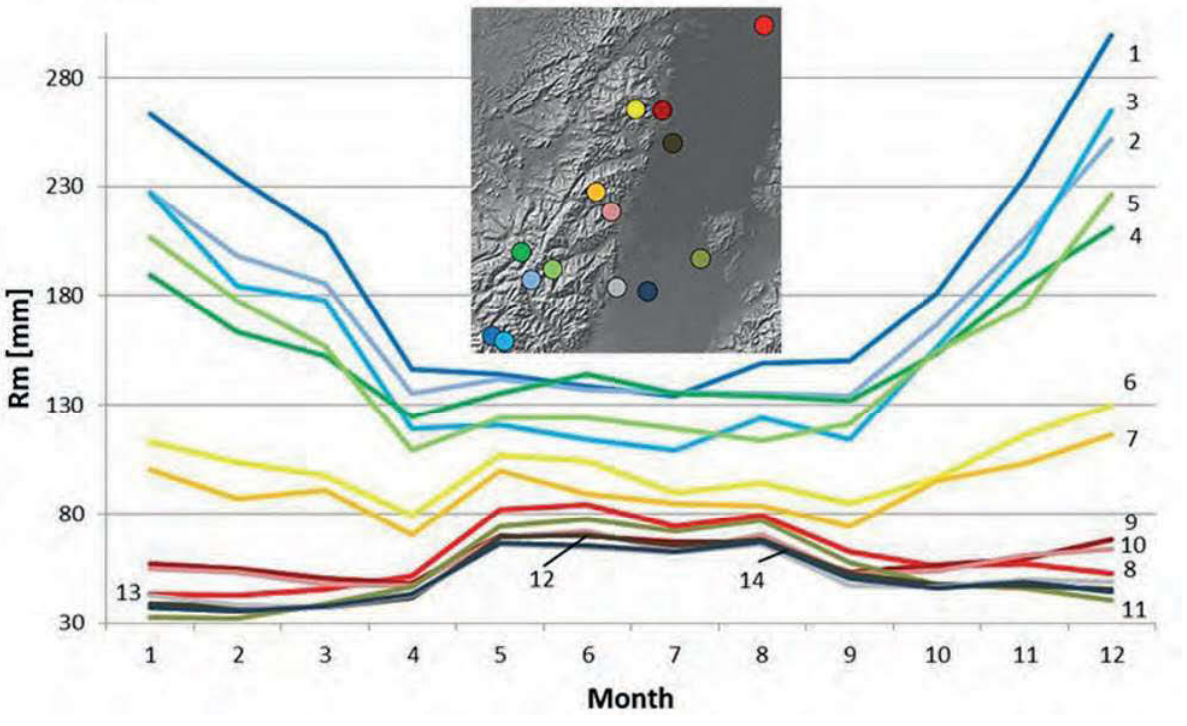

Fig. XVIII Average monthly rainfall ($\overline{Rm}$). Numbers represent stations listed in Table 1.

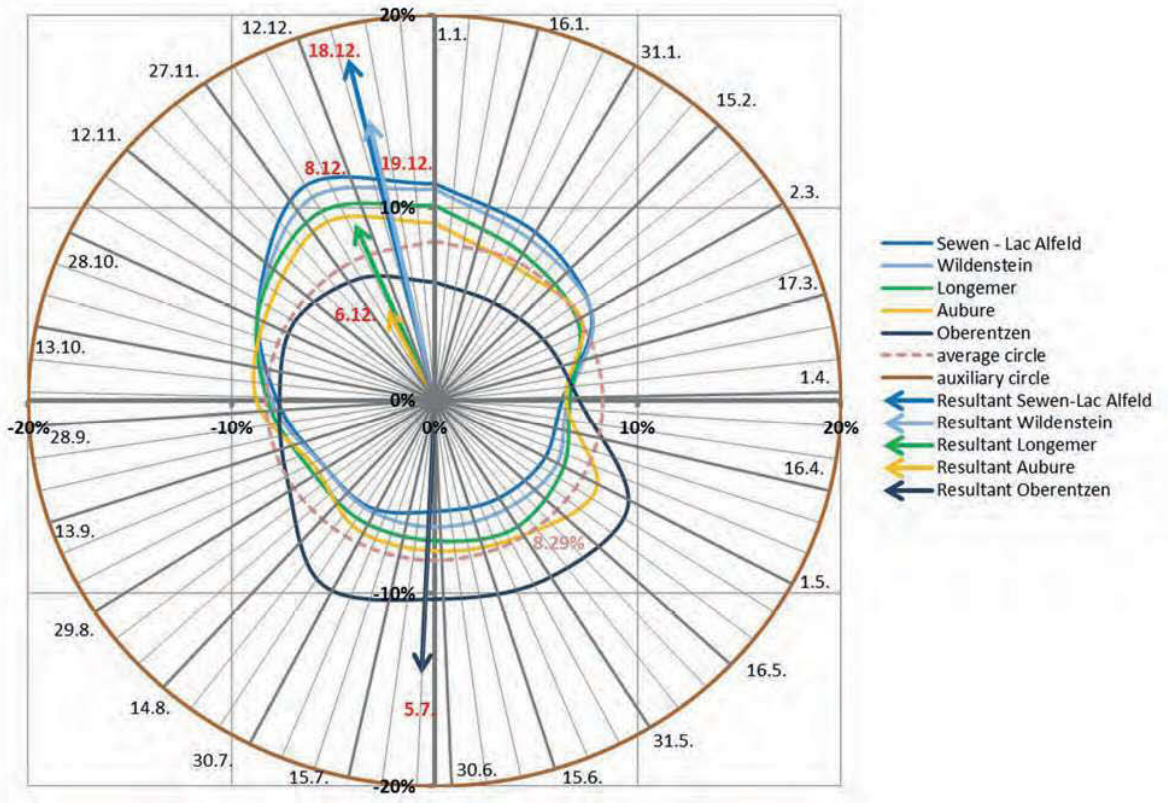

Fig. XIX Intra-annual variability of rainfall at 5 selected stations. The curve links the mean monthly rainfalls and the vector points in the direction of the date representing the centre of gravity of humid period.

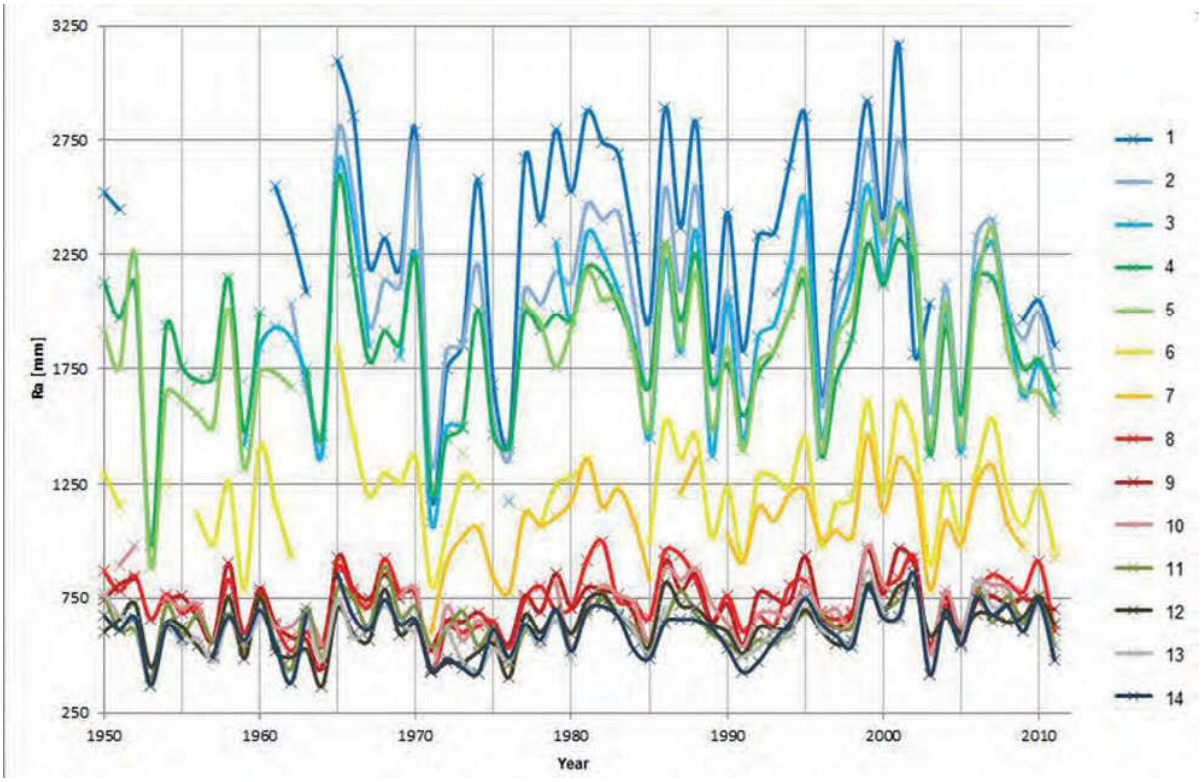

Fig. XX Inter-annual variability of annual rainfall *Ra* for the period 1950–2011. The graph shows the evolution of *Ra* in time. Gaps correspond to years with missing data (Table 1). Stations are listed in the order of descending *Ra*. Station numbers are identified in Table 1.

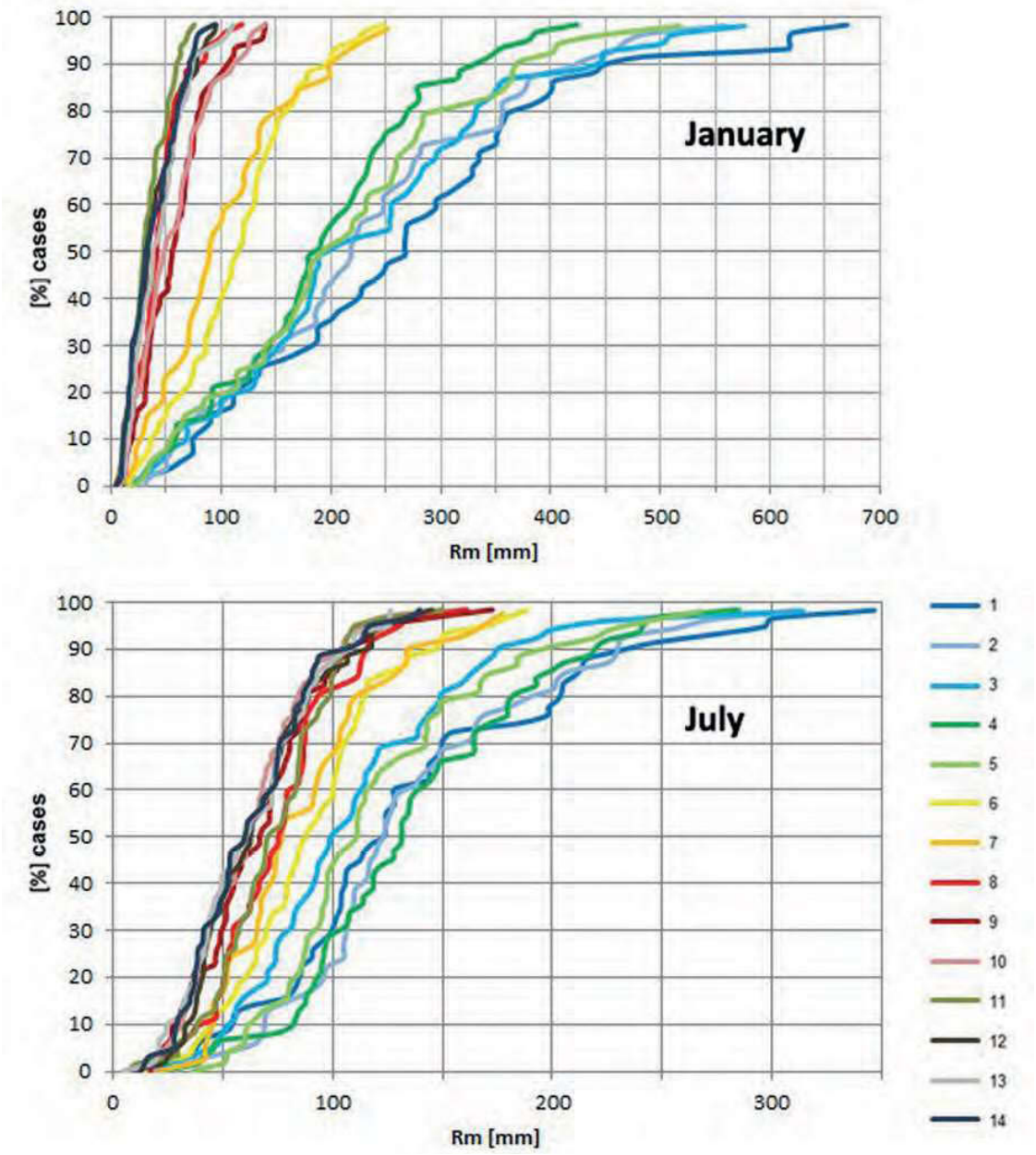

Fig. XXI Inter-monthly variability of monthly rainfall *Rm* for January and July. The cumulative distribution function for January (on the upper graph) and July (on the lower graph) for 14 meteorological stations and are presented for 1950–2011. Numbers represent stations listed in Table 1.

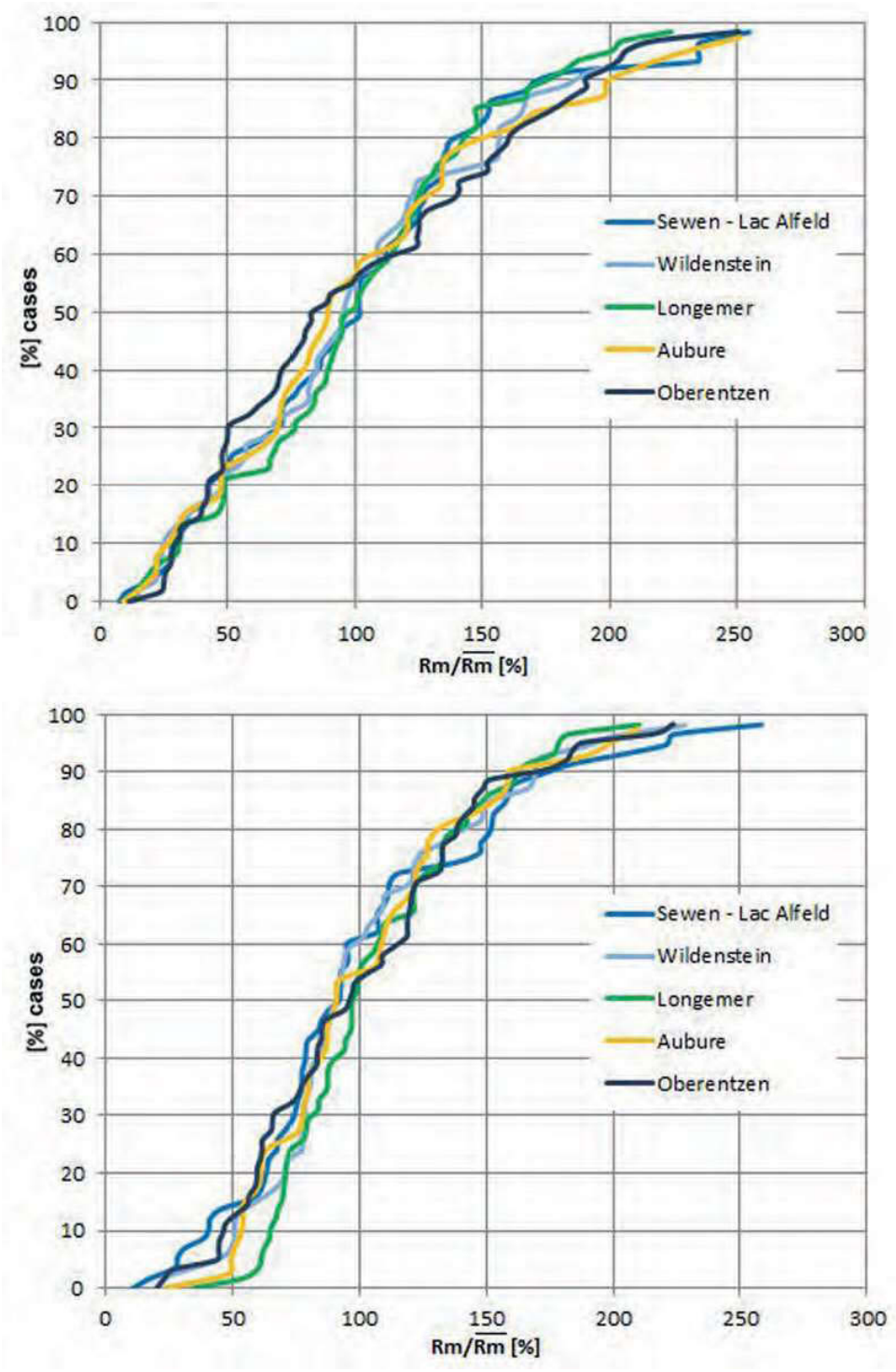

Fig. XXII As in Figure 5 but related to the average monthly rainfall for 5 selected stations.

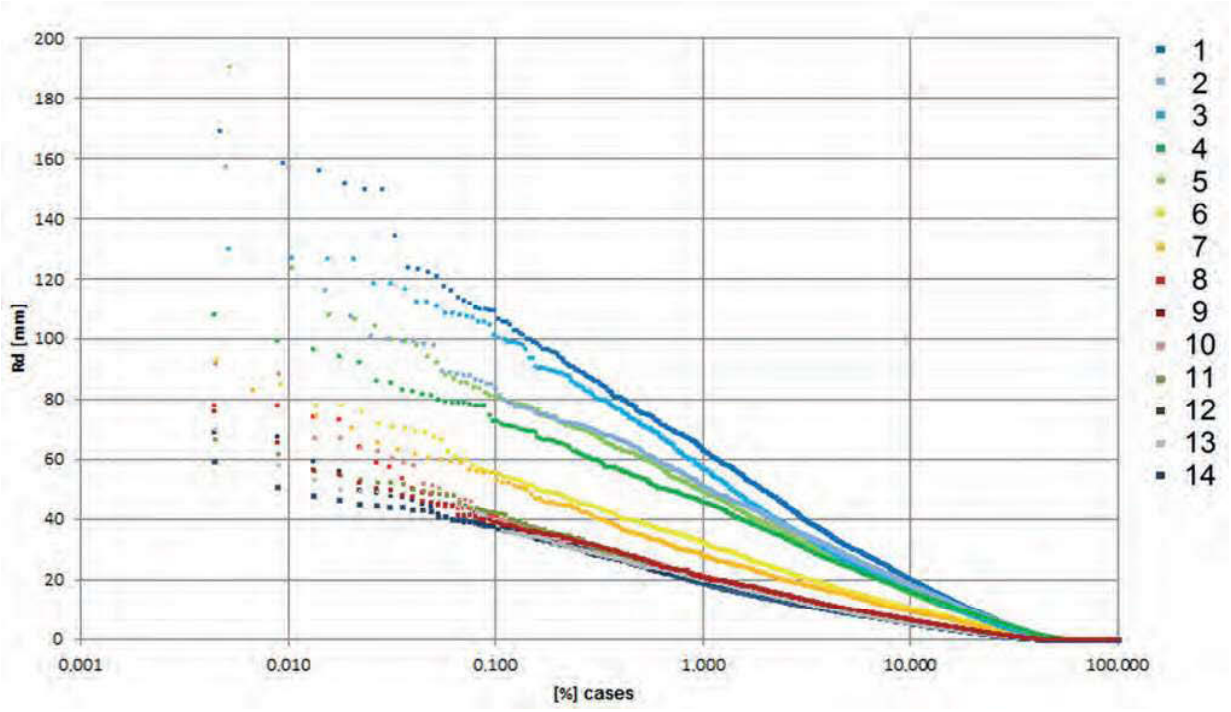

Fig. XXIII The variability of daily precipitation totals (*Rd*). Stations are listed in the order of descending annual rainfall, station numbers are identified in Table 1. The x-axis is expressed in logarithmic scale.

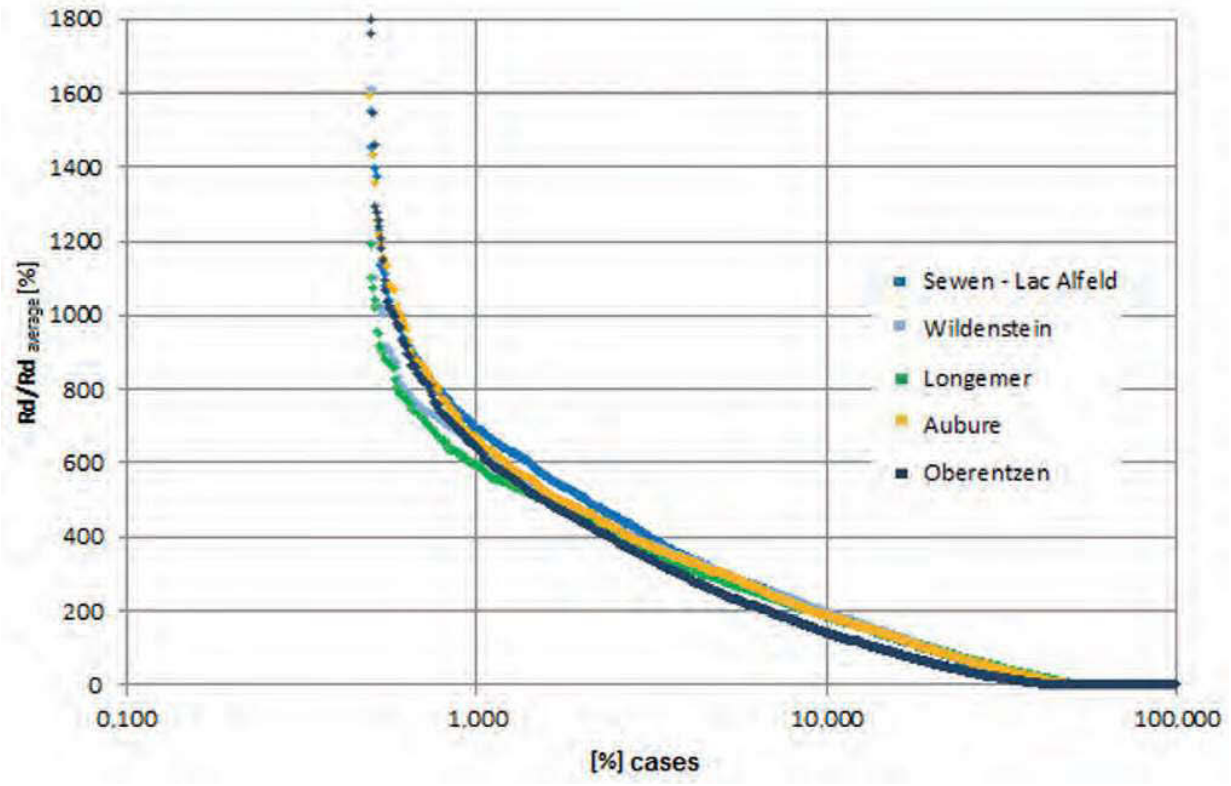

Fig. XXIV As in Figure 7 but related to the average daily rainfall for 5 selected stations. The x-axis and y-axis are expressed in logarithmic scale.

7. Article II: ‘Seasonality of mean and heavy precipitation in the area of the Vosges Mountains: dependence on the selection criterion’

The second article (Minářová *et al.*, 2017a) entitled ‘Seasonality of mean and heavy precipitation in the area of the Vosges Mountains: dependence on the selection criterion’ broadens the previous article in its first part, where it provides a detailed analysis of temporal distribution of precipitation in the Vosges Mountains based on much larger dataset of daily precipitation totals from 168 stations during 1960—2013, and thus including rain gauges on Lorraine windward side. The broader dataset enabled reclassifying the stations based on the temporal distribution of precipitation and mean annual totals into four classes: (i) mountainous gauges with winter precipitation maxima and highest mean annual totals, (ii) leeward slope gauges with two precipitation maxima (primary in winter, secondary in summer), (iii) lee gauges (in the Upper Rhine Plain) with summer precipitation maxima and lowest mean annual totals, and newly (iv) windward side (oceanic) not topographically influenced gauges with even distribution of precipitation and maxima in autumn.

The second part of the article concentrates on 1—10 days extreme precipitation totals based on POT, BM, and RP pointwise approaches with varying criteria. The influence of selection criterion on extreme precipitation characteristics is discussed on the example of the seasonal distribution of the events. The paper concludes that the tested approaches do not provide a definite answer on how to define the extreme precipitation events, and the spatial event-adjusted evaluation method (Müller and Kaspar, 2014) is suggested to be tested in future research.

INTERNATIONAL JOURNAL OF CLIMATOLOGY
Int. J. Climatol. **37**: 2654–2666 (2017)
Published online 22 August 2016 in Wiley Online Library
(wileyonlinelibrary.com) DOI: 10.1002/joc.4871

RMetS
Royal Meteorological Society

Seasonality of mean and heavy precipitation in the area of the Vosges Mountains: dependence on the selection criterion

Jana Minářová,[a,b]* Miloslav Müller[a,c] and Alain Clappier[b]

[a] *Department of Physical Geography and Geoecology, Faculty of Science, Charles University in Prague, Czech Republic*
[b] *Laboratory Image, City, Environment, National Center for Scientific Research & University of Strasbourg, France*
[c] *Institute of Atmospheric Physics, Academy of Sciences of the Czech Republic, Prague, Czech Republic*

ABSTRACT: The seasonal distribution of mean precipitation and heavy rainfalls during 1960–2013 was analysed based on daily precipitation totals from 168 rain gauging stations in the Vosges Mountains area, north-eastern France. Concerning mean precipitation, an ancient Hrudička's index designed as a half-time of precipitation during a year, surprisingly well expresses the seasonality of precipitation and its clear correlation with the mean annual totals in the studied region. The annual course of mean precipitation leads to a distinction of four groups of stations with respect to the position of stations: MT, mountainous stations with maxima of precipitation in winter and an overall highest mean annual totals; LSp, stations situated on leeward slopes of the Vosges Mountains with two maxima of precipitation (primary in winter and secondary in summer); URP, leeward stations located in the Upper Rhine River Plain with the most humid summer season, and the lowest mean annual totals; WSd, windward stations not influenced by the Vosges Mountains, with relatively evenly distributed precipitation, and slight maxima in autumn.

For the heavy precipitation, 1–10-days totals have been considered to be 'heavy' subsequent to applying the three common methods – peaks over threshold (POT), block maxima (BM), and return period estimates based on generalized extreme value distribution. Varying criteria have been employed. The BM method for annual maxima indicates that the heavy rainfall generally occurs during the most humid season although it can also occur anytime during the year. The POT and return period estimates methods reveal that the seasonality of extremes is threshold-dependent and that probably the threshold sensitivity is also related to the degree of orographic influence – higher occurrence of summer events in the lee while lesser occurrence of winter events in mountains, at higher threshold and shorter duration of event.

KEY WORDS Vosges Mountains; seasonality; annual course; extreme; heavy rainfall; precipitation; POT; GEV

Received 8 January 2016; Revised 15 July 2016; Accepted 22 July 2016

1. Introduction

The Vosges Mountains, situated in the north-eastern France, represent the first barrier to the predominant western airflow from the Atlantic Ocean. By their position, almost perpendicular to the airflow and a relatively high altitudinal differences between the mountain range and the Upper Rhine River Plain situated in the lee, differences in both spatial and temporal distributions of precipitation have been detected (e.g. Sell, 1998; Minárova, 2013). The correct understanding of these differences with an emphasis on extreme precipitation (Alexander *et al.*, 2006) is of particular interest for risk management of the natural hazards frequently occurring in this area (e.g. flooding, landslides).

The analysis of the seasonality of precipitation, i.e. the annual course of precipitation, might show the main contrast between a more oceanic character on the windward side and a more semi-continental behaviour on the leeward side (Sell, 1998). The seasonality of mean precipitation in the Vosges Mountains region has already been studied by Minárova (2013), which led to a distinction of three categories of stations based on the average monthly precipitation totals. However, the insufficiency of data on the windward side (only one representative station on this side was available in this study) could produce some inaccurate results. Thus, in this study, the mean annual course of precipitation was re-examined taking into account a much larger data set that is mostly extended in this windward western part of the region.

As for the heavy precipitation in the Vosges Mountains, Arnaud *et al.* (2007, 2008) and Cantet *et al.* (2010) dealt with the modelling and prediction of extreme rainfall within different climate regimes over France. Using the method SHYPRE (Simulated HYdrographs for flood PRobability Estimation), they coupled the stochastic generator of hourly rainfall data from 251 rain gauge stations with a rainfall–runoff model to estimate the flood risk at any point in the studied area (1×1 km spatial resolution). Besides, these studies also provide information about the spatial variation of heavy rainfall. However, these are only based on rainfall data from eight meteorological stations

* Correspondence to: J. Minářová, Department of Physical Geography and Geoecology, Faculty of Science, Charles University in Prague, Albertov 6, 128 43 Praha 2, Prague, Czech Republic. E-mail: jana.minarova@natur.cuni.cz; or jana.minarova@live-cnrs.unistra.fr

in the area of interest of this study and from two stations situated in the Vosges Mountains. This seems to be insufficient in terms of the variety of microclimates and a very complex relief of the Vosges Mountains (with, e.g. abrupt Alsatian slopes, rather gentle Lorrain slopes). Thus more regional studies are necessary. Only papers coming from the *Convective and Orographically induced Precipitation Study* campaign directly dealt with the issue of heavy rainfall in the Vosges Mountains (e.g. Labbouz *et al.*, 2013; Planche *et al.*, 2013). Nevertheless, they were either aimed at more physical micro- to meso-scale phenomena (e.g. the enhanced convection near the mouths of leeward valleys or a further intensification of one cellular convective system over the Rhine River Valley), or were based on observations at a limited area of the Vosges Mountains. Other studies that considered heavy rainfall in the Vosges Mountains were mostly of hydrological rather than climatological interest (e.g. the issue of an international Workshop in Koblenz Krahe *et al.*, 2001). On the other hand, a considerable amount of papers has focused on floods in the Rhine River and its prediction (most recently Pelt *et al.*, 2014).

Thus, the necessity to analyse heavy precipitation from a climatological point of view is evident. In addition, the interest is reinforced by the possible large socio-economic impacts related to the natural hazards in connection with heavy rainfall that is to become even more extreme and frequent in future (Beniston and Stephenson, 2004; Alexander *et al.*, 2006; Klein Tank *et al.*, 2006; Beniston *et al.*, 2007; Cutter *et al.*, 2008).

For a heavy precipitation analysis, its definition is needed even if it remains complex (Stephenson, 2008). In this analysis, we do not limit the study to one commonly used approach rather we test three most current methods dealing with weather and climate extremes – peaks over threshold (POT) (e.g. used by Gizaw and Gan, 2016; used as a basis for widely used ETCCDI/CRD Climate Change Indices (2011); or for other climate extremes indices: e.g. Sillmann *et al.*, 2013; Niedzwiedz *et al.*, 2015); block maxima (BM) (described by, e.g. Embrechts *et al.*, 2011; used by, e.g. Woeste, 2010); and return period (RP) values estimated on the basis of the generalized extreme value (GEV) distribution (used by Bertoldo *et al.*, 2015; Maugeri *et al.*, 2015; Dyrrdal *et al.*, 2016).

The article is organized as follows: after this introduction section, the description of data and of the methods used is presented in Section 2. Section 3 comprises the results of both the seasonality of mean precipitation (Section 3.1) and of heavy precipitation (Section 3.2). The latest is further divided into four sub-sections according to the three methods used; the fourth sub-section provides a comparison of the three methods and the discussion. Section 4 summarizes the findings.

2. Data and methods

2.1. Data

The study is based on daily precipitation totals during the period 1960–2013 that have been obtained from 'Météo-France' rain gauging network. The data set covers the data from 168 meteorological stations and the related metadata, i.e. the information about the changes on station (e.g. location, measuring instrument).

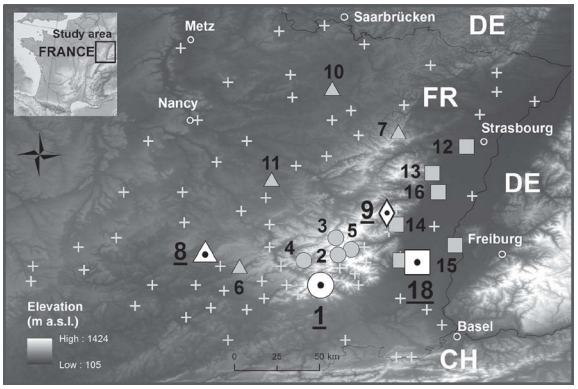

Figure 1. Study area of the Vosges Mountains and the spatial distribution of the 84 meteorological analysed stations. The 18 and 4 further selected stations are labelled by numbers, according to Table 1, in bold and underlined, respectively. The shape corresponds to the four categories of stations further displayed in Figure 2.

The digital elevation model of the broader Vosges Mountains region used as base map for the analysis comes from the 'GeoMapApp', which provides 'global multi-resolution topography' model with the horizontal resolution of about 100 m node spacing (http://www.marine-geo.org/tools/maps_grids.php). All the maps for this study have been generated using 'Esri ArcGIS 10.2' software.

2.2. Methods

Since the data set comprises some large gaps in measurement, only the stations covering more than half of the 54-year-long study period have been further analysed, i.e. 84 in our case (their locations are displayed in Figure 1). The data from the remaining stations have been used for a regular verification of results. No interpolation was conducted to fill in the gaps in data due to missing values in the new data set.

In view of the fact that the 'Météo-France' provided only raw data, it was necessary to test its homogeneity. For this purpose, the 'RHtests_dlyPrcp' R-package (Wang *et al.*, 2010; Wang and Feng, 2013) was used (http://etccdi.pacificclimate.org/software.shtml), which is designed specifically for testing the daily amounts of precipitation considering the metadata. The entering error of measurement had to be fixed. For this article, a value of 0.4 mm was determined on the basis of history of the stations, i.e. the maximum error of different used rain gauges for data acquisition. WMO is suggesting using the value of 0.2 mm or if feasible of 0.1 mm, so for the older models of rain gauges a value of 0.4 mm was selected. In addition, we tested the lower values (0.1, 0.2, and 0.3 mm) of error of measurement and the results of non-homogeneity or homogeneity of series on stations were the same. A negligible difference of the order of 10^{-3} mm between levels was observed after conducting homogenization of

the non-homogenized series. Personal communication with the main author of the R-package Pr. Wang was also of great help in choosing the value of the error of measurement. According to this test, only two meteorological stations have showed a non-homogeneity of series (i.e. 'Aillevillers' and 'Foucogney') and thus have slightly been corrected. Further details of the homogenization technique can be found in Wang *et al.* (2010) and Wang and Feng (2013). The mean of adjusted precipitation values of a station is slightly lower (in order of 10^{-2} mm) as compared to the mean of its equivalent raw data, and is thus insignificant.

A classical climatological analysis has been performed. The mean annual and monthly rainfall totals (R_a and R_m, respectively) per station have been calculated; followed by the determination of seasonal course of mean precipitation as well as the classification of stations into four major groups according to their seasonal behaviours and geographical positions (Section 3.1). The seasons correspond to climatological seasons, e.g. the spring comprising of entire months of March, April, and May.

In addition, the Hrudička's (1933a) index of the half-time of precipitation was calculated. This variable, $T_{1/2Ra}$, is generally used to express the degree of ombric continentality. It equals the length of months when one-half of the mean annual rainfall total (R_a) is accumulated, starting from 1 April. The shorter the duration, the higher the ombric continentality (Hrudička, 1933b). Mean monthly totals are used as input, which means that the mean of whole month totals is taken with the supposition of evenly distributed precipitation within the calendar month. The index is computed on one decimal place, which accounts for number of months and days of precipitation in a month and not the specific days of precipitation in any part of the month. This implies the assumption that the even distribution of precipitation has been considered. This broader assumption does not crucially influence the results because a mean climatological variable, i.e. continentality, is sought. In this article, Hrudička's index is used to show the dependence of precipitation seasonality on R_a.

Three methods have been used to define the heavy precipitation totals – (1) POT, (2) BM, and (3) RPs (Coles, 2001; Katz *et al.*, 2002; Coelho *et al.*, 2008; Katz, 2010). For the whole study period (1960–2013), we calculated 1–10 days totals (rainy days) which have not been interrupted by a day without precipitation (non-rainy day) using the standard window moving procedure. The window moving procedure was applied with time windows from 1 to maximum 10 days not interrupted by a day with zero precipitation in our case. If there was no precipitation in any day, we moved to the next day directly. If there was precipitation, it was 1-day total, but if also the next day there was precipitation, it was 2-day total, if also the second next day there was precipitation, it was 3-day total, and this until the 9th next day, which would have resulted in 10-day total if all the consecutive days were with precipitation. After interruption by a non-rainy day, we moved to the next day with precipitation and we repeated the same procedure until the last day of our study period.

The considered limit of 10 days is higher than that usually used in studies on Central Europe (e.g. 1–5 days used by Müller and Kaspar, 2014; Müller *et al.*, 2015), but it seems to fit well with the geographical position of the Vosges Mountains. As the Vosges Mountains are the first barrier in the airflow direction from the ocean, it has still the characteristics of oceanic climate, i.e. precipitation maxima generally related to longer lasting events and occurring in winter half of the year. Contrarily, the majority of other Central European mountain ranges, e.g. the very closely located Black Forest (*Klimaatlas Oberrhein Mitte-Süd/Atlas Climatique du Fossé Rhénan Méridional*, 1996), have transitional or continental climate whereby the majority of precipitation occurs in summer, and is thus more connected with convection and shorter lasting events. Moreover, according to Pelt *et al.* (2014) approximately 10-day events particularly can cause flooding in this area, e.g. flooding on the Rhine River.

Afterwards, the three previously enumerated methods were applied on the produced data set of events. For the POT, four thresholds (95th, 97.5th, 99th, and 99.9th percentile) were fixed. Although the percentiles lower than those chosen reflect other phenomena and processes mainly related to general rainfall patterns, but if one is interested in (very) heavy rainfall, lower percentiles lead to selection of such a big sample of events that the characteristics of heavy rainfall itself might hide. Thus, lower percentiles have not been considered to avoid taking a sample of numerous events while the analysis is aimed at extremes. Three time blocks, i.e. seasonal, 1- and 2-year maxima have been employed for the BM method. Here, only the results for the most commonly used 1-year precipitation maxima are presented.

At last, the RP values had been estimated from the established empirical GEV distribution. The parameters of the GEV distribution are based on the annual 1–10-day maxima, and have been calculated using the maximum likelihood in 'MatLab'. The GEV curves are used to calculate the RP values. For this study, 2-, 5- and 10-year return levels have been computed and the results of the first two have been discussed further in the following. Overall, three data sets of heavy precipitation events emerged from the three methods, which were compared with one another.

Finally, the seasonal distribution of heavy precipitation events within the three data sets was determined according to the first (starting) day of the event. The analysis of sensitivity of the starting day (i.e. date) of an event when compared to other days of that event, e.g. the middle or last day of the event, does not show any influence on the final result of the seasonal distribution analysis. For the POT method, the frequency per months is shown later.

In general, the significant results were displayed for the 18 stations, which have been selected randomly considering their position towards the Vosges Mountains as a criterion. Then this random selection has been assessed according to the metadata. The results are further displayed for 1- and 5-day lasting events and in the case of the BM for 4-, 7-, and 10-day events.

Table 1. List of 18 selected stations with their geographical position and mean annual rainfall total R_a [a].

No.	Station	Longitude (°)	Latitude (°)	Altitude (m a.s.l.)	Mean R_a (mm)
1	**Sewen-Lac Alfeld**	6.873	47.815	620	**2283**
2	Wildenstein	6.960	47.975	560	2055
3	Longemer	6.948	48.068	745	1859
4	Saulxures	6.777	47.945	465	1839
5	Mittlach-Erbe	7.028	48.005	552	1806
6	Fougerolles	6.440	47.922	473	1547
7	Dabo-Rosskopf	7.278	48.627	455	1342
8	**Bains**	6.262	48.003	319	**1282**
9	**Aubure**	7.222	48.197	796	**1092**
10	Mittersheim	6.932	48.860	234	902
11	Roville	6.607	48.382	278	902
12	Strasbourg	7.640	48.548	150	730
13	Barr	7.460	48.407	193	720
14	Kayserberg	7.267	48.138	246	707
15	Neuf-Brisach	7.575	48.025	195	642
16	Ebersheim	7.493	48.308	164	621
17	Rouffach-Chs	7.290	47.953	208	610
18	**Oberentzen**	7.378	47.943	203	**605**

The stations in bold are examined in more details further in the study. [a]Arranged in descending order by mean R_a.

In the end, a comparison of the three used methods was conducted and a correspondence analysis (CA) in *R* was performed taking into consideration the events selected by the three different methods and their (1–10 days) duration.

3. Results and discussion

3.1. Mean precipitation and its seasonality

As shown in Table 1, there is a great difference in mean annual rainfall total (R_a) of the 18 selected meteorological stations, which is around 1600 mm between the wettest (no. 1) and the driest (no. 18) station situated at a flight distance of only 40 km. With respect to the position of stations in the study area, showed on the top in Figure 1, the R_a increases from the West to the East towards the mountain range, where it reaches maximum values and then decreases rapidly to the lowland in the lee. As stated by Minárova (2013) and many others (e.g. *Klimaatlas Oberrhein Mitte-Süd/Atlas Climatique du Fossé Rhénan Méridional*, 1996; Sell, 1998), this may be due to the position of the Vosges Mountains that lie nearly perpendicular to the predominant western airflow which results in orographic intensification of precipitation on one side and the rain shadow on the other.

The mean monthly totals of the 18 selected stations for the study period 1960–2013 are depicted in Figure 2. The stations have been classified into four groups according to the annual course of precipitation: MT, stations with winter maximum of precipitation and the overall highest totals (no. 1–5; represented by dashed lines); LSp, stations (no. 9; broken line) with two maxima of precipitation (primary in winter and secondary in late spring) on the leeward slopes; URP, stations with summer maximum of precipitation situated in the lee, i.e. the Upper Rhine River Plain, with the lowest totals (no. 12–18; solid lines); and WSd, stations on windward side not influenced by the orographic barrier of the Vosges Mountains with slight autumn maxima and evenly distributed mostly precipitation (no. 6–8 and 10–11; dotted lines). Although the 'Aubure' (no. 9) station shows relatively similar behaviour as stations no. 6–8 and 10–11, it is unique and was put into separate category since it is situated already on the leeward slope behind the main ridge of the Vosges Mountains in the main airflow direction from West to East contrary to the other stations (no. 6–8, 10–11) which are situated on the windward side of the Vosges Mountains. This similar behaviour between the LSp and WSd categories will be focused in more details in future research.

It is plausible that the single representative of the LSp category may have limited the validity of the interpretation of its results and of the further analyses. However, it was the only station facing leeward slope in the area which was fulfilling our criterion of data measurement spanning over half of the 54-year-long study period or more. Therefore, the same analysis was performed also for the 'Le Hohewald' station, which is likewise situated on the leeward slopes of the Vosges Mountains (as no. 9). This station was first excluded from the study, because its measurements did not span over more than half of the 54-year-long study period, it was used only to verify the results. The results showed that according to its mean annual course, it corresponds well with the station no. 9 and thereby falls into the LSp category as well. This is in accordance with Minárova (2013). All the further analyses of the following sections were also thoroughly carried out for the 'Le Hohewald' station in order to compare its results with those of the station no. 9 and to support their validity. Thus, only those results and interpretations which arose from both the stations were presented in the article.

The contrast in the annual course of precipitation among different types of stations is in concordance with the changing amount of precipitation as in the case of R_a (Table 1). However, the greatest difference in mean

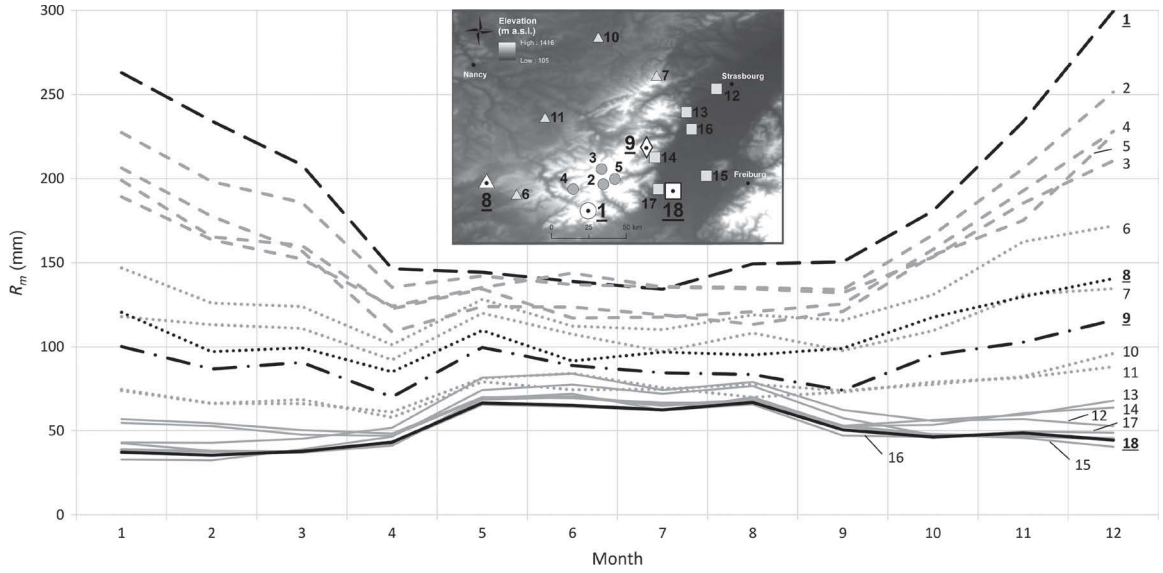

Figure 2. Mean monthly precipitation totals of 18 selected stations in the Vosges Mountains region in 1960–2013. The small map inside the diagram shows (on top) the location of the 18 stations with respect to the orography in that mountain range. Four different categories of the annual course of precipitation are depicted in the graph and in the map on right side as follows: MT, mountain stations – dashed lines, circles (no. 1–5); LPs, stations on the leeward slopes – the broken line, diamond (no. 9); URP, stations in the lee, i.e. the Upper Rhine River Plain – the solid lines, squares (no. 12–18); WSd, stations not influenced by the Vosges Mountains – the dotted lines, triangles (no. 6–8 and 10–11). Each category is symbolized by a representative depicted in bold line according to Table 1 and is highlighted in bold in the map, the shape containing also a point inside.

monthly totals is found in winter and the lowest difference in mean monthly totals is found in summer between MT and URP types. It suggests that the phenomena of orographic intensification of precipitation on one side and of rain shadow on the other are strongest in winter and weakest in summer. This may be related (Gulev *et al.*, 2001; Interklim, 2014) to the more frequent zonal circulation and related cyclonic activity in winter, and less frequent zonal circulation and related cyclonic activity in summer.

Subsequently, the finding was demonstrated by the dependence of the Hrudička's index, the half-time period $T_{1/2Ra}$, on mean annual total, R_a (Figure 3). Although this method is an archival one, it surprisingly shows the evident correlation between the seasonality and the mean annual total; the higher the half-time period, the higher the R_a. The results of the Hrudička's index also suggest that the orographic intensification of precipitation occurs primarily in the colder half of the year in the Vosges Mountains.

The previously introduced categories of stations are also noticeable in Figure 3, where they are depicted by the same shape and format as in Figure 2. The values of $T_{1/2Ra}$ as well as R_a are the lowest at stations type URP marked by squares which represents concentration of precipitation in summer, whereas the highest values of $T_{1/2Ra}$ and R_a at type MTstations marked by circles represent the concentration of precipitation in the colder half-year. The LSp and WSd types almost coincide and are somewhere between the URP and MT, since they show a quite even annual course of precipitation (Figure 2) – for the category LSp, the two maxima of precipitation (in the warmer and the colder half-year) also lead to an overall more even distribution.

The seasonality of mean precipitation for 18 selected stations is summarized in Table 2, which shows the seasonal percentage of mean monthly rainfall totals. The basic finding about the most humid season can again be observed. According to the position of stations (Figure 3), the most humid season is winter in the Vosges Mountains (no. 1), generated by the orographic intensification of precipitation; summer in the lee (no. 15) because of the rain shadow related to the mountain barrier which is especially important in winter; slightly autumn (no. 11) on the windward side.

3.2. Heavy precipitation and its seasonal occurrence

3.2.1. Peaks over threshold

Figure 4 displays the seasonal distribution of heavy precipitation events during the 54-year study period defined by the POT method exceeding the 95th, 97.5th, 99th, and 99.9th percentile. It shows the intra-monthly distribution of 1-day (left) and 5-day (right) heavy precipitation events, respectively for four stations (no. 1, 8, 9, and 18) that were randomly selected based only on their position among the 18 previously chosen stations in order to have one representative per (MT) main ridge, (LSp) leeward slope, (URP) leeward Upper Rhine River Plain, and (WSd) windward side. The overall highest number of events occurred at the 'Sewen-Lac Alfeld' station (no. 1), especially in the colder half of the year (December).

For the representation of category URP situated in the lee (no. 18; solid lines), most of the events occurred in summer and in late spring. Mainly two maxima can generally be recognized – the May maximum and the July–August maximum. The first one is relatively stronger on lower percentiles and corresponds to shorter duration of events whereas the second one is of comparable magnitude (i.e.

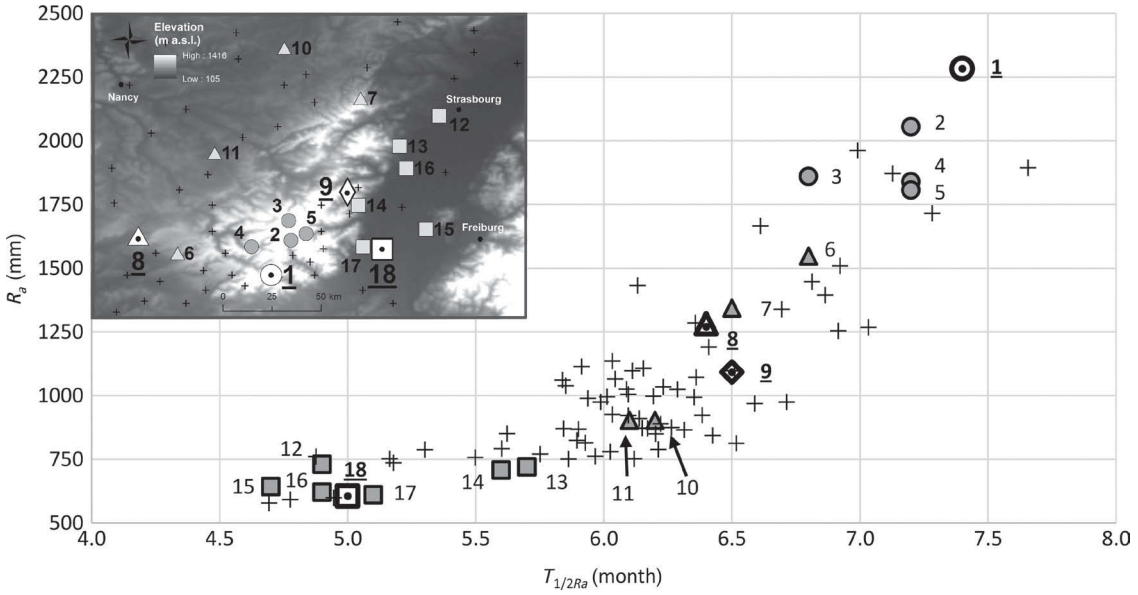

Figure 3. Dependence of half-time of precipitation $T_{1/2Ra}$ on the mean annual rainfall total R_a. Four categories of stations are represented by the diverse shapes for 18 selected stations listed in Table 1; each representative of a category is highlighted in bold and contains a point inside the shape, as in Figure 2. The plus signs represent the remaining studied stations. A small map (left upper corner) displays the topographical position of stations that are of the same shape as in the graph.

Table 2. Seasonal proportional distribution of mean monthly rainfall totals R_m of 18 selected stations on mean annual rainfall total R_a.

		Seasonal occurrence (%)			
No.	Station	Spring	Summer	Autumn	Winter
1	Sewen-Lac Alfeld	21.85	18.49	24.75	***34.91***
2	Wildenstein	22.54	19.85	24.65	*32.96*
3	Longemer	22.13	22.25	25.32	*30.30*
4	Saulxures	22.66	19.30	25.86	*32.18*
5	Mittlach-Erbe	21.57	19.70	24.95	*33.78*
6	Fougerolles	22.82	22.04	26.42	*28.72*
7	Dabo-Rosskopf	24.11	23.35	25.26	*27.29*
8	Bains	22.95	22.11	27.02	*27.91*
9	Aubure	23.85	23.52	*24.90*	*27.73*
10	Mittersheim	22.80	25.12	25.91	*26.17*
11	Roville	23.15	25.50	***25.92***	25.42
12	Strasbourg	24.48	*32.52*	24.00	19.00
13	Barr	23.43	*28.18*	23.47	24.92
14	Kayserberg	23.23	*28.91*	23.61	24.25
15	Neuf-Brisach	**24.86**	***35.18***	23.49	16.47
16	Ebersheim	23.81	*32.83*	23.75	19.61
17	Rouffach-Chs	23.81	*31.50*	23.46	21.24
18	Oberentzen	24.40	*32.15*	24.06	19.39

The maximum value for each station is depicted in italic and underlined and the overall maximum per column is represented in bold.

the number of events) at higher percentiles or even stronger than the May maximum, i.e. observed in the case of events exceeding the 99.9th percentile.

The May maximum might be connected to the global atmospheric circulation. Some stormy and rapidly changing weather occurs in late spring due to the increased atmospheric instability that is related to the differences between the still relatively colder Atlantic Ocean and the relatively warmer European continent, the differences being the highest just in May (e.g. Hupfer *et al.*, 2005, Rohli and Vega, 2011). The July–August maximum is more related to the convection caused by an overheated continent (Sell, 1998).

For the category MT stations (no. 1; dashed lines) situated in the mountains, the heaviest precipitation events occurred in colder half-year with a clear maximum reached in December or in November at the 99.9th percentile. Only at that last percentile, a very slight secondary summer (July) 1-day maximum appeared. Thus the seasonality of extremes is clearly threshold-dependent. The curves show

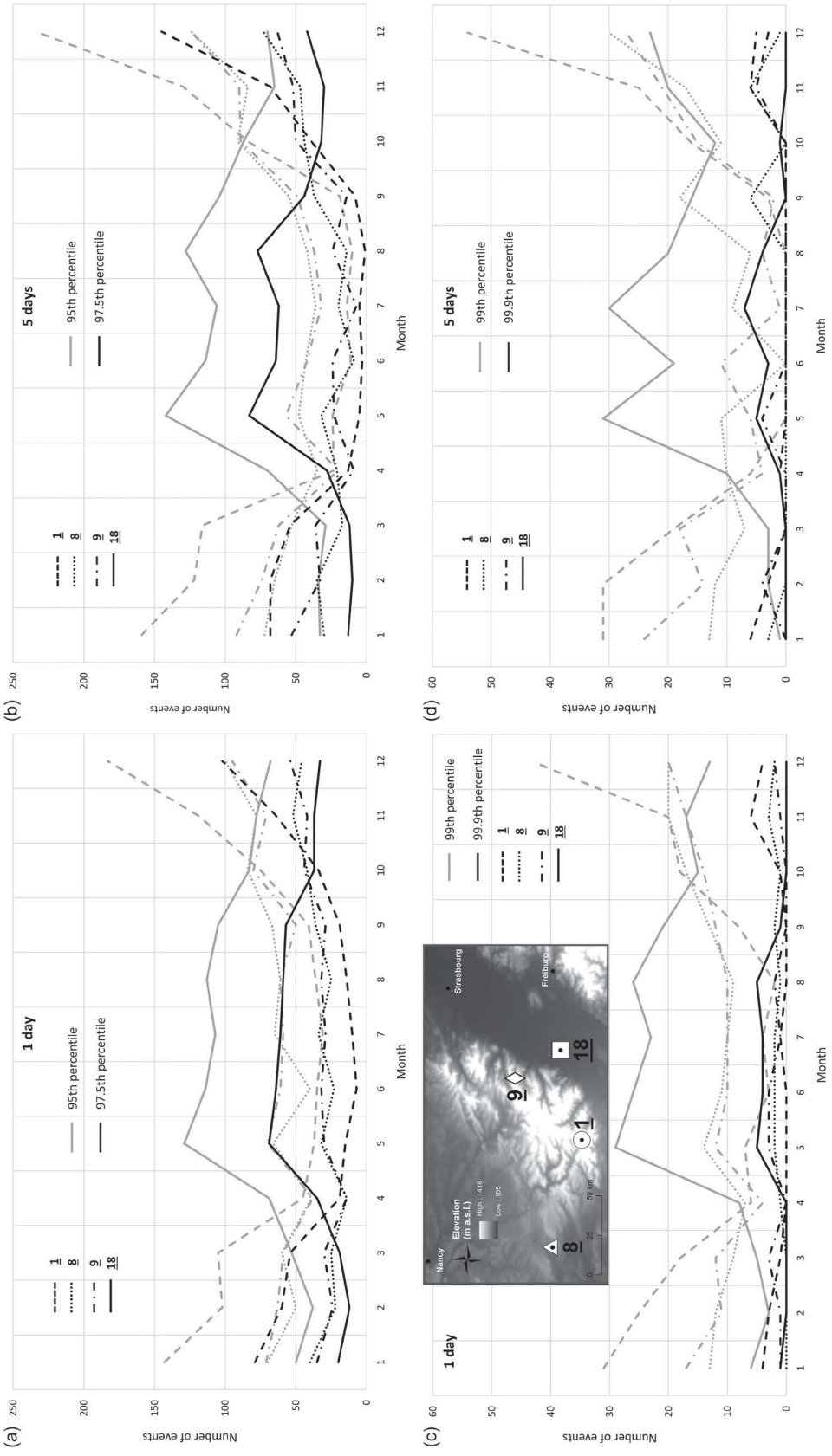

Figure 4. Monthly distribution of 1-day (a and c) and 5-day (b and d) heavy precipitation events for four stations exceeding four different thresholds – 95th, 97.5th (a and b), 99th, 99.9th (c and d) percentiles respectively. The thresholds are distinguished by a diverse grayscale. Each station is one of the representatives of the four categories of stations displayed in Figure 2 and Table 1 in bold. As in Figure 2, the categories of stations are indicated by a different type of line – MT stations by the dashed lines (no. 1); LSp stations by the broken lines (no. 9); URP stations by the solid lines (no. 18); WSd stations by the dotted lines (no. 8).

a changing course of heavy rainfall at different thresholds. It might be for the reason that the summer events are generally shorter (e.g. Ahrens, 2007; Ban *et al.*, 2015) and appear just at higher percentiles. This is also true for the LSp and WSd categories of stations.

Figure 4 indicates that the form of curves of the annual distribution of heavy precipitation occurrence is sensitive to the selected threshold. The differences between stations seem to be higher at 5-day scale rather than on 1-day scale and the curves are also smoother at that scale. This might be due to a greater number of events appearing in marginal seasons (spring and autumn) on the 5-day scale, whereas on the 1-day scale summer events related to convection prevail.

In comparison with the annual course of mean precipitation displayed in Figure 2, if taking lower percentiles as thresholds (e.g. the 95th or 97.5th), the form of the curve of distribution becomes fairly comparable with the mean one. This leads to a suggestion that percentiles lower than 99th are not sufficient to capture the extreme rainfall events although they are often used (e.g. Cioffi *et al.*, 2015; Gizaw and Gan, 2016). WMO recommends to use the 95th and 99th percentile for the analysis of weather extremes (e.g. Klein Tank *et al.*, 2009).

Therefore, the seasonal distribution of occurrence of 1-day (top) and 5-day (bottom) events for the most sensible 99th and 99.9th percentiles has been calculated. The result is displayed in Table 3 for the 18 selected stations.

For the URP stations (no. 14–18), there is a clear intensified concentration in summer at higher threshold. However, two remaining stations from the URP category, no. 12–13, show a concentration at higher percentile rather in autumn at 5-day scale. The reason may lie in the position of stations – they are situated more to the North of the Upper Rhine River Plain, where the Vosges Mountains are appreciably lower. Thus the rain shadow which is strong in winter half of the year is weaker (e.g. Minárova, 2013). For the 5-day lasting events, these stations show a similar seasonal occurrence as it is also in the case of the WSd group of stations.

Contrarily to the URP stations, there is no great increase in the prevailing winter events for the MT stations (no. 1–5) with increasing threshold. Nevertheless, there is an evident decrease in summer events even until 0% at 5-day scale.

The WSd stations situated in front of the Vosges Mountains (no. 6–8 and 10–11) do not evince any great changes, and the season most prone to heavy rainfall differs at some point from one threshold to another.

The results of this sub-section lead to a suggestion that the sensitivity to threshold becomes higher with a higher influence of orography, i.e. of the Vosges Mountains.

3.2.2. Block maxima

The seasonal distribution in relative expression of 1-, 4-, 7-, and 10-day annual maxima for the three selected stations (no. 1, 8, and 18) during 1950–2013 is displayed in Figure 5, based on their position (windward side, ridge, and leeward Upper Rhine River Plain). The position of centres of precipitation gravity (filled-in symbols) is in conformity with the results of the seasonality of mean precipitation (Section 3.1). It confirms a clear transition from a more balanced course with autumn maxima of events on the windward side of the Vosges Mountains (no. 8), i.e. category WSd, to more uneven course in mountains with winter maxima (no. 1) and with summer maxima in the lee (no. 18), i.e. category MT and URP, respectively. The latest two categories MT and URP might undergo the influence of orographic barrier – in MT the highest amounts (above 400 mm at 10-day scale) are at higher locations, which is related to the orographic intensification of precipitation, and in URP the lowest amounts (at all scales the total does not reach 200 mm, and at 1-day and 4-day scale it is sometimes even <50 mm) are in the Upper Rhine River Plain which are linked to the rain shadow, as stated before.

Besides that, the heavy rainfall occurs not only in the most humid season (season with the centre of gravity; Section 3.1) but can also occur in other seasons as well. For example, the station 'Sewen-Lac Alfeld' (no. 1) has experienced some spring (April) and autumn (October) 7- and 10-day events of the same or even higher magnitude than in winter, where the centre of gravity of heavy rainfall is found. Thereby, it is essential to analyse the whole years to capture all the most extreme events and not restrict to only a season or half-year when the long-term means reach their maximum, as it is sometimes found in literature (e.g. Kašpar and Müller, 2014). This is especially true in such an orographically influenced areas in Central Europe that lie between the oceanic and continental climate, as the Vosges Mountains, where the great spatial and temporal differences arise in seasonal distribution of both mean and heavy precipitation.

Notwithstanding that higher duration of event naturally increases its overall totals, Figure 5 also includes some shorter events, which surpass in magnitude the longer lasting events. For example, at the 'Sewen-Lac Alfeld' station (no. 1) the star-crosses indicating the 4-day lasting events are also present in the circle of rainfall totals between 300 and 400 mm. Thus Figure 5 also might serve to compare the extremity of events as well.

From another point of view, the BM method also evinces a limitation because it selects only the one most extreme event per year and thus does not take into consideration the intra-annual climate variability. It leads to a selection of one event even if the year was relatively dry or to leaving out some more extreme events that may occur in the same year. This limitation may be removed using the POT method when on average one event per year is selected, i.e. 54 events within the study period. However, such approach would again lead to the use of the POT method instead of the BM method.

3.2.3. Return periods

The last method of defining the heavy precipitation events is based on the RP estimates that have been calculated from the GEV distribution. Table 4 denotes the results of

Table 3. Seasonal percentage distribution of heavy precipitation 1-day (top) and 5-day (bottom) events at 18 selected stations, listed in Table 1, defined by the POT exceeding 99th and 99.9th percentiles.

Seasonal occurrence (%)											
Method		POT (99th percentile)				POT (99.9th percentile)				POT 99	POT 99.9
No.	Station	Spring	Summer	Autumn	Winter	Spring	Summer	Autumn	Winter	Nb. events	Nb. events
Duration		*1 day*									
1	Sewen-Lac Alfeld	16.23	**5.24**	24.61	*53.93*	5.00	**5.00**	35.00	*55.00*	191	20
2	Wildenstein	18.18	**8.59**	26.26	*46.97*	25.00	**0.00**	25.00	*50.00*	198	20
3	Longemer	15.15	**15.66**	30.81	*38.38*	9.52	**14.29**	33.33	*42.86*	198	21
4	Saulxures	18.27	**6.09**	27.41	*48.22*	10.00	**5.00**	*50.00*	35.00	197	20
5	Mittlach-Erbe	20.25	**7.36**	23.31	*49.08*	11.76	**0.00**	17.65	*70.59*	163	17
6	Fougerolles	16.16	**19.70**	*33.84*	30.30	15.00	**25.00**	*35.00*	25.00	198	20
7	Dabo-Rosskopf	20.21	**23.83**	*31.61*	24.35	25.00	**10.00**	*35.00*	30.00	193	20
8	Bains	18.63	**19.25**	*34.16*	27.95	18.75	**31.25**	*37.50*	12.50	161	16
9	Aubure	18.06	**20.65**	30.32	*30.97*	*35.29*	***35.29***	5.88	23.53	155	17
10	Mittersheim	16.08	***32.16***	31.16	20.60	8.70	**30.43**	*43.48*	17.39	199	23
11	Roville	18.67	**29.52**	*34.94*	16.87	5.88	**23.53**	*47.06*	23.53	166	17
12	Strasbourg	23.62	***40.20***	27.14	9.05	28.57	***42.86***	28.57	0.00	199	21
13	Barr	23.23	***37.37***	23.23	16.16	20.00	***45.00***	25.00	10.00	198	20
14	Kayserberg	22.05	***36.92***	22.56	18.46	15.00	***70.00***	5.00	10.00	195	20
15	Neuf-Brisach	24.49	***47.45***	22.45	5.61	25.00	***70.00***	5.00	0.00	196	20
16	Ebersheim	20.69	***47.78***	25.12	6.40	25.00	***50.00***	20.00	5.00	203	20
17	Rouffach-Chs	24.12	***38.19***	25.63	12.06	5.00	***90.00***	5.00	0.00	199	20
18	Oberentzen	21.83	***39.59***	26.90	11.68	25.00	***65.00***	5.00	5.00	197	20
Duration		*5 days*									
1	Sewen-Lac Alfeld	13.09	**1.05**	23.56	*62.30*	4.76	**0.00**	28.57	*66.67*	191	21
2	Wildenstein	14.80	**0.00**	22.96	*62.24*	15.00	**0.00**	35.00	*50.00*	196	20
3	Longemer	15.74	**6.60**	25.89	*51.78*	5.00	**0.00**	*65.00*	30.00	197	20
4	Saulxures	15.74	**1.02**	26.40	*56.85*	20.00	**0.00**	35.00	*45.00*	197	20
5	Mittlach-Erbe	18.90	**1.22**	20.73	*59.15*	17.65	**0.00**	29.41	*52.94*	164	17
6	Fougerolles	17.17	**14.14**	*36.36*	32.32	10.00	**0.00**	30.00	*60.00*	198	20
7	Dabo-Rosskopf	19.90	**5.76**	36.13	*38.22*	14.29	**0.00**	*57.14*	28.57	191	21
8	Bains	18.42	**9.87**	35.53	*36.18*	0.00	**0.00**	*75.00*	25.00	152	16
9	Aubure	18.06	**11.61**	28.39	*41.94*	25.00	**0.00**	31.25	*43.75*	155	16
10	Mittersheim	13.13	**21.72**	31.82	*33.33*	10.00	**15.00**	*45.00*	30.00	198	20
11	Roville	14.02	**19.51**	*34.76*	31.71	0.00	**0.00**	*88.24*	11.76	164	17
12	Strasbourg	28.64	***44.22***	20.10	7.04	45.00	**5.00**	*50.00*	0.00	199	20
13	Barr	20.20	**20.71**	24.24	*34.85*	15.00	**0.00**	*55.00*	30.00	198	20
14	Kayserberg	17.01	***32.99***	25.26	24.74	0.00	***80.00***	5.00	15.00	194	20
15	Neuf-Brisach	23.71	***52.06***	18.04	6.19	30.00	***70.00***	0.00	0.00	194	20
16	Ebersheim	27.78	***38.89***	23.23	10.10	30.00	***50.00***	20.00	0.00	198	20
17	Rouffach-Chs	19.07	***45.36***	21.13	14.43	25.00	***60.00***	10.00	5.00	194	20
18	Oberentzen	22.34	***37.56***	26.40	13.71	28.57	***66.67***	4.76	0.00	197	21

The maximum value for each station is depicted in italic and underlined. The summer percentages are represented in bold. Interesting values are highlighted in grey. On the right side, the analysed number of events is displayed.

the relative seasonal distribution of 1-day (upper part) and 5-day (lower part) events exceeding 2- and 5-year RP.

Increasing RP at 1-day scale leads to a decrease of concentration of events at MTstations (no. 1–5), except for the 'Longemer' station (no. 3). For that station, it may be related to its position on a sunny slope of a relatively deeper valley, prone in summer to the development of convection and the related convective heavy rainfall (Sell, 1998). On a 5-day resolution, the summer events are not present at all for the MT category or only negligible on both 2- and 5-year level.

On the other hand, Table 4 also shows that for the URP leeward stations (no. 12–18) there is an increase, a decrease, or a stagnation of occurrence of 1-day summer events with an increasing RP. The increase is visible at three stations (no. 14, 17, and 18) situated on the leeward side of the highest part of the Vosges Mountains (i.e. Southern Vosges Mountains), where an increased leeward convection occurring in the warmer half of the year may be expected (Labbouz *et al.*, 2013; Planche *et al.*, 2013). For two of them, stations 'Rouffach-Chs' (no. 17) and 'Oberentzen' (no. 18), summer is the sole season of heavy rainfall with the value of 100%. Unlike these stations, there is a decrease or stagnation of summer events for stations that are situated more to the north of the Upper Rhine River Plain, i.e. no. 12, 13, and 16. It may be caused by a lower mountain barrier in that area, as it has been previously stated for 99.9th percentile in Section 3.2.1. In the case of 'Neuf-Brisach' station (no. 15), the decrease might be related to the proximity of the Black Forest mountain range

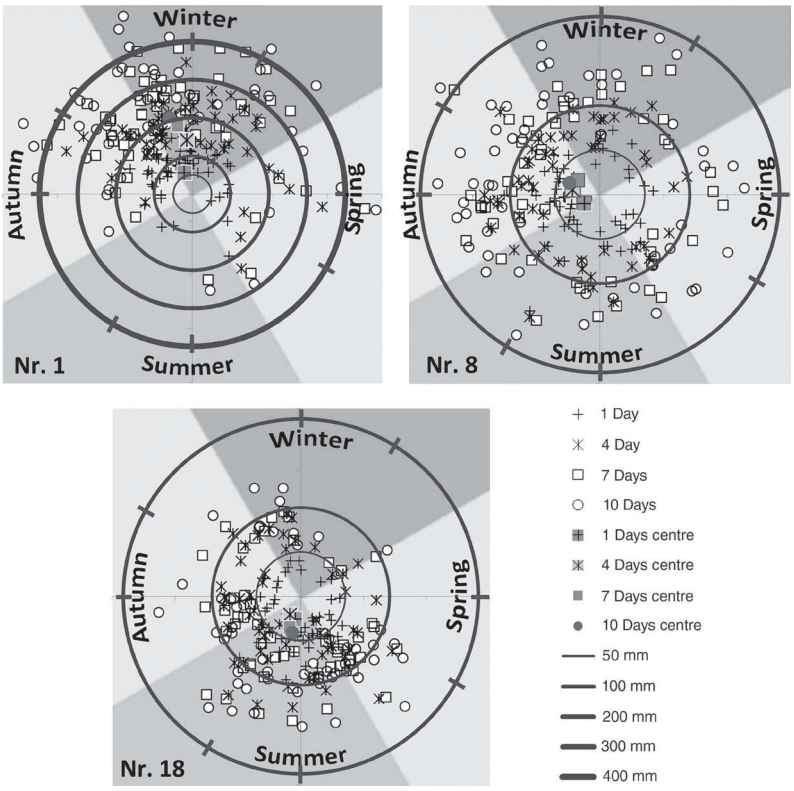

Figure 5. Seasonal distribution for three selected stations (no. 1, 8, and 18) of 1-day (cross), 4-day (cross-star), 7-day (square), and 10-day (small circle) heavy precipitation events within 1960–2013 in relative expression defined by the 1-year BM method. The stations are listed in Table 1 and their geographical position with respect to the topography of the area is displayed in Figure 1. The diagrams show also the centre of gravity of 1-, 4-, 7-, and 10-day lasting events (filled-in symbols of the shape respectively to the duration of event). The circles represent the 50, 100, 200, 300, and 400 mm totals (bolder and wider the line, higher the total). The saturation differentiation separates clockwise the meteorological seasons. The months inside a season are divided by small lines cutting the outer circle.

and its windward influence (Sell, 1998). For the 5-day events, there is an increase of summer events for four out of seven stations type URP and three times a decrease for higher RP. The rather sharp decrease at the 'Strasbourg' station (no. 12) needs to be analysed in further detail, which is planned for the near future research. On that scale, the winter half-year generally longer events might outnumber the increasing occurrence of summer as compared to the shorter events (Ban *et al.*, 2015) on higher threshold, i.e. higher RP.

As in the case of the POT method (Table 3), the categories LSp and WSd of stations (no. 6–11) do not evince any clear tendency in the seasonal distribution that is related to a changing duration of events or RP values. Nevertheless, an obvious higher concentration in some seasons and thus the associated more uneven seasonality is observed on higher RP level; in other word, more zero values are found for 5-year events.

Similar to Section 3.2.1., the seasonality of heavy rainfall events expressed by the RP estimates suggests that the stations influenced by the orographic barrier of the Vosges Mountains are more sensitive to a changing threshold with lower representation of summer events in the mountains and conversely higher concentration in the lee. It might further indicate that the most extreme summer events that occur mainly in the lee are mostly caused by the orography rather than by an increased convection potential on its own, e.g. by the so-called leeward convection (Labbouz *et al.*, 2013; Planche *et al.*, 2013).

3.3. Comparison of methods defining the heavy precipitation events and its discussion

All the three methods used in this study, i.e. POT, BM, and RP estimates, show varying results in terms of the seasonal distribution of heavy precipitation events in the Vosges Mountains area. This is in agreement with Visser and Petersen (2012) who stated that the selection of method might fundamentally influence the results of an analysis of precipitation extremes. Furthermore, the definition of heavy precipitation events is inevitable and crucial for studies dealing with extreme rainfall. This definition is complicated and represents apparently one of the sources of uncertainty of results, which is difficult to quantify (Stephenson, 2008).

The methods used in this study were broadly compared by Müller and Kaspar (2014), who stated that neither the POT method nor the BM method is appropriate for the analysis of precipitation extremes. Firstly, it is because the POT method is based on empirical instead of theoretical distribution. Secondly, the BM method prevents the

Table 4. Seasonal percentage distribution of heavy precipitation 1-day (top) and 5-day (bottom) events at 18 selected stations, listed in Table 1, defined by RP estimates exceeding 2- and 5-years.

Seasonal occurrence (%)											
Method		RP (2 years)				RP (5 years)				RP 2 years	RP 5 years
No.	Station	Spring	Summer	Autumn	Winter	Spring	Summer	Autumn	Winter	Nb. events	Nb. events
	Duration						*1 day*				
1	Sewen-Lac Alfeld	12.50	**6.25**	25.00	*56.25*	10.00	**0.00**	40.00	*50.00*	16	40
2	Wildenstein	11.76	**0.00**	35.29	*52.94*	25.00	**0.00**	12.50	*62.50*	17	37
3	Longemer	10.00	**10.00**	*40.00*	*40.00*	9.09	**18.18**	*45.45*	27.27	20	35
4	Saulxures	11.76	**11.76**	*41.18*	35.29	10.00	**0.00**	*70.00*	20.00	17	37
5	Mittlach-Erbe	15.38	**0.00**	38.46	*46.15*	25.00	**0.00**	12.50	*62.50*	13	34
6	Fougerolles	12.50	**29.17**	*41.67*	16.67	16.67	**33.33**	*41.67*	8.33	24	36
7	Dabo-Rosskopf	17.65	**11.76**	*47.06*	23.53	0.00	**11.11**	*44.44*	*44.44*	17	44
8	Bains	11.11	**22.22**	*38.89*	27.78	9.09	**18.18**	*54.55*	18.18	18	29
9	Aubure	25.00	***31.25***	18.75	25.00	***40.00***	**30.00**	0.00	30.00	16	25
10	Mittersheim	5.88	**23.53**	*47.06*	23.53	14.29	**28.57**	*42.86*	14.29	17	46
11	Roville	6.25	**31.25**	*43.75*	18.75	0.00	**11.11**	*55.56*	33.33	16	41
12	Strasbourg	17.65	***41.18***	*41.18*	0.00	25.00	***37.50***	*37.50*	0.00	17	33
13	Barr	16.67	***33.33***	25.00	25.00	16.67	***33.33***	*33.33*	16.67	12	39
14	Kayserberg	5.88	***64.71***	17.65	11.76	10.00	***80.00***	0.00	10.00	17	37
15	Neuf-Brisach	16.67	***77.78***	5.56	0.00	22.22	***77.78***	0.00	0.00	18	28
16	Ebersheim	33.33	***46.67***	20.00	0.00	*37.50*	***37.50***	25.00	0.00	15	41
17	Rouffach-Chs	13.33	***80.00***	6.67	0.00	0.00	***100.00***	0.00	0.00	15	29
18	Oberentzen	11.11	***72.22***	11.11	5.56	0.00	***100.00***	0.00	0.00	18	27
	Duration						*5 days*				
1	Sewen-Lac Alfeld	12.50	**0.00**	32.50	*55.00*	8.33	**0.00**	33.33	*58.33*	10	24
2	Wildenstein	16.22	**0.00**	32.43	*51.35*	22.22	**0.00**	*44.44*	33.33	8	18
3	Longemer	17.14	**2.86**	34.29	*45.71*	11.76	**5.88**	*47.06*	35.29	11	17
4	Saulxures	18.92	**0.00**	29.73	*51.35*	22.22	**0.00**	27.78	*50.00*	10	18
5	Mittlach-Erbe	14.71	**2.94**	29.41	*52.94*	20.00	**0.00**	26.67	*53.33*	8	15
6	Fougerolles	8.33	**13.89**	*44.44*	33.33	0.00	**25.00**	25.00	*50.00*	12	16
7	Dabo-Rosskopf	18.18	**0.00**	*52.27*	29.55	16.00	**0.00**	*48.00*	36.00	9	25
8	Bains	3.45	**6.90**	*48.28*	41.38	0.00	**0.00**	***69.23***	30.77	11	13
9	Aubure	20.00	**4.00**	*40.00*	36.00	27.27	**0.00**	27.27	*45.45*	10	11
10	Mittersheim	15.22	**4.35**	*43.48*	36.96	14.29	**7.14**	*53.57*	25.00	7	28
11	Roville	17.07	**12.20**	*51.22*	19.51	17.24	**6.90**	*58.62*	17.24	9	29
12	Strasbourg	27.27	**18.18**	*51.52*	3.03	44.44	**5.56**	*50.00*	0.00	8	18
13	Barr	12.82	**17.95**	*43.59*	25.64	15.00	**20.00**	*45.00*	20.00	6	20
14	Kayserberg	13.51	**27.03**	*29.73*	*29.73*	0.00	***53.33***	13.33	33.33	10	15
15	Neuf-Brisach	28.57	***57.14***	10.71	3.57	36.36	***54.55***	9.09	0.00	9	11
16	Ebersheim	24.39	**31.71**	*36.59*	7.32	26.67	***40.00***	33.33	0.00	8	15
17	Rouffach-Chs	17.24	***55.17***	20.69	6.90	33.33	***50.00***	8.33	8.33	8	12
18	Oberentzen	18.52	***55.56***	18.52	7.41	26.67	***66.67***	6.67	0.00	8	15

The maximum value for each station is depicted in italic and underlined. The summer percentages are represented in bold. Interesting values are highlighted in grey. On the right side, the analysed number of events is displayed.

identification of a data set of the most extreme events by selecting one event per some period (e.g. per season, year, 2 years) and that the heavy precipitation is not equally distributed in time. The same has been mentioned in the limitations of the BM method applied on yearly maxima (Section 3.2.2.).

Katz (2010) also indicated that the RP estimates lead to more accurate results even if the stationarity of climate has to be assumed.

However, the results of the three methods defining heavy precipitation events in the presented analysis are to some extent similar, because they lead to the same general rough findings, e.g. they show the same season for the four categories of stations as being the most prone to heavy rainfall, which is in accordance with the most humid season on average. Contrarily, the results also show that they are strongly threshold-dependent. Furthermore, they suggest that the threshold sensitivity increases with an increase in influence of orography, i.e. the Vosges Mountains, which has not yet been described in the literature. The underlying causes of such effect may be related to different weather types responsible for the heavier rainfall events nearer and farer away from the Vosges Mountains range. A strong leeward convection (Labbouz *et al.*, 2013) may also play an important role in this issue. However, a detailed research is needed to be pursued to confirm such hypotheses.

Furthermore, a CA performed on the events selected by the three methods and their duration has shown three groups – (1) The BM method as well as the POT method for the 97.5th percentile are positively correlated with 5- to

9-day events but are negatively correlated with RP method and other percentiles of the POT; (2) the RP method at the 2- and 5-year levels as well as the POT 95th percentile are positively correlated with the 10-day events, while (3) the 10-year RP level belongs to the same group as the POT 99th and 99.9th percentiles that are positively correlated with 1- to 4-day events. The projection of axis was satisfactory with 70.22% for the X-axis and 22.82% for the Y-axis. The variables were not independent (p value $= 10^{-16}$).

The results of the CA seem to well confirm the previous finding that the occurrence of rather shorter events at higher thresholds and RP levels is increasing.

4. Conclusions

We argued at the beginning of the article that a climatological analysis of temporal and spatial distributions of mean and heavy precipitation is needed in the area of the Vosges Mountains in North-Eastern France. To date, the literature has not provided any satisfactory study in this field but this article, based on a larger data set of daily rainfall totals from gauging stations during 1960–2013 and study of the seasonality of both the mean and the 1- to 10-day heavy rainfall offers one.

The findings that we have presented evince the following three main conclusions:

- Seasonality of mean monthly precipitation correlates with the mean annual rainfall total in a complex relief.
- Heavy rainfall events occur mostly in the most humid season on average, but the seasonality of extremes is clearly threshold-dependent and the events can also occur over the whole year, so that an analysis of whole years is required.
- Threshold sensitivity seems to increase with an increase in influence of orographic barrier (reduction of summer events in mountains whereas higher concentration of summer events in the lee of the Vosges Mountains).

Furthermore, the use of three different methods (POT, BM, and RP) defining the heavy rainfall events has enabled a comparison of the three methods and has shown an increasing occurrence of shorter events in warmer half of the year in the lee of the Vosges Mountains at higher thresholds and RP levels. This is important for the risk management of natural hazards related to the heavy rainfall because the awareness of shorter more extreme precipitation events may lead to very efficient warning systems since the time to adopt measures is for such events particularly short and their severity is high. In addition, on higher thresholds or RP levels at shorter time scale more changes in terms of seasonal distribution of events are observed at stations nearer to the Vosges Mountains, as compared to the mean behaviour of precipitation.

The research also raises a question about a particularly high decrease of summer heavy rainfall events at the 'Strasbourg' station (no. 12) with an increasing RP level for the 5-day events. It would be fruitful to pursue further research on the behaviour of heavy rainfall of different RPs in more details mainly at that station, e.g. including weather types or visualizing the most frequently affected area in order to effectively anticipate and prevent the natural disasters that such events may produce in the main city of the French region Alsace Strasbourg.

Moreover, the limited analysis of the presented article to the use of daily rainfall totals also limits at some extent the findings. Therefore, an easier access to more precise precipitation data sets, e.g. hourly rainfall data, would undoubtedly enhance the research about climate extremes. Concerning the radar data, it might be used as an additional source of information. On the other hand, since none of the two French nearest weather radars, i.e. 'Réchicourt-La-Petite' and 'Montancy', is situated after the mountain ridge of the Vosges Mountains in the Upper Rhine River Plain, the use of such data remains very restricted because of the radar shading and its limited coverage. In such case, we propose to combine them with the German radar data. The rainfall data are anyway financially even less accessible than the hourly rain gauging totals.

While this study does not offer a definite answer to the question, which methods might be the best to define heavy precipitation events, we will test in the near future a recently developed event-adjusted evaluation method of precipitation extremes (Müller and Kaspar, 2014), which is more adequate because it does not consider the stations one by one instead considers the spatial distribution. This method may prove the important hypothesis raised by this research about the increasing threshold sensitivity with an increase in influence of orography. As a follow-up to such confirmation, a thorough analysis is also planned to be dedicated to the main causes and processes leading to this effect.

Acknowledgements

We thank 'Météo-France' for providing data and Dr Marek Kašpar and Lukáš Pop M.Sc. for their contribution in computing the GEV parameters in MatLab. We also extend great thanks to Dr Georges Najjar for his helpful comments and discussions, and to Syed Muntazir Abbas M.Phil. for his valuable help especially in improving the language of the manuscript.

References

Ahrens CD. 2007. *Essentials of Meteorology*. Belmont, CA: Cengage Learning.

Alexander LV, Zhang X, Peterson TC, Caesar J, Gleason B, Klein Tank AMG, Haylock M, Collins D, Trewin B, Rahimzadeh F, Tagipour A, Rupa Kumar K, Revadekar J, Griffiths G, Vincent L, Stephenson DB, Burn J, Aguilar E, Brunet M, Taylor M, New M, Zhai P, Rusticucci M, Vazquez-Aguirre JL. 2006. Global observed changes in daily climate extremes of temperature and precipitation. *J. Geophys. Res. Atmos.* **111**(D5): D05109, doi: 10.1029/2005JD006290.

Arnaud P, Fine JA, Lavabre J. 2007. An hourly rainfall generation model applicable to all types of climate. *Atmos. Res.* **85**(2): 230–242, doi: 10.1016/j.atmosres.2007.01.002.

Arnaud P, Lavabre J, Sol B, Desouches C. 2008. Régionalisation d'un générateur de pluies horaires sur la France métropolitaine pour la connaissance de l'aléa pluviographique/Regionalization of an hourly rainfall generating model over metropolitan France for flood hazard estimation. *Hydrol. Sci. J.* **53**(1): 34–47, doi: 10.1623/hysj.53.1.34.

Ban N, Schmidli J, Schär C. 2015. Heavy precipitation in a changing climate: does short-term summer precipitation increase faster? *Geophys. Res. Lett.* **42**: 1165–1172, doi: 10.1002/2014GL062588.

Beniston M, Stephenson DB. 2004. Extreme climatic events and their evolution under changing climatic conditions. *Global Planet. Change* **44**(1–4): 1–9, doi: 10.1016/j.gloplacha.2004.06.001.

Beniston M, Stephenson DB, Christensen OB, Ferro CAT, Frei C, Goyette S, Halsnaes K, Holt T, Jylhä K, Koffi B, Palutikof J, Schöll R, Semmler T, Woth K. 2007. Future extreme events in European climate: an exploration of regional climate model projections. *Clim. Change* **81**(1): 71–95, doi: 10.1007/s10584-006-9226-z.

Bertoldo S, Lucianaz C, Allegretti M. 2015. Extreme rainfall event analysis using rain gauges in a variety of geographical situations. *Atmos. Clim. Sci.* **5**(2): 82–90, doi: 10.4236/acs.2015.52006.

Cantet P, Bacro J-N, Arnaud P. 2010. Using a rainfall stochastic generator to detect trends in extreme rainfall. *Stochastic Environ. Res. Risk Assess.* **25**(3): 429–441, doi: 10.1007/s00477-010-0440-x.

Cioffi F, Lall U, Rus E, Krishnamurthy CKB. 2015. Space-time structure of extreme precipitation in Europe over the last century. *Int. J. Climatol.* **35**: 1749–1760, doi: 10.1002/joc.4116.

Coelho CAS, Ferro CAT, Stephenson DB, Steinskog DJ. 2008. Methods for exploring spatial and temporal variability of extreme events in climate data. *J. Clim.* **21**(10): 2072–2092, doi: 10.1175/2007JCLI1781.1.

Coles S. 2001. *An Introduction to Statistical Modeling of Extreme Values*. Springer: London and New York, NY.

Cutter SL, Gall M, Emrich CT. 2008. Toward a comprehensive loss inventory of weather and climate hazards. In *Climate Extremes and Society*, Díaz HF, Murnane RJ (eds). Cambridge University Press: Cambridge, UK.

Dyrrdal AV, Skaugen T, Stordal F, Førland EJ. 2016. Estimating extreme areal precipitation in Norway from a gridded dataset. *Hydrol. Sci. J.* **61**(3): 483–494, doi: 10.1080/02626667.2014.947289.

Embrechts P, Klüppelberg C, Mikosch T. 2011. *Modelling Extremal Events: For Insurance and Finance*. Springer: New York, NY.

ETCCDI/CRD Climate Change Indices. 2011. *Climate Change Indices: Definitions of the 27 Core Indices*. http://etccdi.pacificclimate.org/list_27_indices.shtml (accessed 2 August 2016).

Gizaw MS, Gan TY. 2016. Possible impact of climate change on future extreme precipitation of the Oldman, Bow and Red Deer River Basins of Alberta. *Int. J. Climatol.* **36**(1): 208–224, doi: 10.1002/joc.4338.

Gulev SK, Zolina O, Grigoriev S. 2001. Extratropical cyclone variability in the Northern Hemisphere winter from the NCEP/NCAR reanalysis data. *Clim. Dyn.* **17**(10): 795–809, doi: 10.1007/s003820000145.

Hrudička, B. 1933a. Doba polovičních srážek a periodická amplituda ročního srážkového průběhu v Československu (The half-time period and periodic amplitude of annual rainfall course in the Czechoslovakia). Spisy vydávané Přírodovědeckou fakultou Masarykovy university: Brno, č. 185, 1–22.

Hrudička B. 1933b. *Příspěvěk k prozkumu ombrické kontinentality v Evropě (Contribution to the research of the ombric continentality in Europe)*. Odbor Československé společnosti zeměpisné, 22 pp.

Hupfer P, Chmielewski F-M, Pethe H, Kuttler W. 2005. *Witterung und Klima: Eine Einführung in die Meteorologie und Klimatologie* (Weather and Climate: Introduction to the Meteorology and Climatology). Vieweg + Teubner Verlag: Stuttgart, Germany.

Interklim. 2014. *Der Klimawandel im böhmisch-sächsischen Grenzraum. Změna klimatu v česko-saském pohraničí* (Climate change in Bohemian-Saxony frontier area). Sächsisches Landesamt für Umwelt, Landwirtschaft und Geologie: Dresden, Germany.

Kašpar M, Müller M. 2014. Combinations of large-scale circulation anomalies conducive to precipitation extremes in the Czech Republic. *Atmos. Res.* **138**: 205–212, doi: 10.1016/j.atmosres.2013.11.014.

Katz RW. 2010. Statistics of extremes in climate change. *Clim. Change* **100**(1): 71–76, doi: 10.1007/s10584-010-9834-5.

Katz RW, Parlange MB, Naveau P. 2002. Statistics of extremes in hydrology. *Adv. Water Resour.* **25**(8–12): 1287–1304, doi: 10.1016/S0309-1708(02)00056-8.

Klein Tank AMG, Peterson TC, Quadir DA, Dorji S, Zou X, Tang H, Santhosh K, Joshi UR, Jaswal AK, Kolli RK, Sikder AB, Deshpande NR, Revadekar JV, Yeleuova K, Vandasheva S, Faleyeva M, Gomboluudev P, Budhathoki KP, Hussain A, Afzaal M, Chandrapala L, Anvar H, Amanmurad D, Asanova VS, Jones PD, New MG, Spektorman T. 2006. Changes in daily temperature and precipitation extremes in central and south Asia. *J. Geophys. Res. Atmos.* **111**(D16): D16105, doi: 10.1029/2005JD006316.

Klein Tank AMG, Zwiers FW, Zhang X. 2009. *Guidelines on Analysis of Extremes in a Changing Climate in Support of Informed Decisions for Adaptation*. World Meteorological Organization: Geneva, Switzerland, 55.

Klimaatlas Oberrhein Mitte-Süd/Atlas Climatique du Fossé Rhénan Méridional (Climatic atlas of the Southern Upper Rhine river Plain). 1996. *REKLIP: Regionales Klimaprojekt/Projet climatologique*. Trinationale Arbeitsgemeinschaft Regio-Klima-Projekt REKLIP. vdf Hochschulvlg: Zürich. ISBN: 978-3-7281-2105-9.

Krahe P, Herpertz D, International Commission for the Hydrology of the Rhine Basin (eds). 2001. *Generation of Hydrometeorological Reference Conditions for the Assessment of Flood Hazard in Large River Basins: Papers Presented at the International Workshop Held on March 6 and 7, 2001 in Koblenz*. International Commission for the Hydrology of the Rhine Basin: Lelystad.

Labbouz L, Van Baelen J, Tridon F, Reverdy M, Hagen M, Bender M, Dick G, Gorgas T, Planche C. 2013. Precipitation on the lee side of the Vosges Mountains: multi-instrumental study of one case from the COPS campaign. *Meteorol. Z.* **22**(4): 413–432, doi: 10.1127/0941-2948/2013/0413.

Maugeri M, Brunetti M, Garzoglio M, Simolo C. 2015. High-resolution analysis of 1 day extreme precipitation in Sicily. *Nat. Hazards Earth Syst. Sci. Discuss.* **3**(4): 2247–2281, doi: 10.5194/nhessd-3-2247-2015.

Minárova J. 2013. Climatology of precipitation in the vosges mountain range area. *Acta Univ. Carol. Geogr.* **48**(2): 51–60.

Müller M, Kaspar M. 2014. Event-adjusted evaluation of weather and climate extremes. *Nat. Hazards Earth Syst. Sci.* **14**(2): 473–483, doi: 10.5194/nhess-14-473-2014.

Müller M, Kašpar M, Valeriánová A, Crhová L, Holtanová E. 2015. Evaluation of precipitation extremes and floods and comparison between their temporal distributions. *Hydrol. Earth Syst. Sci. Discuss.* **12**(1): 281–310, doi: 10.5194/hessd-12-281-2015.

Niedzwiedz T, Lupikasza E, Pinskwar I, Kundzewicz ZW, Stoffel M, Malarzewski L. 2015. Variability of high rainfalls and related synoptic situations causing heavy floods at the northern foothills of the Tatra Mountains. *Theor. Appl. Climatol.* **119**(1–2): 273–284, doi: 10.1007/s00704-014-1108-0.

van Pelt SC, Beersma JJ, Buishand TA, van den Hurk BJJM, Schellekens J. 2014. Uncertainty in the future change of extreme precipitation over the Rhine basin: the role of internal climate variability. *Clim. Dyn.* **44**(7–8): 1789–1800, doi: 10.1007/s00382-014-2312-4.

Planche C, Wobrock W, Flossmann AI, Tridon F, Labbouz L, Van Baelen J. 2013. Small scale topography influence on the formation of three convective systems observed during COPS over the Vosges Mountains. *Meteorol. Z.* **22**(4): 395–411, doi: 10.1127/0941-2948/2013/0402.

Rohli RV, Vega AJ. 2011. *Climatology*. Jones & Bartlett: Sudbury, MA.

Sell Y. 1998. *L'Alsace et les Vosges* (Alsace and the Vosges Mountains). Delachaux et Niestlé: Lausanne, Switzerland.

Sillmann J, Kharin VV, Zhang X, Zwiers FW, Bronaugh D. 2013. Climate extremes indices in the CMIP5 multimodel ensemble: Part 1. Model evaluation in the present climate. *J. Geophys. Res. Atmos.* **118**(4): 1716–1733, doi: 10.1002/jgrd.50203.

Stephenson DB. 2008. Definition, diagnosis, and origin of extreme weather and climate events. In *Climate Extremes and Society*, Díaz HF, Murnane RJ (eds). Cambridge University Press: Cambridge, UK.

Visser H, Petersen AC. 2012. Inferences on weather extremes and weather-related disasters: a review of statistical methods. *Clim. Past* **8**(1): 265–286, doi: 10.5194/cp-8-265-2012.

Wang XL, Feng Y. 2013. *RHtests_dlyPrcp User Manual*. Climate Research Division, Atmospheric Science and Technology Directorate, Science and Technology Branch, Environment Canada: Toronto, ON, Canada. http://etccdi.pacificclimate.org/RHtest/RHtestsV4_User Manual_10Dec2014.pdf (accessed 25 February 2014).

Wang XL, Chen H, Wu Y, Feng Y, Pu Q. 2010. New techniques for the detection and adjustment of shifts in daily precipitation data series. *J. Appl. Meteorol. Climatol.* **49**(12): 2416–2436, doi: 10.1175/2010JAMC2376.1.

Woeste B. 2010. Eine Anwendung der Block Maxima Methode im Risikomanagement. Vol. 111. Westfälische Wilhelms-Universität Münster: Münster, Germany. http://wwwmath.uni-muenster.de/statistik/paulsen/Abschlussarbeiten/Diplomarbeiten/Woeste.pdf (accessed 6 August 2016).

8. Article III: ‘Characteristics of Extreme Precipitation in the Vosges Mountains region (North-Eastern France)’

The third article (Minářová *et al.*, 2017c) entitled ‘Characteristics of Extreme Precipitation in the Vosges Mountains region (North-Eastern France)’ employs in VG the Müller and Kaspar’s method (2014) on the 1—10 day precipitation totals to define the extreme precipitation events (EPEs), which is found objective in selecting the EPEs and applicable also at the regional scale. Strongest EPEs are described in detail including the synoptic situation during the events and hydrological response following the events. Duration, seasonality, affected area, extremity, and synoptic condition are the studied characteristics of the 54 (strongest) EPEs in the paper. Linear trends are also briefly described. The conclusion of the article provides a need of broader study of spatial characteristics of EPEs in VG, and analogous analysis in a similar region in order to compare and generalize the results.

INTERNATIONAL JOURNAL OF CLIMATOLOGY
Int. J. Climatol. (2017)
Published online in Wiley Online Library
(wileyonlinelibrary.com) DOI: 10.1002/joc.5102

RMetS
Royal Meteorological Society

Characteristics of extreme precipitation in the Vosges Mountains region (north-eastern France)

Jana Minářová,[a,b,c]* Miloslav Müller,[b,c] Alain Clappier[a] and Marek Kašpar[c]

[a] *Laboratory Image, City, Environment, National Centre for Scientific Research & University of Strasbourg, France*
[b] *Department of Physical Geography and Geoecology, Faculty of Science, Charles University in Prague, Czech Republic*
[c] *Institute of Atmospheric Physics, Academy of Sciences of the Czech Republic, Prague, Czech Republic*

ABSTRACT: In this research, different characteristics (duration, affected area, extremity, and synoptic conditions) related to extreme precipitation events (EPEs), and the trends in frequency of EPEs in the Vosges Mountains (VG) region (north-eastern France) have been analysed and the events were evaluated on regional scale using the Weather Extremity Index. The index combines three aspects of an EPE – rarity, spatial extent, and duration – and it enables a quantitative comparison of these aspects in a data set of EPEs. In this study, 54 EPEs (which occurred during 1960–2013) were selected using daily precipitation totals from meteorological stations. Although possible maximum duration of an EPE was set to 10 days, all detected EPEs lasted 1–5 days. The prevailing short EPEs (1–2 days) affected smaller areas as compared to long EPEs (3–5 days). Instead of the winter maximum of mean precipitation in the VG, the autumn EPEs prevailed in the data set (40% of all EPEs including the four strongest EPEs). Using the manual and the automated catalogues (Grosswetterlagen and SynopVisGWL, respectively), majority of the 54 EPEs was found associated with the west cyclonic weather type; however, none of the five maximum events was produced by this weather type. The two strongest EPEs were related to the stationary cold front rather than to the expected strong zonal circulation. The EPEs were mostly related to strong southwest airflow and flux of specific humidity. No significant trend was found in frequency of EPEs during the 54 years.

Our results highlight new insights into the extreme precipitation in VG region. We believe that the ranking of EPEs according to their extremity in the VG region provides useful information for local decision making authorities, engineers, and risk managers.

KEY WORDS Vosges Mountains; extreme precipitation; heavy rainfall; WEI; synoptic conditions; trend analysis; precipitation; Grosswetterlagen

Received 2 November 2016; Revised 23 March 2017; Accepted 25 March 2017

1. Introduction

Extreme precipitation has been the major cause of producing localized urban and widespread flooding, and the rainfall induced major landslides which not only result in loss of human life but also cause extensive damage to property and degradation of water quality despite the presence of a more thorough and improved risk management (Cutter *et al*., 2008). Thus, understanding the characteristics of heavy precipitation events is critically important to protect against such events, avoid the consequent losses, and develop the engineering designs and regulations for engineering structures and facilities that can withstand such extreme events. The extreme precipitation has become one of the central issues concerning populations due to the consequential recurring severe floods and according to Intergovernmental Panel on Climate Change (IPCC) because of the threats posed by such events (Barros *et al*., 2014). For climatologists, the main issue related to precipitation extremes is the understanding of extreme precipitation and its as precise as possible prediction. In fact, we are likely to witness an increase in extreme precipitation events (EPEs) in the next decades which may become more severe in likely warmer climate, thereby making the understanding of extreme precipitation even a more crucial topic.

The characteristics of extreme precipitation are not yet fully understood (Stephenson *et al*., 2008). Commonly, the studies dealing with EPEs are event-specific (e.g. Rudolf and Rapp, 2002; Grams *et al*., 2014). Although they provide interesting and important information about an individual event, e.g. of its synoptic conditions, measured record totals, and hydrological and socio-economical consequences, yet they select the event arbitrarily and thus do not allow for an objective comparison among different events. Random comparative studies have also been event-specific leading to event-specific results, e.g. the study by Conradt *et al*. (2013) has compared the August 2002 and June 2013 Central Europeans floods from the perspective of their return period estimates and its consequences.

* Correspondence to: J. Minářová, Department of Physical Geography and Geoecology, Faculty of Science, Charles University in Prague, Albertov 6, 128 43 Praha 2, Prague, Czech Republic. E-mail: jana.minarova@live-cnrs.unistra.fr; jana.minarova@natur.cuni.cz; jana.minarova@ufa.cas.cz

A wider data set of EPEs is needed for the better understanding of EPEs based on an objective method for selection of the data set. Among the objective approaches, the peaks over threshold, return period estimates, and block maxima (described, e.g. by Coles, 2001; Katz *et al*., 2002; Coelho *et al*., 2008; Katz, 2010) are the most commonly used. The threshold approach considers the precipitation total exceeding a defined precipitation threshold value (Štekl, 2001; Muluneh *et al*., 2016; Ngo-Duc *et al*., 2016; Tošić *et al*., 2016; Wang *et al*., 2016a), or a percentile (Allan *et al*., 2015; Wi *et al*., 2015; Blenkinsop *et al*., 2016; Wang *et al*., 2016b; Yin *et al*., 2016). Although the peaks over a defined percentile may lead to more adequate results because of its capability to reflect microclimates, yet they are based on an empirical distribution. By the block maxima approach, one can examine the yearly (or seasonal) daily precipitation maxima (Balling *et al*., 2016; Blanchet *et al*., 2016; Ghenim and Megnounif, 2016). However, it has a limitation that only one most intense precipitation event is selected during a period irrespective of the characteristics of the period (i.e. dry or humid). Contrary to the block maxima and peaks over threshold, Katz (2010) suggested that the return period estimates are more accurate because they are based on theoretical distribution of extreme precipitation (commonly three-parametric generalized extreme value (GEV) distribution).

Minářová *et al*. (2016) have compared the peaks over threshold (percentiles), block maxima, and return period estimates approaches considering the seasonality of heavy rainfall in the Vosges Mountains (VG), north-eastern France. The study concludes that although the three methods give satisfying outcomes, the results remain station or group of stations specific. Therefore, a more suitable event-adjusted technique for evaluation of precipitation extremes developed by Müller and Kaspar (2014) was suggested to be tested. This event-adjusted technique considers the spatial distribution of an EPE, its varying duration, and its rarity computed from return period estimates; thus combining all necessary information about a weather or climate extreme in one index, i.e. Weather Extremity Index (WEI). This quantification of extremity of weather events (WEI) is very useful because of the more objective assessment and easier comparability among different events in a region (Müller and Kaspar, 2014).

The event-adjusted technique is a very promising tool for the evaluation of weather extremes, and it has been applied and elaborated several times since its first publication (Müller *et al*., 2015a, 2015b; Valeriánová *et al*., 2015; Kašpar *et al*., 2016). A study by Schiller (2016) has proved its applicability on radar data beyond the Czech Republic territory (in Germany) as well.

The prime purpose of this research is to analyse different characteristics of the selected data set of EPEs such as the duration, affected area, extremity, and synoptic conditions related to EPEs, and the trends in frequency of EPEs during the study period (1960–2013). For this purpose, the selection of EPEs data set was carried out using the event-adjusted evaluation technique (Müller and Kaspar, 2014). The technique was applied on daily precipitation data from rain gauges in the VG situated in north-eastern France (Figure 1). We believe that our findings can be applied to climate projection analyses, and may conceivably provide useful and interesting information for decision-makers and risk managers. Moreover, this study leads to additional verification of the applicability of the event-adjusted method.

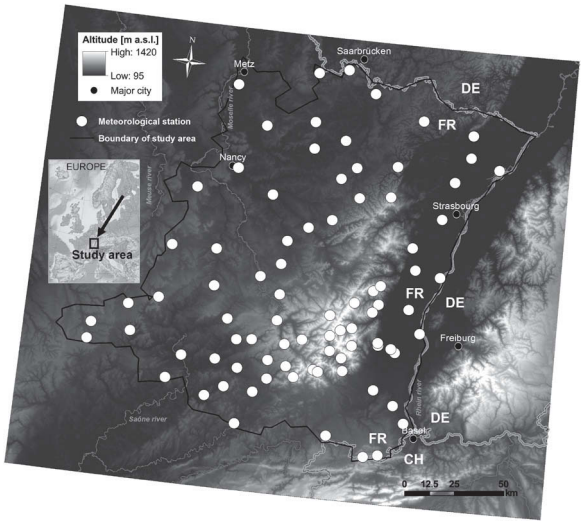

Figure 1. Spatial distribution of the 84 analysed weather stations located in the study area (VG). The relief is represented in grey-scale, with the highest locations displayed in white.

2. Data and methods

2.1. Study area

The study area (Figure 1) comprises of VG and covers Alsace, major part of Lorraine, and some parts of the Franche-Comté regions, north-eastern France. VG culminating at the Grand Ballon (1424 m a.s.l.) are characterized by hilly foreland, relatively gentle western slopes, and steep eastern slopes dipping to the Upper Rhine Plain at an altitude of 200 m a.s.l. (Gley, 1867; Alsatia, 1932; Ernst, 1988; Sell, 1998). Despite various microclimates, the temperate oceanic climate dominates at the western part and near the ridge of VG, and the temperate climate with continental features prevails in the Upper Rhine Plain (Sell, 1998; Météo-France, 2008).

The spatial distribution of precipitation is correlative to altitude and the prevailing westerlies from the Atlantic Ocean. The major precipitation differences are due to the almost perpendicular orientation of the mountain ridge to the dominant airflow direction (Sell, 1998; Météo-France, 2008). During 1960–2013, the highest mean annual precipitation total of 2329 mm was recorded at the Sewen-Lac Alfeld weather station (620 m a.s.l.) in the southern Vosges, 903 mm was recorded at the Rovillé weather station (278 m a.s.l.) on the windward side, and 599 mm at the Colmar–Mayenheim rain gauge in Upper Rhine River

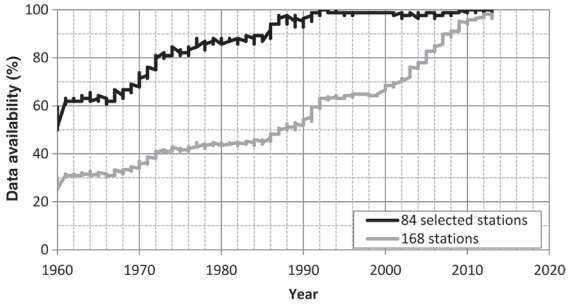

Figure 2. Percentage of stations among 84 selected and all 168 rain gauges showing the availability of daily precipitation data.

Plain due to rain shadow in the lee (Minářová *et al*., 2016).

2.2. Precipitation data set

Daily precipitation non-homogenized totals and metadata from 168 weather stations of the VG were analysed. The data covers the period 1960–2013 and were provided by Météo-France national meteorological network. Due to the fact that some of the time series included large discontinuities, only that data which covered more than half of the study period (i.e. 27 years) was analysed further. This criterion was met by data from 84 weather stations, and the remaining data were used for checking the interim results. The missing values in the new data set of time series from the 84 selected stations were not filled in by interpolation or extrapolation, and the data set was found sufficient for the subsequent analyses. Figure 2 shows the substantial progressive increase of daily data availability for the meteorological stations with time either due to the increase in the number of weather stations or due to the availability of digital precipitation records. The availability of daily precipitation totals has increased from 50–60% in 1960 to 90–100% in 1980 and onwards. Taking into consideration the spatial distribution of the selected 84 stations, the study area VG was adjusted in order to avoid the extrapolation of resulting spatial outputs (Figure 1).

The RHtests_dlyPrcp R-package (Wang *et al*., 2010; Wang and Feng, 2013), designed for testing the daily precipitation totals, was used to test the homogeneity of time series. The package is accessible at http://etccdi.pacificclimate.org/software.shtml. The computation includes the metadata of weather stations. In our case, 0.4 mm was selected as a suitable value for the error of data measurement in the test based on the estimated maximum error of the different rain gauges used for data measurement in our study area, despite the commonly used value of 0.2 mm for such analyses, which is also suggested by the WMO (World Meteorological Organization, 2008). Lower values (0.1, 0.2, and 0.3 mm) would have produced similar results, as documented by Minářová *et al*. (2016).

The test highlighted two non-homogenous time series recorded at the Aillevillers and Foucogney meteorological stations, which were adjusted according to the homogenization technique described by Wang *et al*. (2010) and Wang and Feng (2013). The mean of adjusted daily precipitation totals from both the stations is negligibly lower (in order of 10^{-2} mm) than the equivalent of its raw data.

The non-zero daily precipitation totals were studied further, and the 1–10 days precipitation totals were assessed using the event-adjusted evaluation technique (Section 2.3) in order to select the EPEs. The limit of 10 days in the VG area was set based on the characteristics of mean precipitation in VG and the Czech Republic, and is in good agreement with the hydrological studies in the areas. For instance, van Pelt *et al.* (2014) stated that 10-day precipitation events in particular tend to result in flooding in the Upper Rhine River catchment.

2.3. Event-adjusted evaluation technique of weather and climate extremes

The event-adjusted evaluation method of weather and climate extremes (Müller and Kaspar, 2014) was applied in order to obtain a data set of EPEs and to perform comparison among events. This technique introduces the WEI, which quantifies the extremity of an event on the basis of three parameters, i.e. rarity, spatial extent, and duration of an event; all varying and combined in one single index. In the first step, the return periods of precipitation are estimated at individual sites for various time windows separately. Then the resulting point return period data are interpolated spatially, and in the third step that area and time window is identified in which the event has the maximum extremity, which is termed as WEI.

The technique starts by assessment of rarity, which is based on return period estimates of 1 to x-day precipitation totals (1–10 days in our case) at rain gauges individually. The return period was estimated using three-parametric GEV distribution that is widely used for analysis of heavy rainfall. The three parameters of the GEV were calculated based on precipitation annual maxima values by means of L-moments (Hosking and Wallis, 2005). Since such local analysis may create variations in the estimates of GEV parameters and high quantiles, the maximum return period estimate was set to 1000 years. To express the spatial aspect of weather extremity, the maximum return period estimates from individual gauges are not considered. Instead, the resulting rain gauge return period estimates from the gauges were expressed in their common logarithmic equivalents that were interpolated using ordinary kriging interpolation method into a regular grid of 2×2 km resolution. The interpolated logarithmic values were transformed back to return period estimates N during t days (i.e. 1–10 days) at grid points i. The values of grid points (N_{ti}) were sorted in decreasing order, since the area affected by an EPE can be discontinuous. The analysis starts at the grid point with the highest value of return period estimate N, and other grid points are added one by one according to the decreasing value of return period estimates, i.e. the area a increases with each addition of the grid point. The spatial geometric mean G_{ta} is calculated step-by-step for n grid points.

The WEI is defined based on the spatial geometric mean as follows (Müller and Kaspar, 2014):

$$\mathrm{WEI}\left[\log(\text{years})\,\mathrm{km}\right] = \max\left(E_{ta}\right) = \max\left(\log\left(G_{ta}\right)R\right) = \max\left(\frac{\sum_{i=1}^{n}\log\left(N_{ti}\right)\sqrt{a}}{n\sqrt{\pi}}\right) \quad (1)$$

where N_{ti} is the return period estimate in years at a grid point i for t days, and a is the area in km^2 comprising n grid points. The resulting E_{ta} is the indicator of extremity of a weather/climate event, and it corresponds to the multiplication of a common logarithm of the spatial geometric mean G_{ta} of return period estimates N_{ti} by the radius of a circle R in km whose area is equal to that delimited by the spatial geometric mean G_{ta}.

The Equation (1) implies that the maximum value of E_{ta} is considered. It corresponds to the inflection point of its curve which represents an optimized combination between rarity and affected area. In fact, at the beginning pixels of high return period estimates are accumulated and the area and E_{ta} increase inflection point of E_{ta}, when it starts decreasing since newly accumulated pixels are of low return period estimates and the decrease of the return period estimates prevails over the increase in the accumulated area a.

The final WEI corresponds to the first maximal E_{ta} among non-zero E_{ta} values computed for 1–10 days (t) overlapping events, starting from the duration of 1 day. All the 1-day E_{ta} values included in an event longer than one day have also to be non-zero values so that the daily precipitation totals within the event are all considerable as sufficiently significant, i.e. as extreme. For further details about the computation and reasons of WEI, we refer the reader to (Müller and Kaspar, 2014).

In contradiction to the widely used approaches for evaluating precipitation extremes (annual block maxima or peaks over threshold), the WEI consists of areal assessment of events – it enables to optimize and delimit the area affected by the extreme precipitation within a wider precipitation field.

Based on the highest WEI independent values (irrespective of their 1–10 days duration), we selected and further examined the first 54 EPEs in this study; one EPE per year of the study period.

2.4. Other data sets

Two catalogues of the weather types were used to analyse the synoptic conditions during the EPEs; a manual 'Grosswetterlagen' catalogue (GWLc, Werner and Gerstengarbe, 2010) and an automated SynopVisGWL-catalogue (SVGc, James, 2007; James, 2015; personal communication). Subsequently, a weather type was assigned to each EPE. For EPEs lasting longer than one day, the most frequent weather type during such EPEs was taken into consideration. If the weather types were of similar frequency during an EPE, the weather type assigned to the day of the highest 1-day E_{ta} value was considered.

Since the GWLc provides qualitative rather than quantitative information about synoptic situation during EPEs, the ERA-40 gridded reanalysis (2.5°a horizontal resolution) daily data (Uppala *et al*., 2005) provided by ECMWF for the study area (5°–10°E, 47.5°–50°N) at two isobaric levels (500 and 850 hPa) at 12 UTC were used to quantify synoptic conditions during EPEs that occurred during 1960–2010. The velocity of meridional and zonal airflow components was derived to provide information about wind direction during EPEs. Meridional and zonal flux of specific humidity was calculated since it was suggested as one of predictors of extreme large-scale precipitation by Müller *et al*. (2009).

The cartographical outputs were constructed in Esri's ArcGIS 10.3 software using a high resolution (100 × 100 m) global multi-resolution topography model obtained from GeoMapApp (http://www.marine-geo.org/tools/GMRTMapTool/) as base map.

2.5. Analysis approach

The three strongest EPEs and the EPE that affected the largest area in the VG were described in detail, i.e. their synoptic situation was analysed in conjunction with the precipitation totals and river discharges. The synoptic situation was described mostly based on National Centers for Environmental Prediction/National Center for Atmospheric Research (NCEP/NCAR) reanalysis data (Kalnay *et al*., 1996), and the data from Koblenz Global Runoff Data Centre (GRDC) was used to examine the river discharges.

The seasonality of EPEs was analysed according to the occurrence of the first day of event in meteorological seasons (e.g. spring for 1 March to 31 May), and a division between summer half-year (SHY) (from April to September) events and winter half-year (WHY) events (from October to March) was also derived from the first day of event. No influence of the selection of first day of event compared to the second, third until the last day was detected in the conducted sensitivity analysis. In order to shorten the terms, summer (warm) half-year events and winter (cold) half-year events are written as SHY events (SHY EPEs) and WHY events (WHY EPEs), respectively.

The resulting duration of events served to divide the EPEs between short and long. Various characteristics of short/long EPEs and SHY/WHY EPEs were studied: affected area, extremity (expressed by WEI), inter-annual changes, and synoptic conditions. The relationship between duration, affected area, and extremity was expressed through correlation coefficient at 1 and 5% p-value levels, and the covariance was also computed.

The inter-annual changes were examined using simple linear regression for different durations. The synoptic conditions were analysed based on the two GWLc and values of synoptic variables (Section 2.4). For the later, the daily means of the derived synoptic variables (meridional and

Table 1. The 10 first EPEs from 54 selected EPEs ranged in the decreasing order of their extremity (WEI)

EPE	Starting date	Duration (days)	WEI [log(years)km]	Affected area (%)	N_{max} (years)	Rd_{max} (mm)	GWLc	SVGc
1	*11 November 1996*	*2*	*120.21*	*47*	*1000*	*68.6*	*NEa*	*HFa*
2	**12 September 1986**	**5**	**118.86**	**68**	**437**	**61.2**	**TrW**	**Sz**
3	17 September 2006	1	115.86	35	1000	142.0	TM	TB
4	*02 October2006*	*2*	*109.28*	*65*	*316*	*72.0*	*WS*	*WW*
5	**23 May 1983**	**4**	**102.83**	**75**	**357**	**81.3**	**SEz**	**WS**
6	10 May 1970	2	92.29	31	1000	83.8	TM	SEz
7	*28 October 1998*	*1*	*91.58*	*40*	*1000*	*109.0*	*WS*	*WS*
8	*25 February 1997*	*1*	*81.66*	*42*	*265*	*106.9*	*NEa*	*HNFa*
9	22 July 1995	1	69.16	21	476	82.0	Wz	NWz
10	*13 February 1990*	*2*	*62.88*	*31*	*546*	*156.2*	*TM*	*SEz*

From left to right: number of event, starting day, WEI values, affected area as a percentage of the whole study area, maximum return period level (N_{max}) at a station, maximum daily precipitation total (Rd_{max}) at a station, and the weather types based on GWLc and SVGc. Winter half-year EPEs are given in italic and long EPEs (i.e. 3–5 days EPEs) are displayed in bold.

zonal airflow components and meridional and zonal flux of specific humidity) were calculated in VG (i.e. six grid points), and the highest absolute values (i.e. minimum or maximum) of variables during EPEs were assigned to each EPE following Müller *et al*. (2009) and Kašpar and Müller (2014), who suggested that the anomalies are essential for heavy rainfall. We are aware that the non-availability of quantitative variables during 2011–2013 may influence our results. However, following Zolina *et al*. (2005, 2013) we consider the influence less significant, since 3 years represent less than 6% of the study period.

3. Results and discussion

3.1. The three strongest EPEs

The maximum EPE (WEI = 120) started on 11 November 1996 and lasted 2 days (Table 1, Figure 3(a)). On 11 November, the highest daily precipitation total was recorded at the Bains rain gauge station (67.3 mm). On 12 November, even 68.6 mm total was measured at the Terre-Natale station situated not far away from the Bains station (the position of both stations is westward from the southern VG). The study area was under the influence of a stationary cold front separating warm and moist air over western Mediterranean and Central Europe from the cold air which earlier penetrated along the West-European coast up to Portugal. A strong temperature gradient in lower troposphere positioned below the front side of an upper-level trough remained for both days over the VG region, as it is obvious from NCEP/NCAR reanalysis data (Kalnay *et al*., 1996). As a result, heavy precipitation occurred mostly in the southwestern (SW) part of the VG and was not related to orography, which is rather typical for stationary cold front. Subsequent to this EPE, according to data from GRDC, a very strong increase in discharge generated a heavy flood on 14 and 15 November at the Moselle River with mean daily discharges of 1350 $m^3 s^{-1}$ recorded at the hydrological station in Cochem. Flooding was documented in the Saône River Basin on 13 November in the villages of Monthureux-sur-Saône and Bourbéville, where house-marks can still be found (EPTB, n.d.).

The second EPE of nearly the same magnitude (WEI = 119, Table 1) started on 12 September 1986 and lasted 5 days. It affected larger area as compared to the 1996 EPE (68% of the study area, Figure 3(b)). Badonviller weather station situated west–north-west of the Middle VG recorded 61.2 mm on 14 September. As in the case of the 1996 EPE, a stationary cold front prevailed over the region. In 1986, westwards of the front, a trough was present at higher altitudes, and there was an advection of warm and moist air in the foreground of the front. Then shallow lows or frontal waves passed at the front interface and resulted in heavy precipitation in the region. The discharge significantly increased from 12 to 18 September at the Meuse River, Saar River, and mainly Moselle River, where the mean daily discharge increased from 33 to 681 $m^3 s^{-1}$ in Perl, and from 86 to 927 $m^3 s^{-1}$ in Cochem (GRDC).

The third EPE (WEI = 116) occurred on 17 September 2006 (Table 1). Among the three strongest EPEs it was the most recent, and due to its very short (1-day) duration it affected the least part of the study area (35%, Figure 3(c)). The highest daily rainfall total of 142.0 mm was recorded at the Padoux rain gauge (343 m a.s.l.) situated southeast of Nancy and north of Épinal. No strong pressure gradient was influencing the area that day, and according to the SVGc (James, 2007), the synoptic situation was classified to be low over British Isles. Nevertheless, a shallow trough was also situated over Germany, Alps, and northern Italy. The shallow low was present in the early morning of 17 September, and moved towards southeast during the day. The combined influence of shallow low pressure, dominant eastern airflow, and divergence at 300 hPa level in the study area suggests favourable conditions for an EPE. This can also be supported by 90% relative humidity at 700 hPa and intense vertical movements. In addition, convection might have played a role because such precipitation occurs frequently in autumn when the eastern airflow prevails in Central Europe (Tolasz *et al*., 2007). No orographical effect seems to occur in the third EPE as for the other two strongest EPEs. Though discharges at the Moselle River were not as high as in previous two cases, the increase was more rapid: between 17 and 19 September, mean daily

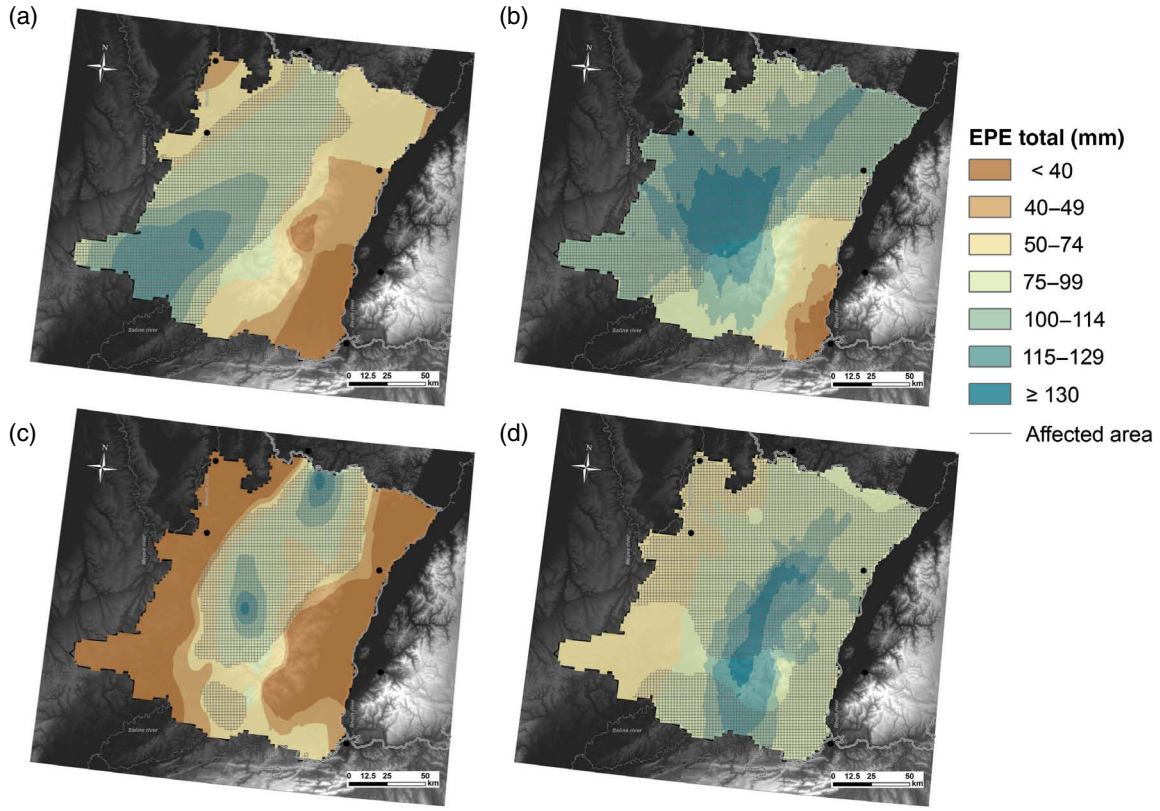

Figure 3. Gridded precipitation totals in study area for (a–c) the three strongest EPEs (EPEs 1–3 in Table 1) and (d) the EPE that affected the largest part of VG (EPE 5 in Table 1). The grey grid represents the area affected by EPEs using WEI. The grid resolution is 2 × 2 km. [Colour figure can be viewed at wileyonlinelibrary.com].

discharge increased from 27 to 426 $m^3 s^{-1}$ and from 67 to 538 $m^3 s^{-1}$ in Perl and in Cochem, respectively (GRDC). A house-mark in the village of Darney demarcates local flooding in the Saône River Basin (EPTB, n.d.).

Overall, the three heaviest EPEs were of similar WEI magnitude, and affected the study area according to their duration, i.e. shorter EPE affected smaller part of the VG. The return period estimates of the three strongest EPEs were very short (if detectable by the WEI) in the VG, whereas the longest return period levels were mostly detected on the windward Lorraine side. This may suggest comparatively lower orographical influence during the events. The two strongest EPEs were not related to the expected strong zonal circulation but to stationary cold fronts.

3.2. Seasonal distribution of EPEs

The seasonal distribution of 54 EPEs in meteorological seasons (Figure 4) shows that the EPEs occurred in all seasons (9 EPEs in spring and winter, 15 EPEs in summer) but most frequently in autumn (21 EPEs). The autumnal predominance of EPEs matches with the seasonality of mean precipitation in the study area only on the windward side of the VG, where the autumn is the most humid season (Section 2.1). The seasonality can also be documented by similar representation of SHY and WHY EPEs with 30 SHY EPEs found in the data set of 54 EPEs (Table S1, Supporting information).

The seasonal distribution suggests that the EPEs can occur irrespective of the mean precipitation season, which is in good agreement with Minářová *et al*. (2016). This may also be valid for the strongest EPEs as well since the ten strongest EPEs also occurred in all seasons (Table 1). However, the strongest EPEs (WEI value higher than 100) occurred mainly in autumn and spring, which is in contradiction to Minářová *et al*. (2016), who found the strongest events in peak summer. This might be related to the difference between station-to-station approach used in Minářová *et al*. (2016), which enables detection of even very local (peak summer) convective storms. The areal assessment by WEI in this study produced more reliable results for the area of interest.

3.3. Duration, affected area, and extremity of EPEs

3.3.1. Duration

The maximal duration of 54 EPEs was 5 days, i.e. 6–10 days EPEs did not occur (Figure 5). 1- and 2-days EPEs were the most frequent (26 and 19 EPEs, respectively). The short duration of EPEs is against our expectation, which was based on the general behaviour of precipitation in the VG area where precipitation lasts rather longer on average (Parlow, 1996; Minářová, 2013).

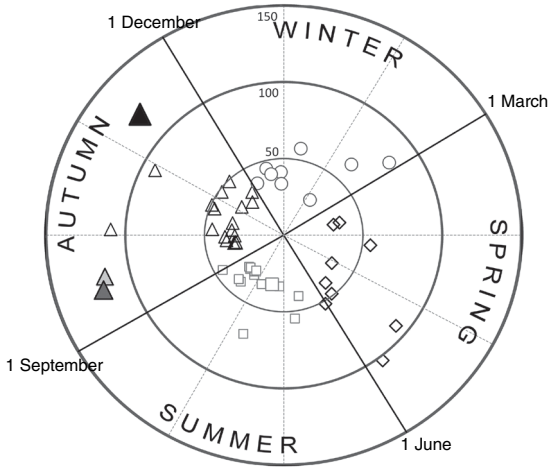

Figure 4. Seasonality of the 54 EPEs. The black squares represent spring EPEs, grey squares summer EPEs, triangles autumn EPEs and circles are used for winter EPEs. The first, second and third strongest EPE (Table 1) is represented by black, dark grey and light grey bigger triangle, respectively. Note that the EPEs were considered as vectors with the direction corresponding to the first day of an EPE, and the magnitude equal to the WEI value of the EPE [log(years)km], and calendar days in a year are displayed on an equally divided concentric circle.

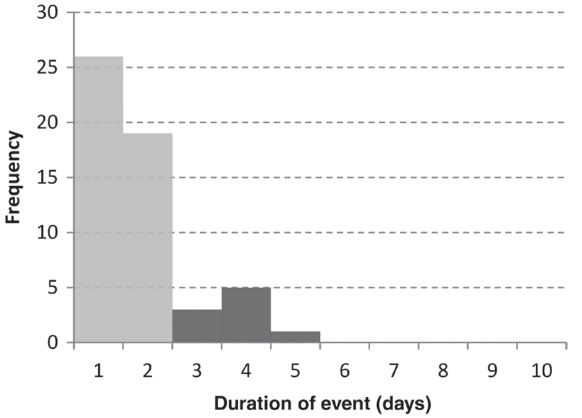

Figure 5. Frequency of 54 EPEs with respect to their duration: short EPEs are represented in light grey colour and long EPEs in dark grey colour.

The short duration may be explained by leeward convection, which is generally short lasting (Houze, 2014) and has been documented in the leeward side of the VG by the Convective and Orographically induced Precipitation Study campaign (Planche *et al*., 2013). Nevertheless, since the leeward convection mostly occurs in summer in Europe (Barry, 2008), short duration of EPEs in the VG area, which occurred mostly in autumn, is more likely related to rapid changes in precipitation activity during precipitation event in the area. In fact, the event-adjusted method enables to distinguish the most anomalous 1- to *x*-day EPE within a more continuous precipitation period, which also suggests that there can be more episodes of heavy rainfall within a precipitation sequence but separated by no or less extreme precipitation resulting in the decrease of the E_{ta}. Moreover, since the WEI tends to increase with increasing duration of event (and area) by definition, the short duration of EPEs found in VG suggests its plausibility.

Given that the study was limited to precipitation totals available only at daily resolution, return levels at a resolution of 3- or 1-h were not computable. This limitation hindered any comparison of 1- to 3-h return levels with the 1-day EPEs, which may categorize the 1-day EPEs into stratiform and convective.

We propose to consider 1–2 days EPEs as short EPEs, and 3–5 days EPEs as long EPEs because 1–2 days EPEs evince much higher frequency clearly differentiating them from 3 to 5 days EPEs (Figure 5). This division is maintained hereafter.

3.3.2. *Extremity and affected area*

The more frequent short EPEs were of similar range (WEI values 28–120) as compared to long EPEs (35–119) although less extreme in general (Figure 6). It may imply that the long EPEs are more severe. However, the ten strongest EPEs comprise only two long events (Table 1), suggesting that the relationship between duration and extremity of EPEs is more complicated.

Figure 6 also shows that short EPEs tend to affect smaller areas. Most commonly they affected 17–39% of the study area. It is in good agreement with the expectations since the short lasting heavy rainfall events affect smaller area as compared to the long lasting events due to likely restricted time for changes in circulation patterns (Houze, 2014). However, the area affected by short EPEs (6–72% of the VG area) is similar to that by long EPEs (16–75%). The reason for the similarity could be that the data set of long EPEs was too small (only 9 of the 54 EPEs were long) to show substantial differences from short EPEs.

The correlation coefficients calculated between pairs of variables [duration, extremity (WEI), and size of the area affected by 54 EPEs] showed that the pairs of variables are positively correlated (99% probability, except for the pair duration-extremity, where it was significant at the confidence level of 95%). The covariance was higher for the pair affected area-extremity (cov = 215.4, $r = 0.45$) than for duration-size of the affected area (cov = 6.5, $r = 0.43$). The stronger positive correlation between the size of the affected area and extremity is natural due to the definition of the WEI value, which increases with the size of the area.

The correlation coefficients were also calculated for the same variables for short and long EPEs, and SHY and WHY EPEs, separately. The short EPEs showed no correlation between the duration and extremity of events, and duration and size of the affected area of events; only the extremity and size of the affected area were positively correlated ($r = 0.35$ at $\alpha = 5\%$). The long EPEs exhibited the same results between three pairs of variables as the short EPEs ($r = 0.68$ at $\alpha = 5\%$ for the pair extremity-affected area). The SHY EPEs showed positive correlation between all the variables ($r = 0.49$ for duration-extremity, $r = 0.55$ for duration-size of the affected area, and $r = 0.58$ for extremity-size of the affected area at $\alpha = 1\%$), whereas

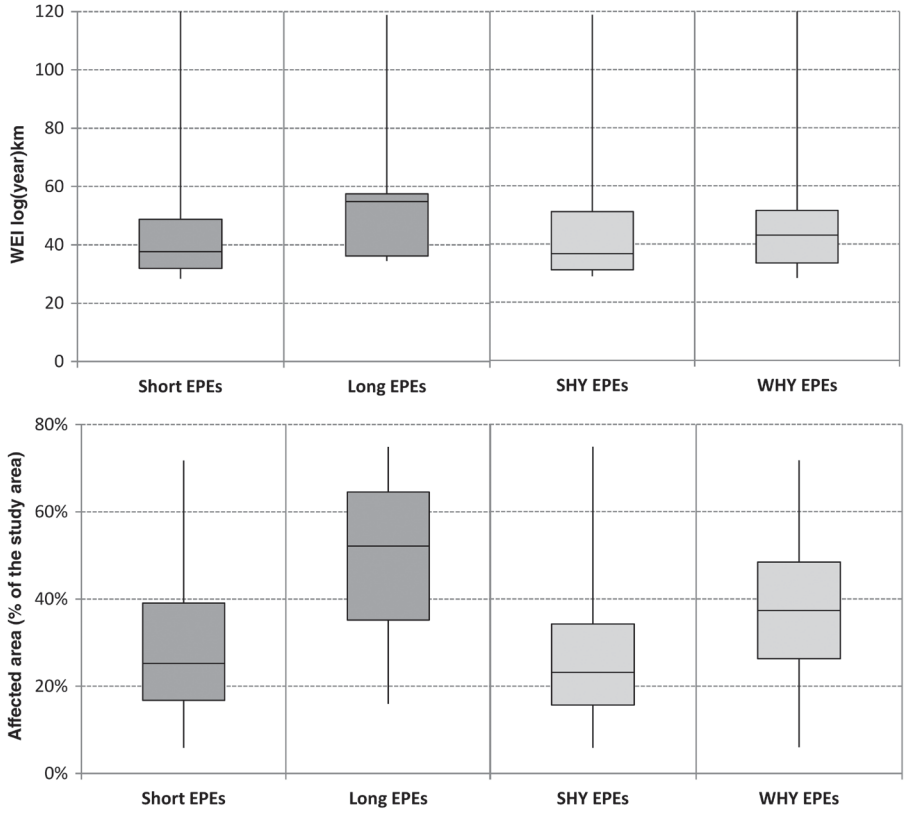

Figure 6. Boxplots for the (top) extremity and (bottom) affected area of (left) short and long EPEs (divided based on Figure 5), and (right) SHY and WHY EPEs.

for WHY EPEs no correlation between the variables was found. The results thus suggest that except the natural positive correlation between the affected area and extremity of EPEs following the definition of WEI, the relationships between the variables are not straightforward and the positive correlations are mostly due to the SHY EPEs.

3.3.3. The largest EPE

The EPE affecting the largest part of the study area (75%, Figure 3(d)) started on 23 May 1983 and lasted 4 days. It was the fifth strongest EPE (Table 1). The highest daily rainfall total of 81.3 mm was measured on 24 May at the Orbey-Lac Blanc rain gauge, situated in the VG westwards from Colmar. The event was connected with a low situated above northern Italy and Central Europe. Whereas above Poland daily temperature maxima surpassed 25 °C, the study area was situated in very cold air at the rear side of the cyclone; e.g. daily air temperature maxima were only about 10 °C in Strasbourg. A strong moisture flux approached the region from the north as warm and moist air turned around the low. The hydrological response was extra strong with maximum daily discharges over 2000 $m^3 s^{-1}$ in Perl and even more than 3000 $m^3 s^{-1}$ in Trier and Cochem (GRDC). The increase in discharge was ranked as the second-largest not only at Moselle since 1951 but also at German rivers Main and Neckar. However, huge flooding was also partly due to a particularly high saturation of the catchments, e.g. because of antecedent precipitation and flooding from April 1983 (EPE No. 12 in Table S1). Besides, it is worth noticing that the area affected by the EPE does not correspond with the area of highest precipitation (Figure 3(d)). It is related to both the WEI method that adjusts the affected area based on decreasing order of return period estimates in pixels instead of their location, and the climatic characteristics of the region, i.e. 4-day totals above 130 mm are not as extreme in southern High Vosges where the mean annual total is >2000 mm, as in northern Low Vosges where the mean annual total is below 800 mm. Thus the WEI enables capturing the area affected by EPEs objectively.

3.4. Inter-annual changes in EPEs

The inter-annual changes of maximal annual WEI values of events show that the extremity (WEI) of events was lower at the beginning of the study period and got higher mostly since 1980 (Figure 7). The lower extremity at the beginning of the study period might be connected with lesser availability of data (Figure 2) and limitations of the available instruments in measuring heavy rainfall (e.g. gauge overflow or wind influence on unshielded gauges). The EPEs being stronger since 1980 is in good agreement with the Beck's (2011) findings and with the findings of IPCC (2014), which showed likely increase in intensity of EPEs in Europe.

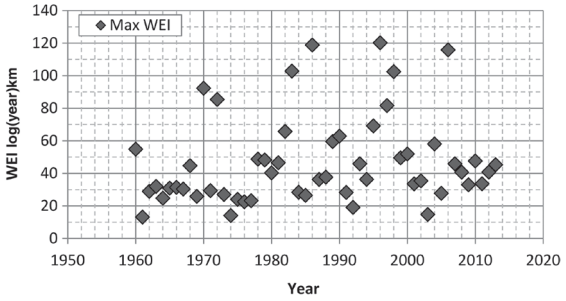

Figure 7. Inter-annual changes in maximum annual WEI values of events during the study period 1960–2013.

No significant increasing trend was identified in the frequency of EPEs unlike reported by IPCC (2014), which might be related to regional differences that have been suggested in the report. We tested 1, 3, 6, 18, and 27 years equally long-time intervals (divisible of 54 years study period) since the trend analysis can be influenced by the selected number of time intervals. All resulted in insignificant linear trends at $\alpha = 0.01$, $\alpha = 0.05$, and $\alpha = 0.10$ except for three equal time slices (i.e. 18-years) that showed an increasing trend in frequency of EPEs in VG at $\alpha = 0.10$. The trend analysis can also be influenced by the trend curve. Nevertheless, the other trend curves such as exponential, polynomial of second degree and logarithmic also resulted in insignificant trends for the analysed time slices and α.

Figure 8(a) shows that the short and long EPEs were the most frequent during 1980–1990 and no long EPE occurred during 1961–1977 and since 2005. Both the long and short EPEs experienced an insignificant trend during the period (at $\alpha = 0.01$, $\alpha = 0.05$, and $\alpha = 0.10$). The increase in numbers in short events in the latest period correspond with the climate projections by Klimaveränderung und Konsequenzen für die Wasserwirtschaft (KLIWA) (Söder *et al.*, 2009) who predicted increase in frequency of very short heavy rainfall.

The SHY EPEs were less frequent during 1990–2000 and the WHY EPEs were the most frequent during 1978–2002; only two WHY EPEs occurred out of the period 1978–2002 (Figure 8(b)). The trends in SHY and WHY EPEs were both insignificant (at $\alpha = 0.01$, $\alpha = 0.05$, and $\alpha = 0.10$), suggesting their difficult prediction. A similar regional study has been performed for the period 1931–2010 by KLIWA (climate change and its consequences for water management) in southern Germany (KLIWA, 2011). In five regions of the Rhine River Basin situated close to the VG area (from Basel to the tributary basin of Schwarzbach), the authors found increasing trends (significance lower than 80%) in 1-day maximum regional precipitation for both the summer (May–October) and winter (November–April) halves of the hydrological year.

In order to minimize the influence of trend analysis related to the arbitrary number of time slices, the SHY and WHY EPEs were also studied for 2, 3, 6, 9, and

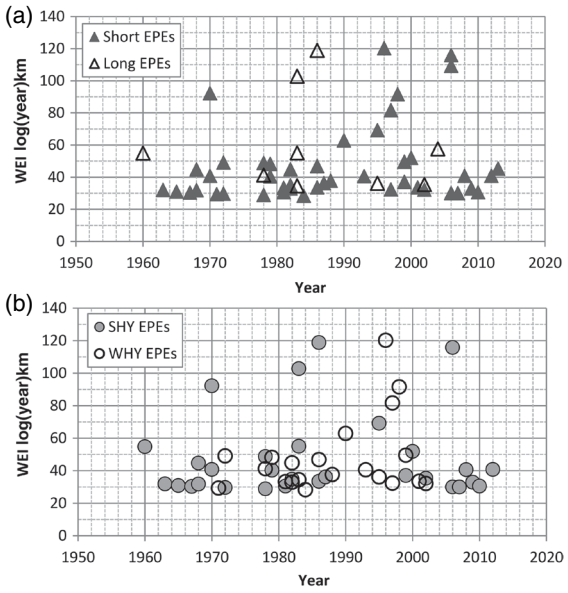

Figure 8. Inter-annual changes in (a) short and long EPEs (Figure 5), and (b) SHY and WHY EPEs during the study period 1960–2013.

18 equally long-time slices (not depicted). The results confirmed the general trend that was found in Figure 8, i.e. higher representation of SHY EPEs at the beginning and in the end of the study period, interrupted by a period of preponderance of WHY events.

3.5. Synoptic conditions of EPEs

Figure 9 displays the weather types that occurred during EPEs (the abbreviations are explained in Table 2). It shows that the west cyclonic weather type (Wz) prevailed during all 54 and 27 first EPEs for both the GWLc and SVGc. It is in good agreement with REKLIP (1995), where it was found that the precipitation in VG is often related to Wz. According to GWLc, the other most frequent weather types during the 54 EPEs were low over Central Europe (TM), trough over Western Europe (TrM) and south-shifted westerly circulation (WS). The TM weather type can cause precipitation on the eastern side of the VG and in the Upper Rhine River Plain when northern or northeastern airflow prevails in the area (REKLIP, 1995). According to SVGc, the north-west cyclonic (NWz) and south-shifted westerly (WS) weather types were among the most frequent during the 54 EPEs (i.e. after Wz). Two more weather types related to EPEs were found in SVGc contrary to the GWLc, although both catalogues include equal number of types.

Although Wz prevailed during the 54 EPEs, it was not related to any of the five strongest EPEs for both the GWLc and SVGc, and to any of the first 11 EPEs for SVGc (Figure 9). This suggests that Wz is not the prevailing synoptic pattern during the very EPEs in VG and that there is a discrepancy between the most frequent weather types during EPEs and the ones producing strongest EPEs, although we are aware about the low number of representatives for the strongest EPEs.

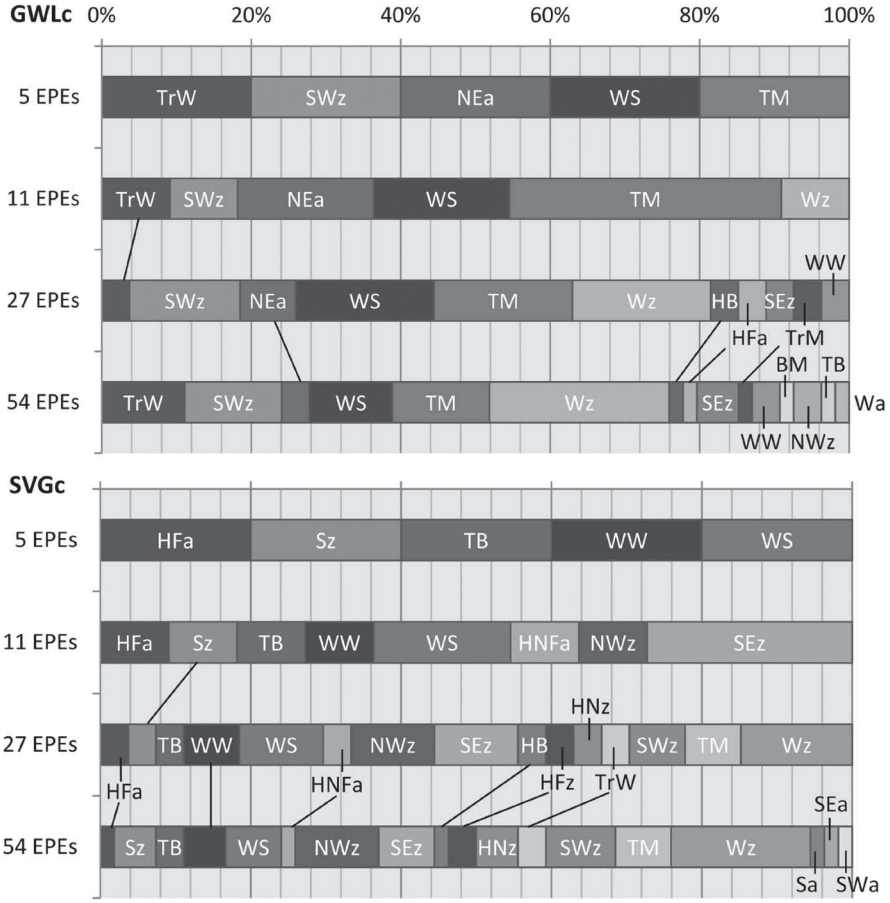

Figure 9. Relative representation of the weather types (explained in Table 2) based on (top) GWLc and (bottom) SVGc that occurred during 5, 11, 27 strongest EPEs (ranking according to Table S1), and all 54 EPEs.

Among the five strongest EPEs no weather type dominated, i.e. the synoptic pattern was diverse. It is in accordance with the general conjecture about various characteristics of the strong EPEs or their strong sensitivity on selected data set (Stephenson *et al*., 2008).

Although based on widely used GWLc and automated SVGc, some rather unusual weather patterns such as anticyclonic weather are linked to EPEs, more frequently in the case of subjective GWLc. It may be connected to the fact that the weather types over Europe from GWLc and SVGc are assessed from the view of Central Europe, VG being situated at its most western part, and at large scale. It suggests that the results are catalogue-dependent and not so precise for very regional analyses. Thus the synoptic conditions during EPEs were also assessed quantitatively.

Figure 10 shows that the EPEs occurred mostly in strong SW airflow at 850 hPa and in western, SW and southern airflow at 500 hPa level. Similar findings can be found in REKLIP (1995), where the SW airflow was related to high precipitation totals (Rd > 100 mm) in VG. Analogous direction and strong values are also found for the flux of specific humidity. Figure 10 shows clearly that strong values of synoptic variables are frequently responsible for extreme precipitation. This corresponds to Müller and Kašpar (2010), who found that usually strong moisture fluxes accompany hydrometeorological extremes in this part of Europe. The strongest EPEs occurred when strongest values of variables were measured, which is especially true for the airflow at 500 hPa level. Other synoptic variables can be analysed such as vertical velocity and relative vorticity with respect to EPEs, while our analysis was restricted to the aforementioned accessible variables. Another quantitative approach introducing a Circulation Extremity Index proposed by Kašpar and Müller (2014) can provide the in-depth study of circulation causes of the EPEs and can be tested in future.

Two EPEs were missed in the quantitative analysis of synoptic variables since they occurred after 2010, i.e. beyond the available data set. However, these EPEs were not among the strongest (20th and 25th in 54 EPEs, Table S1) and they represented <4% of EPEs, thus their influence on the results was considered negligible and the results accurate (Zolina *et al*., 2005, 2013).

3.6. Comparison of WEI with standard indices

The ten strongest EPEs defined by WEI (Table 1) were compared with standard indices, i.e. exceeding a defined precipitation threshold value at a station (Štekl, 2001;

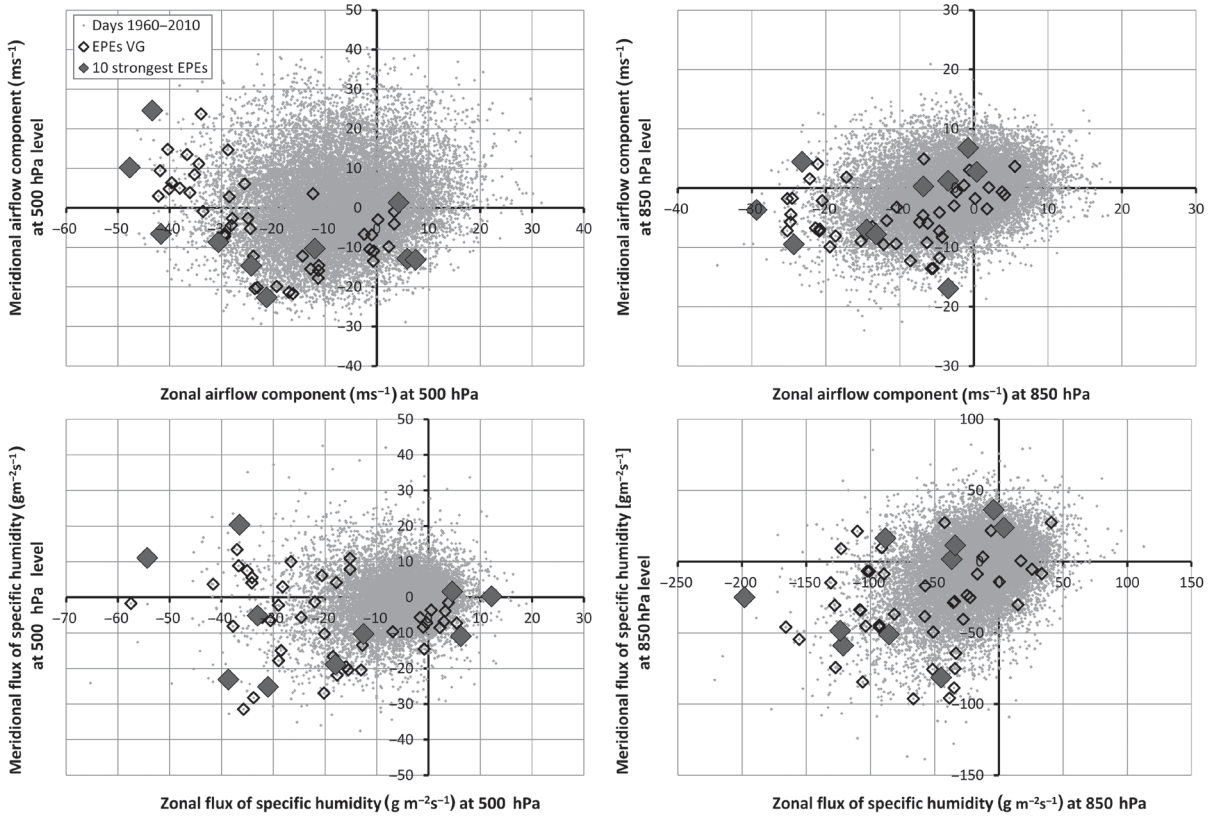

Figure 10. Zonal and meridional (top) airflow component and (bottom) flux of specific humidity at (left) 500 hPa and (right) 850 hPa levels during study period on daily basis and absolute maxima during 54 and 10 strongest EPEs.

Muluneh *et al*., 2016; Ngo-Duc *et al*., 2016; Tošić *et al*., 2016; Wang *et al*., 2016a), and mean areal precipitation totals MAP (e.g. Wang *et al*., 2000; Konrad, 2001). Since the EPEs in VG lasted 1–5 days and a fixed duration in both the methods is required, the 1-, 3-, and 5-days totals were considered. The threshold precipitation total was set to 100 mm for 1-day totals (according to REKLIP, 1995), 200 mm for 3-days totals and 300 mm for 5-days totals.

Figure 11 shows that the WEI values correspond with 1-day maximum precipitation totals if the EPE lasted 1-day (Table 1, e.g. EPE from 17 September 2006). The 3-day totals match with WEI values in most cases except some EPEs, for which a station-to-station approach may result in longer duration of such EPEs. The highest fluctuation as compared to WEI values is found for 5-day point maximum precipitation totals, which may be due to only one 5-day EPE found through WEI. Figure 11 also demonstrates that the fixed duration of EPEs can lead to some uncertainties. For instance, if 3- or 5-days totals are considered, the ninth strongest EPE from 1995 may be considered longer than it obviously was or not considered at all. Thus the major advantage of WEI is that it enables to adjust the duration for each EPE without any arbitrary criterion. Even the maximum allowed duration of precipitation totals does not influence the results of WEI if it is fixed sufficiently long, as in our case.

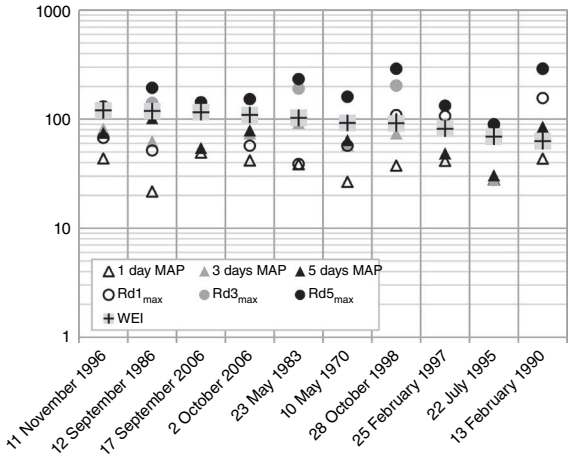

Figure 11. The ten strongest EPEs characterized by the WEI, 1- and 3-days mean areal precipitation totals (1 day MAP and 3 days MAP, respectively), and maximum 1- and 3-days precipitation totals at a rain gauge ($Rd1_{max}$ and $Rd3_{max}$, respectively). Note that the *y*-axis is at logarithmic scale since the totals are in mm and the WEI in log(years)km.

The 3-days MAP was best matching with decreasing WEI values, and the 1-day MAP showed most fluctuation as compared to WEI. More differences of 1-day MAP from WEI may be related to the fact that the short events generally affect much smaller area than the whole study

Table 2. Explication of the abbreviations of the weather types used in GWLc and SVGc that occurred during EPEs in VG (Figure 9).

BM	Zonal Ridge across Central Europe
HB	High over the British Isles
HFa	Scandinavian High, Ridge Central Europe
HFz	Scandinavian High, Trough Central Europe
HNFa	High Scandinavia–Iceland, Ridge Central Europe
HNz	Icelandic High, Trough Central Europe
NEa	North-east anticyclonic
Nz	North cyclonic
NWz	North-west cyclonic
Sa	South anticyclonic
SEa	South-east anticyclonic
SEz	South-east cyclonic
SWa	South-west anticyclonic
SWz	South-west cyclonic
Sz	South cyclonic
TB	Low over the British Isles
TM	Low over Central Europe
TrM	Trough over Central Europe
TrW	Trough over Western Europe
Wa	West anticyclonic
WS	South-shifted westerly
WW	Westerly, Block Eastern Europe
Wz	West cyclonic

region. In fact, the size of the area affected by EPEs was only 50% of the study area on average. Thus in comparison to MAP where a fixed area is needed, and to point specific totals, the adjustable size of the affected area by EPEs through WEI is another valuable advantage. The results are in good agreement with Müller *et al*. (2015b), who discussed the WEI with the standard indices for the Czech Republic.

Figure 11 shows that the ranking of EPEs also depends on the assessment method, however a comparison in the ranking of ten first EPEs based on each aforementioned method highlights that seven out of ten first EPEs based on WEI were also recorded by at least one of other method among the ten strongest. Thus the WEI method can be considered capable of providing relevant results, and its adjustable duration and size of the area affected by EPEs make it unique and simple tool for the analysis of weather and climate extremes.

4. Conclusions

The event-adjusted evaluation technique of weather extremes (Müller and Kaspar, 2014) was applied to select a data set of EPEs in the VG region situated at the Western–Central Europe frontier in order to conduct further analyses to better understand the characteristics of selected EPEs. Similar to Schiller (2016), who used the WEI for evaluation of heavy rainfall in Germany in her master thesis (supported by German Weather Service), this study confirms that the WEI is also applicable in France and at regional scale. Based on WEI calculated for Germany and its states, Schiller (2016) showed the non-linear change of WEI values with the size of the considered area. On the other hand, the WEI values can be easily converted to make them comparable among regions of different sizes. The WEI has thus huge potential and can also be applied on grid of high resolution, remote sensing data, and data of shorter periods, e.g. seasonal data.

The main aim of the paper was to investigate various characteristics of the 54 selected EPEs, for the first time in VG to provide new insights into the extreme precipitation in the region. The EPEs data set was appropriate since maximum EPEs caused floods or significant increases in runoff. The results show that autumn was the major season of EPEs though the EPEs occurred in all meteorological seasons. SHY EPEs were slightly more represented than the WHY EPEs. The EPEs lasted 1–5 days, although the analysis permitted up to 10 days duration of events. Short EPEs (1–2 days, most frequent) and SHY EPEs tended to affect smaller areas as compared to the long EPEs (3–5 days) and WHY EPEs. The correlation coefficients showed positive correlation between the extremity (WEI) of EPE and the size of the area affected by the EPE. The positive correlation between the size of the affected area and duration of EPEs was strongest for SHY EPEs. No significant trend was identified in the frequencies of all EPEs, of long and short EPEs, and of SHY and WHY EPEs during the study period. Given that the three most extreme events occurred during the last 30 years, there is a potential to extend the trend analysis of precipitation in future.

Based on both GWLc and SVGc, the west cyclonic weather type occurred most often during the EPEs. However, the strongest EPEs were frequently related to different weather types and mostly to stationary cold front rather than to the expected strong zonal circulation. The quantitative analysis of synoptic variables showed strong SW airflow and flux of specific humidity to be responsible for most of EPEs.

We believe that the ranking of EPEs according to their extremity in the VG region provides useful information for local decision makers and risk managers. We also believe that our findings can be significant for climate projections. Furthermore, we hope that the event-adjusted evaluation technique of weather extremes will attract wider attention and will be applied by researchers in many regions.

Our future work will not only be concentrated on a more detailed analysis of the spatial distribution of EPEs in VG but will also be focused on the comparison of these findings with the results from similar regions.

Acknowledgements

The authors thank Météo-France, ECMWF (ERA-40 re-analysis) and Global Runoff Data Centre (GDRC, 56068 Koblenz, Germany) for providing data, and the BGF (French Government scholarship) to grant the research during 15 months. They also thank Dr Lukáš Pop for his help in computing the three parameters of the GEV in MatLab. They extend great thanks to Syed Muntazir

Abbas, MPhil, who gave valuable remarks during the revision of the manuscript, and substantially improved the language of the manuscript.

Supporting information

The following supporting information is available as part of the online article:

Table S1. 54 selected EPEs ranged in the decreasing order of their extremity (WEI). From left to right: number of event, starting day, WEI values, affected area as a percentage of the whole study area, maximum return period level (N_{max}) at a station, maximum daily precipitation total (Rd_{max}) at a station, and the weather types based on GWLc and SVGc. Winter half-year EPEs are highlighted by italic and long EPEs (i.e. 3–5 days) are displayed by bold.

References

Allan RP, Lavers DA, Champion AJ. 2015. Diagnosing links between atmospheric moisture and extreme daily precipitation over the UK. *Int. J. Climatol.* **36**(9): 3191–3206. https://doi.org/10.1002/joc.4547.

Alsatia. 1932. *L´Alsace: précis de la géographie régionale des départements Haut-Rhin et Bas-Rhin*. Alsatia: Colmar, France.

Balling RC, Keikhosravi Kiany MS, Sen Roy S, Khoshhal J. 2016. Trends in extreme precipitation indices in Iran: 1951–2007. *Adv. Meteorol.* 2016: e2456809. https://doi.org/10.1155/2016/2456809.

Barros V, Field C, Dokke D, Mastrandrea M, Mach K, Bilir T, Chatterjee M, Ebi K, Estrada Y, Genova R, Girma B, Kissel E, Levy A, MacCracken S, Mastrandrea P, White L. 2014. *Climate Change 2014: Impacts, Adaptation, and Vulnerability. Part B: Regional Aspects. Contribution of Working Group II to the Fifth Assessment Report of the Intergovernmental Panel on Climate Change*. Cambridge University Press: Cambridge, UK.

Barry RG. 2008. *Mountain Weather and Climate*, 3rd edn. Cambridge University Press: Cambridge, UK.

Beck J-S. 2011. *2000 Ans de Climat en Alsace et en Lorraine*. Éd. Coprur: Strasbourg, France.

Blanchet J, Molinié G, Touati J. 2016. Spatial analysis of trend in extreme daily rainfall in southern France. *Clim. Dyn.* : 1–14. https://doi.org/10.1007/s00382-016-3122-7.

Blenkinsop S, Lewis E, Chan SC, Fowler HJ. 2016. Quality-control of an hourly rainfall dataset and climatology of extremes for the UK. *Int. J. Climatol.* **37**(2): 722–740. https://doi.org/10.1002/joc.4735.

Coelho CAS, Ferro CAT, Stephenson DB, Steinskog DJ. 2008. Methods for exploring spatial and temporal variability of extreme events in climate data. *J. Clim.* **21**(10): 2072–2092. https://doi.org/10.1175/2007JCLI1781.1.

Coles S. 2001. *An Introduction to Statistical Modeling of Extreme Values*. Springer: London; New York, NY.

Conradt T, Roers M, Schröter K, Elmer F, Hoffmann P, Koch H, Hattermann FF, Wechsung F. 2013. Comparison of the extreme floods of 2002 and 2013 in the German part of the Elbe River basin and their runoff simulation by SWIM-live. *Hydrol. Wasserbewirtsch.* **57**(5): 241–245. https://doi.org/10.5675/HyWa-2013,5-4.

Cutter SL, Barnes L, Berry M, Burton C, Evans E, Tate E, Webb J. 2008. A place-based model for understanding community resilience to natural disasters. *Glob. Environ. Change* **18**(4): 598–606. https://doi.org/10.1016/j.gloenvcha.2008.07.013.

EPTB. (n.d.). *Reperes de crue - Saône/Programme d'Actions de Prévention des Inondations*. EPTB Saône Doubs.

Ernst F. 1988. *Panorama de la géographie physique de l'Alsace; et Les régions naturelles de l'Alsace*. Conjonture Alsacienne.

Ghenim AN, Megnounif A. 2016. Variability and trend of annual maximum daily rainfall in northern Algeria. *Int. J. Geophys.* **2016**: 1–11. https://doi.org/10.1155/2016/6820397.

Gley G. 1867. *Géographie physique, industrielle, administrative et historique des Vosges*. V.e Gley Impr. V.e & Durand Libraire: Épinal, France.

Grams CM, Binder H, Pfahl S, Piaget N, Wernli H. 2014. Atmospheric processes triggering the central European floods in June 2013. *Nat. Hazards Earth Syst. Sci.* **14**(7): 1691–1702. https://doi.org/10.5194/nhess-14-1691-2014.

Hosking JRM, Wallis JR. 2005. *Regional Frequency Analysis: An Approach Based on L-Moments*. Cambridge University Press: Cambridge, UK.

Houze RA. 2014. *Cloud Dynamics*. Academic Press: Oxford, UK.

IPCC. 2014. Climate Change 2014. Synthesis Report. Contribution of Working Groups I, II and III to the Fifth Assessment Report of the Intergovernmental Panel on Climate Change [Core Writing Team, Pachauri RK, Meyer LA (eds.)]. IPCC: Geneva, Switzerland, 151 pp.

James PM. 2007. An objective classification method for Hess and Brezowsky Grosswetterlagen over Europe. *Theor. Appl. Climatol.* **88**(1–2): 17–42. https://doi.org/10.1007/s00704-006-0239-3.

Kalnay E, Kanamitsu M, Kistler R, Collins W, Deaven D, Gandin L, Iredell M, Saha S, White G, Woollen J, Zhu Y, Leetmaa A, Reynolds R, Chelliah M, Ebisuzaki W, Higgins W, Janowiak J, Mo KC, Ropelewski C, Wang J, Jenne R, Joseph D. 1996. The NCEP/NCAR 40-year reanalysis project. *Bull. Am. Meteorol. Soc.* **77**(3): 437–471. https://doi.org/10.1175/1520-0477(1996)077<0437:TNYRP>2.0.CO;2.

Kašpar M, Müller M. 2014. Combinations of large-scale circulation anomalies conducive to precipitation extremes in the Czech Republic. *Atmos. Res.* **138**: 205–212. https://doi.org/10.1016/j.atmosres.2013.11.014.

Kašpar M, Müller M, Crhová L, Holtanová E, Polášek JF, Pop L, Valeriánová A. 2016. Relationship between Czech windstorms and air temperature. *Int. J. Climatol.* **37**(1): 11–24. https://doi.org/10.1002/joc.4682.

Katz RW. 2010. Statistics of extremes in climate change. *Clim. Change* **100**(1): 71–76. https://doi.org/10.1007/s10584-010-9834-5.

Katz RW, Parlange MB, Naveau P. 2002. Statistics of extremes in hydrology. *Adv. Water Resour.* **25**(8–12): 1287–1304. https://doi.org/10.1016/S0309-1708(02)00056-8.

KLIWA. 2011. *Klimawandel in Süddeutschland Veränderungen von meteorologischen und hydrologischen Kenngrößen*. Monitoring report. Deutscher Wetterdienst: Offenbach, Germany, 58 pp.

Konrad CE. 2001. The most extreme precipitation events over the eastern United States from 1950 to 1996: considerations of scale. *J. Hydrometeorol.* **2**(3): 309–325. https://doi.org/10.1175/1525-7541(2001)002<0309:TMEPEO>2.0.CO;2.

Météo-France. 2008. *Climatologie des Vosges*. Météo-France au service des Vosges: le centre dépertemental d´Épinal: Épinal, France, 10 pp.

Minářová J. 2013. Climatology of precipitation in the Vosges Mountain range area. *AUC Geogr.* **48**(2): 51–60.

Minářová J, Müller M, Clappier A. 2016. Seasonality of mean and heavy precipitation in the area of the Vosges Mountains: dependence on the selection criterion. *Int. J. Climatol.* **37**(5): 2654–2666. https://doi.org/10.1002/joc.4871.

Müller M, Kašpar M. 2010. Quantitative aspect in circulation type classifications – an example based on evaluation of moisture flux anomalies. *Phys. Chem. Earth Parts A/B/C* **35**(9–12): 484–490. https://doi.org/10.1016/j.pce.2009.09.004.

Müller M, Kaspar M. 2014. Event-adjusted evaluation of weather and climate extremes. *Nat. Hazards Earth Syst. Sci.* **14**(2): 473–483. https://doi.org/10.5194/nhess-14-473-2014.

Müller M, Kašpar M, Řezáčová D, Sokol Z. 2009. Extremeness of meteorological variables as an indicator of extreme precipitation events. *Atmos. Res.* **92**(3): 308–317. https://doi.org/10.1016/j.atmosres.2009.01.010.

Müller M, Kašpar M, Valeriánová A, Crhová L, Holtanová E. 2015a. Evaluation of precipitation extremes and floods and comparison between their temporal distributions. *Nat. Hazards Earth Syst. Sci.* **12**(1): 281–310. https://doi.org/10.5194/hessd-12-281-2015.

Müller M, Kašpar M, Valeriánová A, Crhová L, Holtanová E, Gvoždíková B. 2015b. Novel indices for the comparison of precipitation extremes and floods: an example from the Czech territory. *Hydrol. Earth Syst. Sci.* **19**(11): 4641–4652. https://doi.org/10.5194/hess-19-4641-2015.

Muluneh A, Bewket W, Keesstra S, Stroosnijder L. 2016. Searching for evidence of changes in extreme rainfall indices in the Central Rift Valley of Ethiopia. *Theor. Appl. Climatol.* : 1–15. https://doi.org/10.1007/s00704-016-1739-4.

Ngo-Duc T, Tangang FT, Santisirisomboon J, Cruz F, Trinh-Tuan L, Nguyen-Xuan T, Phan-Van T, Juneng L, Narisma G, Singhruck P, Gunawan D, Aldrian E. 2016. Performance evaluation of RegCM4 in simulating extreme rainfall and temperature indices over the CORDEX-Southeast Asia region. *Int. J. Climatol.* **37**(3): 1634–1647. https://doi.org/10.1002/joc.4803.

Parlow E. 1996. The regional climate project REKLIP – an overview. *Theor. Appl. Climatol.* **53**(1–3): 3–7. https://doi.org/10.1007/BF00866406.

van Pelt SC, Beersma JJ, Buishand TA, van den Hurk BJJM, Schellekens J. 2014. Uncertainty in the future change of extreme precipitation over the Rhine basin: the role of internal climate variability. *Clim. Dyn.* **44**(7–8): 1789–1800. https://doi.org/10.1007/s00382-014-2312-4.

Planche C, Wobrock W, Flossmann AI, Tridon F, Labbouz L, Van Baelen J. 2013. Small scale topography influence on the formation of three convective systems observed during COPS over the Vosges Mountains. *Meteorol. Z.* **22**(4): 395–411. https://doi.org/10.1127/0941-2948/2013/0402.

REKLIP. 1995. *Klimaatlas Oberhein Mitte-Süd: REKLIP, Regio-Klima-Projeckt*. Vdf Hochschulverl: Zürich, Switzerland.

Rudolf B, Rapp J. 2002. Das Jahrhunderthochwasser der Elbe: Synoptische Wetterentwicklung und klimatologische Aspekte. *DWD Klimastatusbericht* : 172–187.

Schiller J. 2016. *Eine Sensitivitätsanalyse des Weather Extremity Index (WEI) nach Müller und Kaspar zur Beschreibung extremer Niederschläge unter Verwendung radarbasierter Niederschlagsmessungen des Deutschen Wetterdienstes*. University of Cologne: Cologne, Germany.

Sell Y. 1998. *L'Alsace et les Vosges*. Delachaux et Niestlé: Lausanne, Switzerland.

Söder M, Conrad M, Gönner T, Kusch W. 2009. *Les changements climatiques en Allemagne du Sud: Ampleur – Conséquences – Stratégies*. Brochure. Klimaveränderung und Konsequenzen für die Wasserwirtschaft (KLIWA): Mainz, Germany, 1–20.

Štekl J (ed). 2001. *Extrémni denní srážky na území České Republiky v období 1879–2000 a jejich synoptické příčny (Extreme Daily Precipitation on the Territory of the Czech Republic in the Period 1879–2000 and Their Synoptic Causes)*. Český hydrometeorologický ústav: Praha, Slovakia.

Stephenson DB, Diaz HF, Murnane RJ. 2008. *Definition, Diagnosis, and Origin of Extreme Weather and Climate Events*. Cambridge University Press: New York, NY.

Tolasz R, Brázdil R, Bulíř O, Dobrovolný P, Dubrovský M, Hájková L, Halásová O, Hostýnek J, Janouch M, Kohut M, Krška K, Křivancová S, Květoň V, Lepka Z, Lipina P, Macková J, Metelka L, Míková T, Mrkvica Z, Možný M, Nekovář J, Němec L, Pokorný J, Reitschläger JD, Richterová D, Rožnovský J, Řepka M, Semerádová D, Sosna V, Stříž M, Šercl P, Škáchová H, Štěpánek P, Štěpánková P, Trnka M, Valeriánová A, Valter J, Vaníček K, Vavruška F, Voženílek V, Vráblík T, Vysoudil M, Zahradníček J, Zusková I, Žák M, Žalud Z. 2007. *Altas podnebí Česka (Climate Atlas of Czechia)*. Český hydrometeorologický ústav, Universita Palackého: Olomouc, Czech Republic.

Tošić I, Unkašević M, Putniković S. 2016. Extreme daily precipitation: the case of Serbia in 2014. *Theor. Appl. Climatol.* : 1–10. https://doi.org/10.1007/s00704-016-1749-2.

Uppala SM, KÅllberg PW, Simmons AJ, Andrae U, Bechtold VDC, Fiorino M, Gibson JK, Haseler J, Hernandez A, Kelly GA, Li X, Onogi K, Saarinen S, Sokka N, Allan RP, Andersson E, Arpe K, Balmaseda MA, Beljaars ACM, Berg LVD, Bidlot J, Bormann N, Caires S, Chevallier F, Dethof A, Dragosavac M, Fisher M, Fuentes M, Hagemann S, Hólm E, Hoskins BJ, Isaksen L, Janssen PAEM, Jenne R, Mcnally AP, Mahfouf J-F, Morcrette J-J, Rayner NA, Saunders RW, Simon P, Sterl A, Trenberth KE, Untch A, Vasiljevic D, Viterbo P, Woollen J. 2005. The ERA-40 re-analysis. *Q. J. R. Meteorol. Soc.* **131**(612): 2961–3012. https://doi.org/10.1256/qj.04.176.

Valeriánová A, Crhová L, Holtanová E, Kašpar M, Müller M, Pecho J. 2015. High temperature extremes in the Czech Republic 1961–2010 and their synoptic variants. *Theor. Appl. Climatol.* **127**(1): 17–29. https://doi.org/10.1007/s00704-015-1614-8.

Wang D, Smith MB, Zhang Z, Reed S, Koren VI. 2000. Statistical comparison of mean areal precipitation estimates from WSR-88D, operational, and historical gage networks. *15th Annual Conference on Hydrology, 80th Meeting of the AMS,* Long Beach, CA, 10–14 January.

Wang Q, Wang M, Fan X, Zhang F, Zhu S, Zhao T. 2016a. Trends of temperature and precipitation extremes in the Loess Plateau Region of China, 1961–2010. *Theor. Appl. Climatol.* : 1–15. https://doi.org/10.1007/s00704-016-1820-z.

Wang XL, Chen H, Wu Y, Feng Y, Pu Q. 2010. New techniques for the detection and adjustment of shifts in daily precipitation data series. *J. Appl. Meteorol. Climatol.* **49**(12): 2416–2436. https://doi.org/10.1175/2010JAMC2376.1.

Wang XL, Feng Y. 2013. *RHtests_dlyPrcp User Manual*. Climate Research Division, Atmospheric Science and Technology Directorate, Science and Technology Branch, Environment Canada, Toronto, Ontario, Canada. http://etccdi.pacificclimate.org/RHtest/RHtests_dlyPrcp_UserManual_10Dec2014.pdf (accessed 25 February 2014).

Wang Y, Xu Y, Lei C, Li G, Han L, Song S, Yang L, Deng X. 2016b. Spatio-temporal characteristics of precipitation and dryness/wetness in Yangtze River Delta, eastern China, during 1960–2012. *Atmos. Res.* **172–173**: 196–205 https://doi.org/10.1016/j.atmosres.2016.01.008.

Werner PC, Gerstengarbe F-W. 2010. PIK Report No. 119 – Katalog Der Grosswetterlagen Europas nach Paul Hess und Helmut Brezowsky 7, verbesserte und ergänzte Auflage. Potsdam-Institut für Klimafolgenforschung e.V.

Wi S, Valdés JB, Steinschneider S, Kim T-W. 2015. Non-stationary frequency analysis of extreme precipitation in South Korea using peaks-over-threshold and annual maxima. *Stoch. Environ. Res. Risk Assess.* **30**(2): 583–606. https://doi.org/10.1007/s00477-015-1180-8.

World Meteorological Organization. 2008. *Guide to Meteorological Instruments and Methods of Observation*. World Meteorological Organization: Geneva, Switzerland.

Yin J, Xu Z, Yan D, Yuan Z, Yuan Y, Yang Z. 2016. Simulation and projection of extreme climate events in China under RCP4.5 scenario. *Arab. J. Geosci.* **9**(2): 1–9. https://doi.org/10.1007/s12517-015-2022-1.

Zolina O, Simmer C, Belyaev K, Gulev SK, Koltermann P. 2013. Changes in the duration of European wet and dry spells during the last 60 years. *J. Clim.* **26**(6): 2022–2047. https://doi.org/10.1175/JCLI-D-11-00498.1.

Zolina O, Simmer C, Kapala A, Gulev S. 2005. On the robustness of the estimates of centennial-scale variability in heavy precipitation from station data over Europe. *Geophys. Res. Lett.* **32**(14): L14707. https://doi.org/10.1029/2005GL023231.

9. Article IV: ‘Duration, rarity, affected area, and weather types associated with extreme precipitation in the Ore Mountains (Erzgebirge) region, Central Europe’

The fourth article (Minářová *et al.*, 2017b) entitled ‘Duration, rarity, affected area, and weather types associated with extreme precipitation in the Ore Mountains (Erzgebirge) region, Central Europe’ is focused on EPE characteristics in the Ore Mountains (OM). The EPEs are defined the same way as in VG, i.e. using the WEI (Müller and Kaspar, 2014), because in VG, it was found to best represent the EPEs due to the event-adjusted spatial extent and duration. Three strongest summer half-year and winter half-year EPEs, as well as the EPE affecting smallest area, are synoptically detailed together with the hydrological consequences of the events. Many characteristics and trends of EPEs are analysed based on a dataset of 54 strongest EPEs. The synoptic situation is described using the two weather type catalogues (i.e. GWLc and SVGc), which results in catalogue-dependent outcomes. It is the reason why the paper ends up with a recommendation of a quantitative (instead of qualitative) approach while analysing the synoptic conditions during EPEs. A comparison with the results of EPE characteristics in OM with those in similar low mountain range region (i.e. VG) is also awaited in the paper to further the research.

INTERNATIONAL JOURNAL OF CLIMATOLOGY
Int. J. Climatol. (2017)
Published online in Wiley Online Library
(wileyonlinelibrary.com) DOI: 10.1002/joc.5100

RMetS
Royal Meteorological Society

Duration, rarity, affected area, and weather types associated with extreme precipitation in the Ore Mountains (Erzgebirge) region, Central Europe

Jana Minářová,[a,b,c]* Miloslav Müller,[c,d] Alain Clappier,[e] Stephanie Hänsel,[f] Andreas Hoy,[f] Jörg Matschullat[f] and Marek Kašpar[g]

[a] *Laboratory Image, City, Environment, National Centre for Scientific Research & University of Strasbourg, France*
[b] *Department of Physical Geography and Geoecology, Faculty of Science, Charles University in Prague, Czech Republic*
[c] *Institute of Atmospheric Physics, Academy of Sciences of the Czech Republic, Prague, Czech Republic*
[d] *Department of Physical Geography and Geoecology, Faculty of Science, Charles University in Prague, Czech Republic*
[e] *Laboratory Image, City, Environment, National Centre for Scientific Research & University of Strasbourg, France*
[f] *TU Bergakademie Freiberg, Interdisciplinary Environmental Research Centre, Germany*
[g] *Institute of Atmospheric Physics, Academy of Sciences of the Czech Republic, Prague, Czech Republic*

ABSTRACT: Extreme precipitation events (EPEs) in the Ore Mountains (OM) were studied based on daily precipitation observations from 1960 to 2013. The OM are a low mountain range situated in the Czech-German border area. The Weather Extremity Index (WEI) resulting from an event-adjusted evaluation technique was used to select 54 EPEs of 1-10 days duration. The WEI combines rarity, spatial extent, and duration of an event in one index and provides quantitative information about its extremity. Based on their duration, the 54 EPEs were classified into short (1-2 days) and long events (3-10 days), showing different characteristics and trend behaviour. The EPEs (including the three strongest events) occurred most frequently in late spring and summer. The three strongest EPEs as well as EPEs, which occurred during the winter half-year (WHY EPEs), affected comparatively larger areas; with WHY EPEs being generally longer. EPE frequency does not show any significant trend during the study period; it fluctuated mostly similar to summer half-year EPEs. The most frequent weather type (according to two versions of the German Grosswetterlagen concept) related to EPEs was Trough over Central Europe (TrM). Nevertheless, many differences were noticed between the original (manual) catalogue and its automated version (SynopVis-Grosswetterlagen); the later able to better reflect the weather types associated with 54 EPEs.

KEY WORDS Krušné hory; heavy rainfall; WEI; synoptic conditions; trend analysis; Grosswetterlagen (large-scale weather pattern)

Received 5 December 2016; Revised 27 February 2017; Accepted 23 March 2017

1. Introduction

Extreme precipitation is one of the primary causes for many natural disasters such as flooding and induced landslides. The next decades in Europe are likely to see a rise in weather extremes, including heavy rainfall (Pachauri *et al.*, 2014). Hence, there is an increased risk to societies associated with extreme precipitation events (EPEs), such as human casualties, extensive property damage, losses in agriculture, degradation of water quality, and cuts of electricity or purified water supply (Barros *et al.*, 2014). Improved knowledge about the characteristics of precipitation extremes (such as duration, rarity, affected area, and the associated weather types) at different spatial and temporal scales is therefore essential to avoid and/or minimise the foreseen risks associated with EPEs. Thus, this research is dedicated to fill in the knowledge gap related to the analysis of different characteristics of precipitation extremes in the Ore Mountains (OM).

Large-scale EPEs received much attention in Central Europe following the heavy precipitation and subsequent flood of August 2002. The event affected particularly Austria, the Czech Republic, and eastern Germany (Thieken *et al.*, 2005; Brazdil *et al.*, 2006; Boucek, 2007). This single event is frequently considered as a milestone for more detailed analyses of heavy rainfall in Europe to develop more efficient warning systems, protect citizens, raise public awareness, and improve risk management (Thieken *et al.*, 2007; Socher and Boehme-Korn, 2008; Kienzler *et al.*, 2015). On 12 August 2002, exceptionally high daily rainfall totals were recorded in the OM (OM; Erzgebirge in German, Krušné hory in Czech). The highest amount of 312 mm was registered (from 0600 to 1800 UTC) at the German DWD weather station Zinnwald, located in the eastern part of the Erzgebirge ridge. This amount was the

* Correspondence to: J. Minářová, Laboratory Image, City, Environment, National Centre for Scientific Research & University of Strasbourg, 3 rue de l'Argonne, F-67000, Strasbourg, France. E-mail: jana.minarova@live-cnrs.unistra.fr; jana.minarova@natur.cuni.cz; jana.minarova@ufa.cas.cz

highest observed rainfall total in Central Europe (except for high Alpine regions) since 1947, and the third highest since the onset of a dense rain gauge network in the late 19th century (Munzar *et al.*, 2011). Prior to this event, only two other daily totals have exceeded 300 mm (Munzar *et al.*, 2011): (i) at Nová Louka (Neuwiese) station in the Jizera Mountains in northern Czechia (345 mm on 29 July 1897), and (ii) at the Semmering station in Austria (323 mm on 05 July 1947).

Although several studies have addressed extreme precipitation in (parts of) the OM, these were generally limited to administrative units or to one of the two countries (e.g. Parlow, 1996; Štekl, 2001), considering only parts of the OM. The project INTERKLIM (2014) is an exception. It has been conducted across the OM region, yet heavy rainfall analysis was not the main focus in this project. Other studies were mainly event-specific or focused on larger regions or river basins (e.g. Rudolf and Rapp, 2002; Grams *et al.*, 2014). Their selection of heavy precipitation events was generally impact-based. Extremity estimates of such events were also assessed, mostly based on event consequences, e.g. return-period estimates of the subsequent flooding (Gumbel, 1941; Botero and Francés, 2010; Conradt *et al.*, 2013; Hirabayashi *et al.*, 2013). However, not every heavy rainfall leads to flooding. Thus an objective method to evaluate and to select EPEs is needed.

The usual approach to determine EPEs for impact studies is based on exceeding specific rainfall totals (Štekl, 2001; Muluneh *et al.*, 2016; Ngo-Duc *et al.*, 2016; Tošić *et al.*, 2016; Wang *et al.*, 2016) or return period values at a specific point. Extreme value analyses using methods such as peak over threshold, block maxima, and return periods (described e.g. by Coles (2001), Katz *et al.* (2002), Coelho *et al.* (2008), Katz (2010)) are widely used. Minářová *et al.* (2016) compared these three approaches in a study on the seasonality of heavy rainfall in the Vosges Mountains in north-eastern France. While these are very useful objective tools, they have limitations in the analysis of precipitation extremes because they are calculated pointwise. This led Müller and Kaspar (2014) to their proposal of an event-adjusted evaluation method of precipitation extremes, which they named Weather Extremity Index (WEI). The method is unique in quantifying the extremity of events as it combines the spatial extent (areal evaluation), intensity, and event duration (time evaluation) into one index, thus facilitating event comparison. Several studies employed the WEI (Müller and Kaspar, 2014; Müller *et al.*, 2015; Valeriánová *et al.*, 2017; Kašpar *et al.*, 2016), but the studies were focused on the entire Czech Republic. Schiller (2016) applied the WEI to the German territory by using radar data to evaluate precipitation events. Her study showed that the WEI is well applicable to daily precipitation data representing large-scale precipitation events. In the current study, the event-adjusted evaluation method by Müller and Kaspar (2014) has been tested at a regional scale to characterise EPEs in the OM which has a complex relief.

The main objective of the present study is to study the EPEs in the OM to gain insight into the aspects of the EPE genesis and the related characteristics. Several perspectives have to be considered in parallel, i.e. duration, extremity, spatial extent, seasonality, causal synoptic conditions, and temporal changes. Understanding these EPE characteristics is important to develop strategies against the risks posed by EPEs, to prevent subsequent losses, and to develop engineering designs and regulations for building structures and facilities that can withstand such extreme events. Thus, the results of this study can not only serve in risk management of natural hazards related to heavy rainfall in the study region but can also be used in the parameterization of regional climate models.

2. Data and methods

2.1. Study area

The study area (40 600 km^2) comprises parts of the Czech Republic and Germany in Central Europe (Figure 1). It covers substantial parts of Saxony and the eastern edge of Thuringia in Germany and consists of selected meteorological stations in the Karlovarský kraj (Carlsbad) and Ústecký kraj (Ústí nad Labem) regions in the Czech Republic. The OM are mid-elevation mountain ranges; their highest points are Klínovec (Keilberg in German; 1.244 m a.s.l.) on the Czech side and Fichtelberg (1.215 m a.s.l.) on the German side.

The climate of OM region is characterised by a transition between western European more oceanic and eastern European dominantly continental climates. Westerlies from the Atlantic Ocean dominate the circulation pattern. A diverse set of microclimatic peculiarities can be found due to the complex relief of the study region (Pechala and Böhme, 1975). Elevation is the most influencing factor responsible for the observed regional air temperature differences, i.e. the lowest average temperature is found at the highest altitudes. For instance, the mean annual temperature at the Fichtelberg weather station (1.213 m a.s.l.) was 2.9 °C from 1961 to 1990, while it was 8.7 °C in the northern OM forelands at Dresden airport (222 m a.s.l.) (SMUL, 2008).

Differences in precipitation are not only influenced by altitude but also by orography, e.g. the exposition of the ridge towards the prevailing airflow in particular (INTERKLIM, 2014). The highest precipitation amounts were recorded at the highest elevations and on the windward (German) side. A total of 1285 mm was the mean annual total 1961-1990 at the Fichtelberg weather station (SMUL, 2008). These locations are susceptible to the orographic enhancement of precipitation, whereas the typical rain shadow is found on the leeward side in the Czech lowland basin, where the lowest annual precipitation totals of the whole Czech territory (410-500 mm on average) were recorded (DWD DDR and HMÚ ČSSR, 1975; INTERKLIM, 2014).

2.2. Climatological data

Our analysis is based on daily precipitation totals measured from 1960 to 2013 at 167 meteorological stations, covering

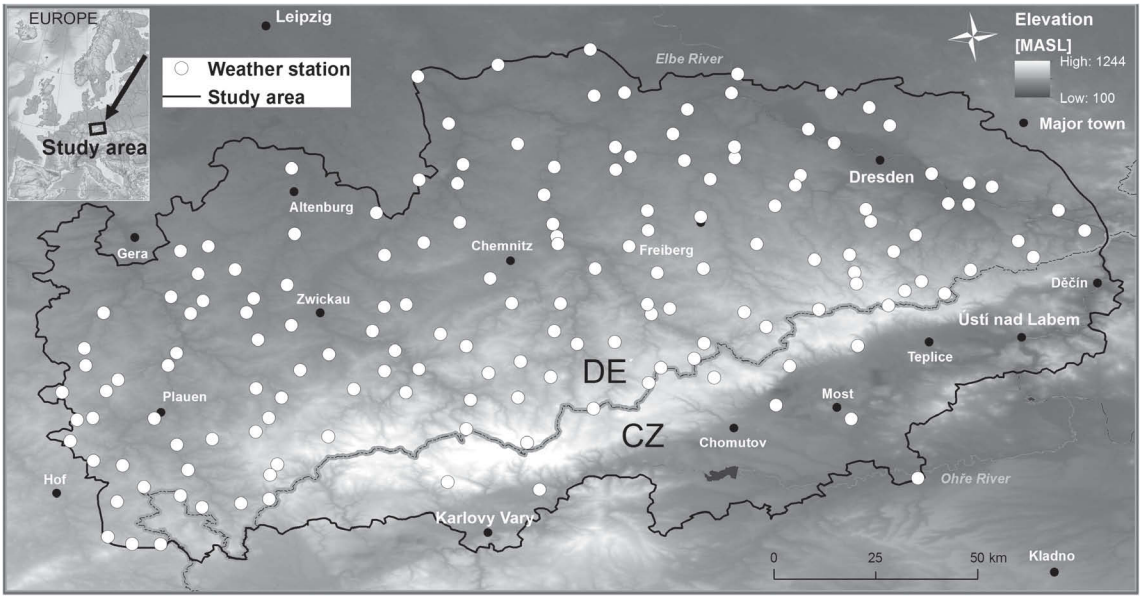

Figure 1. Study area in the Ore Mountains, and the spatial distribution of the 167 analysed weather stations. The relief is represented in grey-scale with the highest locations displayed in white.

the larger area of the OM. Quality-controlled data with metadata from the German and Czech national networks, i.e. *Deutscher Wetterdienst* (DWD) and *Czech Hydrometeorological Institute* (CHMI) are used. Unfortunately, data provided by CHMI reach until 2005 and include only 10 stations. The low number of weather stations for the Czech territory may limit the robustness of results at the more regional scale. However, the weather patterns are regionally more uniform on the leeward (Czech) side than on the windward (German) side (Whiteman, 2000; Barry, 2008), suggesting that the lower density of data series at the Czech side might not influence our results substantially. Moreover, the WEI method used in this study provides areal information (at the 2×2 km grid resolution) rather than station-to-station specific information; we did not aim at the local scale in this paper.

Not all stations cover the complete study duration. Figure 2 shows the fluctuations in data availability. A sharp increase is visible since 1969 (from 50% to 90%). This mostly relates to the digital availability of precipitation data from that time, and less to an increase in the number of precipitation gauges. After a period of broad data availability, a decrease in the number of available stations can be noticed since the Millennium, and especially since 2006. This decline directly corresponds with the shutdown of many sites by DWD, due to maintenance costs and limited financial resources. An increase in shorter gaps is related to the automation of many locations, which are thus simply more vulnerable to measurement failures. However, all the data series considered span more than half of the study period (i.e. 27 years). They were thus considered to be sufficient for identification and characterization of the most EPEs in the study area. No inter- or extrapolation of the data series was performed.

The homogeneity of the daily precipitation time series was examined using the *RHtests_dlyPrcp* R-package accessible at http://etccdi.pacificclimate.org/software.shtml (Wang *et al.*, 2010; Wang and Feng, 2013), considering the available metadata. For instance, changes from Hellmann rain gauge to tipping-bucket in 1990 and to PLUVIO devices with automated readings since 2000 by DWD (Zolina, 2014) and similar changes from previous METRA 886 to automated gauges since 1995 by CHMI (Kněžínková *et al.*, 2010; Zolina *et al.*, 2014) were included in the test as metadata. The systematic errors of METRA 886 were related to evaporation losses, wet buckets, and aerodynamic effects. According to Kyselý (2009), the Czech rain gauges did not experience major inhomogeneities and no significant relocation of gauges were recorded during 1965–2005. The collecting surface of the Czech and German gauges was similar, i.e. 200 cm^2, and the gauges were similarly equipped by antifreeze chemical since 1950 (Kněžínková *et al.*, 2010; Zolina *et al.*, 2014). A fixed data measurement error of 0.2 mm was used in the homogeneity test. This corresponds to the value commonly used for such analyses as suggested by the WMO (World Meteorological Organization, 2008). The test did not reveal major inhomogeneities in the time series. Our results, focusing on individual areal precipitation events within the series, are quite robust against minor inconsistencies between the two national datasets and the minor inhomogeneities that are present in almost all long-term climate time series due to relocations of stations and changes in measuring devices and/or principles.

2.3. Weather types catalogues

Two catalogues were used for the synoptic analysis, the manual catalogue of the Grosswetterlagen classification

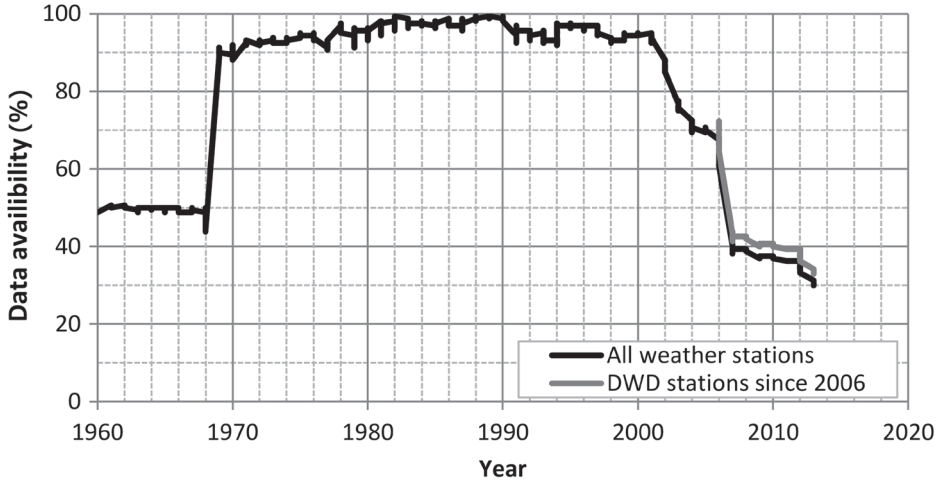

Figure 2. Availability of daily precipitation data during 1960–2013 for (black line) all 167 rain gauge stations, and for (grey line) 157 available stations since 2006 from DWD.

GWLc (Werner and Gerstengarbe, 2010) and the automated SynopVisGWL-catalogue SVGc (James, 2007 and James, 2015; personal communication). One weather type was allocated to each selected EPE (EPE; Section 2.4). If the EPE was lasting longer than 1 day, the most prevailing weather type during the whole EPE was considered. If more weather types had the same representation, then the weather type associated with day/s of highest precipitation extremity (highest variable E_{ta} discussed below in Section 2.4) was considered.

The Grosswetterlagen concept focuses on Central Europe, although it is applicable in most other parts of Europe. The concept is based on the geographical position of low and high-pressure systems, and fronts and their movement. The main advantage of the Grosswetterlagen concept is that it focuses on both the large-scale synoptic patterns and the local weather characteristics. It is highly intuitive and easily comprehensible for non-specialists. However, the manual GWLc may be limited by a certain subjectivity of the classifying specialists (HMI, 1972; Hess and Brezowsky, 1977; Hoy *et al.*, 2012b; Stryhal and Huth, 2016).

The automated SVGc is more objective even if not completely objective (hybrid classification based on specifications provided by the scientists). It is based on an arbitrary given number of pre-selected weather types, because a purely automated classification may omit some infrequent weather types, which might be significant (James, 2007). A more detailed comparison between the GWLc and SVGc can be found in (Hoy *et al.*, 2012a, 2012b).

2.4. Digital elevation model

A *Global Multi-Resolution Topography* (GMRT; resolution of 100×100 m grid spacing) model acquired from *GeoMapApp* (http://www.marine-geo.org/tools/maps_grids.php) was used as a base map to generate further maps in *Esri's ArcGIS 10.3* software.

2.5. Event-adjusted evaluation method: WEI

The event-adjusted evaluation method of weather (climate) extremes is based on the computation of the WEI (proposed by Müller and Kaspar (2014)) as follows:

$$\mathrm{WEI}\ \left[\log(\mathrm{year})\,\mathrm{km}\right] = \max\left(E_{ta}\right) = \max \frac{\left(\sum_{i=1}^{n} \log\left(N_{ti}\right)\sqrt{a}\right)}{n\sqrt{\pi}} \quad (1)$$

where N_{ti} is the return period estimate in a grid point i and time period t and a is the corresponding area consisting of n grid points. The variable E_{ta} indicating the extremity of an event is defined by a product of the areal mean of common logarithms of return period estimates and of a radius of a circle of an equivalent area to the region which the areal geometric mean is calculated in. The max in Equation (1) suggests that the maximum value of the variable E_{ta} is taken as WEI.

First, the common logarithms of return period estimates are interpolated using Ordinary Kriging to a regular 2×2 km resolved grid for each day and time window considered (i.e. 1–10 days). For the interpolation, no external drift such as elevation and use of co-kriging is needed since the distribution of return period estimates is rather flat and no significant correlation was found between the altitude and return period estimates. The return period values are estimated from the commonly applied three-parametric Generalized Extreme Value GEV distribution. Subsequently, the gridded values of common logarithms of return period are transformed back to return period estimates, which are arranged in descending order. The grid point with the highest value is taken as the first, and then stepwise second highest, third highest, and so on (i.e. irrespective of the location of grid points in the study area) are accumulated in order to optimise the area affected by EPE with its rarity. The calculated E_{ta} for

the stepwise-accumulated grid points increases at the beginning because the area increases and still high return period estimates are accumulated. This increase stops at an inflection point (WEI), which is considered as the optimised value between the rarity and affected area of an event, beyond this point the E_{ta} starts decreasing due to the inclusion of pixels with lower return period estimates, which outweighs the increase in accumulated area.

WEI values provide an objective ranking of the extremity of all precipitation events considered (i.e. of varying duration) with extreme events producing the highest WEI values. As the transition from extreme to less and less extreme until non-EPEs is naturally smooth and the WEI depends on the size of the considered area, no critical value of E_{ta} is fixed to distinguish the 'extreme' events from 'non-extreme' events; only the zero value of E_{ta} indicates insignificant precipitation. However, the user has to fix the number of additionally considered precipitation events, based on length of the studied period, climatological characteristics of the study region, and the purpose of further analysis. For instance, the ten first events can be further analysed, or the number can be set proportionally to the study period (i.e. 1 per 2 years on average). More details about the event-adjusted evaluation technique can be found in Müller and Kaspar (2014).

In this paper, the return period estimates are calculated for events of 1-10 days duration. The maximum length of 10 days was selected in order to test whether or not long events also occur in the study area, since previously maximum 5-days totals were analysed using this method in the Czech Republic (Müller and Kaspar, 2014). The 10-day duration is considered to be sufficiently high; longer events are not expected to occur in the area. The final duration of an event is given by the first maximal E_{ta} value (WEI) of the E_{ta} values calculated for all considered durations starting from the duration of day 1. The final duration of an event has to meet the condition that all the 1-day E_{ta} values included in the event are non-zero values, i.e. the precipitation was strong enough during all the duration of the event to be still considered as an EPE.

The major advantage of the WEI is that it combines all relevant information to characterize the extremity of an event into one index, i.e. rarity (return period estimates computed from the GEV distribution), duration, and spatial extent of an event. In addition, the optimization of the affected area is objective since the pixels are not accumulated starting from an arbitrary fixed location in the study area, and it enables to include pixels even from non-neighbouring parts of the study area. It also provides better comparability of weather events compared with the commonly used methods such as peak over threshold (POT) or block maxima (BM).

For the computation of WEI, the study area was adjusted in order to reduce the need of extrapolation. Thus the study area that first followed the boundaries of Czech and German (sub)regions was reduced at few parts with respect to the spatial distribution of stations, i.e. if only a few stations were located in the much bigger (sub)region, the new boundary simply contoured the considered stations.

2.6. Analysis approach

The 54 events with the highest WEI values are considered as reference EPEs (EPEs), i.e. on average one representative per year. These events were further analysed statistically and synoptically from different points of views, e.g. frequency and seasonality. The seasonality was examined based on the date of the first day of the EPE, which was assigned to the meteorological season (e.g., spring spanning from March 01 to May 31) and to one of the two half-years. The warmer summer half-year (SHY) comprises April to September, while the colder winter half-year (WHY) covers October to March. A sensitivity analysis was performed in order to compare the results if the EPEs were represented by a day other than the first day; only up to 4% of EPEs were noticed to be influenced, which was considered negligible.

The seasonal distribution of EPEs is displayed in a polar chart. The radius of concentric circles is equal to the WEI values. Concentric circles were divided evenly into 365 parts (Julian days). Each EPE is expressed by a direction vector, representing its date within a year and a magnitude equal to its WEI value. Principal Component Analysis (PCA) was performed in order to examine the relationship between extremity, duration, affected area, and the most frequent EPE weather types from GWLc and SVGc. Inter-annual changes in the frequency of EPEs, of SHY/WHY EPEs, and of short (1–2 days)/long (3–10 days) EPEs were examined using least-squares linear regression. Non-parametric Mann–Kendall Test for monotonic trend was used to estimate the statistical significance of the results (Mann, 1945; Kendall, 1975; Hirsch *et al.*, 1982; Hirsch and Slack, 1984). The results are discussed in Section 3.4

3. Results and discussion

3.1. Characteristics of EPEs

3.1.1. Event duration

The 54 selected EPEs are listed in Table 1. They are clearly separated into two groups with respect to their duration (Figure 3): (i) short duration events (1 to 2 days; maximum frequency at 2 days) and (ii) long duration events (3 to 10 days; maximum frequency at 6 days). The short duration events (33 EPEs) were more frequent than the long duration events (21 EPEs). The differentiation into 'short' (1–2 days) and 'long' (3–10 days) EPEs is kept hereafter. The short duration of EPEs is in good agreement with Zolina (2014), who found the mean duration of wet spells mostly to be around 2 days (i.e. 1.8 to 2.2 days in SHY and > 2.2 days in WHY) at stations in Saxony. In general, long EPEs tend to reach slightly higher WEI magnitude and a greater range of the WEI value as compared with short EPEs (Figure 4(a)).

The clear differentiation into two duration classes may be related to different precipitation features, e.g. stationarity and spatial extent of weather systems. One day events may, during the SHY, often be related to convective

Table 1. A total of 54 selected EPEs arranged in the decreasing order of their extremity (WEI).

EPE	Date	Season	Duration (dd)	WEI (log[year]km)	Affected area (%)	GWLc	SVGc
1	**28 September 2013**	**Spring**	**7**	**134.46**	**100**	**TM**	**TM**
2	11 August 2002	Summer	2	120.59	88	TrM	TrM
3	**01** August **1983**	**Summer**	**6**	**116.41**	**92**	**NEz**	**NEz**
4	07 August 1978	Summer	2	77.71	84	Nz	Nz
5	22 July 2010	Summer	2	64.24	95	TrW	NEz
6	***27* December *1986***	***Winter***	***7***	***61.24***	***89***	***NWz***	***NWz***
7	31 August 1995	Summer	2	60.51	84	Nz	Nz
8	***19 October 1974***	***Autumn***	***8***	***59.50***	***84***	***TM***	***TM***
9	**25 September 2010**	**Autumn**	**4**	**58.97**	**84**	**TM**	**HFz**
10	***15 October 1960***	***Autumn***	***3***	***57.88***	***95***	***TB***	***HFz***
11	18 July 1981	Summer	2	55.84	55	TrM	TrM
12	22 August 1975	Summer	1	54.74	42	Wz	TrM
13	07 May 1978	Spring	1	53.50	73	TM	HFz
14	**27 June 1966**	**Summer**	**3**	**52.53**	**62**	**NWz**	**Nz**
15	***06 November 2007***	***Autumn***	***8***	***50.86***	***84***	***NWz***	***Nz***
16	**01 July 1992**	**Summer**	**6**	**50.18**	**60**	**HNz**	**HNFz**
17	20 August 1970	Summer	2	48.90	30	TB	SEz
18	23 April 1980	Spring	2	45.49	66	TM	NEz
19	**20 September1979**	**Autumn**	**5**	**44.91**	**96**	**NEz**	**TrM**
20	***05 December 1974***	***Winter***	***4***	***40.76***	***66***	***Wz***	***NWa***
21	02 August 1970	Summer	1	40.06	12	HFa	HNFa
22	30 July 2011	Summer	1	39.82	46	TrM	Na
23	21 July 1980	Summer	1	38.66	56	Wz	Wz
24	07 July 2001	Summer	1	37.56	32	SEa	SEz
25	***16 November 2004***	***Autumn***	***8***	***37.11***	***92***	***NWz***	***NWz***
26	07 July 1996	Summer	2	35.71	72	TrM	TrM
27	**08 June 1995**	**Summer**	**8**	**35.47**	**35**	**TrM**	**TM**
28	**07 August 2007**	**Summer**	**5**	**34.93**	**60**	**TM**	**HFz**
29	15 June 2007	Summer	1	34.37	49	SWz	TB
30	01 August 1991	Summer	2	32.84	38	HFa	HFz
31	***10 January 1976***	***Winter***	***6***	***32.56***	***82***	***Wz***	***NWa***
32	10 August 1964	Summer	2	31.65	33	HNFz	NEz
33	29 May 1986	Spring	2	30.50	86	TrW	TrM
34	18 June 1977	Summer	2	30.10	71	Na	HNz
35	19 June 1969	Summer	1	28.80	58	TB	Sz
36	05 August 2006	Summer	2	28.76	70	TM	NEz
37	13 May 1995	Spring	1	28.01	34	TrM	TM
38	06 August 2010	Summer	2	25.71	29	TrM	TrM
39	17 June 1991	Summer	1	24.38	92	TrW	TrM
40	***27 October 1998***	***Autumn***	***6***	***24.24***	***79***	***Wz***	***NWz***
41	10 May 1965	Spring	2	23.56	34	Wz	Na
42	16 July 1965	Summer	1	23.36	19	NEz	NEz
43	04 August 1986	Summer	1	23.34	19	BM	Sz
44	**04 July 1999**	**Summer**	**5**	**23.30**	**49**	**SWz**	**SWz**
45	**02 June 1971**	**Summer**	**10**	**23.19**	**55**	**HNz**	**HNFz**
46	*12 October 1980*	*Autumn*	*2*	*22.99*	*77*	*WS*	*TM*
47	10 **June** 1965	Summer	1	22.79	6	HNFz	HFz
48	**13 July 1984**	**Summer**	**7**	**22.79**	**71**	**TrM**	**Nz**
49	27 September 2007	Autumn	2	22.18	46	TM	SEz
50	10 August 1977	Summer	1	22.08	38	NEz	NEz
51	**22 July 1989**	**Summer**	**6**	**21.99**	**42**	**HFz**	**Hfa**
52	06 August 2013	Summer	1	21.36	23	TrW	TrW
53	18 June 1999	Summer	1	20.93	45	BM	BM
54	***16 December 1987***	***Winter***	***5***	***20.81***	***77***	***Wz***	***Wa***

From left to right: number of EPEs, starting day, season to which the starting day belongs, WEI values, affected area as a percentage of the whole study area, and the weather types based on GWLc and SVGc (abbreviations explained in Figure 9). Winter half-year (October–March) EPEs are highlighted in italics and long EPEs (Figure 3) are displayed in bold.

rainfall. They yet represent the second highest frequency (16 EPEs) among all EPEs (Figure 3). The most frequent 2-days events (17 EPEs) may be related to recurrent convective precipitation over the area and stratiform precipitation. The stratiform longer-lasting (widespread) precipitation appears to be prioritised more by WEI.

However, the prevailing 1–2 days in the EPE dataset can be considered accurate because it corresponds with the meteorological features in OM, although the accuracy of EPE duration can also be shown by a fitted distribution such as truncated geometric, which was found to be a good approximation for wet spells (Deni *et al.*, 2010; Zolina,

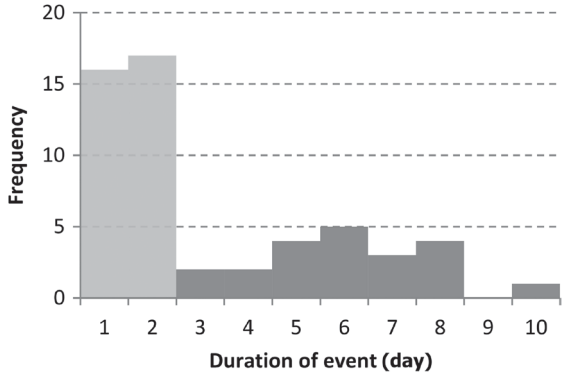

Figure 3. Frequency of different durations of the 54 selected heavy rainfall events (EPEs).

2014). During prevailing (westerly/northwesterly) zonal circulation, the systems move fast so that the EPEs are short. Longer EPEs can occur during the Vb cyclones (Bebber, 1891) that get stationary over Central Europe (mostly Moravia, Poland). However, the Vb cyclones have to move retrograde from their track to affect the OM (as it was the case in August 2002), which cannot last long because the system is pushed sooner or later eastwards by westerlies, resulting again in 1–2 day EPEs. Long EPEs in OM might mainly be related to either slow moving cut-off low or to strong zonal circulation, when many successive cyclones from West/Northwest cross over the area (DWD DDR and HMÚ ČSSR, 1975; Pechala and Böhme, 1975).

The use of daily totals limits the identification of individual rainfall events – the WEI may include two or more separate (or reproducing) convective intense precipitation events during a day and particularly at longer time scales. Further studies on the possibility of separating individual rainfall events using the WEI methodology based on higher resolved datasets are needed. One such study is under investigation by the authors of the method.

3.1.2. Extremity and affected area

WEI values are positively correlated with the affected area – longer events tend to affect larger parts of the study area (35–100%), whereas the short events affect a wider range of the area sizes, from very small (e.g. 6% in June 1965) to almost the entire area (up to 95% of the study area) – Figures 4(b) and 5.

The spatially least extended EPE of 10 June 1965, affected only 2.6% of the study area; it was a 1-day summer event and the 47th heaviest (WEI = 23) in the dataset of EPEs (Table 1). Its short duration, occurrence in the summer season and very small extension suggests its convective origin. It can thus be assumed that the WEI method enables capturing convective EPEs even at the daily scale if they are intense enough, although stratiform precipitation events are generally favoured.

It is also noticeable from Figure 5 that a comparatively large difference between the three strongest rainfall events (the three highest WEI values) and other EPEs exists in the WEI values. The three heaviest EPEs reached WEI values

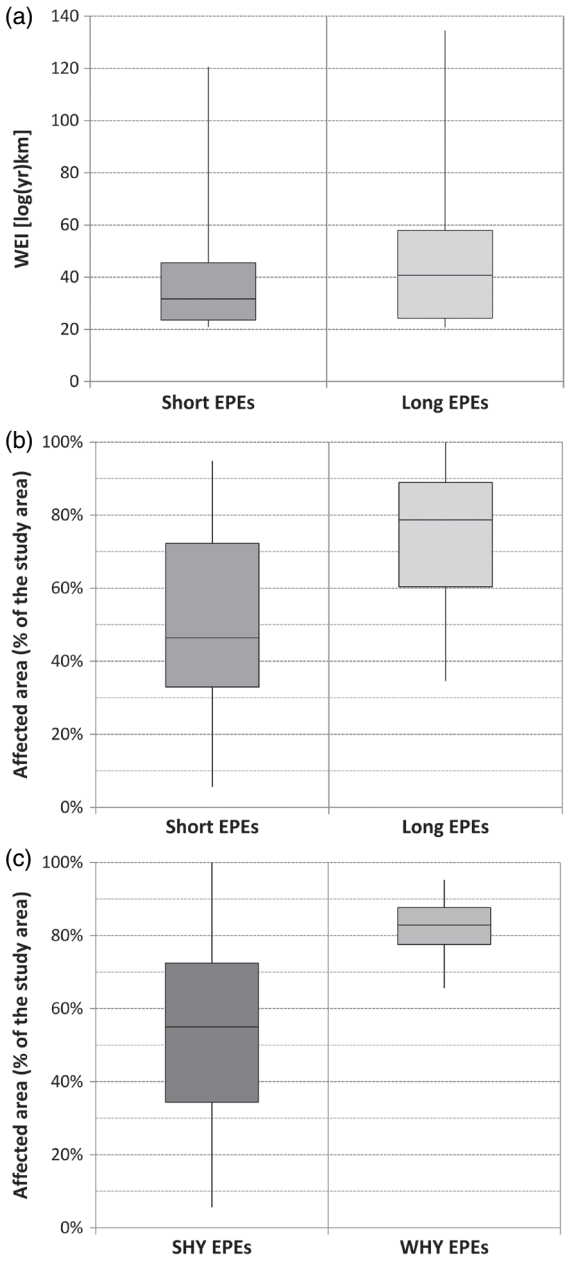

Figure 4. Box-and-Whiskers plot for short and long EPEs and their (a) WEI values, (b) affected area; and (c) for summer half-year (SHY) and winter half-year (WHY) EPEs and their affected area. The short and long EPEs are differentiated according to Figure 3.

above 100 (Table 1), while all other events remained below 80. The three highest WEI values comprise a large area affected by extreme precipitation (88–100%) and exceptionally high return period estimates (exceeding 400 years at some locations). These three exceptionally extreme events are characterized in more detail in Section 3.2

Generally, we found lower WEI values than those calculated by Müller *et al.* (2015) for the whole Czech Republic. This relates to the WEI computation that involves the

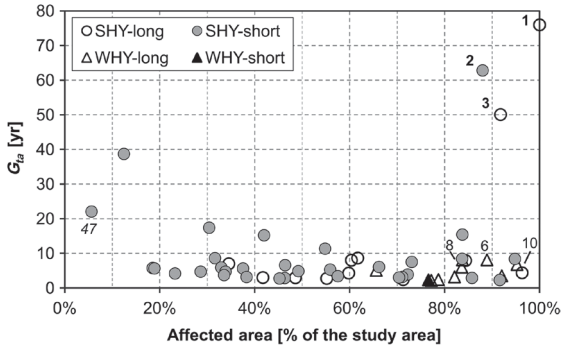

Figure 5. Relationship between the affected area, mean rarity of precipitation totals Gta, duration (long/short) and occurrence in summer half-year (SHY) and winter half-year (WHY) of the 54 EPEs. The Gta is the spatial geometric mean of the return period estimates. The long EPEs and short EPEs are differentiated according to Figure 3. Labels represent the ranking (Table 1) of the following EPEs: (bold) three strongest events, (normal) three WHY strongest events, and (italics) the event affecting less area.

area affected by extreme precipitation. The larger the study area, the larger the WEI values may potentially get. In addition, the correlation of extremity (WEI), affected area (Area) and duration of the EPEs according to the PCA (Figure 6) shows that the variable Area is almost equally positively correlated with both WEI and duration (stronger with WEI), while the variables WEI and duration are not correlated ($r = -0.02$). Projection over the two first components is acceptable (almost 86%).

The selected study area strongly influences EPE ranking, i.e. a shift or enlargement of the study area changes the WEI values and the identification and ranking of EPEs. Nonetheless, some of these events (44 % absolute hits) can also be found in similar studies for the larger territory of the Czech Republic (e.g. Müller *et al.*, 2015), although some differences in the EPE duration were identified (e.g. the August 2002 considered as 2-days event in our study lasted 3 days in their study). These differences are due to the different size and geographical location of the study areas, covering different parts of the relevant precipitation field that is moving over the area.

3.1.3. Seasonal differences

Figure 5 also shows that EPEs generally affected large areas (approx. 66–95% of the study region) during the WHY (October to March); nevertheless, they occurred more frequent in the SHY as compared to the WHY (44 SHY EPEs *vs* 10 WHY EPEs). Despite their large spatial extent (Figure 4c), none of the WHY EPEs was found among the five heaviest events.

Adding supplementary variables (distinction of SHY and WHY EPEs) in the PCA, a correspondence between SHY and WHY EPEs can be observed along the direction of duration but not along the direction of *WEI* (Figure 6). The duration tends thereby to be affected by the seasonality. This is not the case for the *WEI*. The duration appears to be longer in the WHY than in the SHY. This corresponds with the expectation that precipitation events last longer in winter than in summer (Ban *et al.*, 2015), although two of the three strongest EPEs were long and occurred during the SHY (Table 1). However, these events are outliers in the results of PCA (Figure 6).

Most EPEs occurred during the main precipitation season (Pechala and Böhme, 1975), the summer months (35 EPEs) – Figure 7. Table 1 shows that almost all short EPEs occurred in summer except two 1-day EPEs (out of 16) which were recorded during May, and five 2-days EPEs (out of 17) which occurred twice in May, and once in April, September, and October (Table 1). The obvious link between short EPEs and their occurrence in summer (or in transition periods) is expectable and confirms the importance of summer circulation patterns including (recurrent) convection in the development of EPEs in the area.

While intense heavy rainfall events occurred most frequently in July and August (11 and 15 EPEs, respectively), months of maximal mean precipitation, the most recent and heaviest event from May 28 to 03 June 2013 appeared at the transition from spring to summer. Most spring EPEs occurred in late spring (May, 5 EPEs). Autumn events were more equally distributed over the three autumn months and did not show a concentration in the transition month between summer and autumn (September). The more equal distribution of autumn EPEs might be related to the thermal inertia of sea – the surface temperature (SST) of the Mediterranean Sea is higher in autumn than in spring. This warmer sea increases the potential of cyclones with a high precipitable water content moving towards Central Europe during all autumn (Pechala and Böhme, 1975; Oliver, 2008).

3.2. Significant events

3.2.1. Three strongest events

All of the three strongest events occurred in SHY. The most recent EPE in the study period 1960–2013 was the most intense (WEI = 134) and the most widespread in our dataset (the entire study area of 40 600 km^2 was affected). The EPE started on 28 May 2013, and lasted 7 days (Table 1, Figure 8(a)). This event was characterized by widespread prolonged heavy precipitation over Central Europe associated with a cut-off low. Grams *et al.* (2014) described in detail the atmospheric conditions triggering this event. The largest recorded daily precipitation total of 107.5 mm during the EPE was detected in our study area on 1 June at station Rechenberg-Bienenmühle-Holzhau; situated in the eastern part of the mountain range. The 2013-event led to widespread flooding, mainly along the rivers Elbe and Danube (e.g. Stein and Malitz, 2013), with severe economic losses and many casualties (Merz *et al.*, 2014; Schröter *et al.*, 2015).

The second heaviest EPE is the well-known August 2002 event (WEI = 121, August 11–12, 88% of the study area affected). It resulted in many casualties and socio-economic losses (Table 1, Figure 8(b)). Many authors (e.g. Rudolf and Rapp, 2002; Mudelsee *et al.*, 2004) stated that the event was associated with the Vb van Bebber's track of cyclone taking its origin over the

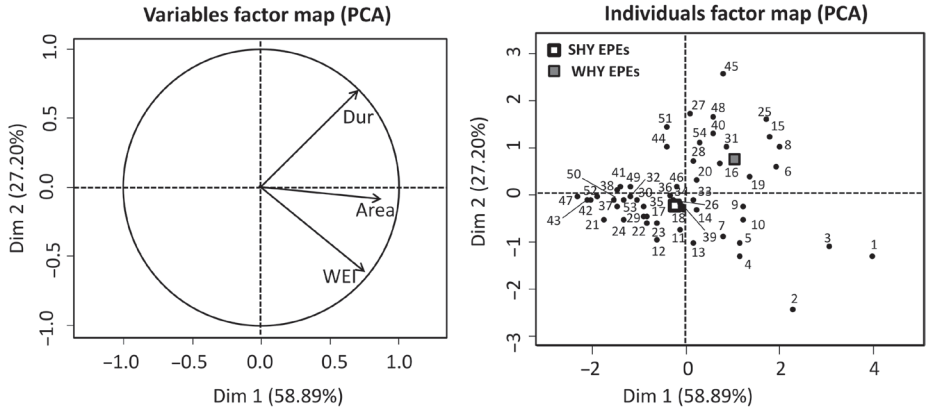

Figure 6. (Left) Correlation of extremity, affected area and duration of the EPEs, and (right) the relationship between the EPEs and the seasonality (SHY and WHY EPEs), according to the PCA. Note that WEI expresses the extremity, area is the size of the area affected by EPEs, and Dur stands for the duration of EPEs.

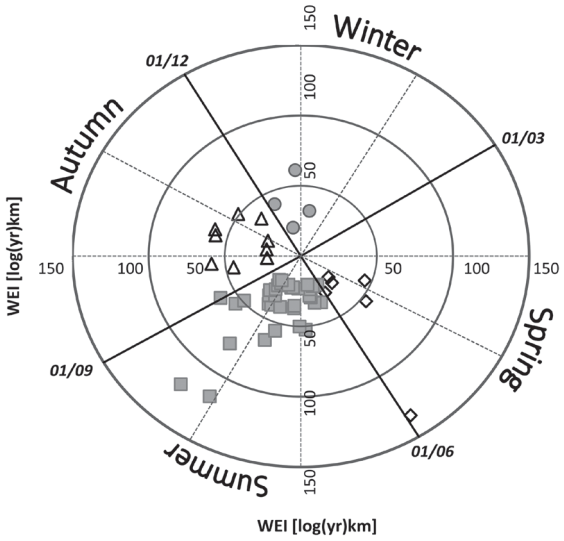

Figure 7. Seasonal distribution of the 54 EPEs. The diamonds represent spring EPEs, squares summer EPEs, triangles autumn EPEs, and circles are used for winter EPEs.

Mediterranean Sea (Bebber, 1891). This event was of great importance (Munzar *et al.*, 2011) because of the 312 mm daily rainfall total recorded at the Zinnwald weather station (Section 1), and a total of 354 mm was recorded during 24 h starting from 0300 UTC on 12 August 2002. This EPE generated severe and extensive flooding (of the Elbe river and several tributaries) with discharges surpassing centennial values in various regions (Ulbrich *et al.*, 2003). In the OM, some flash floods were recorded as well (Goldberg and Bernhofer, 2003), partly related to an additional orographical intensification of precipitation and to local convection within the stratiform cloudiness (e.g. James *et al.*, 2004). This August 2002 event was ranked by Müller *et al.* (2015) as the third heaviest in the context of the Czech Republic territory during the 1961–2010 period. Its duration was set to 3 days (the system moved afterwards eastwards from the OM).

The third most important EPE started on 01 August 1983 (WEI = 116) and lasted 6 days (Table 1, Figure 8(c)). This event was remarkable not only in the Saxon part of the OM but also in Karlovarský kraj region, occupying most of the Czech side of the OM study region. The regional August monthly total (130 mm) exceeded the long-term total of 1961–1990 by 89%, according to the free online-available CHMI historical data (http://portal.chmi.cz/, accessed February 2016), while the monthly total was the seventh wettest in 1960–2010 at the Karlovy Vary (Carlsbad) weather station. Müller *et al.* (2015) described this event as the fourth most significant EPE during 1961–2010 in the entire Czech Republic; in our study area, it was the third most significant since it affected 92% of the OM. This event reached the highest daily totals on 04 August in the Saxon part of the OM study region. Up to 93.3 mm were recorded in Leipzig (Noack *et al.*, 2014), and 112.0 mm at the Ostrau weather station to the northwest of Dresden. Similar to the 2013-event, the 1983-event was also connected to a cut-off low with respect to NCEP/NCAR Reanalysis (Kalnay *et al.*, 1996), but only limited flooding was registered mostly because the soil was highly unsaturated; an extreme drought was observed before the event (Müller *et al.*, 2015).

3.2.2. *Strongest WHY events*

The strongest WHY EPE occurred at the turn of the year 1986/1987 (7-days event starting December 27, 1986; WEI = 61; Table 1, Figure 8(d)). It is the sixth heaviest event within the 54 studied EPEs; its WEI value is much lower than those of the three heaviest events (Section 3.2.1.). The EPE affecting 89% of the study area developed within a zonal flux with mostly northwestern cyclonic airflow in the OM susceptible to an intensified precipitation (Kalnay *et al.*, 1996). This event was significant because of its hydrological response: a maximum peak discharge of 1810 $m^3 s^{-1}$ was measured on 04 January 1987 at the Děčín station on the Elbe river, where the average discharge is 312 $m^3 s^{-1}$ and the m-daily discharge of 94.3 $m^3 s^{-1}$ is exceeded 364 days in a year during 1981–2010 (Brázdil,

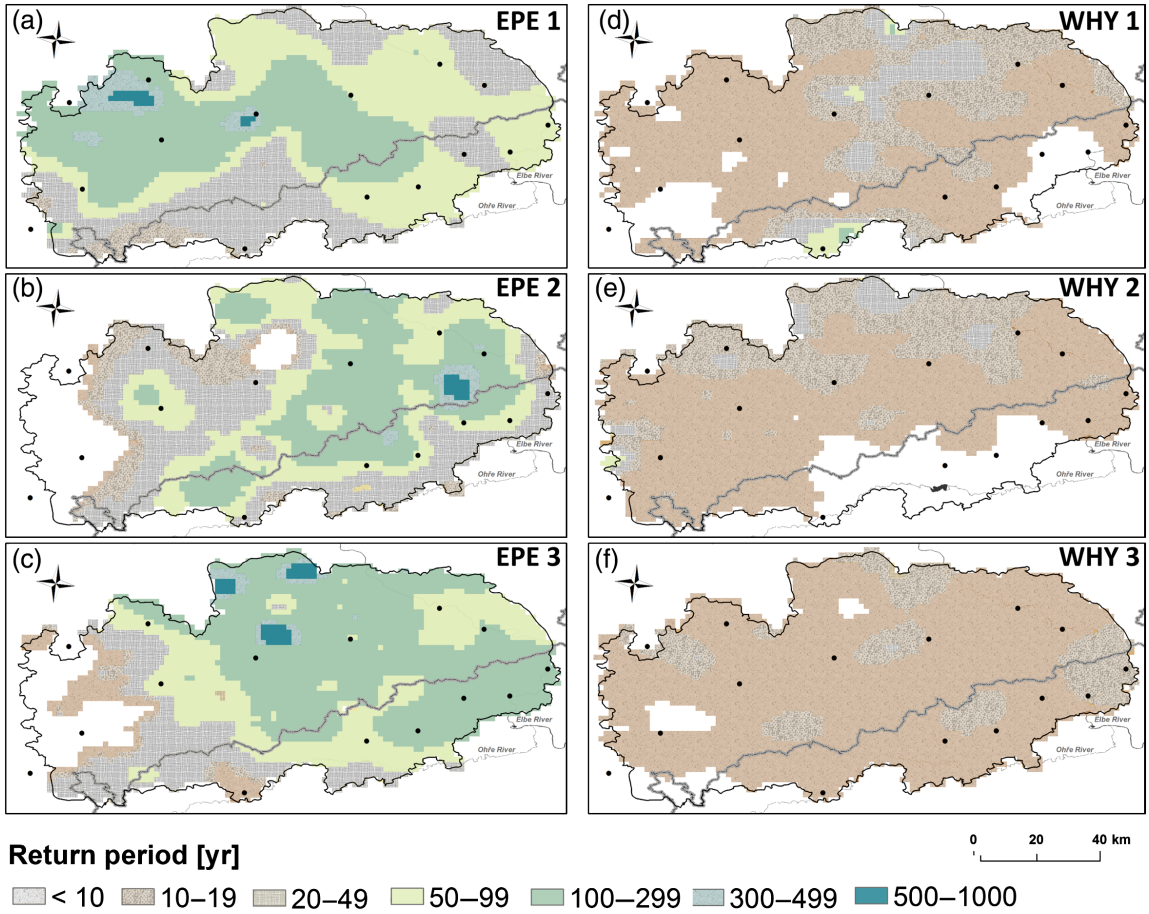

Figure 8. Gridded return period estimates within the area affected by EPEs based on WEI technique for (left) the three strongest EPEs (EPE 1–3) and (right) three strongest WHY EPEs (WHY 1–3). The grid resolution is 2 × 2 km. The black dots represent the cities in the region. Further information about the EPEs is indicated in Table 1. [Colour figure can be viewed at wileyonlinelibrary.com].

2006). The hydrological response was not only related to the EPE itself but was enhanced by substantial thawing during the EPE. Although the snow cover increased during the first day of the event from 46 to 56 cm at the Nová Ves v Horách weather station (725 m a.s.l.), it was reduced to 20 cm during the next 4 days due to maximum temperatures slightly above 0 °C. Mixed or liquid precipitation occurred at the end of December 1986, and this precipitation intensified the thawing process and significantly contributed to the hydrological response.

The second strongest WHY EPE with a WEI value of 60 occurred from 19 to 26 October 1974, and affected 84% of the study area (Table 1, Figure 8(e)). Central Europe was influenced by a trough at that time and the airflow to the OM region was from northwest to north (Werner and Gerstengarbe, 2010). This airflow direction is particularly prone to generate an EPE due to the orographic effect of the OM, leading to an intensification of precipitation on the windward side of the OM (Pechala and Böhme, 1975). Starting 03 October the daily precipitation totals were very low with a maximal value of 8 mm on 09 October at the Fichtelberg weather station. During the EPE, the precipitation occurred as snow particularly at higher altitudes. The snow cover increased at Fichtelberg weather station from 10 cm on 17 October up to 70 cm on 24–25 October, including slightly decreasing values (5 cm loss) during 18–20 October because of maximum air temperatures slightly above 0 °C (http://www.wetteronline.de/rueckblick). Thus precipitation did not get immediately effective for a hydrological response. However, subsequent to the EPE several flooding occurred at the Saale River and Mulde River, where the sixth and seventh highest increase in discharge was recorded during 1951–2002 (Müller *et al.*, 2009a). This WHY EPE is in good agreement with Brázdil (2006). He stated that winters (December–March) in the 1970s were characterized by higher precipitation (especially rainfall) totals. This was associated with a more frequent positive phase of the North Atlantic Oscillation (NAO) responsible for more frequent and stronger zonal circulation in Central Europe. Nevertheless, all of the four strongest WHY EPEs were followed by a significant hydrological response, which is also true for the three strongest SHY EPEs discussed above.

The third most extreme WHY event started on 15 October 1960. It lasted 3 days (WEI = 58; Table 1, Figure 8(f)) and affected the largest part of the territory (95 %)

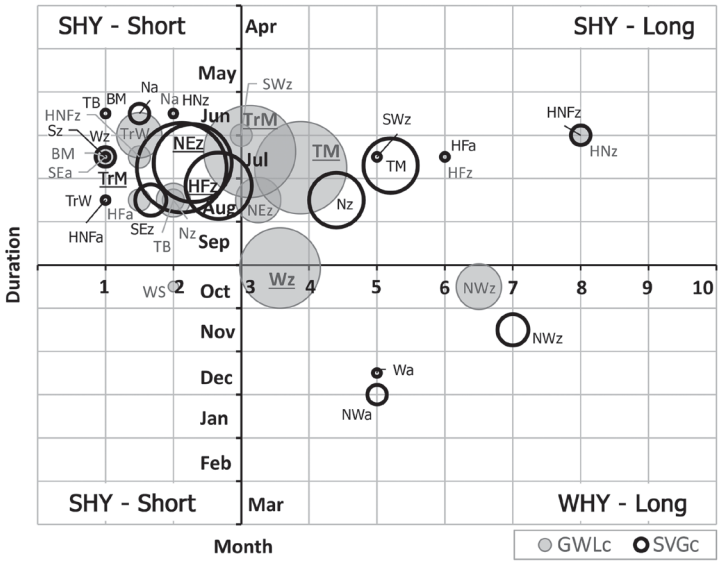

BM	Zonal Ridge across Central Europe
HFa	Scandinavian High, Ridge Central Europe
HFz	**Scandinavian High, Trough Central Europe**
HNFa	High Scandinavia-Iceland, Ridge Central Europe
HNFz	High Scandinavia-Iceland, Trough Central Europe
HNz	Icelandic High, Trough Central Europe
Na	North anticyclonic
NEz	**North-East cyclonic**
NWa	North-West anticyclonic
NWz	North-West cyclonic
Nz	North cyclonic
SEa	South-East anticyclonic
SEz	South-East cyclonic
SWz	South-West cyclonic
Sz	South cyclonic
TB	Low over the British Isles
TM	**Low over Central Europe**
TrM	**Trough over Central Europe**
TrW	Trough over Western Europe
Wa	West anticyclonic
WS	South-Shifted West cyclonic
Wz	**West cyclonic**

Figure 9. Frequency of weather types (size of circles) related to the 54 EPEs according to GWLc (filled-in circles, grey labels) and SVGc (empty circles, black labels in italics), and mean duration and mean monthly distribution of EPEs corresponding with weather types; the three predominant weather types of GWLc and SVGc are highlighted in bold.

among the three strongest WHY EPEs. As in August 2002 (Section 3.2.1.) and based on archived weather maps, Central Europe was influenced by a Vb cyclone that moved from North-Eastern France north-eastwards. Although the manual subjective GWLc of weather types (Werner and Gerstengarbe, 2010) shows that Central Europe was influenced by a low over the British Isles during the event, rather high pressure over the British Isles was found according to NCEP/NCAR reanalysis, which is typical for the Vb cyclones. Unlike the GWLc, according to the automated SVGc (James, 2007), the event was reasonably associated with a trough over Central Europe (Table 1). No flood of 2-years or higher return period was recorded in the Ohře river basin (Louny hydrological station) or at the last Czech hydrological station at the Elbe river in Děčín (Brázdil, 2006). However, a small catchment-wide flood was recorded in the Mulde river catchment with return period estimates of discharges from 2 (e.g. Pockau and Nossen hydrological stations) to 4 years (e.g. Niederschlema, Wechselburg and Golzern hydrological stations) according to Petrow *et al.* (2007).

3.3. Synoptic conditions of EPEs

The GWLc method shows that EPEs in the OM regions occur mostly (Figure 9) when a low (TM) or a trough (TrM) is situated over Central Europe, or during the West cyclonic weather type (Wz). Similar to GWLc, the SVGc (SynopVisGWL-catalogue) method leads to the highest frequency of EPEs associated with TrM (8 EPEs). However, instead of the TM and Wz, the North-Eastern cyclonic pattern (NEz) and trough over Central Europe and Scandinavian high (HFz) appear among the three most frequent weather types associated with heavy rainfall in the OM. Both GWLc and SVGc differ in frequency associated with heavy precipitation (e.g. Wz associated with seven EPEs for GWLc and one EPE for SVGc), in number of representatives (17 GWLc *vs* 20 SVGc weather types) and in mean duration of EPEs related to a weather type (1–2 days for EPEs associated with Scandinavian high and ridge over Central Europe HFa weather type for GWLc, and 6 days for HFa related EPEs for SVGc). Fewer differences between GWLc and SVGc are found in the mean monthly distribution of EPEs related to weather types.

According to the GWLc, EPEs related to the low-pressure systems over and east from Central Europe (TrM, TM, and NEz) occurred more often in SHY (July–August in particular) and lasted 3–4 days on average. This agrees with Müller and Kašpar (2010), who detected strong moisture flux from the northern quadrant as a typical feature for maximum discharge increases at Mulde River from May to October. On the contrary, EPEs associated with the cyclonic situations from North-West (NWz) occurred more likely in the winter half-year (WHY) and lasted longer (7 days on average). This corresponds to our previous findings (Figure 4c) showing a greater area affected by heavy rainfall in WHY in general and thereby their rather long duration. The SVGc method reveals a similar seasonal pattern for the TrM, TM, NEz and NWz weather types. Moreover, it is also characterized by a longer duration of EPEs related to TM weather conditions on average (5–6 days) and by the short duration of EPEs connected with the TrM (1–3 days on average). Surprisingly, the western cyclonic weather type (Wz) did not occur during the EPEs in winter months according to both the GWLc and SVGc. However, the results may be influenced by the computation of mean duration and the mean monthly occurrence of EPEs per a weather type.

Based on components *WEI* and duration (Figure 6), the PCA reveals that the weather types associated with five

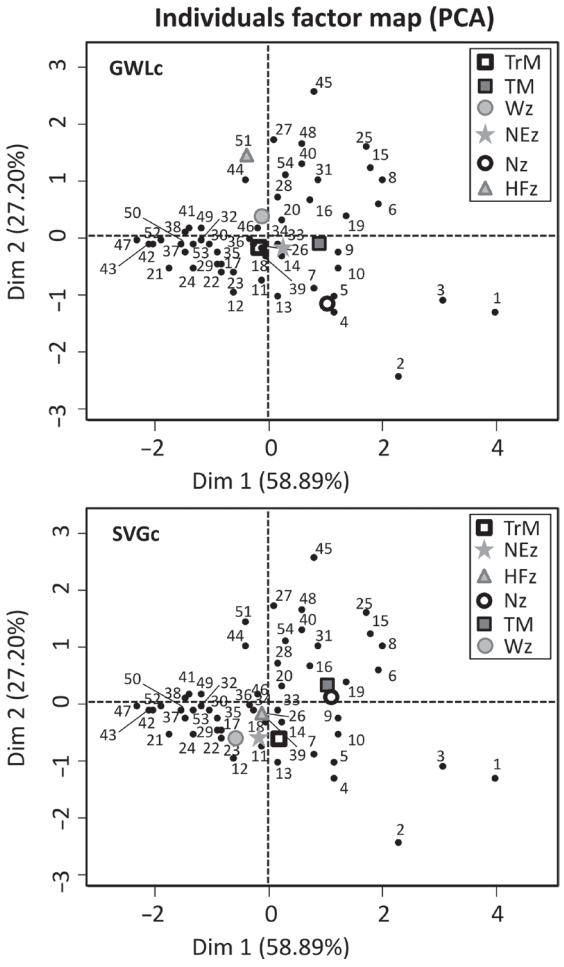

Figure 10. PCA of the 54 EPEs, their extremity, duration and different weather types according to the (top) GWLc and (bottom) SVGc classifications. The abbreviations of weather types are explained in Figure 9. The weather types are ordered according to their frequency, only those related to five or more EPEs from both the GWLc and SVGc are considered (the remaining weather types are for easier comparison between the GWLc and SVGc).

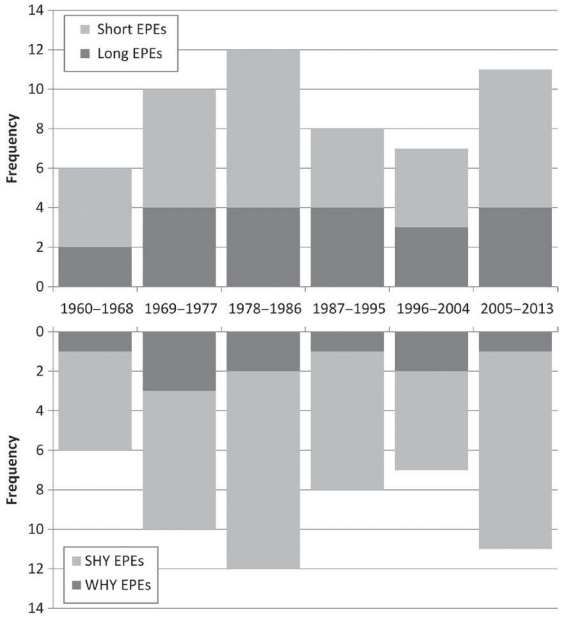

Figure 11. Frequency of (top) short and long EPEs (division according to Figure 3), and (bottom) of summer half-year (SHY) and winter half-year (WHY) EPEs during 1960–2013 divided into six equally long periods.

and more EPEs are better correlated with *WEI* for GWLc and with duration for SVGc (Figure 10). For SVGc all the displayed weather types are of medium extremity (*WEI*), for GWLc it is valid apart from the weather types HFz and Nz (North cyclonic) showing low and high extremity, respectively. The TrM and NEz tend to be of medium duration and TM of longer duration for both the GWLc and SVGc. Taking into consideration Figure 6, the Figure 10 also shows that the EPEs related to TrM and NEz tend to occur in SHY according to both catalogues. The PCA thus confirms the findings from Figure 9.

Many differences were found between the GWLc and SVGc methods. A thorough analysis (not presented here) comparing both the catalogues with NCEP/NCAR reanalysis for each EPE individually revealed that SVGc provides more convincing results as compared to the GWLc. For instance, during the two EPEs starting on 01 August 1991 (29th EPE in Table 1) and 15 October 1960 (discussed above in Section 3.2.2.), the GWLc showed less plausible weather types than SVGc. The automated SVGc seems to be more accurate based on the 54 analysed EPEs from OM region.

3.4. Trends in EPEs

Based on the inter-annual changes in frequency of EPEs, short/long EPEs, and SHY/WHY EPEs during 1960–2013, no significant trend (at 90% and higher confidence levels) was identified. The Sen's estimate resulted in completely flat distribution, which might be related to a limited number of representatives. Thus the results were not depicted, instead, clusters of EPEs during 9-years periods (i.e. divisible of 54 years long study period) were created to increase the number of representatives, and the frequency of EPEs in clusters was discussed and shown in Figure 11.

Despite the insignificant EPE trends, results of INTERKLIM (2014) showed an increase in the number of very wet days (daily totals *Rd* exceeding 95th^{h} percentile) and extremely wet days (*Rd* exceeding 99th percentile), and in days with strong precipitation (*Rd* greater than 10 mm) and extreme precipitation (*Rd* greater than 30 mm) at many rain gauges in the Bohemia-Saxony border during 1961–1990 as compared with 1991–2010. However, many regional dissimilarities in trends were also shown, and the analysis considered only changes in daily totals (instead of events), as compared with the EPEs (i.e. 1–10 days totals). The heavy rainfall was not defined the same way, e.g. the number of representatives was much higher in their analysis. In addition, the threshold 30 mm for extreme precipitation might be underestimated, e.g. for mountainous stations due to the differences in microclimates such as the dependence

of precipitation on altitude (Barry, 2008). The analysis of INTERKLIM (2014) also resulted in a decrease of wet spells ($Rd > 1$ mm) at all considered stations suggesting that the results are definition-dependent.

The changes in clusters of EPEs (Figure 11) show two periods of increased frequency of EPEs – at the turn of 1970s and 1980s (1969–1986), and at the end of the study period. The periods of increased frequency in EPEs might have been influenced by natural variability, especially in atmospheric circulation patterns. For instance, the warm (positive) phase of the Atlantic Multidecadal Oscillation (AMO) is accompanied by low-pressure anomalies. The AMO is in its positive warm phase since the mid-1990s, possibly leading to intensified heavy precipitation activity over the Atlantic Ocean and in Europe (Knight *et al.*, 2006). However, the frequency in EPEs averaged for the last two clusters (1996–2013) was not exceptionally high.

The frequency of long EPEs did not substantially vary from cluster to cluster (2–4 EPEs per cluster), and the short EPEs increased in the first half of the study period (1960–1986) and between the last two clusters (1996–2013). The clusters of SHY EPEs varied in frequency similarly to the entire EPEs dataset during the study period, which might be related to the high representation of SHY EPEs in the whole dataset of EPEs. The clusters of WHY EPEs exhibited negligible changes in frequency (1–3 EPEs per cluster) and were likely connected with the North Atlantic Oscillation (NAO) as the NAO produces the largest climate anomalies particularly during the colder half-year (Hurrell, 2005). On the other hand, Zolina (2014) found an increasing linear trend in mean wet spells ($Rd \geq 1$ mm) in WHY (up to 4% per decade) in Saxony during 1950–2008, whereas no clear trend in SHY (from −3 to 4% per decade) despite decreasing trend at many locations. However, especially the linear trends in the fractional contribution of rainfall during wet spells differing in durations (i.e. 1-day, 2–4 days and ≥ 5 days long) did not result in any significant trend at many locations in Saxony. This is in good agreement with our findings about EPEs that have mixed durations, although the EPEs are defined in a different way and represent much smaller dataset as compared to wet spells.

4. Conclusions

Müller and Kaspar's (2014) methodology of an event-adjusted evaluation of EPEs was applied successfully beyond the Czech Republic territory at a regional scale in OM, the area with complex relief. The resulting dataset of 54 EPEs is in good agreement with known heavy rainfall episodes in the OM region.

The WEI is easily computable and valuable for comparing the extremeness of different events within a defined study area. The index enables quantification and thus better comparability of extreme weather events. However, the comparability between EPEs from regions of different size needs an adjustment of the WEI values, as the WEI can reach higher values with increasing size of the considered area. With fixed study area borders some locations of extreme precipitation might be excluded. This leads to a different evaluation of extremity for a shifted or extended study area. Nonetheless, the event-adjusted evaluation method provides a powerful tool to investigate extreme precipitation. It has a huge potential for a wider use, e.g. in other regions, with data of different time resolution (hour, days, weeks, months), and weather prediction and climate model data, and so on.

The selected 54 EPEs were analysed in detail in order to gain insight into the characteristics of the heavy precipitation events in OM, which was the main purpose of the study. Based on the duration of EPEs, these were classified into long (≥3 days) and short (≤ 2 days) events within the OM region. However, the probability that long events include several shorter ones is high. The majority of EPEs occurred in summer or late spring, being often connected with a low or a trough over Central Europe. The extremity of the SHY events seems to increase with the size of the affected area. WHY EPEs generally affected a larger area. Based on the manual GWLc and the automated SVGc catalogues, the EPEs were most frequently related to a trough situated over Central Europe. However, many differences were found between the two catalogues. SVGc provided more plausible weather types associated with 54 EPEs in our dataset. Two of the three most extreme events occurred in the 21st Century. Nevertheless, no significant trend was found during the study period in EPEs, short and long EPEs, and SHY and WHY EPEs.

Our results clearly are a useful aid for decision makers in the OM area, especially when the Flood Extremity Index (FEI) is to be computed (Müller *et al.*, 2015). Insurance services analysing precipitation-related natural hazards may benefit from the classification of weather extremes during assembly of their contracts.

We are currently investigating the selected EPEs via the event-adjusted method in other low mountains in Central Europe. We intend to compare the results with those presented here for the OM region. Another recently studied issue is a quantitative evaluation of circulation anomalies (Müller *et al.*, 2009b) and their combinations (Kašpar and Müller, 2014) which were connected with the presented EPEs and can be considered as typical for precipitation extremes in the studied area.

Acknowledgements

We thank DWD (Deutscher Wetterdienst) and CHMI (Czech Hydrometeorological Survey) for data, and DBU (Deutsche Bundesstiftung Umwelt) for their support of our research. We acknowledge M.Phil. Syed Muntazir Abbas for his valuable remarks during the revision of the manuscript.

References

Ban N, Schmidli J, Schär C. 2015. Heavy precipitation in a changing climate: does short-term summer precipitation increase faster? *Geophys. Res. Lett.* **2014**: GL062588. https://doi.org/10.1002/2014GL062588.

Barros V, Field C, Dokke D, Mastrandrea M, Mach K, Bilir T, Chatterjee M, Ebi K, Estrada Y, Genova R, Girma B, Kissel E, Levy A, MacCracken S, Mastrandrea P, White L. 2014. *Climate Change 2014: Impacts, Adaptation, and Vulnerability. Part B: Regional Aspects. Contribution of Working Group II to the Fifth Assessment Report of the Intergovernmental Panel on Climate Change*. Cambridge University Press: Cambridge, UK.

Barry RG. 2008. *Mountain Weather and Climate*, 3rd edn. Cambridge University Press: Cambridge, UK.

van Bebber WJ. 1891. *Die Zugstrassen der barometrischen Minima nach den Bahnenkarten der deutschen Seewarte für den Zeitraum 1875-1890*.

Botero BA, Francés F. 2010. Estimation of high return period flood quantiles using additional non-systematic information with upper bounded statistical models. *Hydrol. Earth Syst. Sci.* **14**(12): 2617–2628. https://doi.org/10.5194/hess-14-2617-2010.

Boucek J. 2007. August 2002 catastrophic flood in the Czech Republic. In *Extreme Hydrological Events: New Concepts for Security*, Vasiliev OF, VanGelder P, Plate EJ, Bolgov MV (eds). Springer: Dordrecht, The Netherlands, 59–68.

Brázdil R (ed). 2006. *Historické a současné povodně v České republice*. Masarykova University [u.a.]: Brno, Czech Republic.

Brazdil R, Kotyza O, Dobrovolny P. 2006. July 1432 and August 2002 – two millennial floods in Bohemia? *Hydrol. Sci. J.* **51**(5): 848–863. https://doi.org/10.1623/hysj.51.5.848.

CHMI. n.d. *CHMI Portal*: *Info for you*: *Historical Data*: *Weather*: *Territorial precipitation*. (accessed February 2016).

Coelho CS, Ferro CT, Stephenson DB, Steinskog DJ. 2008. Methods for exploring spatial and temporal variability of extreme events in climate data. *J. Clim.* **21**(10): 2072–2092. https://doi.org/10.1175/2007JCLI1781.1.

Coles S. 2001. *An Introduction to Statistical Modeling of Extreme Values*. Springer: London; New York, NY.

Conradt T, Roers M, Schröter K, Elmer F, Hoffmann P, Koch H, Hattermann FF, Wechsung F. 2013. Comparison of the extreme floods of 2002 and 2013 in the German part of the Elbe River basin and their runoff simulation by SWIM-live. *Hydrol. Wasserbewirtschaftung* **57**(5): 241–245. https://doi.org/10.5675/HyWa-2013,5-4.

Deni SM, Jemain AA, Ibrahim K. 2010. The best probability models for dry and wet spells in Peninsular Malaysia during monsoon seasons. *Int. J. Climatol.* **30**(8): 1194–1205. https://doi.org/10.1002/joc.1972.

DWD DDR, HMÚ ČSSR. 1975. *Podnebí a počasí v Krušných horách*. SNTL – Nakladatelství technické literatury: Praha.

Goldberg V, Bernhofer C. 2003. The flash flood event in the catchment of the river Weisseritz (eastern Erzgebirge, Saxony) from 12 to 14 August 2002 – meteorological and hydrological reasons, damage assesment and disaster management. Paper presented at the EGS – AGU – EUG Joint Assembly, 5134.

Grams CM, Binder H, Pfahl S, Piaget N, Wernli H. 2014. Atmospheric processes triggering the central European floods in June 2013. *Nat. Hazards Earth Syst. Sci.* **14**(7): 1691–1702. https://doi.org/10.5194/nhess-14-1691-2014.

Gumbel EJ. 1941. The return period of flood flows. *Ann. Math. Stat.* **12**(2): 163–190.

Hess P, Brezowsky H. 1977. *Katalog der Grosswetterlagen Europas: (1881-1976)*. Deutscher Wetterdienst: Offenbach a.M, Germany.

Hirabayashi Y, Mahendran R, Koirala S, Konoshima L, Yamazaki D, Watanabe S, Kim H, Kanae S. 2013. Global flood risk under climate change. *Nat. Clim. Change* **3**(9): 816–821. https://doi.org/10.1038/nclimate1911.

Hirsch RM, Slack JR. 1984. A nonparametric trend test for seasonal data with serial dependence. *Water Resour. Res.* **20**(6): 727–732. https://doi.org/10.1029/WR020i006p00727.

Hirsch RM, Slack JR, Smith RA. 1982. Techniques of trend analysis for monthly water quality data. *Water Resour. Res.* **18**(1): 107–121. https://doi.org/10.1029/WR018i001p00107.

HMI. 1972. *Katalog povětrnostních situací pro území ČSSR*. SNTL: Prague, Czech Republic.

Hoy A, Jaagus J, Sepp M, Matschullat J. 2012a. Spatial response of two European atmospheric circulation classifications (data 1901–2010). *Theor. Appl. Climatol.* **112**(1–2): 73–88. https://doi.org/10.1007/s00704-012-0707-x.

Hoy A, Sepp M, Matschullat J. 2012b. Atmospheric circulation variability in Europe and northern Asia (1901 to 2010). *Theor. Appl. Climatol.* **113**(1–2): 105–126. https://doi.org/10.1007/s00704-012-0770-3.

Hurrell JW. 2005. *North Atlantic Oscillation. Encyclopedia of World Climatology*. Springer-Verlag: Berlin, 536–539.

INTERKLIM. 2014. *Der Klimawandel im böhmisch-sächsischen Grenzraum. Změna klimatu v česko-saském pohraničí*. Sächsisches Landesamt für Umwelt: Dresden, Germany.

James PM. 2007. An objective classification method for Hess and Brezowsky Grosswetterlagen over Europe. *Theor. Appl. Climatol.* **88**(1–2): 17–42. https://doi.org/10.1007/s00704-006-0239-3.

James P, Stohl A, Spichtinger N, Eckhardt S, Forster C. 2004. Climatological aspects of the extreme European rainfall of August 2002 and a trajectory method for estimating the associated evaporative source regions. *Nat. Hazard. Earth Syst. Sci.* **4**(5/6): 733–746.

Kalnay E, Kanamitsu M, Kistler R, Collins W, Deaven D, Gandin L, Iredell M, Saha S, White G, Woollen J, Zhu Y, Leetmaa A, Reynolds R, Chelliah M, Ebisuzaki W, Higgins W, Janowiak J, Mo KC, Ropelewski C, Wang J, Jenne R, Joseph D. 1996. The NCEP/NCAR 40-year reanalysis project. *Bull. Am. Meteorol. Soc.* **77**(3): 437–471. https://doi.org/10.1175/1520-0477(1996)077<0437:TNYRP>2.0.CO;2.

Kašpar M, Müller M. 2014. Combinations of large-scale circulation anomalies conducive to precipitation extremes in the Czech Republic. *Atmos. Res.* **138**: 205–212. https://doi.org/10.1016/j.atmosres.2013.11.014.

Kašpar M, Müller M, Crhová L, Holtanová E, Polášek JF, Pop L, Valeriánová A. 2016. Relationship between Czech windstorms and air temperature. *Int. J. Climatol.* **37**(1): 11–24. https://doi.org/10.1002/joc.4682.

Katz RW. 2010. Statistics of extremes in climate change. *Clim. Change* **100**(1): 71–76. https://doi.org/10.1007/s10584-010-9834-5.

Katz RW, Parlange MB, Naveau P. 2002. Statistics of extremes in hydrology. *Adv. Water Resour.* **25**(8–12): 1287–1304. https://doi.org/10.1016/S0309-1708(02)00056-8.

Kendall MG. 1975. *Rank Correlation Methods*. Griffin: Oxford, England.

Kienzler S, Pech I, Kreibich H, Mueller M, Thieken AH. 2015. After the extreme flood in 2002: changes in preparedness, response and recovery of flood-affected residents in Germany between 2005 and 2011. *Nat. Hazard. Earth Syst. Sci.* **15**(3): 505–526. https://doi.org/10.5194/nhess-15-505-2015.

Kněžínková B, Brázdil R, Štěpánek P. 2010. Porovnávání měření srážek srážkoměrem METRA 886 a automatickým člunkovým srážkoměrem MR3H ve staniční síti Českého hydrometeorologického ústavu. *Meteorol. zprávy* **63**: 147.

Knight JR, Folland CK, Scaife AA. 2006. Climate impacts of the Atlantic Multidecadal Oscillation. *Geophys. Res. Lett.* **33**(17): L17706. https://doi.org/10.1029/2006GL026242.

Kyselý J. 2009. Trends in heavy precipitation in the Czech Republic over 1961–2005. *Int. J. Climatol.* **29**(12): 1745–1758. https://doi.org/10.1002/joc.1784.

Mann HB. 1945. Nonparametric tests against trend. *Econometrica* **13**(3): 245–259. https://doi.org/10.2307/1907187.

Merz B, Elmer F, Kunz M, Mühr B, Schröter K, Uhlemann-Elmer S. 2014. The extreme flood in June 2013 in Germany. *La Houille Blanche* **1**: 5–10. https://doi.org/10.1051/lhb/2014001.

Minářová J, Müller M, Clappier A. 2016. Seasonality of mean and heavy precipitation in the area of the Vosges Mountains: dependence on the selection criterion. *Int. J. Climatol.* https://doi.org/10.1002/joc.4871.

Mudelsee M, Börngen M, Tetzlaff G, Grünewald U. 2004. Extreme floods in central Europe over the past 500 years: role of cyclone pathway "Zugstrasse Vb": extreme floods in central Europe. *J. Geophys. Res.* **109**(D23): D23101. https://doi.org/10.1029/2004JD005034.

Müller M, Kašpar M. 2010. Quantitative aspect in circulation type classifications – an example based on evaluation of moisture flux anomalies. *Phys. Chem. Earth A/B/C* **35**(9–12): 484–490. https://doi.org/10.1016/j.pce.2009.09.004.

Müller M, Kaspar M. 2014. Event-adjusted evaluation of weather and climate extremes. *Nat. Hazard. Earth Syst. Sci.* **14**(2): 473–483. https://doi.org/10.5194/nhess-14-473-2014.

Müller M, Kašpar M, Matschullat J. 2009a. Heavy rains and extreme rainfall-runoff events in Central Europe from 1951 to 2002. *Nat. Hazard. Earth Syst. Sci.* **9**(2): 441–450.

Müller M, Kašpar M, Řezáčová D, Sokol Z. 2009b. Extremeness of meteorological variables as an indicator of extreme precipitation events. *Atmos. Res.* **92**(3): 308–317. https://doi.org/10.1016/j.atmosres.2009.01.010.

Müller M, Kašpar M, Valeriánová A, Crhová L, Holtanová E, Gvoždíková B. 2015. Novel indices for the comparison of precipitation extremes and floods: an example from the Czech territory. *Hydrol. Earth Syst. Sci.* **19**(11): 4641–4652. https://doi.org/10.5194/hess-19-4641-2015.

Muluneh A, Bewket W, Keesstra S, Stroosnijder L. 2016. Searching for evidence of changes in extreme rainfall indices in the Central Rift Valley of Ethiopia. *Theor. Appl. Climatol.* : 1–15. https://doi.org/10.1007/s00704-016-1739-4.

Munzar J, Auer I, Ondráček S. 2011. Central European one-day precipitation record. *Hist. Geogr.* **64**(4): 107–112.

Ngo-Duc T, Tangang FT, Santisirisomboon J, Cruz F, Trinh-Tuan L, Nguyen-Xuan T, Phan-Van T, Juneng L, Narisma G, Singhruck P, Gunawan D, Aldrian E. 2016. Performance evaluation of RegCM4 in simulating extreme rainfall and temperature indices over the CORDEX-Southeast Asia region. *Int. J. Climatol.* **37**(3): 1634–1647. https://doi.org/10.1002/joc.4803.

Noack P, Jacobs F, Börngen M. 2014. *Leipzig. Alle Wetter!: Alltägliches – Besonderes –Extremes*. Leipzig.

Oliver JE. 2008. *Encyclopedia of World Climatology*. Springer Science & Business Media: Dordrecht, The Netherlands.

Pachauri RK, Allen MR, Barros VR, Broome J, Cramer W, Christ R, Church JA, Clarke L, Dahe Q, Dasgupta P, Dubash NK, Edenhofer O, Elgizouli I, Field CB, Forster P, Friedlingstein P, Fuglestvedt J, Gomez-Echeverri L, Hallegatte S, Hegerl G, Howden M, Jiang K, Jimenez Cisneroz B, Kattsov V, Lee H, Mach KJ, Marotzke J, Mastrandrea MD, Meyer L, Minx J, Mulugetta Y, O'Brien K, Oppenheimer M, Pereira JJ, Pichs-Madruga R, Plattner G-K, Pörtner H-O, Power SB, Preston B, Ravindranath NH, Reisinger A, Riahi K, Rusticucci M, Scholes R, Seyboth K, Sokona Y, Stavins R, Stocker TF, Tschakert P, van Vuuren D, van Ypserle J-P. 2014. *Climate Change 2014: Synthesis Report. Contribution of Working Groups I, II and III to the Fifth Assessment Report of the Intergovernmental Panel on Climate Change*. IPCC: Geneva, Switzerland.

Parlow E. 1996. The regional climate project REKLIP – an overview. *Theor. Appl. Climatol.* **53**(1–3): 3–7. https://doi.org/10.1007/BF00866406.

Pechala F, Böhme W (eds). 1975. *Podnebí a počasí v Krušných horách*. SNTL: Praha.

Petrow T, Merz B, Lindenschmidt K-E, Thieken AH. 2007. Aspects of seasonality and flood generating circulation patterns in a mountainous catchment in south-eastern Germany. *Hydrol. Earth Syst. Sci. Discuss.* **4**(2): 589–625.

Rudolf B, Rapp J. 2002. Das Jahrhunderthochwasser der Elbe: Synoptische Wetterentwicklung und klimatologische Aspekte. *DWD Klimastatusbericht* : 172–187.

Schiller J. 2016. *Eine Sensitivitätsanalyse des Weather Extremity Index (WEI) nach Müller und Kaspar zur Beschreibung extremer Niederschläge unter Verwendung radarbasierter Niederschlagsmessungen des Deutschen Wetterdienstes*. University of Cologne: Cologne, Germany.

Schröter K, Kunz M, Elmer F, Mühr B, Merz B. 2015. What made the June 2013 flood in Germany an exceptional event? A hydrometeorological evaluation. *Hydrol. Earth Syst. Sci.* **19**(1): 309–327. https://doi.org/10.5194/hess-19-309-2015.

SMUL. 2008. *Sachsen im Klimawandel – Eine Analyse*. Sächsisches Staatsministerium für Umwelt und Landwirtschaft: Dresden, Germany.

Socher M, Boehme-Korn G. 2008. Central European floods 2002: lessons learned in Saxony. *J. Flood Risk Manage.* **1**(2): 123–129. https://doi.org/10.1111/j.1753-318X.2008.00014.x.

Stein C, Malitz G. 2013. Das Hochwasser an Elbe und Donau im Juni 2013, Berichte des Deutschen Wetterdienstes.

Štekl J (ed). 2001. *Extrémni denní srážky na území České Republiky v období 1879-2000 a jejich synoptické příčny = Extreme Daily Precipitation on the Territory of the Czech Republic in the Period 1879-2000 and Their Synoptic Causes*. Český hydrometeorologický ústav: Praha.

Stryhal J, Huth R. 2016. Classifications of atmospheric circulation. *Geophys. J. R. Astron. Soc.* **121**(2): 300–323.

Thieken AH, Muller M, Kreibich H, Merz B. 2005. Flood damage and influencing factors: new insights from the August 2002 flood in Germany. *Water Resour. Res.* **41**(12): W12430. https://doi.org/10.1029/2005WR004177.

Thieken AH, Kreibich H, Mueller M, Merz B. 2007. Coping with floods: preparedness, response and recovery of flood-affected residents in Germany in 2002. *Hydrol. Sci. J.* **52**(5): 1016–1037. https://doi.org/10.1623/hysj.52.5.1016.

Tošić I, Unkašević M, Putniković S. 2016. Extreme daily precipitation: the case of Serbia in 2014. *Theor. Appl. Climatol.* : 1–10. https://doi.org/10.1007/s00704-016-1749-2.

Ulbrich U, Brücher T, Fink AH, Leckebusch GC, Krüger A, Pinto JG. 2003. The central European floods of August 2002: Part 1 – rainfall periods and flood development. *Weather* **58**(10): 371–377. https://doi.org/10.1256/wea.61.03A.

Valeriánová A, Crhová L, Holtanová E, Kašpar M, Müller M, Pecho J. 2017. High temperature extremes in the Czech Republic 1961–2010 and their synoptic variants. *Theor. Appl. Climatol.* **127**(1): 17–29. https://doi.org/10.1007/s00704-015-1614-8.

Wang XL, Feng Y. 2013. RHtests_dlyPrcp User Manual. Climate Research Division, Atmospheric Science and Technology Directorate, Science and Technology Branch, Environment Canada, Toronto, Ontario, Canada, Retrieved February 2017, 17 pp.

Wang XL, Chen H, Wu Y, Feng Y, Pu Q. 2010. New techniques for the detection and adjustment of shifts in daily precipitation data series. *J. Appl. Meteorol. Climatol.* **49**(12): 2416–2436. https://doi.org/10.1175/2010JAMC2376.1.

Wang Q, Wang M, Fan X, Zhang F, Zhu S, Zhao T. 2016. Trends of temperature and precipitation extremes in the Loess Plateau Region of China, 1961–2010. *Theor. Appl. Climatol.* : 1–15. https://doi.org/10.1007/s00704-016-1820-z.

Werner PC, Gerstengarbe F-W. 2010. PIK Report No. 119 – Der Grosswetterlagen Europas nach Paul Hess und Helmut Brezowsky 7, verbesserte und ergänzte Auflage.

Whiteman CD. 2000. *Mountain Meteorology: Fundamentals and Applications*. Oxford University Press: Oxford, UK.

World Meteorological Organization. 2008. *Guide to Meteorological Instruments and Methods of Observation*. World Meteorological Organization: Geneva, Switzerland.

Zolina O. 2014. Multidecadal trends in the duration of wet spells and associated intensity of precipitation as revealed by a very dense observational German network. *Environ. Res. Lett.* **9**(2): 025003. https://doi.org/10.1088/1748-9326/9/2/025003.

Zolina O, Simmer C, Kapala A, Shabanov P, Becker P, Mächel H, Gulev S, Groisman P. 2014. Precipitation variability and extremes in Central Europe: new view from STAMMEX results. *Bull. Am. Meteorol. Soc.* **95**(7): 995–1002. https://doi.org/10.1175/BAMS-D-12-00134.1.

10. Article V: ‘Comparison of synoptic conditions and characteristics of extreme precipitation between the Ore Mountains and the Vosges Mountains’

In the fifth article (Minářová *et al.*, [submitted]) entitled ‘Comparison of synoptic conditions and characteristics of extreme precipitation between the Ore Mountains and the Vosges Mountains’, the first part is dedicated to detailed analysis of synoptic conditions during 54 EPEs in the Ore Mountains (OM) and the Vosges Mountains (VG) individually, based on derived (previously recommended) synoptic quantitative variables such as components of wind direction, flux of specific humidity, and vertical velocity (in p-system) at 500 and 850 hPa levels. The analysis enables to categorize the synoptic situation during which the EPEs occur. Based on the results of Pearson’s chi-squared test (Greenwood and Nikulin, 1996) at 1 % significance level and Cramér's V (Cramér, 1946), the second (major) part of the paper focuses on relationships and in/dependence among the EPE characteristics that were qualitatively categorized. It discusses the significantly dependent pairs of temporal, spatial, and synoptic attributes using the chi-squared residuals that provide the information about the positive/negative association between the categories of the characteristics. The paper thus provides a picture about the dis/similarities in the behaviour of EPEs in OM as compared to that in VG and points out whether the extreme precipitation patterns typical in Central Europe (OM) can also be expected in its western part (VG) as it is the case of mean precipitation patterns which exhibits central European features on the lee side of VG (i.e. Upper Rhine Plain).

Title

Comparison of synoptic conditions and characteristics of extreme precipitation between the Ore Mountains and the Vosges Mountains

Affiliation of authors:

Jana Minářová (ORCID id: 0000-0001-8870-9126)

Laboratory Image, City, Environment, National Centre for Scientific Research & University of Strasbourg (3 rue de l'Argonne, F-67000, Strasbourg), Strasbourg, France

jana.minarova@live-cnrs.unistra.fr

Department of Physical Geography and Geoecology, Faculty of Science, Charles University in Prague (Albertov 6, 128 43 Praha 2), Prague, Czech Republic

jana.minarova@natur.cuni.cz

Institute of Atmospheric Physics, Academy of Sciences of the Czech Republic (Boční II 1401, 141 31 Praha 4), Prague, Czech Republic

jana.minarova@ufa.cas.cz

+33 (0)6 83 58 03 96

+420 737 432 486

Dr. Miloslav Müller

Institute of Atmospheric Physics, Academy of Sciences of the Czech Republic (Boční II 1401, 141 31 Praha 4), Prague, Czech Republic

Department of Physical Geography and Geoecology, Faculty of Science, Charles University in Prague (Albertov 6, 128 43 Praha 2), Prague, Czech Republic

muller@ufa.cas.cz

+420 272 016 024

Pr. Alain Clappier

Laboratory Image, City, Environment, National Centre for Scientific Research & University of Strasbourg (3 rue de l'Argonne, F-67000, Strasbourg), Strasbourg, France

alain.clappier@live-cnrs.unistra.fr

+33 (0)3 68 85 08 96

Dr. Marek Kašpar

Institute of Atmospheric Physics, Academy of Sciences of the Czech Republic (Boční II 1401, 141 31 Praha 4), Prague, Czech Republic

kaspar@ufa.cas.cz

+420 272 016 024

Abstract

Understanding the characteristics of extreme precipitation events (EPEs) not only helps in mitigating the hazards associated with it but will also reduce the risks by improved planning based on detailed information, and provide basis for making better engineering decisions which can withstand the recurring and likely more frequent events predicted in future in the context of global climate change. In this study, the synoptic conditions and other characteristics (extremity, temporal and spatial characteristics) of the 54 EPEs that occurred during 1960—2013 were compared between two low mountain ranges situated in Central Europe; the Ore Mountains (OM) and Vosges Mountains (VG). The EPEs were defined using the Weather Extremity Index, which quantifies the extremity of events.

Intense flux of specific humidity prevailed during the EPEs in OM and VG. The EPEs were most frequently associated with lows in OM (Central European pattern) and troughs in VG (western European pattern). However, the EPEs in VG were also related to Vb cyclones, which confirms that the central European features of precipitation occurs in VG as well. Significant dependencies between the temporal characteristics and synoptic conditions were found in OM and VG, which might represent a common feature of low mountain ranges in Central Europe. The relationships of spatial characteristics of EPEs were site-specific, suggesting the need for individual analyses. The comparison of EPEs between the two low mountain ranges might be of its first kind, and contributes to the understanding of EPE characteristics in Central Europe.

Keywords

Erzgebirge, Krušné hory, heavy rainfall, Weather Extremity Index, synoptic pattern, precipitation

1. Introduction

Extreme precipitation has been the focus of atmospheric sciences since 1990s due to the direct impacts, such as the threat posed to the safety of transport, and the indirect impacts such as flooding, erosion, and landsliding which affect large areas even beyond the area of rainfall occurrence. To be able to reduce these impacts (e.g., loss of lives, large scale damages to agriculture resources and property, and contamination of clean water), the emphasis on recognition, description, and prediction of precipitation extremes has become more crucial specially in the context of global climate change (Beniston and Stephenson 2004), i.e. an increase in the frequency of weather and climate extremes has been predicted (Pachauri et al. 2014). As documented by simulations of the development in 21st century by Euro-Cortex, almost all European countries might experience an increase in the frequency of extreme precipitation (Söder et al. 2009; Vautard not dated).

Despite the improved prediction of heavy rainfall and enhanced communication with decision makers to issue warnings (Cavalcanti 2012), considerable causalities and dire financial impacts were induced by the two relatively recent episodes: the heavy rainfall events and related floods in the middle Danube and the Elbe catchments in 2002 and 2013 in Central Europe (Van der Schrier, et al. 2013; Thieken et al. 2005; Brazdil et al. 2006; Boucek 2007). It demonstrates the ongoing vulnerability of European societies to weather extremes and demands more detailed insight into the characteristics and conditioning factors of heavy rainfall (e.g., synoptic conditions) in Europe at diverse temporal and spatial scales in Europe to make the risk management and warning systems more efficient (Thieken et al. 2007; Socher and Boehme-Korn 2008; Kienzler et al. 2015).

Since the spatial distribution of (mean) precipitation in orographic areas is very complex and not all the processes have satisfactorily been understood (Prudhomme and Reed 1998; Roe et al. 2003; Smith 2006), the spatial distribution of precipitation extremes in orographic areas is even more complicated and needs further attention. Recent papers dealing with heavy rainfall in orographic areas in Europe mostly considered the Alps and the Carpathian Mountains (e.g., Bartholy and Pongracz 2005; Bartholy and Pongrácz 2007; Foresti and Pozdnoukhov 2012; Awan and Formayer 2016). However, in Central Europe, there are many low mountain ranges which are densely populated (especially on their leeward side) as compared to the Alps and the Carpathian Mountains, thus more vulnerable to the damages associated with natural disasters. In addition, the future projections of heavy rainfall in the region are vague (Solomon et al. 2007; Pachauri et al. 2014), which makes the region of Central Europe more appealing for further analyses (Alexander et al. 2006; Solomon et al. 2007; Pachauri et al. 2014)(Alexander et al. 2006; Solomon et al. 2007; Pachauri et al. 2014).

The current study focuses on several characteristics (duration, affected area, and extremity) and synoptic conditions during extreme precipitation in two low mountain ranges situated in Central Europe: Vosges Mountains (northeastern France) and the Ore Mountains (also named as Krušné hory or Erzgebirge at the Czech-German border). The selection of study areas is related to the orographic effect that is responsible for huge difference in precipitation totals between the windward and leeward sides; with the leeward sides considered to be one of the driest regions of the respective countries, i.e. France (Sell 1998) and the Czech Republic (Pechala and Böhme 1975; Tolasz et al. 2007). Besides the similar morphology, the two study areas differ in mean annual course of precipitation depending on the continentality (Section 2.1). Moreover, the extreme precipitation in the Vosges Mountains is compared with that in the Ore Mountains (middle Central Europe) to see whether the typical central European meteorological patterns related to extreme precipitation, such as Vb cyclones (Bebber

1891; Nissen et al. 2013; Messmer et al. 2015), are also typical in the Vosges Mountains that are situated westernmost in Central Europe.

To the best of our knowledge, only the project INTERKLIM (2014) has partly dealt with heavy rainfall across the whole Ore Mountains using the threshold-based definition of extremes; and in the Vosges Mountains a very local case study has been conducted to examine the leeward convection under the COPS campaign (Labbouz et al. 2013). We analysed the heavy rainfall in both regions separately (Minářová et al. 2017a [in press], b [in press]) using the event-adjusted evaluation method for precipitation extremes proposed by Müller and Kaspar (2014). This paper provides new results, i.e. a quantitative comparison of conditions leading to extreme precipitation, and a comparison of the characteristics of the extreme precipitation between the two study regions. The comparison results in highlighting the similarity/dissimilarity of the characteristics of extreme precipitation between the two regions. The results of this study can be used to understand similar characteristics in other low mountain ranges in Central Europe, such as Schwarzwald in Germany, Eifel at Germany-Belgium border, and Giant or Ore Mountains in the Czech Republic. The attributes of the extreme precipitation in both areas compared in this study have been defined the same way, contrary to the works of previous publications that were site specific, and used different definitions of heavy rainfall, which makes the comparison difficult. The results of such comparison will contribute to understand the patterns of heavy rainfall and its characteristics in other similar areas in Central Europe not yet studied in detail, and thus will help in mitigating the natural disasters and subsequent losses associated with extreme precipitation.

2. Data and Methods

2.1. Study areas

The study areas generally follow the boundaries of the administrative units comprising the Ore Mountains and the Vosges Mountains. At places, the boundaries were reduced corresponding to the spatial distribution of the weather stations (i.e. the large extra areas in the administrative units beyond the meteorological stations were omitted from the selection) in order to reduce the need of extrapolation of weather data. The two study areas, i.e. Ore and Vosges mountains, have some morphological and relief-related climatological similarities while they differ in mean annual course of precipitation, as described in the following.

2.1.1. Ore Mountains region (OM)

The study area comprising Ore Mountains (OM) and its surrounding area (40,600 km^2) is situated at the Czech-German border (Fig. 1a). The Ore Mountains is a low mountain range, which culminates at Klínovec Mountain (1,244 m a.s.l.). The slopes on German side are gentle as compared to the slopes on the Czech side. Typical climate in OM is temperate with the western major airflow from the Atlantic Ocean, and is transitional from the oceanic climate that dominates in Western Europe to a continental climate that prevails in Eastern Europe, (DWD DDR and HMÚ ČSSR 1975).

Complex relief is responsible for diverse microclimates in OM and is involved in producing the orographic effect on precipitation (Pechala and Böhme 1975), which is primarily related to the almost perpendicular orientation of the mountain range against the prevailing airflow direction and causes differences in precipitation totals between the (wetter) windward German side due to the orographic enhancement of precipitation and the (drier) leeward Czech side due to rain shadow (INTERKLIM 2014). The precipitation differences are also related to the elevation differences, which are displayed in Fig. 2a for the 5 classes of weather stations (the

classes are based on mean monthly totals from 167 weather stations during 1960—2013 that were used for Principal Component Analysis PCA and subsequent Hierarchical Clustering on Principal Components HCPC).

2.1.2. Vosges Mountains region (VG)

The study area comprising Vosges Mountains VG (31,400 km^2) is situated in northeastern France (Fig. 1b), and constitutes a broader area of the low mountain range, which culminates at Grand Ballon (1,424 m a.s.l.). Likewise OM, the VG has gentle windward (western) slopes and steeper leeward (eastern) slopes that dip towards the Upper Rhine Plain (Gley 1867; Alsatia 1932; Ernst 1988; Sell 1998). The Vosges Mountains represent a frontier between the temperate oceanic climate in its western part, and continental in the eastern part, mainly Upper Rhine Plain. It also includes microclimatic peculiarities (Sell 1998; Météo-France 2008).

Similar to OM, elevation, prevailing westerlies from the Atlantic Ocean, and the orographic effect related to the nearly perpendicular position of the mountain ridge to the prevailing airflow are among the most important factors responsible for differences in precipitation in the region (Sell 1998; Météo-France 2008). In VG, the differences in mean annual precipitation totals between the wettest and driest stations during 1960—2013 were up to 1,730 mm due to the orographic enhancement of precipitation on one side, and the rain shadow on the other (Minářová et al. 2016). The precipitation differences can be seen in Fig. 2b for the 5 classes (clusters) of rain gauges (the classes are based on mean monthly totals from 84 gauges during 1960—2013 that were used for PCA and subsequent HCPC).

2.2. Precipitation time series

In this paper, the daily precipitation totals during 1960—2013, obtained from *Météo-France*, *Deutscher Wetter Dienst* (DWD) and *Czech Hydrometeorological Institue* (CHMI) rain gauging networks, have been analysed. The metadata (e.g., changes in location, measuring instrument) was also acquired with the datasets.

The analysed datasets include data obtained at 168 meteorological stations in the Vosges Mountains study region (VG) and 167 meteorological stations in the Ore Mountains study region (OM). The data from Czech (leeward) side of the OM are available for 10 weather stations and span from 1960—2005 only. It may affect the results but not significantly since at regional scale, a higher uniformity of weather patterns is found on the (Czech) leeward side as compared to the (German) windward side (Whiteman 2000; Barry 2008).

Due to the installation of weather stations in VG with time, and the installation and shutting down of weather stations in OM, not all the stations could record data for the entire study period (54 years). Therefore, only the stations which recorded data for more than half of the study period (i.e. 27 years) were used for identification and characterization of the most extreme precipitation events (EPEs) in the study areas. The 27 years of observations were not bound to the beginning or the end of the 54-years period. In OM all the 167 stations, while in VG only 84 out of 168 (half of the stations) measured the daily precipitation totals for more than 27 years, because in VG the installation of rain gauges increased with time. The criterion of omitting the time series from stations that did not record data for more than half of the study period resulted in VG in an increase in the daily data availability from 35—62 % in the 1960s, and from 50 to almost 100 % since the 1980s.

The accuracy of calculating mean and capturing inter-annual changes is related to the completeness of data. Completeness of the yearly time series means that the data at the particular station is available for every day in a year i.e. for 365 days in a year. In VG, the missed values are up to a maximum of 5%, while in OM, it is up to a

maximum of 9% during half of the study period, which according to (Zolina et al. 2013) is acceptable for accurately estimating precipitation durations and their variability.

Relocation of stations and changes in measuring devices or its principles introduce inhomogenities in the time series. *RHtests_dlyPrcp* R-package http://etccdi.pacificclimate.org/software.shtml (Wang et al. 2010; Wang and Feng 2013) was conducted to test whether the daily precipitation time series are homogenous. The test considered the metadata including the changes in measuring devices. No significant relocation and inhomogeneities were noticed for the Czech rain gauges during 1965—2005 ((Kyselý 2009), thus a fixed data measurement error of 0.2 mm was used for OM as suggested by the WMO (World Meteorological Organization 2008). In VG, a value of 0.4 mm was used while considering the maximum error estimated for the changes in rain gauges. Minářová et al. (2016) have suggested that lower values (0.2 and 0.3 mm) produce similar results. No major inhomogeneities were noticed in the time series, except for 2 stations in VG which were homogenized. However, the difference between the raw data and the homogenized data of the 2 stations is insignificant, i.e. lower than the resolution of the time series (in the order of 10^{-2} mm). Thus, despite minor inconsistencies in the three national weather networks, the results from the analysed time series are considered robust.

Further analysis (Section 2.5) of time series was based on 1—10 days consecutive non-zero precipitation totals from individual stations. The threshold of 10 days was assumed to be sufficiently high since longer lasting extreme precipitation events were not awaited to occur in any of the study areas. The length of events lower than 10 days was not considered adequate based on the study from Pelt et al. (2014), who suggested that mainly the 10-days rainfall events are prone to induce flooding in Upper Rhine river basin, i.e. in VG.

The uneven spatial distribution of stations was considered not to substantially influence the robustness of our results, as described below (Section 2.5), since during the process of definition of heavy rainfall events only common logarithms of return period estimates from stations are interpolated into a regular grid. The common logarithms of return period estimates (and the return period estimates) exhibit flat distribution, which makes their interpolation to the uneven spatial distribution of stations much less sensitive as compared to the interpolation of precipitation totals (e.g., Šercl 2008). For instance, the insignificant dependence of return period estimates (N) on altitude as compared to the dependence of precipitation totals (R) on altitude (complex for extremes) is shown in Fig. 3 for the 4-day (4D) extreme precipitation event (starting on May 23, 1984) that affected the largest area of the VG.

2.3. Synoptic variables

Synoptic variables (wind velocity, geopotential height, the flux of specific humidity and vertical velocity) at 500 and 850 hPa isobaric levels (measured at 12 UTC) were derived from the NCEP/NCAR (National Centers for Environmental Prediction/National Center for Atmospheric Research) daily data reanalysis (Kalnay et al. 1996) in gridded form at 2.5° horizontal resolution for the period 1960—2010 (Uppala et al. 2005). Mean daily data (except geopotential height) from 6 grid points covering each study area (10–15°E and 50.0°–52.5°N in OM, while 5–10°E and 47.5°–50.0°N in VG) were used in the analysis of synoptic conditions occurring during extreme precipitation events. If an extreme precipitation event lasted longer than 1-day, the value of the day with the highest daily extremity of precipitation E_{ta} (defined in Section 2.5) was assigned to the event.

Meridional and zonal airflow components, and components of the flux of specific humidity were computed to know the direction of the airflow and flux of specific humidity; the positive and negative vertical velocity in p-system showed whether air was descending or ascending in meso-alpha scale according to Orlanski (1975),

respectively. The directional fluxes of specific humidity were considered to provide relevant information about extreme precipitation (Müller et al. 2009). A quantitative approach was also suggested to reflect the synoptic conditions during precipitation extremes (Müller and Kašpar 2010; Kašpar and Müller 2014a) better than qualitative approach such as the widespread "Grosswetterlagen" concept that provides the weather types over Europe (Werner and Gerstengarbe 2010).

2.4. Digital Elevation Model (DEM) and cartographic outputs

For the relief related information, Digital Elevation Models (DEM) comprising the two study areas were obtained from *GeoMapApp* (http://www.marine-geo.org/tools/maps_grids.php). The horizontal resolution of the *GeoMapApp*'s gridded *Global Multi-Resolution Topography* model is 100 m. The map outputs were produced in *Esri*'s *ArcGIS 10.5* software, where the DEMs were used as base maps, and in *Golden* software *Surfer 10*.

Ordinary Kriging with raster cell size of 2 km was used for interpolating the common logarithms of return period estimates into a regular grid (see below). The Ordinary Kriging was based on Gaussian semi-variogram model, and the maximum searching radius was set to variable. Cokriging or other geo-statistical methods with external drifts that could include orography in the interpolation were not considered in this paper since the return period estimates were found not sensitive to orography (Fig. 3).

2.5. Precipitation extremes: Event-adjusted evaluation method

Precipitation extremes were defined using the event-adjusted evaluation method proposed by (Müller and Kaspar 2014), which allows for quantitative estimation of the extremity of individual heavy rainfall events and their comparison using the variable extremity E_{ta} for a given duration t of an event, which affects an area a. At the beginning, return period estimates of precipitation totals (1—10 days in this study) are used to assess the rarity. The return period estimates are computed at individual rain gauges using the Generalized Extreme Value (GEV) distribution with maximal value of 1,000 years. The approximation of precipitation totals by GEV was found convenient on the basis of the goodness of fit test based on the L-kurtosis τ4 of the fitted distribution and the regional average L-kurtosis τ4R (Hosking and Wallis 1997). This is in good agreement with Kyselý and Picek (2007), who have shown that the GEV approximates the precipitation time series well and is suitable for the estimation of extreme precipitation events in the Czech Republic. Common logarithms of return period estimates calculated at individual gauges are subsequently interpolated into a regular grid (2 km horizontal resolution) using the Ordinary Kriging. No influence of orography on return period estimates was proved (Fig. 3), thus the orography was not considered in the interpolation. In the next step (computation of E_{ta}), the values of return period estimates at resulting grid points are taken one by one in their decreasing order, i.e. irrespective of their position in the study region.

The E_{ta} corresponds to the multiplication of the radius of a circle R [km] over an area a [km^2], that is equal to the area consisting of i number of included grid points, and the common logarithm of the spatial geometric mean G_{ta} of return period estimates N_{ti} [years] for a given duration t [days], i.e. the E_{ta} (Müller and Kaspar 2014):

$$E_{ta}[\log(\mathrm{yr})\mathrm{km}] = \log(G_{ta})\, R = \frac{\sum_{i=1}^{n} \log(\mathrm{N_{ti}})\sqrt{a}}{n\sqrt{\pi}} \qquad (1)$$

Based on the step-by-step inclusion of grid points with lower and lower return period estimate, the E_{ta} stops increasing at one point (maximum E_{ta}), i.e. the enlarging area does not counterbalance the inclusion of substantially reduced values of return period estimates. This maximal value of E_{ta} is taken as the Weather

Extremity Index (WEI) value, and the corresponding area *a* is the area affected by a heavy rainfall event. However, the WEI varies with duration *t* of the event (1—10 days considered in this study). The final duration of the event is determined as the first maximal E_{ta} value consecutively calculated for 1-day, 2-days up to 10 days long events, where all the events must overlap, and their 1-day (daily) E_{ta} values must be above zero, i.e. the daily precipitation totals during the event are significantly high or extreme. The given duration of the event determines the final WEI value of the event, and thereby the size of the area that it affected.

The WEI provides quantitative information about the extremity of weather events including the size of the area affected by an event, which is adjusted along with the rarity (return period estimates) and duration based on the two foregoing characteristics (area and rarity) of the event, i.e. the WEI reflects three important characteristics of extreme weather events. Further details can be found in the original work of Müller and Kaspar (2014) about the WEI.

The smooth transition from extreme to non-extreme precipitation events signifies that no critical value of WEI can be suggested to differentiate between the extreme and less extreme events, i.e. the researcher should fix the dataset of further analysed events e.g., with respect to the length of the study period, climatological features of the study region, and the aim of the study. Either a specific WEI-value threshold (e.g., WEI = 30) or an arbitrary number of precipitation events (e.g., 3, 10, 20 events) can be used to fix the dataset. In this paper, 54 EPEs (i.e. extreme precipitation events) from each study area have been compared since it implies on average one EPE per year during the study period.

2.6. Comparative Methods

Different characteristics of EPEs (duration, affected area, extremity) and synoptic conditions during EPEs in OM and VG were expressed as categorical variables (described below) in order to test their dependence. Resulting dependence/independence between variables found in both OM and VG suggests a typical feature of EPEs in other low mountain ranges in Central Europe as well, while a dependence/independence found in only one of the study areas indicates a specific feature of EPEs in the particular area, which thus might unlikely be generalized.

Based on a contingency table between the pairs of variables (e.g. duration and affected area), the Pearson's chi-squared test of independence (Greenwood and Nikulin 1996) was calculated at 1 % significance level. When the test resulted in chi-squared value $\chi 2$ exceeding the critical value of $\chi 2$ at the confidence level, the null hypothesis (two variables are independent) was rejected, the chi-squared residuals examined and the Cramér's V (Cramér 1946) calculated. The Cramér's V is a measure of the association between the two variables and it varies from 0 (i.e. no association between the two variables) to +1 (i.e. the two variables are identical) inclusive. Cramér's V shows the percentage of the maximum possible variation of the two variables, and its square is considered the mean square correlation between the two variables. Since the Cramér's V tend to be 1 without meaningful evidence of correlation with increasing difference between the number of rows and number of columns, and the $\chi 2$ values tend to increase with the number of cells, the derived categorical variables of the EPEs characteristics were defined to maximum 4 categories.

2.6.1. Temporal Characteristics of EPEs

Two categories of EPEs were defined on the basis of frequency of durations of EPEs: short EPEs (lasting 1—2 days) and long EPEs (3—10 days). The distinction corresponds to the frequency distribution of 1—10 days EPEs in the dataset of EPEs, with 1—2 days (short) EPEs occurring much more frequent as compared to the 3—10

days (long) EPEs in both OM and VG. Two and four categories of EPEs were defined based on their occurrence in halves of the year (summer half-year SHY from April to September / winter half-year WHY) and meteorological seasons (i.e. spring covering calendar days from March 01 to May 31), respectively. The occurrence of EPEs in SHY/WHY and seasons was assigned according to the calendar date of the first day of the EPE. A sensitivity analysis proved that the selection of the first day as compared to second and up to 10^{th} day of the EPE has no significant influence on the seasonal distribution of EPEs (only up to 2—3 EPEs from 54 EPEs in OM and VG were influenced by the change of the assigned date).

2.6.2. Spatial Characteristics of EPEs

Besides the temporal characteristics of EPEs, spatial characteristics of EPEs were also included in the comparison. For easy comparison between the OM and VG, the area affected by the EPEs was expressed as the percentage of the total of each study area. Four categories of EPEs were defined based on the percentage of the area that the EPEs affected, as follows: local EPEs (affecting less than 20 % of the study area), district EPEs (affecting 20—49 % of the area), regional EPEs (50—79 %) and large EPEs (≥ 80 % of the study area was affected by the EPEs).

Based on the location of the centre of gravity of return period estimates of precipitation during EPEs in the orographic area, the EPEs were divided into 3 categories (Fig. 1): EPEs affecting mountains MT (> 450 m a.s.l. in OM, and > 400 m a.s.l. on the windward side, and 300 m a.s.l. on the leeward side of the Vosges Mountains, starting from the mountain ridges in both regions), foreland F (west-northwestwards of the ridges), and lee L (covering Podkrušnohorské pánve basins in OM and the Upper Rhine river Plain in VG). The fixed elevation limits for EPEs affecting MT cannot be similar in OM as in VG since the mean altitude of OM is greater than that of VG, where the mean altitude is lowered by low situated Upper Rhine Plain. Nevertheless, based on the obvious elevation characteristics of the individual study area in DEM (Fig. 1), the selected elevation limits are considered convenient in both areas because the delimitation accurately captures the mountain ranges and separates them from their surroundings. An extra (fourth) category called “total” T was added to the 3 categories of the relief to ensure the case when very long return period estimates were scattered in MT, L, and F without any specific predominance. In this case, the calculated coordinates of centre of gravity would not be meaningful.

Geographical location (latitude, longitude) of the centre of gravity of return period estimates of precipitation during EPEs allows also for a categorization of EPEs with respect to cardinal points as follows: EPEs affecting southern part of the study area S and northern part N in VG, and western W and eastern E part in OM. OM and VG were divided into two parts based on the mean perpendicular line to the main mountain ridge as displayed in Fig. 1a and Fig. 1b, respectively. The division was motivated considering the prevailing direction of airflow (Section 2.1) and ensured that the division differed from the previously described characteristics of the relief. A third category C was used for the case when the longest return period estimates were not concentrated in neither the southern nor the northern part, similar to the category T for relief.

2.6.3. Extremity and synoptic conditions of EPEs

The categorization of EPEs according to their extremity was based on the WEI values. Since the WEI values vary non-linearly with the size of the study area, as demonstrated by Schiller (2016), and the OM and VG differ in size, the WEI values from one study area have to be transformed to be comparable with those of the second area. The conversion is possible through computation of maximum theoretical WEI value in the two regions, i.e.

1,000 years is the return period estimate of precipitation in all grid points and the area affected is equal to the size of the study area. In our case, the WEI values from OM remained the same, while the WEI values from VG were converted as if the VG area was the same size as that of the OM. The converted (i.e. comparable) WEI values corresponded to the multiplication of the previous WEI values in VG by the ratio of the maximum theoretical WEI value in OM to that in VG. Based on the extremity (WEI values), the EPEs were arbitrarily classified into 4 categories: E1 (WEI < 35), E2 (WEI from 35—49), E3 (50—99) and E4 (WEI ≥ 100).

Synoptic variables (Section 2.3) enabled the categorization of EPEs to EPEs with airflow/flux of specific humidity from Southeast SE, Southwest SW, Northwest NW and Northeast NE at 500 and 850 hPa isobaric levels. The vertical velocity (at 500 and 850 hPa levels) was not used in any categorization of EPEs, e.g. into those with large-scale ascents and descents, since the large-scale ascents are largely associated with extreme precipitation (Kašpar and Müller 2014b). A thorough analysis of the results of synoptic variables and along with the pressure field led to a distinction of four categories of synoptic situation per study area, during which the EPEs occurred. The categorization was personally discussed with and was approved by the specialist on the synoptic situations over Europe, Dr. Hoy, author of e.g. (Hoy et al. 2012a, b).

3. Results and Discussion

Ten strongest EPEs from both the OM and the VG are presented in Table 1 and Table 2, respectively. Comparison of the WEI values from OM with those converted from VG shows that four of the 5 overall strongest EPEs occurred in VG, which suggests that the EPEs are stronger in VG as compared to OM. In OM, 60 % of the ten strongest EPEs were long and 7 of the 10 EPEs occurred in SHY (Table 1), whereas in VG 80 % of the ten strongest EPEs were short and 5 of the 10 EPEs occurred in WHY (Table 2). No local EPE was identified among the ten strongest in both OM and VG. The studied datasets of 54 EPEs showed that in both OM and VG, the EPEs were mostly short, i.e. lasted 1—2 days. More information about the characteristics of EPEs in VG and OM individually can be found in (Minářová et al. 2017a [in press], b [in press]).

Table 1 and Table 2 also show that the majority of the strongest EPEs was associated with a low and a trough in OM and VG, respectively. In VG, 2 EPEs were associated with lows (Table 2), a usual synoptic pattern responsible for large-scale heavy rainfall in Central Europe (Messmer et al. 2015), including the EPE (starting from May 23, 1983) that affected the largest area of VG. The results from the analysis of quantitative synoptic variables during EPEs are described in more details in the following part; for OM in Section 3.1 and for VG in Section 3.2. Section 3.3 discusses dependencies between various characteristics of EPEs (i.e. temporal and synoptic characteristics, and characteristics of extremity and spatial distribution) that were studied to compare the behaviour of EPEs between the two study regions.

It is worth noticing that since three EPEs in OM and two EPEs in VG occurred during 2011—2013, they were not included in the analysis of synoptic variables that were available until 2010. Nevertheless, it was less than 6 % and 4 % of events in the dataset of EPEs in OM and VG, respectively, which according to Zolina et al. (2013) does not influence the accuracy of the results.

3.1. Synoptic conditions of EPEs in OM

In OM, the analysis of synoptic variables shows that the EPEs are identifiable at 850 hPa isobaric level, and they correspond to strong negative vertical velocity, i.e. strong ground-level ascending air motion. It is in good

agreement with Kašpar and Müller (2014b), who found the negative anomalies in vertical velocity at 850 hPa level as a predictor of EPEs in East Bohemia (Czech Republic).

Four clusters of synoptic situations inductive to EPEs were identified: a low, strong zonal circulation, a trough, and strong meridional circulation. The low and the strong zonal circulation which were most frequent synoptic situations during the 54 EPEs in the dataset are shown (1 exemplary EPE per each pattern) in Fig. 4. The low (Fig. 4a) occurred during 61 % of 54 EPEs and during 9 of the 10 strongest EPEs (Table 1), and included the Vb lows (Bebber 1891), cut-off lows and other shallow lows. The Vb cyclones and cut-off lows are well-known to be prone to large-scale heavy rainfall in Central Europe in particular (Nissen et al. 2013; Messmer et al. 2015). The Vb cyclones are generated or intensified over the northwestern Mediterranean region due to strong thermal interface between the lower (warmer) and higher (colder) levels. The Vb cyclones, particularly warm and humid shallow systems in summer, are shifted towards northeast (Vb track) due to strong southwestern airflow in the upper atmosphere, where they might get stationary. The stationarity of the cyclone over Central to Eastern Europe along with very warm and moist air are responsible for prolonged large-scale heavy rainfall (Bebber 1891; Nissen et al. 2013). Although some of the lows were not observable using the synoptic variables at 500 hPa level (not depicted), all the lows were observable at 850 hPa level (Fig. 4a), which confirms the importance of 850 hPa level in the analysis of synoptic conditions in the region (Müller and Kašpar 2010; Kašpar and Müller 2014b).

Strong zonal (western) circulation was the second most frequent synoptic pattern related to EPEs, and sixth strongest EPE (Table 1) in OM (16 %). The zonal circulation was observable at both the 500 and 850 hPa levels (Fig. 4b). The wind and the depicted flux of specific humidity was mainly from northwest (NW), which corresponds with the direction perpendicular to the mountains and thus is particularly prone to orographic enhancement of precipitation on the western windward side and in the mountains of the region (Pechala and Böhme 1975; INTERKLIM 2014).

The trough was characterized by mixed patterns during EPEs, most likely because the direction of airflow and flux of specific humidity depends on the exact position of the trough in the region. The region was more often influenced by the front side of the trough as compared to the rear side. Based on NCEP/NCAR reanalysis data (Kalnay et al. 1996), the strong meridional airflow during EPEs corresponded with sharp frontal zone.

3.2. Synoptic conditions of EPEs in VG

In VG, anomalies in flux of specific humidity represented the EPEs (as in OM). Contrary to OM, the vertical velocity could not clearly show the EPEs because the results showed positive values (i.e. descending air) during one third of EPEs for the vertical velocity at 850 hPa level (not depicted). The large-scale positive values are very unlikely to produce large-scale heavy rainfall in the same area (Oliver 2008; Houze 2014). Nevertheless, a detailed analysis revealed that the biased results were related to the computed averages from the 6 selected grid points comprising also the leeward (northern) side of the Alps, which is under the influence of descending air behind the orographic barrier during e.g. southwestern airflow (Barry 2008). Moreover, the air ascents are generally found inclined in the direction opposite to the airflow, and are accompanied by strong air descents in nearby areas in the direction of the airflow (i.e. bipolar distribution). It was the case during all the one third EPEs associated seemingly with descending air on average, i.e. the grid points westwards from the 6 selected grid points recorded negative values of vertical velocity (air ascents). It suggests that in VG, the vertical velocity can also be used for the analysis but adjusted selection of grid points is needed during individual EPEs.

Four clusters of synoptic situations related to EPEs were differentiated based on the studied synoptic variables, i.e. a trough situated over VG, VG under strong zonal (western) or northwestern (NW) circulation, and a low influencing the region (Fig. 5). 50 % of EPEs and half of the 10 strongest EPEs occurred when a trough was situated over the region (Table 2). The trough (Fig. 5a), generally related with stationary cold front (Minářová et al. 2017b [in press]), in most of the cases produced southwestern airflow and flux of specific humidity to VG, which induces the orographic enhancement of precipitation on the southwestern slopes of the mountains that are comparatively higher than e.g., on the northwestern slopes (Fig. 1b). The southwestern airflow direction was also identified to be related to precipitation totals exceeding 100 mm in Alsace in REKLIP (1995).

The lows (Fig. 5b), frequently originating over Po Plain and moving northwards to north-eastwards, were characterised by inducing extreme precipitation within eastern (northeast—southeast) direction of airflow and flux of specific humidity to VG. The lows are in fact mostly the Vb cyclones (Bebber 1891), which suggests on their importance in generating extreme precipitation even in VG, the westernmost edge of Central Europe, as it was the case of the fifth strongest EPE (Table 2). It agrees with Messmer et al. (2015) who found that the Vb occurs also northwards from the Alps. The occurrence of Vb cyclones during EPEs in VG also suggests that the region at least partly belongs to Central Europe hydro-meteorologically delimited. The lows over Bay of Biscay were more typical for southwestern airflow in the region.

One third of the EPEs occurred within strong western zonal circulation (Fig. 5c). The northwestern zonal circulation together with the western zonal circulation influenced VG during 44 % of EPEs, and corresponded to an increased horizontal gradient of air pressure in the areas of lower pressure, where the air ascents prevail (i.e. negative vertical velocity in p-system). Although the 500 hPa level better represents EPEs associated with the two most dominant patterns (i.e. trough and zonal circulation), the lower 850 hPa level is needed for the identification of the lows, as in OM (Section 3.1).

3.3. Comparison of characteristics of EPEs in OM and VG

Table 3 and Table 4 summarize the significant dependencies at 1 % p-value between various characteristics of EPEs in OM and VG, respectively. In OM, the characteristics were significantly dependent on the occurrence in half-year and meteorological season, although more dependent on half-year, whereas in VG they were significantly dependent on the occurrence during seasons. The lower dependence of characteristics on half-year as compared to that on season may in VG correspond to the April—September definition of SHY instead of March—August. The comparison between the two datasets of 54 EPEs revealed that 3 EPEs from VG overlapped with those in OM, most significantly the EPE from the end of October 1998 (6^{th} strongest EPE in VG, Table 2) related to strong zonal circulation also affected OM as 40^{th} strongest EPE in the dataset (Minářová et al. 2017a [in press]).

3.3.1. Temporal characteristics of EPEs

In both OM and VG, the seasonal distribution of EPEs did not correspond with the seasonality of mean precipitation, the EPEs instead of occurring only in the season with the highest monthly totals on average occurred in all seasons (Minářová et al. 2017a [in press], b [in press]). A strong dependence was found between the duration of EPEs (short/long) and half-year (HY) and/or season of their occurrence. In OM, the Crámer's V was 0.5 for the dependence HY-duration and season-duration, and the distances between the observed and theoretical values showed positive association of long EPEs with WHY, and winter and autumn, while negative

with SHY, and summer and spring, and *vice versa* for the short EPEs (Table 3). It is in a good agreement with the expectation that the long events occur mostly in WHY and winter season since the circulation is more pronounced over Europe during that time (Barry 2008; Oliver 2008).

In VG, although the duration and HY show no significant inter-dependence, the duration and season were significantly dependent with positive association between the long EPEs and its occurrence in spring and winter, and between the short EPEs and summer and autumn (Table 4). The insignificant dependence found for the HY and duration might be influenced by the definition of SHY, and the substantially less representatives of the long EPEs (9) as compared to the short EPEs (45) in the dataset of EPEs in VG.

3.3.2. Synoptic patterns of EPEs

Table 1 and Table 2 showed that the lows are associated with 9 of the ten strongest EPEs in OM and two of the ten strongest EPEs in VG, respectively. It suggests an increasing number of events associated with lows (Vb cyclones in particular) from Western to Eastern Europe. However, such hypothesis needs further analyses in other morphologically similar areas e.g. in eastern part of Central Europe (for instance Malá Fatra or Nízké Beskydy mountains in Slovakia).

The direction of flux of specific humidity and wind were significantly dependent on HY and season in both OM and VG (Crámer's V from 0.3—0.4). Only the dependence of flux of specific humidity at 850 hPa level and HY was found insignificant in VG which is likely again related to the definition of SHY (April—September instead of March—August). The dependence of the synoptic variables on HY and season correspond mainly with the mean seasonal circulation patterns in Europe. Fig. 6a shows that over the year, most of the EPEs in VG occurred within western airflow at 500 hPa level (Fig. 6a) and southwestern airflow at 850 hPa level (Fig. 6b), which agrees with general circulation over the area found in REKLIP (1995), while in OM the EPEs occurred mostly within northeastern to southern airflow at 500 hPa level (Fig. 6a) and northern airflow at 850 hPa level (Fig. 6b). The northern airflow corresponds with the usual position of the lows (mostly over Poland) responsible for almost two thirds of the EPEs in the region. The strongest EPEs in OM (Table 1) were related to northeastern and northwestern airflow at 500 and 850 hPa level, respectively, and to the NW flux of specific humidity at 850 hPa level. The NW direction is mainly responsible for strong orographic enhancement of precipitation in OM (DWD DDR and HMÚ ČSSR 1975; Pechala and Böhme 1975). In VG, the strongest EPEs were also connected to induced orographic enhancement of precipitation mainly in the Southern Vosges Mountains and by southwestern airflow at 850 hPa level, southwestern to western airflow at 500 hPa level, and southwestern flux of specific humidity at 850 hPa level (Table 2).

The duration of EPEs was significantly dependent on all synoptic variables of EPEs in OM (Crámer's V 0.3—0.4). The long EPEs in OM were positively associated with northwestern and in some cases with southwestern airflow, while the short EPEs were positively dependent on northeastern and southeastern direction of airflow (not depicted). The dependence seems to be robust since the northwestern wind direction is typical for winter events, when also long EPEs are expected (Section 3.3.1), whereas the short EPEs expected to occur more frequently in summer are often related to eastern wind direction.

The synoptic situation was significantly dependent on HY and season in both OM and VG with the Crámer's V from 0.4—0.6. The chi-squared residuals showed positive association of lows and meridional circulation in SHY, and of zonal circulation and troughs in WHY in OM (Table 3). It is in good agreement with the literature, when e.g., the Vb cyclones often related to summer heavy rainfall events induce strong northern (meridional)

airflow to the region (Pechala and Böhme 1975; SMUL 2008; INTERKLIM 2014; Messmer et al. 2015), whereas during winter when the circulation in mid-latitudes is more pronounced and the zonal circulation more frequent (Oliver 2008; Houze 2014), the heavy rainfall is more often associated with zonal circulation. In VG, the positive associations were found between spring EPEs and troughs and lows, summer EPEs and troughs and lows, autumn EPEs and zonal circulation, and winter EPEs and NW and zonal circulation (Table 4). The zonal circulation related to autumn and winter EPEs agrees with expectations, as in OM. The troughs related to spring and summer EPEs in VG might correspond with an increased potential thermal difference between warm air (near the ground or from southern latitudes) and cold air (aloft or from Arctic) during the seasons (REKLIP 1995; Oliver 2008).

3.3.3. Extremity and spatial characteristics of EPEs

The area affected by EPEs in VG was comparatively smaller to that affected by EPEs in OM; no large EPEs could be identified in VG, while in OM these were the strongest. The affected area in OM was significantly dependent on HY (Crámer's V 0.4) with positive association of WHY EPEs having regional to large affected area, and negative association of SHY EPEs with local to regional area affected by EPEs (Table 3) because in SHY the stationary cold fronts influences OM much less frequent as compared to WHY. It is in conformity with more frequent widespread precipitation systems in WHY in Western and Central Europe (Houze 2014). In VG, the area affected by EPEs was significantly dependent on the duration of EPEs (Crámer's V 0.4) with positive association between the long EPEs and regional (i.e. largest in VG) spatial extent (Table 4). It suggests that in VG, the actual precipitation fields are rather smaller as compared to those in OM, although they might be more unstable.

The extremity of EPEs in VG showed significant dependence on the wind direction at 500 hPa level (Crámer's V 0.3) with the strongest E4 EPEs positively associated with NE wind direction (Table 4). The expected significant dependence of extremity on size of the area affected by EPEs (from the definition of WEI) was found only in OM (Crámer's V 0.3). The dependent characteristics in OM showed that stronger events (E3, E4) tend to affect large areas, i.e.≥ 80 % of the study area (not depicted). It might be due to most frequent association of EPEs in OM with stationary lows (western sector), which induces longer precipitation that can affect greater area. Contrary to OM, in VG the extremity of EPEs may increase with the duration rather than area affected by EPEs.

The characteristic relief was significantly dependent on the size of the affected area, extremity and cardinal points of EPEs in OM (Crámer's V 0.4, 0.3 and 0.6, respectively). The EPEs that affected the mountains the most were of district to regional extent, and positively associated with E1 EPEs (i.e. least strong). The EPEs that affected the leeward side were positively associated with the expected local EPEs and E3 to E4 EPEs with total area T (Table 3). In VG (Table 4), the relief and season were significantly dependent (Crámer's V 0.3) — the EPEs affecting the most the leeward side of the Vosges Mountains were positively associated with summer, which is in conformity with mixed patterns and leeward convection in summer in the region (Sell 1998; Labbouz et al. 2013). The winter EPEs were positively associated with those affecting the most the mountains, which fits in stronger orographic enhancement of precipitation in winter (Barry 2008).

The characteristic relief was also significantly dependent on the characteristic cardinal points in OM and VG (Crámer's V 0.6 and 0.8, respectively). As expected, the EPEs affecting the W part of OM were positively associated with foreland and those affecting E with the mountains, despite the higher elevation of the Western Ore Mountains than the Eastern Ore Mountains (Fig. 1a), and the leeward side (Table 3). However, the Eastern

Ore Mountains were also associated with heavy rainfall due to the Vb cyclones (Bebber 1891), and August 2002 event in particular (Munzar et al. 2011). In VG, the EPEs that affected the southern part were positively associated with those strongest in mountains, whereas the EPEs that affected the northern part the most were related to those affecting the foreland or the lee (Table 4). It might be related to lower potential orographic effect on precipitation in the northern part of the area due to lower elevation of mountains in that part as compared to the highest elevated southern part, where the orographic effect can be most efficient (Fig. 1b).

The spatial distribution of the superimposed and averaged return period estimates of SHY and WHY EPEs for OM (10 WHY EPEs out of 54 EPEs) is displayed in Fig. 7 and for VG (24 WHY EPEs out of 54 EPEs) in Fig. 8. The EPEs with the longest return period estimates are not found in mountains where the highest totals are mostly recorded, but often on the windward side (in SHY in OM and in SHY and WHY in VG). In OM, longer return period estimates are typical in SHY (Fig. 7a) in comparison with WHY (Fig. 7b), whereas in VG they are of similar length (up to around 50 years) in SHY (Fig. 8a) and WHY (Fig. 8b). It might be related to the differences in mean annual course of precipitation between OM and VG with more seasonal differences in the annual course in various parts of VG (Fig. 2). However, Fig. 7 and Fig. 8 show that the EPEs are spatially rather inhomogeneous in OM as compared to the EPEs in VG, where they are more concentrated in specific regions, i.e. northwestern windward and northeastern lee side in SHY and northern and southwestern windward side in WHY. In WHY, the spatial distribution in VG might be related to the extratropical cyclonic zone shifted southwards during winter (Oliver 2008), and the troughs in southwest-northeast direction influencing mainly the southwestern part of the region, where the orographic enhancement of precipitation plays crucial role in producing EPEs of high return period levels.

Despite rather inhomogeneous spatial distribution of averaged return period levels in OM, it can be observed that in SHY (Fig. 7a) the highest return period estimates affected mostly the area northwards of the main mountain ridge; its central and eastern part in particular. This is in good agreement with literature attributing the record daily precipitation total (i.e. 312 mm on August 12, 2002 at Zinnwald weather station) in the Eastern Ore Mountains (Munzar et al. 2011), although the mean elevation of Eastern Ore Mountains is lower than that of the Western Ore Mountains (Fig. 1a). In WHY (Fig. 7b), the highest average return period estimates of the EPEs are more concentrated to a north-south oriented belt that is situated in the middle of the study area. The belt comprises also the lee (Czech) side of the mountains, which might be in contradiction to the assumed stronger orographic effect (i.e. rain shadow in the lee) in winter (Barry 2008). However, the Vb cyclones affecting also the lee side can occur in winter as well even if they are generally weaker than in summer (Messmer et al. 2015), and most of the time affect areas eastwards from OM. During the cases when it affects OM, the precipitation amounts are then considerable.

3.3.4. Summary of the dependent characteristics of EPEs in OM and VG

The above described significant dependencies are demonstrated on the EPEs in OM in Fig. 9a and Fig. 10, and on the EPEs in VG in Fig. 9b. Fig. 9a confirms that in OM, the short EPEs occurred mostly in SHY and long EPEs in WHY. The NW flux of specific humidity at 850 hPa isobaric level prevailed during WHY and long EPEs, while the other directions of the flux were related to SHY and short EPEs. The SHY EPEs were mostly of smaller spatial extent (district to local), though some large EPEs (including the strongest) were also identified in SHY. Low (or meridional circulation) was the dominant synoptic situation related to EPEs in OM in SHY, while in WHY it was the zonal circulation or trough. The strongest EPEs (E3—E4) occurred mainly in second half of

calendar year (especially in summer months) and the E4 EPEs affected the largest area, up to 100 % (Fig. 10). The WHY EPEs affected large to regional area of OM (not less than 50 % of OM), and were severe in the mountains or affected the total area. The largest SHY EPEs occurred heavily in foreland or mountains and the least spatially extended EPEs affected mostly the lee of the mountains. The eastern part of OM was the most affected by EPEs in SHY, except of EPEs affecting the foreland that were more associated with western part of the region. The results which are in conformity with fragmentary information about heavy rainfall in smaller or broader part of the region (e.g., SMUL 2008; INTERKLIM 2014) provide integral picture about the EPEs in OM.

In VG, the EPEs demonstrate the dependence of season on other characteristics of EPEs (Fig. 9b); the NW wind direction at 500 hPa occurred during winter EPEs, SW wind direction mostly during autumn or summer EPEs, and spring EPEs were rather related to northern wind direction. The SW wind direction was typical for EPEs associated with trough and affecting mostly foreland or mountains, while the NW wind direction in winter corresponded with EPEs from zonal to NW circulation affecting also foreland and mountains of VG. All the five EPEs associated with low occurred within SE to eastern airflow, none of them occurred in winter. Long EPEs corresponded with western airflow and affected the foreland or mountains the most. These findings provide new insights to the topic about heavy rainfall in VG, very limitedly dealt in literature except (Minářová et al. 2017b [in press]).

The similar dependencies of the characteristics of EPEs on half-year / season in OM / VG, respectively, are that the low was related to SHY / summer EPEs, and zonal circulation to WHY / winter EPEs. Short EPEs tend to occur in SHY / summer, whereas the long EPEs are more associated with WHY / winter. The NW wind direction or flux of specific humidity in WHY / winter is related to EPEs. The similarities of EPEs in OM and VG suggest that the temporal characteristics and synoptic conditions of EPEs might be typical features in similar low mountain ranges in Central Europe. On the other hand, the spatial characteristics and extremity of EPEs did not show significant similarities between OM and VG, they seem to be more complex and unique for each studied mountain range.

4. Conclusion

Synoptic conditions and other characteristics (extremity, and temporal and spatial characteristics) of EPEs were compared between two low mountain ranges situated in Central Europe, i.e. OM and VG. Based on the daily precipitation data from rain gauges during 54 years, the EPEs were defined using WEI, which provided a quantitative assessment of extremity of events, including rarity, and variable duration and spatial extent.

The 54 strongest EPEs from both regions were first analysed from the perspective of synoptic conditions in individual regions separately. In OM, strong air ascent (vertical velocity) and anomalies in flux of specific humidity at 850 hPa level were confirmed to be the common synoptic feature for all EPEs. The EPEs were most frequently associated with lows (cut-off lows and Vb cyclones in particular) over Central Europe and strong zonal circulation, and both synoptic conditions induced the orographically enhanced precipitation in OM during EPEs. As in OM, the orographic enhancement (mostly within southwestern direction of airflow) also plays a substantial role in producing most of EPEs in VG. In VG, the 500 hPa isobaric level of flux of specific humidity was sufficient for the identification of EPEs related to troughs and zonal circulation (most frequent synoptic situation related to EPEs). However although less frequent, the lows were identifiable mostly only at 850 hPa

levels, which suggests the importance of 850 hPa level in VG as well. Among the lows also the Vb cyclones were identified in VG, which is a typical feature related to EPEs in Central Europe. It suggested Central European hydro-meteorological features in VG, and a hypothesis about a successively increasing occurrence of Vb cyclones in the eastwards direction in Central Europe that needs to be confirmed in further research of other datasets of EPEs.

Secondly, the analysis of dependence between 12 pairs of characteristics of EPEs in OM and VG showed that the duration of EPEs and synoptic situation during EPEs are significantly dependent on seasonal occurrence of EPEs in both OM and VG. The long EPEs (3—10 days) were positively associated with WHY / winter and short EPEs with SHY / summer. Short EPEs dominated in both the datasets and the EPEs occurred in all seasons irrespective of the main precipitation season in both regions. The similarities of the characteristics of EPEs in both OM and VG might also be relevant in other low mountain ranges in Central Europe. Slightly higher extremity of EPEs was found in VG as compared to OM. The spatial characteristics of EPEs showed rather different results from OM to VG. For instance, the spatial distribution of rarity showed that the windward side of the Vosges Mountains is the most affected by EPEs in both SHY and WHY, while in OM it is more heterogeneous with longer return periods in central and Eastern Ore Mountains in SHY. The long EPEs tended to affect larger area as compared to those affected by short EPEs. The area affected by EPEs in OM was generally greater than that in VG, and no large EPE was identified in VG. The more dissimilar dependencies between spatial characteristics of EPEs from one region to another might represent a specific feature of EPEs in the given region, thereby suggesting that these characteristics must be analysed in other low mountain ranges rather individually.

Contrary to the previous studies that were mostly based on one study region and generally used different definitions of heavy rainfall, in this study the EPEs and their characteristics have been defined the same way for the two similar Central European low mountain regions. To the best of our knowledge, the comparison of greater dataset of EPEs between them might be of its first kind, and contributes to broadening the understanding of heavy rainfall characteristics not only in OM and VG, but also in other similar areas in Central Europe not yet studied in detail. The study might also contribute to mitigating the natural disasters and subsequent losses associated with extreme precipitation. The future research will be dedicated to further investigation of the same characteristics of EPEs compared among more similar areas to confirm our results and the hypothesis about the West-East gradient in the occurrence of lows such as Vb cyclones associated with EPEs in Central Europe.

Acknowledgements

We thank *Météo-France, DWD (Deutscher Wetterdienst),* and *CHMI (Czech Hydrometeorological Survey)* for provided precipitation data, and NCEP/NCAR re-analysed gridded data of synoptic variables. We extend great thanks to the *BGF* (*French Government scholarship*) and *DBU* (*Deutsche Bundesstiftung Umwelt*), and project CRREAT (reg. number: CZ.02.1.01/0.0/0.0/15_003/0000481) call number 02_15_003 of the Operational Programme Research, Development and Education for financially supporting the research for 15 and 6 months, respectively. We also thank M.Phil. Syed Muntazir Abbas for his valuable remarks during the revision of the manuscript and the language corrections.

Reference list

Alexander LV, Zhang X, Peterson TC, et al (2006) Global observed changes in daily climate extremes of temperature and precipitation. J Geophys Res Atmospheres 111:D05109. doi: 10.1029/2005JD006290

Alsatia (1932) L´Alsace : précis de la géographie régionale des départements Haut-Rhin et Bas-Rhin. Alsatia, Colmar

Awan NK, Formayer H (2016) Cutoff low systems and their relevance to large-scale extreme precipitation in the European Alps. Theor Appl Climatol 1–10. doi: 10.1007/s00704-016-1767-0

Barry RG (2008) Mountain Weather and Climate Third Edition, 3rd edn. Cambridge University Press, Cambridge

Bartholy J, Pongracz R (2005) Tendencies of extreme climate indices based on daily precipitation in the Carpathian Basin for the 20th century. Idojárás 109:1–20.

Bartholy J, Pongrácz R (2007) Regional analysis of extreme temperature and precipitation indices for the Carpathian Basin from 1946 to 2001. Glob Planet Change 57:83–95. doi: 10.1016/j.gloplacha.2006.11.002

Bebber WJ van (1891) Die Zugstrassen der barometrischen Minima nach den Bahnenkarten der deutschen Seewarte für den Zeitraum 1875-1890.

Beniston M, Stephenson DB (2004) Extreme climatic events and their evolution under changing climatic conditions. Glob Planet Change 44:1–9. doi: 10.1016/j.gloplacha.2004.06.001

Boucek J (2007) August 2002 catastrophic flood in the Czech Republic. In: Vasiliev OF, VanGelder P, Plate EJ, Bolgov MV (eds) Extreme Hydrological Events: New Concepts for Security. Springer, Dordrecht, pp 59–68

Brazdil R, Kotyza O, Dobrovolny P (2006) July 1432 and August 2002 - two millennial floods in Bohemia? Hydrol Sci J-J Sci Hydrol 51:848–863. doi: 10.1623/hysj.51.5.848

Cavalcanti IFA (2012) Large scale and synoptic features associated with extreme precipitation over South America: A review and case studies for the first decade of the 21st century. Atmospheric Res 118:27–40. doi: 10.1016/j.atmosres.2012.06.012

Cramér H (1946) Mathematical methods of statistics. Princeton University Press, Princeton

DWD DDR, HMÚ ČSSR (1975) Podnebí a počasí v Krušných horách. SNTL - Nakladatelství technické literatury, Praha

Ernst F (1988) Panorama de la géographie physique de l'Alsace ; et Les régions naturelles de l'Alsace.

Foresti L, Pozdnoukhov A (2012) Exploration of alpine orographic precipitation patterns with radar image processing and clustering techniques. Meteorol Appl 19:407–419. doi: 10.1002/met.272

Gley G (1867) Géographie physique, industrielle, administrative et historique des Vosges, 3rd edn. V.e Gley Impr. V.e & Durand Libraire, Épinal

Greenwood PE, Nikulin MS (1996) A guide to chi-squared testing. Wiley, New York

Hosking JRM, Wallis JR (1997) Regional Frequency Analysis: An Approach Based on L-Moments. Cambridge University Press

Houze RA (2014) Cloud Dynamics. Academic Press

Hoy A, Jaagus J, Sepp M, Matschullat J (2012a) Spatial response of two European atmospheric circulation classifications (data 1901–2010). Theor Appl Climatol 112:73–88. doi: 10.1007/s00704-012-0707-x

Hoy A, Sepp M, Matschullat J (2012b) Atmospheric circulation variability in Europe and northern Asia (1901 to 2010). Theor Appl Climatol 113:105–126. doi: 10.1007/s00704-012-0770-3

INTERKLIM (2014) Der Klimawandel im böhmisch-sächsischen Grenzraum. Změna klimatu v česko-saském pohraničí. Sächsisches Landesamt für Umwelt, Dresden

Kalnay E, Kanamitsu M, Kistler R, et al (1996) The NCEP/NCAR 40-Year Reanalysis Project. Bull Am Meteorol Soc 77:437–471. doi: 10.1175/1520-0477(1996)077<0437:TNYRP>2.0.CO;2

Kašpar M, Müller M (2014a) Combinations of large-scale circulation anomalies conducive to precipitation extremes in the Czech Republic. Atmospheric Res 138:205–212. doi: 10.1016/j.atmosres.2013.11.014

Kašpar M, Müller M (2014b) Combinations of large-scale circulation anomalies conducive to precipitation extremes in the Czech Republic. Atmospheric Res 138:205–212. doi: 10.1016/j.atmosres.2013.11.014

Kienzler S, Pech I, Kreibich H, et al (2015) After the extreme flood in 2002: changes in preparedness, response and recovery of flood-affected residents in Germany between 2005 and 2011. Nat Hazards Earth Syst Sci 15:505–526. doi: 10.5194/nhess-15-505-2015

Kyselý J (2009) Trends in heavy precipitation in the Czech Republic over 1961–2005. Int J Climatol 29:1745–1758. doi: 10.1002/joc.1784

Kyselý J, Picek J (2007) Regional growth curves and improved design value estimates of extreme precipitation events in the Czech Republic. Clim Res 33:243–255. doi: 10.3354/cr033243

Labbouz L, Van Baelen J, Tridon F, et al (2013) Precipitation on the lee side of the Vosges Mountains: Multi-instrumental study of one case from the COPS campaign. Meteorol Z 22:413–432. doi: 10.1127/0941-2948/2013/0413

Messmer M, Gómez-Navarro JJ, Raible CC (2015) Climatology of Vb cyclones, physical mechanisms and their impact on extreme precipitation over Central Europe. Earth Syst Dyn 6:541–553. doi: 10.5194/esd-6-541-2015

Météo-France (2008) Climatologie des Vosges. Météo-France au service des Vosges : le centre dépertemental d´Épinal, Épinal

Minářová J, Müller M, Clappier A, et al (2017a) Duration, rarity, affected area, and weather types associated with extreme precipitation in the Ore Mountains (Erzgebirge) region, Central Europe. Press. doi: 10.1002/joc.5100

Minářová J, Müller M, Clappier A (2016) Seasonality of mean and heavy precipitation in the area of the Vosges Mountains: dependence on the selection criterion. Int J Climatol n/a-n/a. doi: 10.1002/joc.4871

Minářová J, Müller M, Clappier A, Kašpar M (2017b) Characteristics of Extreme Precipitation in the Vosges Mountains region (North-Eastern France). Press. doi: 10.1002/joc.5102

Müller M, Kaspar M (2014) Event-adjusted evaluation of weather and climate extremes. Nat Hazards Earth Syst Sci 14:473–483. doi: 10.5194/nhess-14-473-2014

Müller M, Kašpar M (2010) Quantitative aspect in circulation type classifications – An example based on evaluation of moisture flux anomalies. Phys Chem Earth Parts ABC 35:484–490. doi: 10.1016/j.pce.2009.09.004

Müller M, Kašpar M, Řezáčová D, Sokol Z (2009) Extremeness of meteorological variables as an indicator of extreme precipitation events. Atmospheric Res 92:308–317. doi: 10.1016/j.atmosres.2009.01.010

Munzar J, Auer I, Ondráček S (2011) Central European one-day precipitation record. Moravian Geographical Reports 64:107–112.

Nissen KM, Ulbrich U, Leckebusch GC (2013) Vb cyclones and associated rainfall extremes over Central Europe under present day and climate change conditions. Meteorol Z 22:649–660. doi: 10.1127/0941-2948/2013/0514

Oliver JE (2008) Encyclopedia of World Climatology. Springer Science & Business Media

Orlanski I (1975) A rational subdivision of scales for atmospheric processes. Bull Am Meteorol Soc 56:527–530.

Pachauri RK, Allen MR, Barros VR, et al (2014) Climate Change 2014: Synthesis Report. Contribution of Working Groups I, II and III to the Fifth Assessment Report of the Intergovernmental Panel on Climate Change. IPCC, Geneva, Switzerland

Pechala F, Böhme W (eds) (1975) Podnebí a počasí v Krušných horách, 1. vyd. SNTL, Praha

Pelt SC van, Beersma JJ, Buishand TA, et al (2014) Uncertainty in the future change of extreme precipitation over the Rhine basin: the role of internal climate variability. Clim Dyn 44:1789–1800. doi: 10.1007/s00382-014-2312-4

Prudhomme C, Reed DW (1998) Relationships between extreme daily precipitation and topography in a mountainous region: a case study in Scotland. Int J Climatol 18:1439–1453. doi: 10.1002/(SICI)1097-0088(19981115)18:13<1439::AID-JOC320>3.0.CO;2-7

REKLIP (1995) Klimaatlas Oberhein Mitte-Süd: REKLIP, Regio-Klima-Projeckt. Vdf Hochschulverl, Zürich, Suisse

Roe GH, Montgomery DR, Hallet B (2003) Orographic precipitation and the relief of mountain ranges. J Geophys Res Solid Earth 108:n/a–n/a. doi: 10.1029/2001JB001521

Schiller J (2016) Eine Sensitivitätsanalyse des Weather Extremity Index (WEI) nach Müller und Kaspar zur Beschreibung extremer Niederschläge unter Verwendung radarbasierter Niederschlagsmessungen des Deutschen Wetterdienstes. University of Cologne

Sell Y (1998) L'Alsace et les Vosges. Delachaux et Niestlé, Lausanne (Suisse)

Šercl P (2008) Hodnocení metod odhadu plošných srážek (Assessment of methods for Area Precipitation Estimates). Meteorol Zprávy Meteorol Bull 61:33–43.

Smith RB (2006) Progress on the theory of orographic precipitation. Spec Pap 398:1–16.

SMUL (2008) Sachsen im Klimawandel - Eine Analyse. Sächsisches Staatsministerium für Umwelt und Landwirtschaft, Dresden

Socher M, Boehme-Korn G (2008) Central European floods 2002: lessons learned in Saxony. J Flood Risk Manag 1:123–129. doi: 10.1111/j.1753-318X.2008.00014.x

Söder M, Conrad M, Gönner T, Kusch W (2009) Les changements climatiques en Allemagne du Sud: Ampleur – Conséquences – Stratégies. Klimaveränderung und Konsequenzen für die Wasserwirtschaft (KLIWA), Mainz

Solomon S, Quin D, Manning M, et al (2007) Climate Change 2007 - The Physical Science Basis: Working Group I Contribution to the Fourth Assessment Report of the IPCC, IPCC. Cambridge University Press, Cambridge, United Kingdom and New York, NY, USA

Thieken AH, Kreibich H, Mueller M, Merz B (2007) Coping with floods: preparedness, response and recovery of flood-affected residents in Germany in 2002. Hydrol Sci J-J Sci Hydrol 52:1016–1037. doi: 10.1623/hysj.52.5.1016

Thieken AH, Muller M, Kreibich H, Merz B (2005) Flood damage and influencing factors: New insights from the August 2002 flood in Germany. Water Resour Res 41:W12430. doi: 10.1029/2005WR004177

Tolasz R, Brázdil R, Bulíř O, et al (2007) Altas podnebí Česka / Climate Atlas of Czechia, 1st edn. Český hydrometeorologický ústav, Universita Palackého

Uppala SM, KÅllberg PW, Simmons AJ, et al (2005) The ERA-40 re-analysis. Q J R Meteorol Soc 131:2961–3012. doi: 10.1256/qj.04.176

Van der Schrier, G, van den Besselaar E, Leander R, et al (2013) Central European flooding 2013 - Euro4m CIB.

Vautard R Des projections climatiques d'une précision inégalée sur toute l'Europe. http://www.insu.cnrs.fr/node/4634. Accessed 10 Feb 2014

Wang XL, Chen H, Wu Y, et al (2010) New Techniques for the Detection and Adjustment of Shifts in Daily Precipitation Data Series. J Appl Meteorol Climatol 49:2416–2436. doi: 10.1175/2010JAMC2376.1

Wang XL, Feng Y (2013) RHtests_dlyPrcp User Manual. Clim Res Div Atmospheric Sci Technol Dir Sci Technol Branch Environ Can Tor Ont Can Retrieved Febr 25:2014.

Werner PC, Gerstengarbe F-W (2010) PIK Report No. 119 - Katalog Der Grosswetterlagen Europas nach Paul Hess und Helmut Brezowsky 7., verbesserte und ergänzte Auflage.

Whiteman CD (2000) Mountain Meteorology: Fundamentals and Applications. Oxford University Press

World Meteorological Organization (2008) Guide to meteorological instruments and methods of observation. World Meteorological Organization, Geneva, Switzerland

Zolina O, Simmer C, Belyaev K, et al (2013) Changes in the Duration of European Wet and Dry Spells during the Last 60 Years. J Clim 26:2022–2047. doi: 10.1175/JCLI-D-11-00498.1

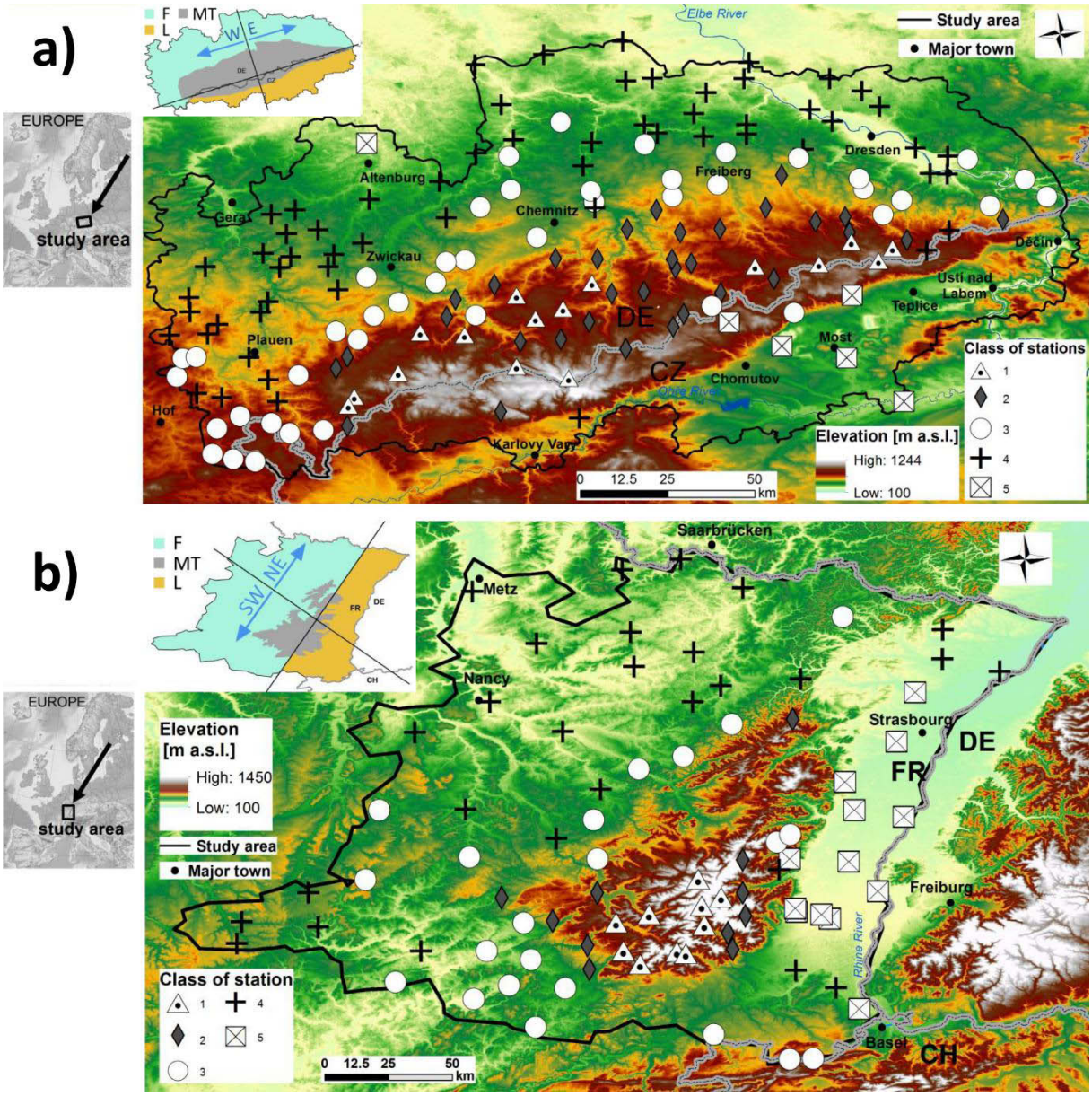

Fig. 1 Study area of the a) the Ore Mountains (OM) and b) the Vosges Mountains (VG), and the spatial distribution of the a) 167 and b) 84 analysed rain gauges, which were divided according to the mean monthly totals during 1960—2013 into 5 classes using Hierarchical Clustering based on Principal Components Analysis. 88.3 % and 94.8 % of variance was expressed by the first component in OM and VG, respectively. The relief is represented in colour-scale, i.e. the highest locations are displayed in white. The inserted scheme maps display the categorization of the study area according to the relief and cardinal points in a) OM and b) VG. F stands for foreland, MT for mountains, L for lee, W for western, E for eastern, SW for southwestern and NE for northeastern part. More details about the categories are given in Section 2.6.2.

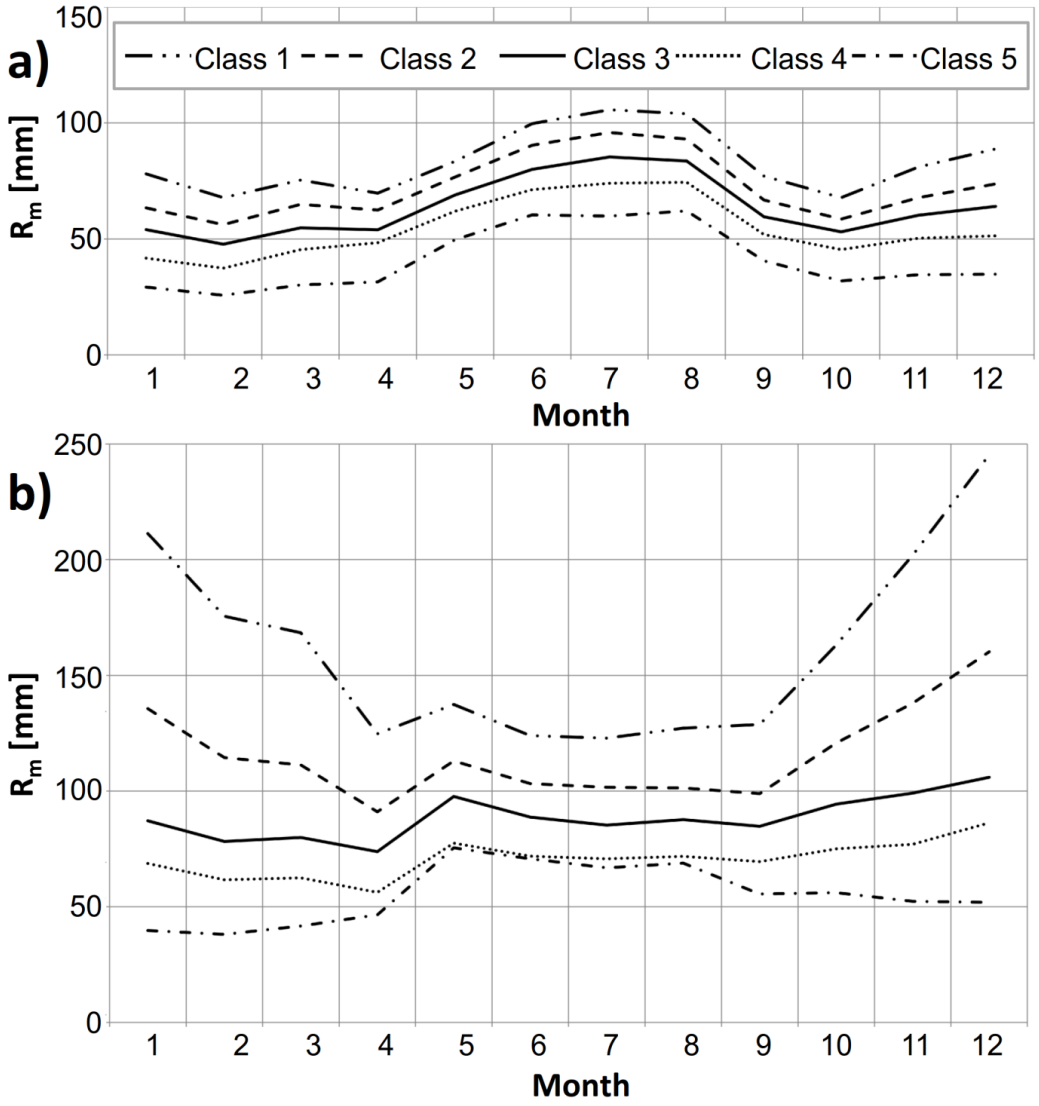

Fig. 2 Mean monthly totals of the classes of stations in a) OM and b) VG resulting from the Hierarchical Clustering based on Principal Components (Fig. 1)

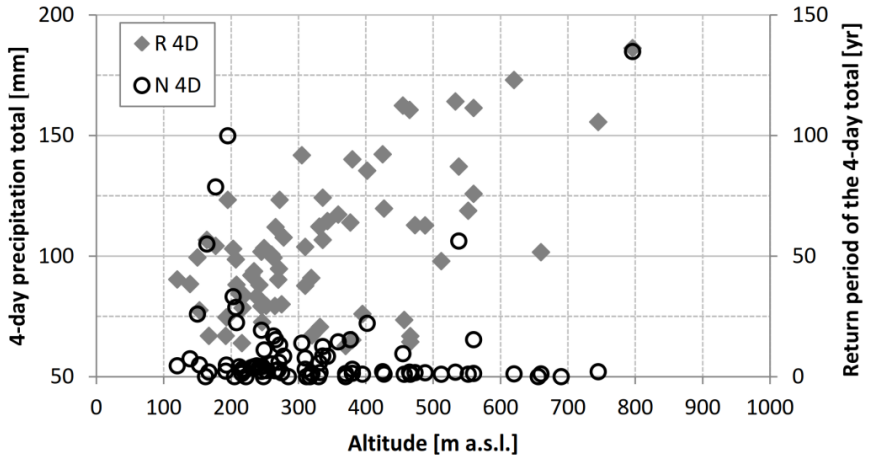

Fig. 3 Dependence on altitude of the 4-day precipitation totals (R 4D) and their return period estimates (N 4D) at 84 stations during the extreme precipitation event on May 23, 1983 that affected the largest area of the VG

Table 1
10 strongest EPEs from OM arranged in the decreasing order of their extremity (WEI). The first column corresponds to the starting day of EPEs. "CardP" stands for the categorization of EPEs based on cardinal points and "x" for no available data. The categorized variables are described in Section 2.6, and for the synoptic situation in Section 3.1. Winter half-year (October—March) EPEs are depicted in italics and long EPEs (3—10 days) are displayed in bold.

Date	Duration [day]	Affected area [km^2]		Relief	CardP	Extremity (WEI [log(yr)km])		Synoptic situation	Wind at 500 hPa	FQUV at 850 hPa
28.05.2013	**7**	**large**	**16060**	**F**	**W**	**E4**	**135**	**low (cut-off)**	**x**	**x**
11.08.2002	2	large	14132	MT	E	E4	121	low (Vb)	NE	NW
01.08.1983	**6**	**large**	**14740**	**F**	**E**	**E4**	**116**	**low (cut-off)**	**NE**	**NW**
07.08.1978	2	large	13448	F	E	E3	78	low (Vb)	SW	NW
22.07.2010	2	large	15224	F	W	E3	64	low	SW	NW
27.12.1986	***7***	***large***	***14280***	***T***	***C***	***E3***	***61***	***zonal***	***NW***	***NW***
31.08.1995	2	large	13440	F	W	E3	61	low (cut-off)	NE	NW
19.10.1974	***8***	***large***	***13452***	***F***	***E***	***E3***	***60***	***low (cut-off)***	***NE***	***NW***
25.09.2010	**4**	**large**	**13556**	**F**	**E**	**E3**	**59**	**low (cut-off)**	**NE**	**NW**
15.10.1960	***3***	***large***	***15296***	***T***	***C***	***E3***	***58***	***low (Vb)***	***SW***	***SE***

Table 2
As Table 1, but from VG; WEI values were converted to be comparable with those from OM (Section 2.6.3), and the synoptic situation categorized in Section 3.2

Date	Duration [day]	Affected area [km^2]		Relief	CardP	Extremity (WEI [log(yr)km])		Synoptic situation	Wind at 500 hPa	FQUV at 850 hPa
11.11.1996	*2*	*district*	*14840*	*F*	*SW*	*E4*	*137*	*trough*	*SW*	*SW*
12.9.1986	**5**	**regional**	**21312**	**T**	**C**	**E4**	**135**	**trough**	**SW**	**SW**
17.9.2006	1	district	11108	T	C	E4	132	low	NE	NE
2.10.2006	*2*	*regional*	*20316*	*MT*	*SW*	*E4*	*124*	*trough*	*SW*	*SW*
23.5.1983	**4**	**regional**	**23512**	**T**	**C**	**E4**	**117**	**low**	**NE**	**NW**
10.5.1970	2	district	9836	L	NE	E4	105	trough	NE	NW
28.10.1998	*1*	*district*	*12636*	*MT*	*NE*	*E4*	*104*	*zonal*	*NW*	*SW*
25.2.1997	*1*	*district*	*13184*	*F*	*NE*	*E3*	*93*	*zonal*	*SW*	*SW*
22.7.1995	1	district	6648	F	NE	E3	79	trough	SW	NW
13.2.1990	*2*	*district*	*9664*	*MT*	*SW*	*E3*	*72*	*zonal (NW)*	*NW*	*NW*

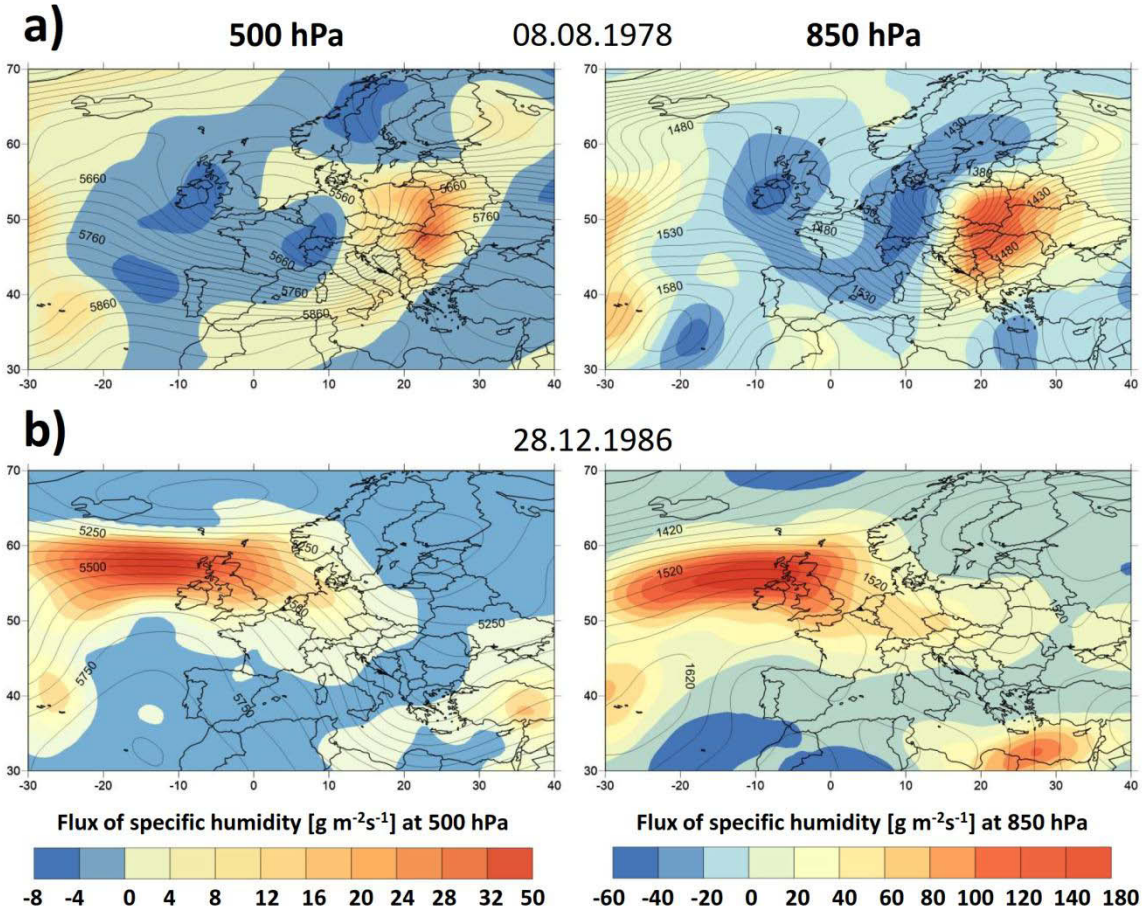

Fig. 4 Meridional (a) and zonal (b) component of flux of specific humidity (colour scale) and geopotential height (contour) at (left) 500 hPa level and (right) 850 hPa level for the two most frequent synoptic patterns during EPEs (the day with highest E_{ta}) in OM: a) low over Central Europe (August 8, 1978), and b) strong zonal circulation (December 12, 1986). More information about the EPEs is given in Table 1.

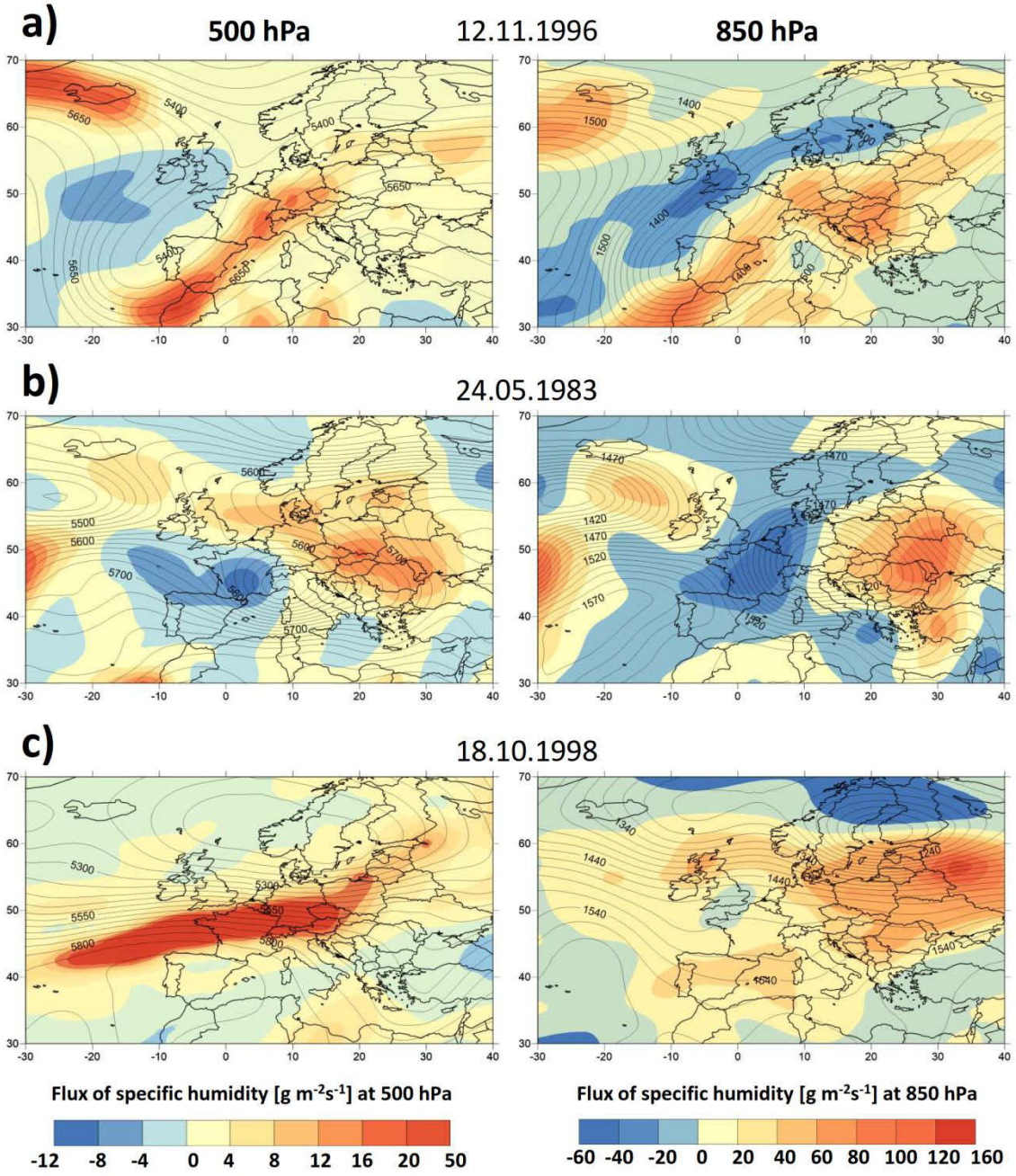

Fig. 5 Meridional (a, b) and zonal (c) component of flux of specific humidity in colour scale and geopotential height in contour at (left) 500 hPa level and (right) 850 hPa level for the three frequent synoptic patterns during EPEs (the day with highest E_{ta}) in VG: a) trough and related southwestern airflow to VG (strongest EPE, November 12, 1996), b) low over Central Europe (May 24, 1983), and c) strong zonal circulation (October 18, 1998). More information about the EPEs is given in Table 2.

Table 3

Chi-squared residuals of the significantly dependent variables at 1 % p-value in OM. The variables and their categories are described in Section 2.6 and 3.1. FQUV stands for the flux of specific humidity and "Card P" for cardinal points. Note that the FQUV at 850 hPa level was selected to be shown because of the strongest dependence on half-year, while other synoptic variables (FQUV at 500 hPa level and wind direction at both 500 and 850 hPa levels) were also significantly dependent on half-year and showed the same (positive/negative) associations.

		SHY	**WHY**						
Duration	short	1,02	-2,06	**Relief**					
	long	-1,27	2,56	F	MT	L	T		
Affected area	local	0,44	-0,89	-0,45	-1,08	4,16	-0,93		
	district	0,85	-1,71	-0,36	0,76	-0,39	-0,19		
	regional	-0,18	0,37	0,52	0,45	-0,52	-0,87		
	large	-0,88	1,78	0,05	-0,67	-1,21	1,54		
FQUV 850 hPa	NE	0,32	-0,64	0,67	1,21	0,11	-1,68	E1	**Extremity**
	SE	0,66	-1,33	0,24	0,03	0,37	-0,55	E2	
	SW	0,58	-1,17	-1,01	-1,44	-0,16	2,14	E3	
	NW	-1,09	2,21	-0,40	-0,77	-0,82	1,84	E4	
Synoptic situation	low	1,16	-2,34	1,86	-0,13	-0,58	-1,97	W	**Card P**
	zonal	-2,14	4,34	-0,21	1,39	1,26	-2,18	E	
	trough	-0,56	1,14	-2,08	-1,80	-1,40	5,60	T	
	meridional	0,58	-1,17						

Table 4

As Table 3, but in VG; the synoptic situation is categorized in Section 3.2. Note that the results for season and the flux of specific humidity at 500 and 850 hPa levels were also significant, and similar associations were found as those depicted for the wind at 500 and 850 hPa levels, respectively.

		Season				**Affected area**		
		Spring	**Summer**	**Autumn**	**Winter**	local	district	regional
Duration	short	-0,91	0,42	0,36	-0,18	0,49	0,29	-1,05
	long	2,04	-0,95	-0,80	0,41	-1,09	-0,64	2,34
Synoptic situation	trough	-0,36	2,31	-0,41	-2,04			
	zonal	0,86	-2,21	0,57	1,20			
	NW	-0,96	-1,32	-0,20	2,91	**Cardinal points**		
	low	0,26	0,46	0,06	-0,93	NE	SW	T
Relief	F	-1,57	-0,75	1,55	0,14	0,94	-0,40	-0,5
	MT	0,46	-1,12	-0,32	1,49	-0,29	1,69	-1,94
	L	1,01	1,59	-1,57	-0,66	0,88	0,51	-1,66
	T	0,37	0,66	0,08	-1,32	-1,75	-2,10	4,74
Wind 850 hPa	NE	-0,68	1,22	-0,14	-0,72			
	SE	-0,88	2,13	-0,67	-0,93			
	SW	-0,92	-1,14	0,93	0,96	**Extremity**		
	NW	2,54	-0,10	-1,08	-0,66	E1	E2	E3	E4
Wind 500 hPa	NE	1,77	-0,14	-0,43	-0,83	-0,93	-1,45	0,56	2,84
	SE	-0,78	1,72	-0,43	-0,83	0,37	0,24	-0,07	-0,73
	SW	-0,75	0,80	0,72	-1,40	0,35	0,93	-1,08	-0,52
	NW	0,05	-1,94	-0,45	3,17	-0,17	-0,64	1,34	-0,57

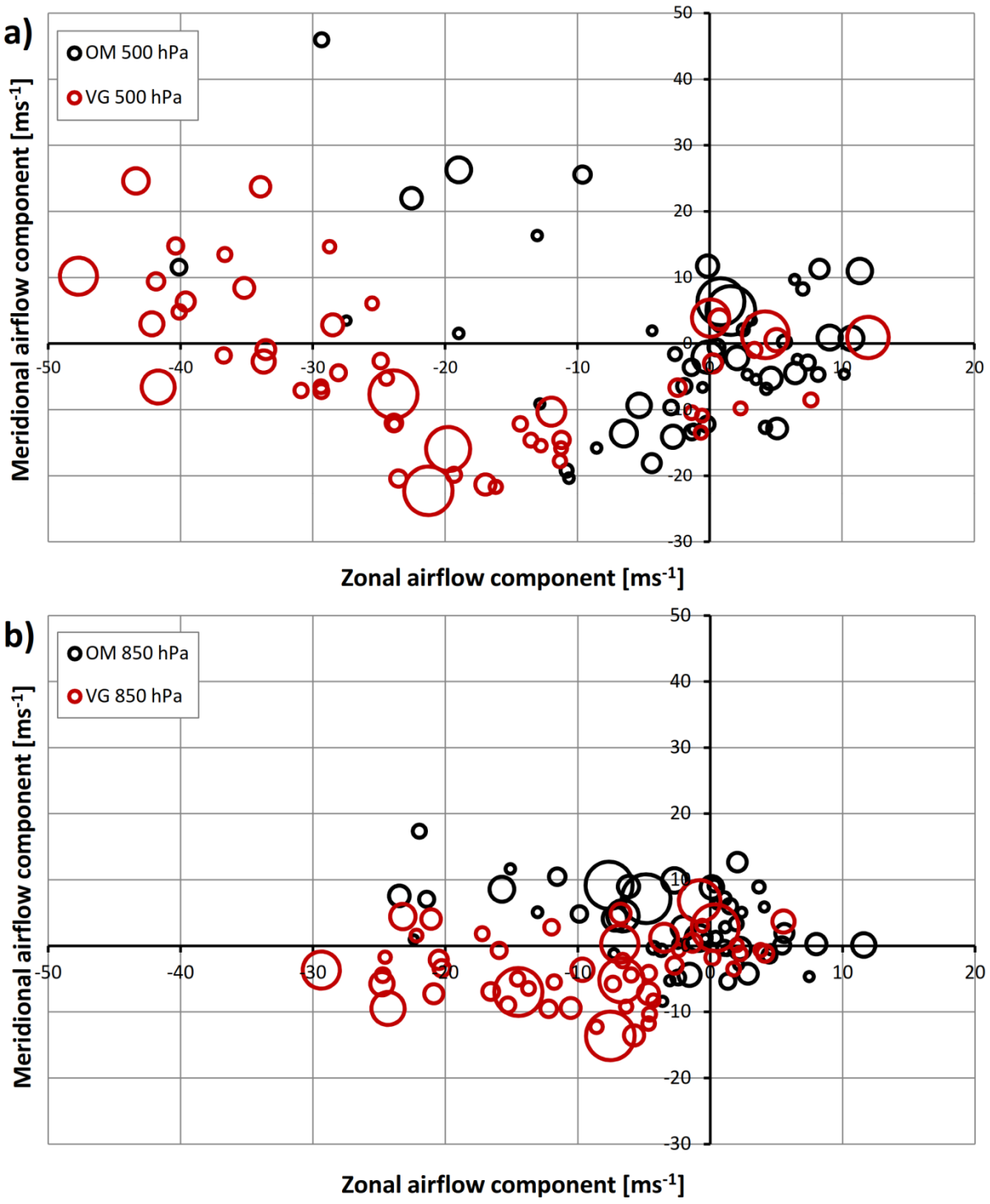

Fig. 6 Zonal and meridional airflow components during EPEs in OM and VG a) at 500 hPa and b) at 850 hPa isobaric levels; the reversed values of the components are displayed to match the cardinal points, e.g. the western and southern airflow correspond to the negative values of zonal and meridional airflow components, respectively

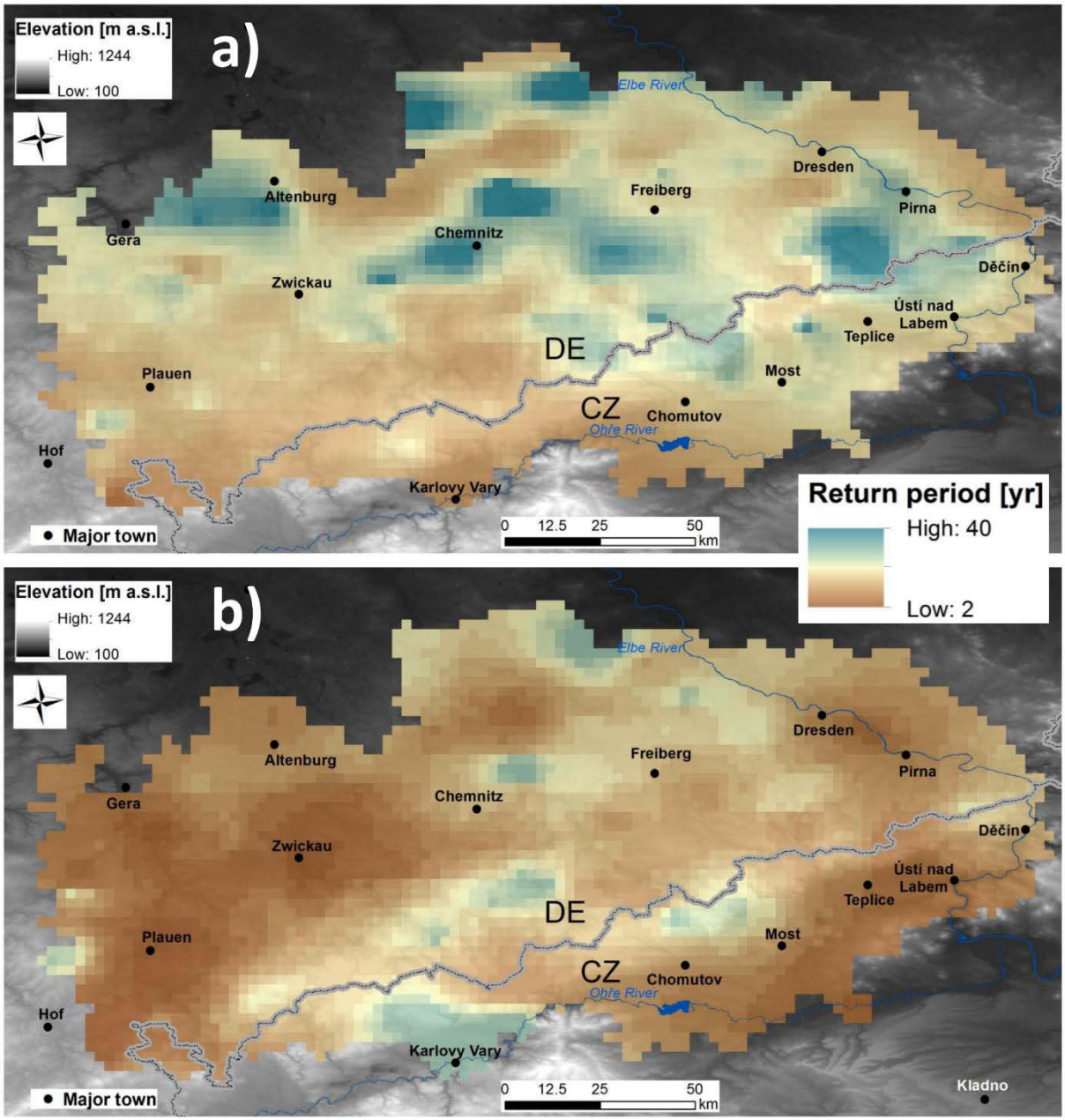

Fig. 7 Superimposed and averaged return period estimates during EPEs in a) SHY and b) WHY in OM

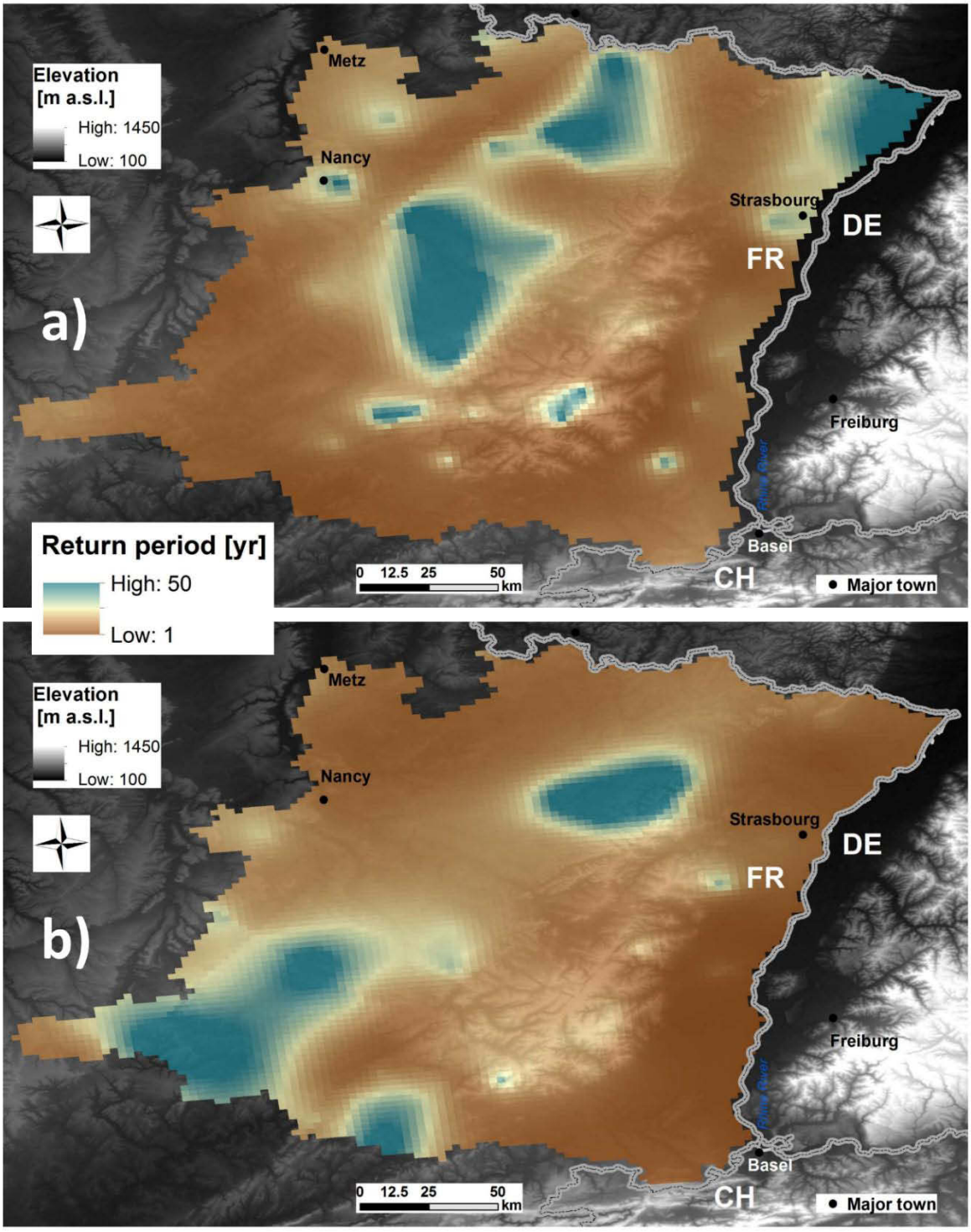

Fig. 8 Superimposed and averaged return period estimates during EPEs in a) SHY and b) WHY in VG

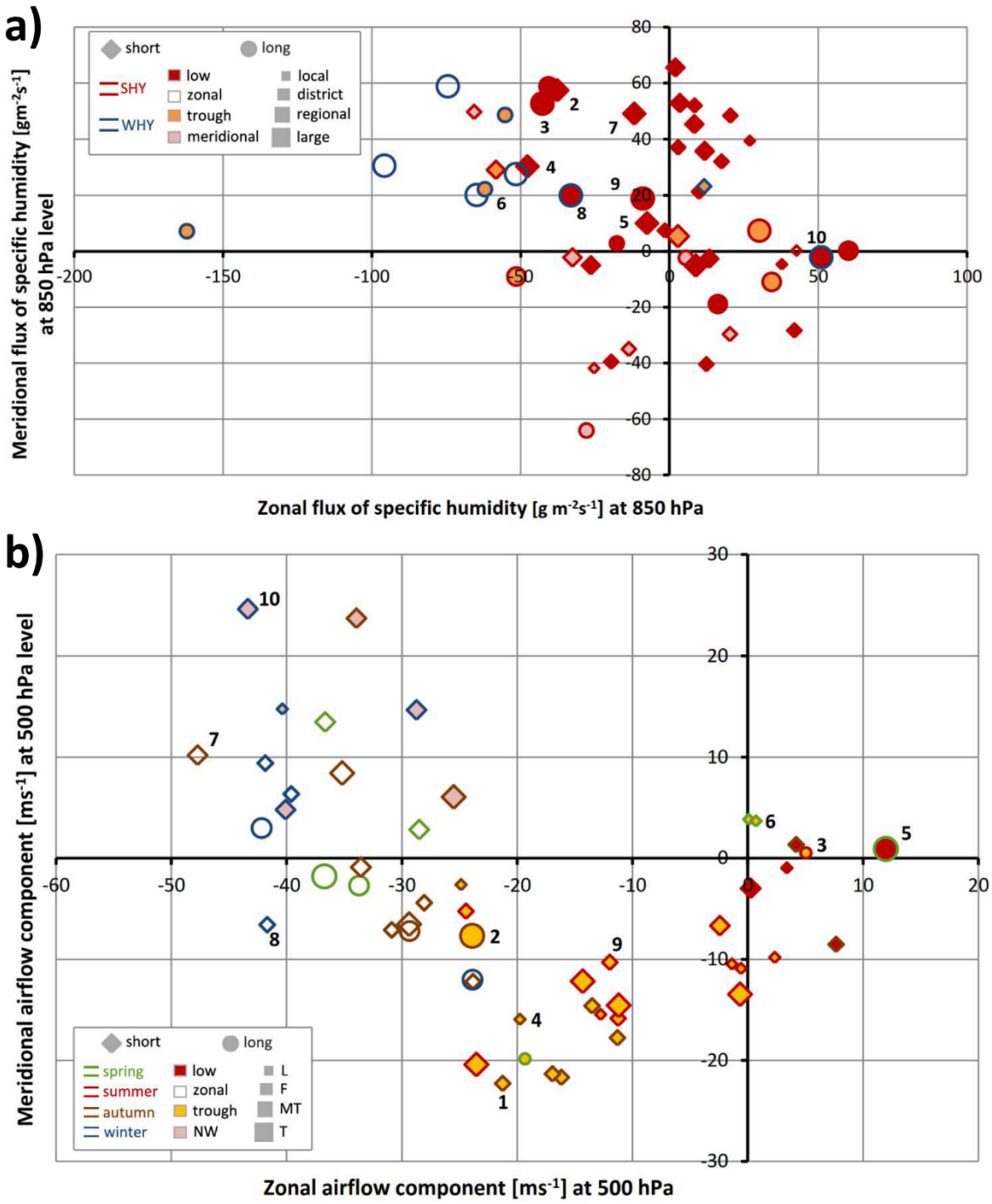

Fig. 9 Significantly dependent characteristics of EPEs: a) characteristics of EPEs in OM: flux of specific humidity at 850 hPa level, half-year (SHY bordered in red, WHY in blue), duration, synoptic situation, and affected area (larger the area larger the symbol), and b) characteristics of EPEs in VG: airflow at 500 hPa level, season (spring EPEs bordered by green, summer by red, autumn by brown, winter by blue), duration, synoptic situation, and relief (size of the symbol). The diamonds depict short EPEs, circles long EPEs, and various filling the synoptic situations that are given in Section 3.1 (a) and 3.2 (b). The description of the categorized characteristics can be found in Section 2.6. Ten strongest EPEs from OM (Table 1) and VG (Table 2) are numbered starting from the strongest (Nr. 1), except one in OM where it was beyond the available synoptic dataset. Note that the reversed values of the components of flux of specific humidity are displayed in (a) to match the cardinal points.

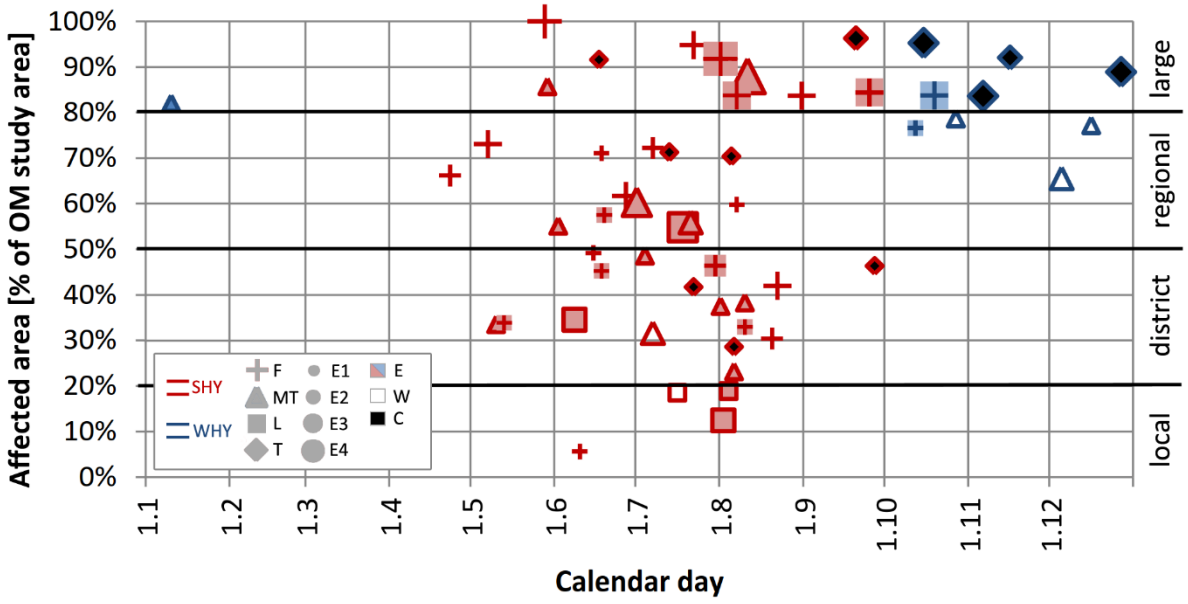

Fig. 10 Dependence of the area affected by EPEs in OM and their annual course, most affected part of the relief (shape of the symbol, roughly the shape in Fig. 1a), extremity (size of the symbol), and most affected part of the area with respect to the cardinal points (filling of the symbols, scheme map in Fig. 1a). SHY and WHY EPEs are bordered in red and blue, respectively. The description of the categories and their abbreviations can be found in Section 2.6.

11. Conclusions and future perspectives

According to IPCC (Pachauri *et al.*, 2014), it is likely that in Europe the frequency and intensity of precipitation extremes will increase in future despite regional differences. Subsequent to the heavy rainfall in August 2002 and June 2013 which induced disastrous flooding in Central Europe (e.g., Conradt *et al.*, 2013), the demand for improving the risk management at regional scales has become an important issue. The risk management should encompass reducing risks and protecting or adapting societies against the natural hazards induced by extreme precipitation (e.g., flooding, landsliding) which result in huge socioeconomic impacts. For an improved risk management, it is necessary to understand the processes and characteristics related to extreme precipitation.

The thesis provides a description and comparison of several characteristics of EPEs between two low mountain ranges in Central Europe – Ore Mountains (OM) situated at the Czech-German border and Vosges Mountains (VG) in northeastern France, based on wider dataset of EPEs during longer period (1960—2013) which were spatially defined, i.e. using event-adjustable parameters, the WEI. The same way of defining the EPEs and quantitative assessment of their extremity enables comparable and robust findings among the EPEs and between the study regions. Based on the current literature review, the up-to-date temporal distribution of precipitation was studied in VG as well, since it provides a basis for the analysis of precipitation extremes.

Major results of the thesis are summarized as follows:

- Main precipitation season in VG changes according to the mean annual totals and relief: highest annual and monthly totals are reached in mountains where winter is the main precipitation season (oceanic feature), and lowest totals in the leeward Upper Rhine Plain where summer is the main precipitation season (continental feature).
- Orographic influence on extreme precipitation seems to be more pronounced at higher thresholds based on the results of the seasonality of extreme precipitation totals defined using the pointwise approaches POT, BM, and RP with varying criteria.
- The areal assessment of extreme precipitation events (EPEs) using WEI (Müller and Kaspar, 2014) was proved to be applicable at the regional scale.
- Computation of maximum theoretical WEI enables a conversion of the WEI values from one region to another so that the extremity of events is objectively comparable.
- The extremity of strongest events was slightly higher in VG as compared to that in OM.
- EPEs lasted most frequently 1—2 days during 1960—2013 in OM and VG, although no 1-day event was found among the 10 strongest in OM, where the longest EPE lasted 10 days. The longest EPE in VG lasted 5 days.
- EPEs in OM affected up to 100 % of the study area (i.e. the strongest event), while the area affected by the EPEs in VG is smaller: the 10 heaviest EPEs affected 21—75 % of VG, whereas more than 80 % of OM.

- Main precipitation season did not correspond with the seasonality of extreme precipitation in VG regardless of the applied definition of extremes (point/areal).
- EPEs occurred in all seasons in both OM and VG, indicating the need of considering all seasons in extreme precipitation analyses.
- Based on the Grosswetterlagen catalogue, the EPEs in OM and VG were related to many and various weather types.
- Based on synoptic data, the Vb cyclones (Bebber, 1891) and cut-off lows, known to be prone to heavy rainfall in Central Europe, were the dominant synoptic conditions during EPEs in OM, while it was stationary fronts related to troughs in VG; however Vb lows were also identified during 2 of the 10 strongest EPEs in VG.
- Significant hydrological response ensued majority of EPEs in OM and VG, however, the strongest precipitation in VG was related to the stationary front rather than to the zonal circulation known to induce widespread flooding in the area.
- Alike temporal aspects of EPEs in OM, those in VG closely depended on the synoptic situation, which might be similar in other low mountain ranges in Central Europe.
- The dependencies between the spatial and other characteristics of EPEs provided more site-specific results and most likely cannot be generalized over other similar areas.

Besides the new and detailed information about characteristics of extreme precipitation in OM and VG which is useful for improving the regional urban planning, mitigating the hazards, and reducing the risks associated with extreme precipitation by e.g., climate change withstanding engineering decisions, the thesis also provides the first objective comparison of EPEs between the two orographic regions. It might motivate for analogous analyses in similar areas in Central Europe which are still not studied in detail in order to provide a whole and precise picture of EPEs in low mountain ranges in Central Europe. Thus, there is still a need for further research in future which will investigate the EPE characteristics in similar regions based on WEI, and gain insight into the occurrence of Vb cyclones during EPEs in the eastwards direction in Central Europe.

12. References (excluding Section 6—10)

Akinremi OO, McGinn SM, Cutforth HW. 1999. Precipitation Trends on the Canadian Prairies. *Journal of Climate* **12**(10): 2996–3003. DOI: 10.1175/1520-0442(1999)012<2996:PTOTCP>2.0.CO;2.

Alexander LV, Zhang X, Peterson TC, Caesar J, Gleason B, Klein Tank AMG, Haylock M, Collins D, Trewin B, Rahimzadeh F, Tagipour A, Rupa Kumar K, Revadekar J, Griffiths G, Vincent L, Stephenson DB, Burn J, Aguilar E, Brunet M, Taylor M, New M, Zhai P, Rusticucci M, Vazquez-Aguirre JL. 2006. Global observed changes in daily climate extremes of temperature and precipitation. *Journal of Geophysical Research: Atmospheres* **111**(D5): D05109. DOI: 10.1029/2005JD006290.

Allaby M. 2007. *Encyclopedia of weather and climate*. Facts on File: New York.

Allan RP, Lavers DA, Champion AJ. 2015. Diagnosing links between atmospheric moisture and extreme daily precipitation over the UK. *International Journal of Climatology* n/a-n/a. DOI: 10.1002/joc.4547.

Alpert P. 1986. Mesoscale Indexing of the Distribution of Orographic Precipitation over High Mountains. *Journal of Climate and Applied Meteorology* **25**(4): 532–545. DOI: 10.1175/1520-0450(1986)025<0532:MIOTDO>2.0.CO;2.

Alsatia. 1932. *L´Alsace : précis de la géographie régionale des départements Haut-Rhin et Bas-Rhin*. Alsatia: Colmar.

AMS. online (n.d.). Heavy rain. *AMS Glossary*.

Andreadis KM, Clark EA, Wood AW, Hamlet AF, Lettenmaier DP. 2005. Twentieth-century drought in the conterminous United States. *Journal of Hydrometeorology* **6**(6).

Augros C, Caumont O, Ducrocq V, Gaussiat N, Tabary P. 2016. Comparisons between S-, C- and X-band polarimetric radar observations and convective-scale simulations of the HyMeX first special observing period. *Quarterly Journal of the Royal Meteorological Society* **142**: 347–362. DOI: 10.1002/qj.2572.

Balling RC, Keikhosravi Kiany MS, Sen Roy S, Khoshhal J. 2016. Trends in Extreme Precipitation Indices in Iran: 1951-2013;2007, Trends in Extreme Precipitation Indices in Iran: 1951–2007. *Advances in Meteorology, Advances in Meteorology* **2016**, **2016**: e2456809. DOI: 10.1155/2016/2456809, 10.1155/2016/2456809.

Ban N, Schmidli J, Schär C. 2015. Heavy precipitation in a changing climate: Does short-term summer precipitation increase faster? *Geophysical Research Letters* **42**(4): 2014GL062588. DOI: 10.1002/2014GL062588.

Barry RG. 2008. *Mountain Weather and Climate Third Edition*. Cambridge University Press: Cambridge.

Barstad I, Smith RB. 2005. Evaluation of an Orographic Precipitation Model. *Journal of Hydrometeorology* **6**: 85–99.

Bauer H-S, Schwitalla T, Wulfmeyer V, Bakhshaii A, Ehret U, Neuper M, Caumont O. 2015. Quantitative precipitation estimation based on high-resolution numerical weather prediction and data assimilation with WRF – a performance test. *Tellus A: Dynamic Meteorology and Oceanography* **67**(1): 25047. DOI: 10.3402/tellusa.v67.25047.

Baulig H. 1950. *Les inondations de décembre 1947*.

Bebber WJ van. 1891. *Die Zugstrassen der barometrischen Minima nach den Bahnenkarten der deutschen Seewarte für den Zeitraum 1875-1890*.

Beck J-S. 2011. *2000 ans de climat en Alsace et en Lorraine*.

Beguería S, Vicente-Serrano SM, López-Moreno JI, García-Ruiz JM. 2009. Annual and seasonal mapping of peak intensity, magnitude and duration of extreme precipitation events across a climatic gradient, northeast Spain. *International Journal of Climatology* **29**(12): 1759–1779. DOI: 10.1002/joc.1808.

Beniston M, Stephenson DB. 2004. Extreme climatic events and their evolution under changing climatic conditions. *Global and Planetary Change* **44**(1–4): 1–9. DOI: 10.1016/j.gloplacha.2004.06.001.

Beniston M, Stephenson DB, Christensen OB, Ferro CAT, Frei C, Goyette S, Halsnaes K, Holt T, Jylhä K, Koffi B, Palutikof J, Schöll R, Semmler T, Woth K. 2007. Future extreme events in European climate: an exploration of regional climate model projections. *Climatic Change* **81**(S1): 71–95. DOI: 10.1007/s10584-006-9226-z.

Bernhofer C, Surke M, Leibniz-Institut für Ökologische Raumentwicklung (eds). 2009. *Das Klima in der REGKLAM-Modellregion Dresden*. Rhombos-Verl: Berlin.

Bertoldo S, Lucianaz C, Allegretti M. 2015. Extreme Rainfall Event Analysis Using Rain Gauges in a Variety of Geographical Situations. *Atmospheric and Climate Sciences* **05**(02): 82–90. DOI: 10.4236/acs.2015.52006.

Blanchet J, Molinié G, Touati J. 2016. Spatial analysis of trend in extreme daily rainfall in southern France. *Climate Dynamics* 1–14. DOI: 10.1007/s00382-016-3122-7.

Blenkinsop S, Lewis E, Chan SC, Fowler HJ. 2016. Quality-control of an hourly rainfall dataset and climatology of extremes for the UK. *International Journal of Climatology* n/a-n/a. DOI: 10.1002/joc.4735.

Bosshard T, Kotlarski S, Zappa M, Schär C. 2013. Hydrological Climate-Impact Projections for the Rhine River: GCM–RCM Uncertainty and Separate Temperature and Precipitation Effects. *Journal of Hydrometeorology* **15**(2): 697–713. DOI: 10.1175/JHM-D-12-098.1.

Botero BA, Francés F. 2010. Estimation of high return period flood quantiles using additional non-systematic information with upper bounded statistical models. *Hydrology and Earth System Sciences* **14**(12): 2617–2628. DOI: 10.5194/hess-14-2617-2010.

Boucek J. 2007. August 2002 catastrophic flood in the Czech Republic. In: Vasiliev OF, VanGelder P, Plate EJ and Bolgov MV (eds) *Extreme Hydrological Events: New Concepts for Security*. Springer: Dordrecht, 59–68.

Brádka J. 1963. O srážkovém stínu za Krušnými horami. *Meteorologické zprávy* **16**(2): 26–28.

Brázdil R. 2002. Meteorologické extrémy a povodně v České republice - přirozený trend nebo následek globálního oteplování? *Geografie - Sborník České geografické společnosti* (4).

Brázdil R, Chromá K, Dobrovolný P, Tolasz R. 2009. Climate fluctuations in the Czech Republic during the period 1961-2005. *International Journal of Climatology* **29**(2): 223–242. DOI: 10.1002/joc.1718.

Brázdil R, Dobrovolný P, Elleder L, Kakos V, Kotyza O, Květoň V, Burianová J, Muller M, Štekl J, Tolasz R, Valášek H. 2005. *Historické a současné povodně v České republice*. Masarykova univerzita v Brně, Český hydrometeorologický ústav v Praze.

Brazdil R, Kotyza O, Dobrovolny P. 2006. July 1432 and August 2002 - two millennial floods in Bohemia? *Hydrological Sciences Journal-Journal Des Sciences Hydrologiques* **51**(5): 848–863. DOI: 10.1623/hysj.51.5.848.

Burt TP, Howden NJK. 2013. North Atlantic Oscillation amplifies orographic precipitation and river flow in upland Britain. *Water Resources Research* **49**(6): 3504–3515. DOI: 10.1002/wrcr.20297.

Cantet P, Bacro J-N, Arnaud P. 2010. Using a rainfall stochastic generator to detect trends in extreme rainfall. *Stochastic Environmental Research and Risk Assessment* **25**(3): 429–441. DOI: 10.1007/s00477-010-0440-x.

Cavalcanti IFA. 2012. Large scale and synoptic features associated with extreme precipitation over South America: A review and case studies for the first decade of the 21st century. *Atmospheric Research* **118**(0): 27–40. DOI: 10.1016/j.atmosres.2012.06.012.

CEMAGREF Aix-en-Provence. 1981. *Bassin du Real Collobrier : analyse de la pluviométrie par la méthode des composantes principales.* CEMAGREF: Aix en Provence.

Chamas V, Kakos V. 1988. Mimořádná průtrž mračen a povodeň na Jílovském potoce dne 1. 7. 1987. *Sborník Československé geografické společnosti* **93**(4): 265–278.

Chen C-S, Lin Y-L, Zeng H-T, Chen C-Y, Liu C-L. 2013. Orographic effects on heavy rainfall events over northeastern Taiwan during the northeasterly monsoon season. *Atmospheric Research* **122**: 310–335. DOI: 10.1016/j.atmosres.2012.10.008.

Chow VT, Maidment DR, Mays LW, Chow VT, Maidment DR, Mays LW. 1988. Applied Hydrology. *McGraw-Hill Series in Water Resources and Environmental Engineering*.

Coelho C a. S, Ferro C a. T, Stephenson DB, Steinskog DJ. 2008. Methods for Exploring Spatial and Temporal Variability of Extreme Events in Climate Data. *Journal of Climate* **21**(10): 2072–2092. DOI: 10.1175/2007JCLI1781.1.

Coles S. 2001. *An Introduction to Statistical Modeling of Extreme Values*. Springer: London ; New York.

Colle BA, Yuter SE. 2007. The Impact of Coastal Boundaries and Small Hills on the Precipitation Distribution across Southern Connecticut and Long Island, New York. *Monthly Weather Review* **135**(3): 933–954. DOI: 10.1175/MWR3320.1.

Colle BA, Zeng Y. 2004. Bulk Microphysical Sensitivities within the MM5 for Orographic Precipitation. Part II: Impact of Barrier Width and Freezing Level. *Monthly Weather Review* **132**(12): 2802–2815. DOI: 10.1175/MWR2822.1.

Conradt T, Roers M, Schröter K, Elmer F, Hoffmann P, Koch H, Hattermann FF, Wechsung F. 2013. Comparison of the extreme floods of 2002 and 2013 in the German part of the Elbe River basin and their runoff simulation by SWIM-live. *Hydrology und Wasserbewirtschaftung* **57**(5): 241–245. DOI: 10.5675/HyWa-2013,5-4.

Cox DR, Isham V. 2000. *Point processes*. Chapman & Hall/CRC: Boca Raton, Fla.

Cramér H. 1946. *Mathematical methods of statistics*. Princeton University Press: Princeton.

Cutter SL, Barnes L, Berry M, Burton C, Evans E, Tate E, Webb J. 2008. A place-based model for understanding community resilience to natural disasters. *Global Environmental Change* **18**(4): 598–606. DOI: 10.1016/j.gloenvcha.2008.07.013.

Davison AC, Gholamrezaee MM. 2012. Geostatistics of extremes. *Proceedings of the Royal Society A: Mathematical, Physical and Engineering Sciences* **468**(2138): 581–608. DOI: 10.1098/rspa.2011.0412.

Davison AC, Padoan SA, Ribatet M. 2012. Statistical Modeling of Spatial Extremes. *Statistical Science* **27**(2): 161–186. DOI: 10.1214/11-STS376.

Dawdy DR, Langbein WB. 1960. Mapping Mean Areal Precipitation. *International Association of Scientific Hydrology. Bulletin* **5**(3): 16–23. DOI: 10.1080/02626666009493176.

Dean WE. 1997. Rates, timing, and cyclicity of Holocene eolian activity in north-central United States: Evidence from varved lake sediments. *Geology* **25**(4): 331. DOI: 10.1130/0091-7613(1997)025<0331:RTACOH>2.3.CO;2.

Décamps H (ed). 2010. *Événements climatiques extrêmes: réduire les vulnérabilités des systèmes écologiques et sociaux*. EDP sciences: Les Ulis.

Denhez F, Petit M, Mazoyer K. 2009. *Atlas du changement climatique: du global au local, changer les comportements*. Autrement: Paris, France.

Desurosne I, Oberlin G. 1994. - 01-Desurosne_&_Oberlin_1994-TPG.pdf. paper presented at the Contrat Etat - Région Rhône Alpes programme de recherche sur les risques naturels bilan des travaux de 1989 à 1993. Préfecture de la Région Rhône-Alpes: Bron.

Diaz HF, Murnane RJ. 2008. *Climate Extremes and Society*. Cambridge University Press.

Dion J. 1972. Etude fréquentielle des précipitations mensuelles du Nord-Est de la France. *Revue Géographique de l'Est* **12**(2): 175–223. DOI: 10.3406/rgest.1972.2355.

Dobesch H, Dumolard P, Dyras I (eds). 2007. *Spatial interpolation for climate data: the use of GIS in climatology and meterology*. ISTE: London ; Newport Beach, CA.

Dobrovolný P, Rybníček M, Kolář T, Brázdil R, Trnka M, Büntgen U. 2015. A tree-ring perspective on temporal changes in the frequency and intensity of hydroclimatic extremes in the territory of the Czech Republic since 761 AD. *Clim. Past* **11**(10): 1453–1466. DOI: 10.5194/cp-11-1453-2015.

Drogue G, Humbert J, Deraisme J, Mahr N, Freslon N. 2002. A statistical–topographic model using an omnidirectional parameterization of the relief for mapping orographic rainfall. *International Journal of Climatology* **22**(5): 599–613. DOI: 10.1002/joc.671.

DWD DDR, HMÚ ČSSR. 1975. *Podnebí a počasí v Krušných horách*. SNTL - Nakladatelství technické literatury: Praha.

Dyrrdal AV, Skaugen T, Stordal F, Førland EJ. 2014. Estimating extreme areal precipitation in Norway from a gridded dataset. *Hydrological Sciences Journal* **0**(ja): null. DOI: 10.1080/02626667.2014.947289.

Embrechts P, Klüppelberg C, Mikosch T. 2011. *Modelling Extremal Events: for Insurance and Finance*. Springer: New York.

Ernst F. 1988. *Panorama de la géographie physique de l'Alsace ; et Les régions naturelles de l'Alsace*. .

Ferro CAT, Hannachi A, Stephenson DB. 2005. Simple Nonparametric Techniques for Exploring Changing Probability Distributions of Weather. *Journal of Climate* **18**(21): 4344–4354. DOI: 10.1175/JCLI3518.1.

Ferro CAT, Stephenson DB. 2011. Deterministic Forecasts of Extreme Events and Warnings. In: Jolliffe IT and Stephenson DB (eds) *Forecast Verification*. John Wiley & Sons, Ltd, 185–201. DOI: 10.1002/9781119960003.ch10.

Fink A, Ulbrich U, Engel H. 1996. Aspects of the January 1995 flood in Germany. *Weather* **51**(2): 34–39. DOI: 10.1002/j.1477-8696.1996.tb06182.x.

Foresti L, Pozdnoukhov A. 2012. Exploration of alpine orographic precipitation patterns with radar image processing and clustering techniques. *Meteorological Applications* **19**(4): 407–419. DOI: 10.1002/met.272.

Fort M. 2015. Impact of climate change on mountain environment dynamics. *Journal of Alpine Research | Revue de géographie alpine* (103–2). DOI: 10.4000/rga.2877.

Franke J, Goldberg V, Eichelmann U, Freydank E, Bernhofer C. 2004. Statistical analysis of regional climate trends in Saxony, Germany. *Climate Research* **27**(2): 145–150. DOI: 10.3354/cr027145.

Frich P, Alexander LV, Della-Marta P, Gleason B, Haylock M, Klein Tank AM, Peterson T. 2002. Observed coherent changes in climatic extremes during the second half of the twentieth century. *Climate Research* **19**(3): 193–212.

Fuhrer O, Schär C. 2005. Banded convection in moist orographic flows. *Hrvatski Meteoroloski Casopis* (40): 50.

Fukutome S, Liniger MA, Süveges M. 2015. Automatic threshold and run parameter selection: a climatology for extreme hourly precipitation in Switzerland. *Theoretical and Applied Climatology* **120**(3–4): 403–416. DOI: 10.1007/s00704-014-1180-5.

Gabl K (ed). 2014. *Bergwetter: Praxiswissen vom Profi zu Wetterbeobachtung und Tourenplanung*. Bruckmann: München.

Gagnon P, Rousseau AN, Mailhot A, Caya D. 2013. A Gibbs sampling disaggregation model for orographic precipitation. *International Journal of Applied Earth Observation and Geoinformation* **22**(0): 16–26. DOI: 10.1016/j.jag.2011.11.002.

Garvert MF, Smull B, Mass C. 2007. Multiscale Mountain Waves Influencing a Major Orographic Precipitation Event. *Journal of the Atmospheric Sciences* **64**(3): 711–737. DOI: 10.1175/JAS3876.1.

Germann U, Galli G, Boscacci M, Bolliger M. 2006. Radar precipitation measurement in a mountainous region. *Quarterly Journal of the Royal Meteorological Society* **132**(618): 1669–1692. DOI: 10.1256/qj.05.190.

Ghenim AN, Megnounif A. 2016. Variability and Trend of Annual Maximum Daily Rainfall in Northern Algeria. *International Journal of Geophysics* **2016**: 1–11. DOI: 10.1155/2016/6820397.

Gley G. 1867. *Géographie physique, industrielle, administrative et historique des Vosges*. V.e Gley Impr. V.e & Durand Libraire: Épinal.

Goldberg V, Bernhofer C. 2003. The flash flood event in the catchment of the river Weisseritz (eastern Erzgebirge, Saxony) from 12.-14. August 2002 - meteorological and hydrological reasons, damage assesment and disaster managment. paper presented at the EGS - AGU - EUG Joint Assembly, 5134.

Grams CM, Binder H, Pfahl S, Piaget N, Wernli H. 2014. Atmospheric processes triggering the central European floods in June 2013. *Nat. Hazards Earth Syst. Sci.* **14**(7): 1691–1702. DOI: 10.5194/nhess-14-1691-2014.

Granger OE. 2005. Precipitation distribution. *Encyclopedia of world climatology*. Springer, 576–582.

Greenwood PE, Nikulin MS. 1996. *A guide to chi-squared testing*. Wiley: New York.

Groisman PY, Knight RW, Easterling DR, Karl TR, Hegerl GC, Razuvaev VN. 2005. Trends in Intense Precipitation in the Climate Record. *Journal of Climate* **18**(9): 1326–1350. DOI: 10.1175/JCLI3339.1.

Gumbel EJ. 1941. The Return Period of Flood Flows. *The Annals of Mathematical Statistics* **12**(2): 163–190.

Haan LD. 1984. A Spectral Representation for Max-stable Processes. *The Annals of Probability* **12**(4): 1194–1204. DOI: 10.1214/aop/1176993148.

Hally A, Caumont O, Garrote L, Richard E, Weerts A, Delogu F, Fiori E, Rebora N, Parodi A, Mihalović A, Ivković M, Dekić L, van Verseveld W, Nuissier O, Ducrocq V, D'Agostino D, Galizia A, Danovaro E, Clematis A. 2015. Hydrometeorological multi-model ensemble simulations of the 4 November 2011 flash flood event in Genoa, Italy, in the framework of the DRIHM project. *Nat. Hazards Earth Syst. Sci.* **15**(3): 537–555. DOI: 10.5194/nhess-15-537-2015.

Hamblyn R, Great Britain, Meteorological Office. 2009. *Extraordinary clouds: skies of the unexpected from bizarre to beautiful*. David & Charles: Newton Abbot.

Hänsel S, Schucknecht A, Böttcher F, Bernhofer C, Matschullat J. 2015. *Niederschlagsveränderungen in Sachsen von 1901 bis 2100 Starkniederschlags- und Trockenheitstrends*. Selbstverlag des Deutchen Wetterdienstes: Offenbach am Main.

Heidenreich M, Bernhofer C (eds). 2011. *Klimaprojektionen für die REGKLAM-Modellregion Dresden*. Rhombos Verl: Berlin.

Hirabayashi Y, Mahendran R, Koirala S, Konoshima L, Yamazaki D, Watanabe S, Kim H, Kanae S. 2013. Global flood risk under climate change. *Nature Climate Change* **3**(9): 816–821. DOI: 10.1038/nclimate1911.

Hirsch F. 1967. Application de l'analyse statistique à l'etude de la pluviométrie: Le bassin versant de la Bruche. *Société Météorologique de France* (7): 27–46.

Hirsch F. 1972. Bassin représentatif de la Bruche: Intensité des pluies dans le bassin, une méthode d'analyse. *Société Météorologique de France* 443–456.

Hirsch RM, Slack JR. 1984. A Nonparametric Trend Test for Seasonal Data With Serial Dependence. *Water Resources Research* **20**(6): 727–732. DOI: 10.1029/WR020i006p00727.

Hirsch RM, Slack JR, Smith RA. 1982. Techniques of trend analysis for monthly water quality data. *Water Resources Research* **18**(1): 107–121. DOI: 10.1029/WR018i001p00107.

Hladný J, Barbořík J. 1967. Studie krátkodobých hydrologických předpovědí v povodí Ohře. *Sborník HMÚ* **1**: 1–38.

Holton JR, Curry JA, Pyle JA (eds). 2003. *Encyclopedia of atmospheric sciences*. Academic Press: Amsterdam ; Boston.

Hosking JRM, Wallis JR. 2005. *Regional Frequency Analysis: An Approach Based on L-Moments*. Cambridge University Press.

Houze RA. 2014. *Cloud Dynamics*. Academic Press.

Hrudička B. 1933. *Příspěvek k prozkumu ombrické kontinentality v Evropě*. Odbor Československé společnosti zeměpisné.

Humbert J, Cloots A-R, Maire G. 1987. *Crues et inondations (genèse, méthodes d'étude, impacts et prévention) : actes du colloque de Strasbourg, 16-18 octobre 1986 publieś par Joël Humbert, Anne-Rose Cloots et Gérard Maire*. .

Hutchinson MF. 1998. Interpolation of rainfall data with thin plate smoothing splines. Part II: Analysis of topographic dependence. *Journal of Geographic Information and Decision Analysis* **2**(2): 152–167.

INTERKLIM. 2014. *Der Klimawandel im böhmisch-sächsischen Grenzraum. Změna klimatu v česko-saském pohraničí.* Sächsisches Landesamt für Umwelt: Dresden.

James PM. 2007. An objective classification method for Hess and Brezowsky Grosswetterlagen over Europe. *Theoretical and Applied Climatology* **88**(1–2): 17–42. DOI: 10.1007/s00704-006-0239-3.

Jiang Q. 2003. Moist dynamics and orographic precipitation. *Tellus A* **55**(4): 301–316.

Jiang Q, Smith RB. 2003. Cloud Timescales and Orographic Precipitation. *Journal of the Atmospheric Sciences* **60**(13): 1543–1559. DOI: 10.1175/2995.1.

Johnson GL, Hanson CL. 1995. Topographic and atmospheric influences on precipitation variability over a mountainous watershed. *Journal of Applied Meteorology* **34**(1): 68–87.

Kakos V. 1975. Meteorologické příčiny povodní v první polovině prosince 1974. *VTEI* (3–4).

Kakos V. 1977. Meteorologické příčiny povodní v oblasti Krušných hor. *VTEI* (9).

Kalnay E, Kanamitsu M, Kistler R, Collins W, Deaven D, Gandin L, Iredell M, Saha S, White G, Woollen J, Zhu Y, Leetmaa A, Reynolds R, Chelliah M, Ebisuzaki W, Higgins W, Janowiak J, Mo KC, Ropelewski C, Wang J, Jenne R, Joseph D. 1996. The NCEP/NCAR 40-Year Reanalysis Project. *Bulletin of the American Meteorological Society* **77**(3): 437–471. DOI: 10.1175/1520-0477(1996)077<0437:TNYRP>2.0.CO;2.

Kaspar M, Müller M, Pecho J. 2013. Comparison of meteorological conditions during May and August 2010 floods in Central Europe. **48**(2): 27–34.

Katz RW. 2010. Statistics of extremes in climate change. *Climatic Change* **100**(1): 71–76. DOI: 10.1007/s10584-010-9834-5.

Katz RW, Parlange MB, Naveau P. 2002. Statistics of extremes in hydrology. *Advances in Water Resources* **25**(8–12): 1287–1304. DOI: 10.1016/S0309-1708(02)00056-8.

Keeping ES. 1962. *Introduction to Statistical Inference*. Courier Corporation.

Kendall MG. 1975. *Rank correlation methods*. Griffin: Oxford, England.

Kienzler S, Pech I, Kreibich H, Mueller M, Thieken AH. 2015. After the extreme flood in 2002: changes in preparedness, response and recovery of flood-affected residents in Germany between 2005 and 2011. *Natural Hazards and Earth System Sciences* **15**(3): 505–526. DOI: 10.5194/nhess-15-505-2015.

King MD, Platnick S, Yang P, Arnold GT, Gray MA, Riedi J, Ackerman SA, Liou K-N. 2004. Remote sensing of liquid water and ice cloud optical thickness and effective radius in the Arctic: Application of airborne multispectral MAS data. *Journal of Atmospheric & Oceanic Technology* **21**(6).

Kirshbaum DJ, Smith RB. 2008. Temperature and moist-stability effects on midlatitude orographic precipitation. *Quarterly Journal of the Royal Meteorological Society* **134**(634): 1183–1199. DOI: 10.1002/qj.274.

Klein Tank AMG, Peterson TC, Quadir DA, Dorji S, Zou X, Tang H, Santhosh K, Joshi UR, Jaswal AK, Kolli RK, Sikder AB, Deshpande NR, Revadekar JV, Yeleuova K, Vandasheva S, Faleyeva M, Gomboluudev P, Budhathoki KP, Hussain A, Afzaal M, Chandrapala L, Anvar H, Amanmurad D, Asanova VS, Jones PD, New MG, Spektorman T. 2006. Changes in daily temperature and precipitation extremes in central and south Asia. *Journal of Geophysical Research: Atmospheres* **111**(D16): n/a–n/a. DOI: 10.1029/2005JD006316.

Konrad II CE. 2001. The most extreme precipitation events over the eastern United States from 1950 to 1996: Considerations of scale. *Journal of Hydrometeorology* **2**(3).

Koutsoyiannis D. 2004. Statistics of extremes and estimation of extreme rainfall, 2, Empirical investigation of long rainfall records. *Hydrological Sciences Journal* **49**(4): 591–610.

Krahe P, Herpertz D, International Commission for the Hydrology of the Rhine Basin (eds). 2004. *Entwicklung einer Methodik zur Analyse des Einflusses dezentraler Hochwasserrückhaltemassnahmen auf den Abfluss des Rheins =: Development of methodologies for the analysis of the efficiency of flood reduction measures in the Rhine basin on the basis of reference floods*. Internationale Kommission für die Hydrologie des Rheingebietes: Lelystad.

Krishbaum DJ, Durran DR. 2004. Factors governing cellular convection in orographic precipitation. *Journal of the atmospheric Sciences* **61**(6).

Küchler W, Sommer W. 2005. *Klimawandel in Sachsen: Sachstand und Ausblick*. Sächsisches Staatsministerium für Umwelt und Landwirtschaft: Dresden.

Kunkel KE, Andsager K, Easterling DR. 1999. Long-Term Trends in Extreme Precipitation Events over the Conterminous United States and Canada. *Journal of Climate* **12**(8): 2515–2527. DOI: 10.1175/1520-0442(1999)012<2515:LTTIEP>2.0.CO;2.

Kunkel KE, Easterling DR, Redmond K, Hubbard K. 2003. Temporal variations of extreme precipitation events in the United States: 1895–2000. *Geophysical Research Letters* **30**(17). DOI: 10.1029/2003GL018052.

Kunkel KE, Karl TR, Brooks H, Kossin J, Lawrimore JH, Arndt D, Bosart L, Changnon D, Cutter SL, Doesken N, Emanuel K, Groisman PY, Katz RW, Knutson T, O'Brien J, Paciorek CJ, Peterson TC, Redmond K, Robinson D, Trapp J, Vose R, Weaver S, Wehner M, Wolter K, Wuebbles D. 2012. Monitoring and Understanding Trends in Extreme Storms: State of Knowledge. *Bulletin of the American Meteorological Society* **94**(4): 499–514. DOI: 10.1175/BAMS-D-11-00262.1.

Kynčil J. 1983. *Povodně v Krušných horách a jejich podhůří v letech 1784-1981: Příspěvek k dějinám čes. hydrologie*. Povodí Ohře, podnik pro provoz a využití vodních toků.

Kynčil J, Lůžek B. 1979. *Historické povodně v povodí Bíliny a Ohře*. Povodí Ohře.

Kyselý J, Picek J. 2007. Regional growth curves and improved design value estimates of extreme precipitation events in the Czech Republic. *Climate Research* **33**: 243–255. DOI: 10.3354/cr033243.

Labbouz L, Van Baelen J, Tridon F, Reverdy M, Hagen M, Bender M, Dick G, Gorgas T, Planche C. 2013. Precipitation on the lee side of the Vosges Mountains: Multi-instrumental study of one case from the COPS campaign. *Meteorologische Zeitschrift* **22**(4): 413–432. DOI: 10.1127/0941-2948/2013/0413.

Lafontaine M. 1986. *Les précipitations sur le massif vosgien, leurs relations avec les types de temps: Océanité et continentalité*. Université Louis Pasteur: Strasbourg.

Lamarre D, Groupement de recherches sur les risques liés au climat (France). 2005. *Les risques climatiques*. Belin: Paris.

Le Moine N, Hendrickx F, Gailhard J. 2013. Rainfall–runoff modelling as a tool for constraining the reanalysis of daily precipitation and temperature fields in mountainous regions. *Cold and*

Mountain Region Hydrological Systems Under Climate Change: Towards Improved Projections 13–18.

Lecarpentier C, Shamsi F. 1972. Les régimes pluviométriques dans la France de l'Est. *Revue Géographique de l'Est* **12**(2): 159–174. DOI: 10.3406/rgest.1972.2354.

Lecolazet R. 1950. *Les précipitations atmosphériques en Alsace et Lorraine : moyennes pluviométriques 1911-1940*. .

Liu K, Fearn ML. 2000. Reconstruction of Prehistoric Landfall Frequencies of Catastrophic Hurricanes in Northwestern Florida from Lake Sediment Records. *Quaternary Research* **54**(2): 238–245. DOI: 10.1006/qres.2000.2166.

Liu K, Fearn ML. 2002. Lake Sediment Evidence of Coastal Geologic Evolution and Hurricane History from Western Lake, Florida: Reply to Otvos. *Quaternary Research* **57**(3): 429–431. DOI: 10.1006/qres.2002.2334.

Maire G. 1979. *Analyse des fortes pluies de 1h à 48h: Bassin de l'Ill, région Alsace*. Ministère de l'agriculture, Université Louis Pasteur: Strasbourg.

Mann HB. 1945. Nonparametric Tests Against Trend. *Econometrica* **13**(3): 245–259. DOI: 10.2307/1907187.

Markham CG. 1970. Seasonality of Precipitation in the United States. *Annals of the Association of American Geographers* **60**(3): 593–597. DOI: 10.1111/j.1467-8306.1970.tb00743.x.

Mastrangelo D, Horvath K, Riccio A, Miglietta MM. 2011. Mechanisms for convection development in a long-lasting heavy precipitation event over southeastern Italy. *Atmospheric Research* **100**(4): 586–602. DOI: 10.1016/j.atmosres.2010.10.010.

Maugeri M, Brunetti M, Garzoglio M, Simolo C. 2015. High-resolution analysis of 1 day extreme precipitation in Sicily. *Natural Hazards and Earth System Sciences Discussions* **3**(4): 2247–2281. DOI: 10.5194/nhessd-3-2247-2015.

Merz B, Elmer F, Kunz M, Mühr B, Schröter K, Uhlemann-Elmer S. 2014. The extreme flood in June 2013 in Germany. *La Houille Blanche* (1): 5–10. DOI: 10.1051/lhb/2014001.

Météo-France. 2008. *Climatologie des Vosges*. Météo-France au service des Vosges : le centre dépertemental d´Épinal: Épinal, 10.

Miglietta MM, Laviola S, Malvaldi A, Conte D, Levizzani V, Price C. 2013a. Analysis of tropical-like cyclones over the Mediterranean Sea through a combined modeling and satellite approach. *Geophysical Research Letters* **40**(10): 2400–2405. DOI: 10.1002/grl.50432.

Miglietta MM, Mastrangelo D, Conte D. 2015. Influence of physics parameterization schemes on the simulation of a tropical-like cyclone in the Mediterranean Sea. *Atmospheric Research* **153**: 360–375. DOI: 10.1016/j.atmosres.2014.09.008.

Miglietta MM, Rotunno R. 2012. Application of Theory to Simulations of Observed Cases of Orographically Forced Convective Rainfall. *Monthly Weather Review* **140**(9): 3039–3053. DOI: 10.1175/MWR-D-11-00253.1.

Miglietta MM, Rotunno R. 2014. Numerical simulations of sheared conditionally unstable flows over a mountain ridge. *Journal of the Atmospheric Sciences* **71**: 1747–1762. DOI: 10.1175/JAS-D-13-0297.1.

Miglietta MM, Zecchetto S, De Biasio F. 2013b. A comparison of WRF model simulations with SAR wind data in two case studies of orographic lee waves over the Eastern Mediterranean Sea. *Atmospheric Research* **120**–**121**: 127–146. DOI: 10.1016/j.atmosres.2012.08.009.

Mills E. 2005. Insurance in a Climate of Change. *Science* **309**(5737): 1040–1044. DOI: 10.1126/science.1112121.

Minářová J. 2013. Climatology of precipitation in the Vosges mountain range area. *AUC GEOGRAPHICA* **48**(2): 51–60.

Minářová J, Müller M, Clappier A. 2017a. Seasonality of mean and heavy precipitation in the area of the Vosges Mountains: dependence on the selection criterion. *International Journal of Climatology* **37**(5): 2654–2666. DOI: 10.1002/joc.4871.

Minářová J, Müller M, Clappier A, Hänsel S, Hoy A, Matschullat J, Kašpar M. 2017b. Duration, rarity, affected area, and weather types associated with extreme precipitation in the Ore Mountains (Erzgebirge) region, Central Europe. *International Journal of Climatology* n/a-n/a. DOI: 10.1002/joc.5100.

Minářová J, Müller M, Clappier A, Kašpar M. [submitted TAAC-D-17-00287]. Comparison of synoptic conditions and characteristics of extreme precipitation between the Ore Mountains and the Vosges Mountains. *Theoretical and Applied Climatology*.

Minářová J, Müller M, Clappier A, Kašpar M. 2017c. Characteristics of extreme precipitation in the Vosges Mountains region (north-eastern France). *International Journal of Climatology* n/a-n/a. DOI: 10.1002/joc.5102.

Müller M, Kaspar M. 2014. Event-adjusted evaluation of weather and climate extremes. *Natural Hazards and Earth System Science* **14**(2): 473–483. DOI: 10.5194/nhess-14-473-2014.

Muluneh A, Bewket W, Keesstra S, Stroosnijder L. 2016. Searching for evidence of changes in extreme rainfall indices in the Central Rift Valley of Ethiopia. *Theoretical and Applied Climatology* 1–15. DOI: 10.1007/s00704-016-1739-4.

Munzar J, Auer I, Ondráček S. 2011. Central European one-day precipitation record. **64**(4): 107–112.

Neiman PJ, Ralph FM, White AB, Kingsmill DE, Persson POG. 2002. The statistical relationship between upslope flow and rainfall in California's coastal mountains: Observations during CALJET. *Monthly weather review* **130**(6).

Ngo-Duc T, Tangang FT, Santisirisomboon J, Cruz F, Trinh-Tuan L, Nguyen-Xuan T, Phan-Van T, Juneng L, Narisma G, Singhruck P, Gunawan D, Aldrian E. 2016. Performance evaluation of RegCM4 in simulating extreme rainfall and temperature indices over the CORDEX-Southeast Asia region. *International Journal of Climatology* n/a-n/a. DOI: 10.1002/joc.4803.

Nicks AD, Igo FA. 1980. A depth-area-duration model of storm rainfall in the Southern Great Plains. *Water Resources Research* **16**(5): 939–945. DOI: 10.1029/WR016i005p00939.

Niedźwiedź T, Łupikasza E, Pińskwar I, Kundzewicz ZW, Stoffel M, Małarzewski Ł. 2015. Variability of high rainfalls and related synoptic situations causing heavy floods at the northern foothills of the Tatra Mountains. *Theoretical and Applied Climatology* **119**(1–2): 273–284. DOI: 10.1007/s00704-014-1108-0.

Nott J. 2006. *Extreme events: a physical reconstruction and risk assessment*. Cambridge, UK, Royaume-Uni.

Oliver JE (ed). 2005. *Encyclopedia of World Climatology*. Springer: Dordrecht, Pays-Bas.

Oliver JE. 2008. *Encyclopedia of World Climatology*. Springer Science & Business Media.

Osborn TJ, Hulme M, Jones PD, Basnett TA. 2000. Observed trends in the daily intensity of United Kingdom precipitation. *International Journal of Climatology* **20**(4): 347–364. DOI: 10.1002/(SICI)1097-0088(20000330)20:4<347::AID-JOC475>3.0.CO;2-C.

Oxford Dictionaries - Extreme. (n.d.). *Oxford Dictionaries | English*.

Pachauri RK, Allen MR, Barros VR, Broome J, Cramer W, Christ R, Church JA, Clarke L, Dahe Q, Dasgupta P, Dubash NK, Edenhofer O, Elgizouli I, Field CB, Forster P, Friedlingstein P, Fuglestvedt J, Gomez-Echeverri L, Hallegatte S, Hegerl G, Howden M, Jiang K, Jimenez Cisneroz B, Kattsov V, Lee H, Mach KJ, Marotzke J, Mastrandrea MD, Meyer L, Minx J, Mulugetta Y, O'Brien K, Oppenheimer M, Pereira JJ, Pichs-Madruga R, Plattner G-K, Pörtner H-O, Power SB, Preston B, Ravindranath NH, Reisinger A, Riahi K, Rusticucci M, Scholes R, Seyboth K, Sokona Y, Stavins R, Stocker TF, Tschakert P, van Vuuren D, van Ypserle J-P. 2014. *Climate Change 2014: Synthesis Report. Contribution of Working Groups I, II and III to the Fifth Assessment Report of the Intergovernmental Panel on Climate Change*. IPCC: Geneva, Switzerland.

Panagoulia D, Economou P, Caroni C. 2014. Stationary and nonstationary generalized extreme value modelling of extreme precipitation over a mountainous area under climate change. *Environmetrics* **25**(1): 29–43. DOI: 10.1002/env.2252.

Paul P. 1982. Le climat de la vallée de la Fecht: Aspects généraux. **19**–**21**(1982): 65–78.

Paul P, Roussel I. 1985. *Les précipitations exceptionnelles d'avril et mai 1983 à l'origine des fortes crues en Alsace et en Lorraine*.

Pechala F, Böhme W (eds). 1975. *Podnebí a počasí v Krušných horách*. SNTL: Praha.

Pelt SC van, Beersma JJ, Buishand TA, Hurk BJJM van den, Schellekens J. 2014. Uncertainty in the future change of extreme precipitation over the Rhine basin: the role of internal climate variability. *Climate Dynamics* **44**(7–8): 1789–1800. DOI: 10.1007/s00382-014-2312-4.

Pfister L. 1994. *L' apport de quelques stations récentes pour la spatialisation des précipitations dans les Hautes-Vosges : analyse critique des données de stations d'altitude exposées au vent*. .

Planche C, Wobrock W, Flossmann AI, Tridon F, Labbouz L, Van Baelen J. 2013. Small scale topography influence on the formation of three convective systems observed during COPS over the Vosges Mountains. *Meteorologische Zeitschrift* **22**(4): 395–411. DOI: 10.1127/0941-2948/2013/0402.

Prudhomme C, Reed DW. 1998. Relationships between extreme daily precipitation and topography in a mountainous region: a case study in Scotland. *International Journal of Climatology* **18**(13): 1439–1453. DOI: 10.1002/(SICI)1097-0088(19981115)18:13<1439::AID-JOC320>3.0.CO;2-7.

Ramos MH, Creutin J-D, Leblois E. 2005. Visualization of storm severity. *Journal of Hydrology* **315**(1–4): 295–307. DOI: 10.1016/j.jhydrol.2005.04.007.

Raška P, Brázdil R. 2015. Participatory responses to historical flash floods and their relevance for current risk reduction: a view from a post-communist country. *Area* **47**(2): 166–178. DOI: 10.1111/area.12159.

Raulin V. 1881. *Sur les observations pluviométriques faites dans l'Est de la France (Alsace, Vosges, Lorraine, Bresse ...) de 1871 à 1880*.

Région Météorologique Nord-Est. 1980a. *Orage et fortes precipitations: nuit du 26 au 27 juillet 1980*. Strasbourg, 3.

Région Météorologique Nord-Est. 1980b. *Orage et fortes precipitations: nuit du 15 au 16 août 1980*. Strasbourg, 4.

Reiners PW, Ehlers TA, Mitchell SG, Montgomery DR. 2003. Coupled spatial variations in precipitation and long-term erosion rates across the Washington Cascades. *Nature* **426**(6967): 645–647. DOI: 10.1038/nature02111.

REKLIP. 1995. *Klimaatlas Oberhein Mitte-Süd: REKLIP, Regio-Klima-Projeckt*. Vdf Hochschulverl: Zürich, Suisse.

Rempp G. 1937. *Le Climat de l'Alsace*.

Ren F, Cui D, Gong Z, Wang Y, Zou X, Li Y, Wang S, Wang X. 2012. An Objective Identification Technique for Regional Extreme Events. *Journal of Climate* **25**(20): 7015–7027. DOI: 10.1175/JCLI-D-11-00489.1.

Řezáčová D (ed). 2007. *Fyzika oblaků a srážek*. Academia: Praha.

Roe GH, Montgomery DR, Hallet B. 2003. Orographic precipitation and the relief of mountain ranges. *Journal of Geophysical Research: Solid Earth* **108**(B6): n/a–n/a. DOI: 10.1029/2001JB001521.

Rohli RV, Vega AJ. 2008. *Climatology*. Jones and Bartlett Publishers: Sudbury (Mass.), Etats-Unis.

Rothé J-P, Herrenschneider A. 1963. *Le Hohneck : aspects physiques, biologiques, et humains, Extrait: Climatologie du Massif du Hohneck*. L'Association philomathique d'Alsace et de Lorraine: Strasbourg.

Rudolf B, Rapp J. 2002. Das Jahrhunderthochwasser der Elbe: Synoptische Wetterentwicklung und klimatologische Aspekte. *DWD Klimastatusbericht* 172–187.

Šálek M. 2007. Orographic intensification of precipitation and its implications for quantitative precipitation estimation by meteorological radars. *Proceedings from the 10 years of disastrous floods in Moravia in 1997*. Czech Hydrometeorological Institute: Brno.

Schenck C. 1976. Les conditions climatiques à Colmar de 1972 à 1975. **55**(1972, 1973, 1974): 107–126.

Schock C. 1994. Étude des précipitations sur l'espace alsacien au sens large de 1949 à 1989. Strasbourg, Université Louis Pasteur.

Schröter K, Kunz M, Elmer F, Mühr B, Merz B. 2015. What made the June 2013 flood in Germany an exceptional event? A hydro-meteorological evaluation. *Hydrol. Earth Syst. Sci.* **19**(1): 309–327. DOI: 10.5194/hess-19-309-2015.

Sell Y. 1998. *L'Alsace et les Vosges*. Delachaux et Niestlé: Lausanne (Suisse).

Sheffield J, Andreadis KM, Wood EF, Lettenmaier DP. 2009. Global and Continental Drought in the Second Half of the Twentieth Century: Severity–Area–Duration Analysis and Temporal Variability of Large-Scale Events. *Journal of Climate* **22**(8): 1962–1981. DOI: 10.1175/2008JCLI2722.1.

Siler N, Roe G. 2014. How will orographic precipitation respond to surface warming? An idealized thermodynamic perspective. *Geophysical Research Letters* **41**(7): 2606–2613. DOI: 10.1002/2013GL059095.

Sinclair MR. 1994. A Diagnostic Model for Estimating Orographic Precipitation. *Journal of Applied Meteorology* **33**(10): 1163–1175. DOI: 10.1175/1520-0450(1994)033<1163:ADMFEO>2.0.CO;2.

Smith MD. 2011. An ecological perspective on extreme climatic events: a synthetic definition and framework to guide future research. *Journal of Ecology* **99**(3): 656–663. DOI: 10.1111/j.1365-2745.2011.01798.x.

Smith RB. 1979. The influence of mountains on the atmosphere. *Advances in Geophysics* **27**: 87–230.

Smith RB. 2003. A linear upslope-time-delay model for orographic precipitation. *Journal of Hydrology* **282**(1–4): 2–9. DOI: 10.1016/s0022-1694(03)00248-8.

Smith RB. 2006. Progress on the theory of orographic precipitation. *Special Paper* **398**: 1–16.

Smith RB, Barstad I. 2004. A Linear Theory of Orographic Precipitation. *Journal of the Atmospheric Sciences* **61**: 1377–1391.

Smith TM, Peterson TC, Lawrimore JH, Reynolds RW. 2005. New surface temperature analyses for climate monitoring: SURFACE TEMPERATURE ANALYSES. *Geophysical Research Letters* **32**(14): n/a-n/a. DOI: 10.1029/2005GL023402.

Socher M, Boehme-Korn G. 2008. Central European floods 2002: lessons learned in Saxony. *Journal of Flood Risk Management* **1**(2): 123–129. DOI: 10.1111/j.1753-318X.2008.00014.x.

Söder M, Conrad M, Gönner T, Kusch W. 2009. *Les changements climatiques en Allemagne du Sud: Ampleur – Conséquences – Stratégies*. Brochure. Klimaveränderung und Konsequenzen für die Wasserwirtschaft (KLIWA): Mainz, 1–20.

Stein C, Malitz G. 2013. *Das Hochwasser an Elbe und Donau im Juni 2013*.

Štekl J, Brázdil R, Kakos V, Jež J, Tolasz R, Sokol Z. 2001. *Extrémní denní srážkové úhrny na území ČR v období 1879-2000 a jejich synoptické příčiny*. Národní klimatický program České republiky: Praha.

Stephenson AG. 2009. High-Dimensional Parametric Modelling of Multivariate Extreme Events. *Australian & New Zealand Journal of Statistics* **51**(1): 77–88. DOI: 10.1111/j.1467-842X.2008.00528.x.

Stephenson DB. 2008. *Definition, diagnosis, and origin of extreme weather and climate events*. Cambridge University Press: New York.

Stern LA, Blisniuk PM. 2002. Stable isotope composition of precipitation across the southern Patagonian Andes. *Journal of Geophysical Research: Atmospheres* **107**(D23): ACL 3-1–ACL 3-14. DOI: 10.1029/2002JD002509.

Strangeways I. 2007. *Precipitation: theory, measurement and distribution*. Cambridge, Royaume-Uni.

Svensson C, Jones DA. 2010. Review of rainfall frequency estimation methods: Review of rainfall frequency estimation methods. *Journal of Flood Risk Management* **3**(4): 296–313. DOI: 10.1111/j.1753-318X.2010.01079.x.

Thieken AH, Kreibich H, Mueller M, Merz B. 2007. Coping with floods: preparedness, response and recovery of flood-affected residents in Germany in 2002. *Hydrological Sciences Journal-Journal Des Sciences Hydrologiques* **52**(5): 1016–1037. DOI: 10.1623/hysj.52.5.1016.

Thieken AH, Muller M, Kreibich H, Merz B. 2005. Flood damage and influencing factors: New insights from the August 2002 flood in Germany. *Water Resources Research* **41**(12): W12430. DOI: 10.1029/2005WR004177.

Thillet J-J, Schueller D. 2010. *Petit manuel de météo montagne*. Glénat: Grenoble.

Tolasz R, Brázdil R, Bulíř O, Dobrovolný P, Dubrovský M, Hájková L, Halásová O, Hostýnek J, Janouch M, Kohut M, Krška K, Křivancová S, Květoň V, Lepka Z, Lipina P, Macková J, Metelka L, Míková T, Mrkvica Z, Možný M, Nekovář J, Němec L, Pokorný J, Reitschläger JD, Richterová D, Rožnovský J, Řepka M, Semerádová D, Sosna V, Stříž M, Šercl P, Škáchová H, Štěpánek P, Štěpánková P, Trnka M, Valeriánová A, Valter J, Vaníček K, Vavruška F, Voženílek V, Vráblík T, Vysoudil M, Zahradníček J, Zusková I, Žák M, Žalud Z. 2007. *Altas podnebí Česka / Climate Atlas of Czechia*. Český hydrometeorologický ústav, Universita Palackého.

Tošić I, Unkašević M, Putniković S. 2016. Extreme daily precipitation: the case of Serbia in 2014. *Theoretical and Applied Climatology* 1–10. DOI: 10.1007/s00704-016-1749-2.

Trapero L, Bech J, Lorente J. 2013. Numerical modelling of heavy precipitation events over Eastern Pyrenees: Analysis of orographic effects. *Atmospheric Research* **123**: 368–383. DOI: 10.1016/j.atmosres.2012.09.014.

Tucker DF. 2005. Precipitation. *Encyclopedia of World Climatology*. Springer: Dordrecht, Pays-Bas, 854.

Ulbrich U, Brücher T, Fink AH, Leckebusch GC, Krüger A, Pinto JG. 2003. The central European floods of August 2002: Part 1 – Rainfall periods and flood development. *Weather* **58**(10): 371–377. DOI: 10.1256/wea.61.03A.

Uppala SM, KÅllberg PW, Simmons AJ, Andrae U, Bechtold VDC, Fiorino M, Gibson JK, Haseler J, Hernandez A, Kelly GA, Li X, Onogi K, Saarinen S, Sokka N, Allan RP, Andersson E, Arpe K, Balmaseda MA, Beljaars ACM, Berg LVD, Bidlot J, Bormann N, Caires S, Chevallier F, Dethof A,

Dragosavac M, Fisher M, Fuentes M, Hagemann S, Hólm E, Hoskins BJ, Isaksen L, Janssen P a. EM, Jenne R, Mcnally AP, Mahfouf J-F, Morcrette J-J, Rayner NA, Saunders RW, Simon P, Sterl A, Trenberth KE, Untch A, Vasiljevic D, Viterbo P, Woollen J. 2005. The ERA-40 re-analysis. *Quarterly Journal of the Royal Meteorological Society* **131**(612): 2961–3012. DOI: 10.1256/qj.04.176.

Van der Schrier, G, van den Besselaar E, Leander R, Verver G, Klein Tank A, Beersma J, van Oldenborgh, GJ, Plieger M, Renshaw R, Bissoli P. 2013. Central European flooding 2013 - Euro4m CIB. .

van Meijgaard E, Jilderda R. 1996. The Meuse flood in January 1995. *Weather* **51**(2): 39–45. DOI: 10.1002/j.1477-8696.1996.tb06183.x.

Vautard R. (n.d.). *Des projections climatiques d'une précision inégalée sur toute l'Europe*.

Wallace JM, Hobbs PV. 2006. *Atmospheric Science: An Introductory Survey*. Academic Press: New York.

Wang H, Chen Y, Chen Z. 2013. Spatial distribution and temporal trends of mean precipitation and extremes in the arid region, northwest of China, during 1960–2010. *Hydrological Processes* **27**(12): 1807–1818. DOI: 10.1002/hyp.9339.

Wang Q, Wang M, Fan X, Zhang F, Zhu S, Zhao T. 2016a. Trends of temperature and precipitation extremes in the Loess Plateau Region of China, 1961–2010. *Theoretical and Applied Climatology* 1–15. DOI: 10.1007/s00704-016-1820-z.

Wang XL, Chen H, Wu Y, Feng Y, Pu Q. 2010. New Techniques for the Detection and Adjustment of Shifts in Daily Precipitation Data Series. *Journal of Applied Meteorology and Climatology* **49**(12): 2416–2436. DOI: 10.1175/2010JAMC2376.1.

Wang XL, Feng Y. 2013. RHtests_dlyPrcp User Manual. *Climate Research Division, Atmospheric Science and Technology Directorate, Science and Technology Branch, Environment Canada, Toronto, Ontario, Canada, Retrieved February* **25**: 2014.

Wang Y, Xu Y, Lei C, Li G, Han L, Song S, Yang L, Deng X. 2016b. Spatio-temporal characteristics of precipitation and dryness/wetness in Yangtze River Delta, Eastern China, during 1960–2012. *Atmospheric Research*. DOI: 10.1016/j.atmosres.2016.01.008.

Wang Y, Zhou L. 2005. Observed trends in extreme precipitation events in China during 1961–2001 and the associated changes in large-scale circulation. *Geophysical Research Letters* **32**(9): L09707. DOI: 10.1029/2005GL022574.

Werner PC, Gerstengarbe F-W. 2010. PIK Report No. 119 - Katalog Der Grosswetterlagen Europas nach Paul Hess und Helmut Brezowsky 7., verbesserte und ergänzte Auflage.

Westra S, Fowler HJ, Evans JP, Alexander LV, Berg P, Johnson F, Kendon EJ, Lenderink G, Roberts NM. 2014. Future changes to the intensity and frequency of short-duration extreme rainfall. *Reviews of Geophysics* **52**(3): 2014RG000464. DOI: 10.1002/2014RG000464.

Whiteman CD. 2000. *Mountain Meteorology: Fundamentals and Applications*. Oxford University Press.

Wi S, Valdés JB, Steinschneider S, Kim T-W. 2015. Non-stationary frequency analysis of extreme precipitation in South Korea using peaks-over-threshold and annual maxima. *Stochastic Environmental Research and Risk Assessment* 1–24. DOI: 10.1007/s00477-015-1180-8.

WMO. online. Heavy rain. *WMO Meteoterm*.

WMO, UNESCO. 2013. *International glossary of hydrology = Glossaire international d'hydrologie = Mezhdunarodnyĭ gidrologicheskiĭ slovar' = Glosario hidrológico internacional*.

Woeste B. (n.d.). Eine Anwendung der Block Maxima Methode im Risikomanagement.

World Meteorological Organization. 2008. *Guide to meteorological instruments and methods of observation.* World Meteorological Organization: Geneva, Switzerland.

World Meteorological Organization. (n.d.). *METEOTERM WMO*.

Wotling G, Bouvier C, Danloux J, Fritsch JM. 2000. Regionalization of extreme precipitation distribution using the principal components of the topographical environment. *Journal of Hydrology* **233**(1–4): 86–101. DOI: 10.1016/S0022-1694(00)00232-8.

Yin J, Xu Z, Yan D, Yuan Z, Yuan Y, Yang Z. 2016. Simulation and projection of extreme climate events in China under RCP4.5 scenario. *Arabian Journal of Geosciences* **9**(2): 1–9. DOI: 10.1007/s12517-015-2022-1.

Zhang Q, Xiao M, Li J, Singh VP, Wang Z. 2014. Topography-based spatial patterns of precipitation extremes in the Poyang Lake basin, China: Changing properties and causes. *Journal of Hydrology* **512**: 229–239. DOI: 10.1016/j.jhydrol.2014.03.010.

Zhang X. 2013. *Climate Change Indices: Definitions of the 27 core indices*. *ETCCDI/CRD Climate Change Indices*.

Zhang X, Alexander L, Hegerl GC, Jones P, Tank AK, Peterson TC, Trewin B, Zwiers FW. 2011. Indices for monitoring changes in extremes based on daily temperature and precipitation data. *Wiley Interdisciplinary Reviews: Climate Change* **2**(6): 851–870. DOI: 10.1002/wcc.147.

Zhang X, Zwiers FW, Li G, Wan H, Cannon AJ. 2017. Complexity in estimating past and future extreme short-duration rainfall. *Nature Geoscience* **10**(4): 255–259. DOI: 10.1038/ngeo2911.

Zhou L, Dai A, Dai Y, Vose RS, Zou C-Z, Tian Y, Chen H. 2009. Spatial dependence of diurnal temperature range trends on precipitation from 1950 to 2004. *Climate Dynamics* **32**(2–3): 429–440. DOI: 10.1007/s00382-008-0387-5.

Zolina O, Demuth S, Detemmerman V, Gulev S, Gutowski W, Klein Tank A, Stephenson D, Stewart R, Trenberth K, Zwiers F. 2010. *WCRP (GEWEX/CLIVAR) and UNESCO (IHP) Metrics and methodologies of estima tion of extreme climate events Workshop*. WCRP Informal/Series Report. UNESCO Headquarter: Paris, France, 1–39.

Zolina O, Simmer C, Belyaev K, Gulev SK, Koltermann P. 2013. Changes in the Duration of European Wet and Dry Spells during the Last 60 Years. *Journal of Climate* **26**(6): 2022–2047. DOI: 10.1175/JCLI-D-11-00498.1.

FACULTY OF SCIENCE
Charles University

Department of Physical Geography and Geoecology

Confirmation of co-authorship

As one of supervisors of PhD thesis of Jana Minářová I confirm that she produced the substantial parts of the research published in four papers listed below. She personally collected and analyzed the data, prepared the figures and tables, and wrote the main parts of the text. The co-authors played the supplementary role as follows: M. Müller and A. Clappier supervised the work and helped with interpretation of the results if necessary. M. Kašpar assisted with calculation of the WEI. German colleagues S. Hänsel, A. Hoy, and J. Matschullat contributed to the synoptic classification and interpretation of precipitation extremes in Ore Mountains.

RNDr. Miloslav Müller, Ph.D.

Minářová J, Müller M, Clappier A. 2017. Seasonality of mean and heavy precipitation in the area of the Vosges Mountains: dependence on the selection criterion. International Journal of Climatology *37*(5): 2654–2666. DOI: 10.1002/joc.4871.

Minářová J, Müller M, Clappier A, Kašpar M. 2017. Characteristics of extreme precipitation in the Vosges Mountains region (north-eastern France). International Journal of Climatology n/a-n/a [in press]. DOI: 10.1002/joc.5102.

Minářová J, Müller M, Clappier A, Hänsel S, Hoy A, Matschullat J, Kašpar M. 2017. Duration, rarity, affected area, and weather types associated with extreme precipitation in the Ore Mountains (Erzgebirge) region, Central Europe. International Journal of Climatology n/a-n/a [in press]. DOI: 10.1002/joc.5100.

Minářová J, Müller M, Clappier A, Kašpar M. [submitted TAAC-D-17-00287]. Comparison of synoptic conditions and characteristics of extreme precipitation between the Ore Mountains and the Vosges Mountains. Theoretical and Applied Climatology.

Department of Physical Geography and Geoecology, Faculty of Science
Charles University, Albertov 6, Prague
128 43, Czech Republic

RNDr. Miloslav Müller, Ph.D.
miloslav.muller@natur.cuni.cz
T: +420 221 951 363

IČO: 00216208
DIČ: CZ00216208

TECHNISCHE UNIVERSITÄT
BERGAKADEMIE FREIBERG
Die Ressourcenuniversität. Seit 1765.

Prof. Dr. Jörg Matschullat
Werner-Bau
03731 39-3399
Joerg.Matschullat@ioez.tu-freiberg.de

Interdisziplinäres Ökologisches Zentrum

Department of Physical Geography and
Geoecology
Attn. Dean of the Faculty of Science
Charles University in Prague
Albertov 6

128 43 Praha 1, Czech Republic

28. Mai 2017

Declaration of authroship on behalf of PhD candidate Jana Minárová

Spectability, dear colleague,

Your doctoral student Jana Minárová asked me to send a declaration on authorship activities for her publication, entitled "Duration, rarity, affected area, and weather types associated with extreme precipitation in the Ore Mountains (Erzgebirge) region, Central Europe".

That work resulted from her 6-month collaboration stay with colleagues of my group at TU Bergakademie Freiberg in Germany. Dr. Andreas Hoy assisted her in the interpretation of weather types catalogues, Dr. Stephanie Hänsel recommended to her some literature sources about precipitation in the Erzgebirge (Krusne Hory) and proposed the trend analysis and boxplot approach for visualizing the relationship of affected area, duration, and WEI of EPEs, and I (Dr. Jörg Matschullat) improved the English language of your manuscript.

M. Kašpar estimated the GEV and WEI, A. Clappier and Dr. Miloslav Müller supervised her work at Charles University, proposed some analytical approaches and helped with the interpretation of results. Mrs. Minárová prepared the data, performed the analyses, and wrote the manuscript following the changes in the structure of the paper proposed by the German colleagues. Obviously 85 to 90% of the workload was on your shoulders and she is the true first author of that nice publication.

Sincerely yours

Prof. Dr. Jörg Matschullat

Anlage: //

Kopie an: Mrs. Minárová